STP 543

HYDROGEN EMBRITTLEMENT TESTING

AMERICAN SOCIETY FOR TESTING AND MATERIALS

HYDROGEN EMBRITTLEMENT TESTING

A symposium
presented at the
Seventy-fifth Annual Meeting
AMERICAN SOCIETY FOR
TESTING AND MATERIALS
Los Angeles, Calif., 25–30 June 1972

ASTM SPECIAL TECHNICAL PUBLICATION 543
Louis Raymond, symposium chairman

List price $29.75
04–543000–26

AMERICAN SOCIETY FOR TESTING AND MATERIALS
1916 Race Street, Philadelphia, Pa. 19103

Library of Congress Catalog Card Number: 73-87352

NOTE

Printed in Baltimore, Md.
January 1974

Foreword

The symposium on Hydrogen Embrittlement Testing was given at the Seventy-fifth Annual Meeting of the American Society for Testing and Materials held in Los Angeles, Calif., 25–30 June 1972. Committee F-7 on Aerospace Industry Methods sponsored the symposium. Louis Raymond, The Aerospace Corporation, served as symposium chairman.

Related ASTM Publications

Fatigue at Elevated Temperatures, STP 520 (1973), $45.50 (04–520000–30)

Fracture Toughness Evaluation by R-Curve Methods, STP 527 (1973), $9.75 (04–527000–30)

Impact Testing of Metals, STP 466 (1970), $21.25 (04–466000–23)

Contents

INTERNAL HYDROGEN EMBRITTLEMENT (IHE)

Testing for Relative Susceptibility

Testing for Hydrogen Pickup During Processing

Mechanical Delay—Time Test Methods

Hydrogen Detection Test Methods

HYDROGEN ENVIRONMENT EMBRITTLEMENT (HEE)

CLOSING COMMENTARIES

Introduction

This symposium attempts to update our knowledge of hydrogen embrittlement by presenting new test methods in comparison to those which have been in use for years. The old test methods have been used to evaluate the classic sources of internal hydrogen embrittlement (IHE), such as pickling and plating. New test methods have been devised to evaluate materials susceptibility to high-pressure gaseous hydrogen environments (HEE), such as found in storage tanks, turbine engines, and power units.

The purpose of the first part of this book dealing with IHE is to present a wide range of methods for measuring, detecting, and testing for the phenomena of hydrogen attack. This portion of the book illustrates the lack of a standardized approach resulting from various philosophies and personal preferences as to test methods. This initial effort should point the way for development of long-needed ASTM methods on the subject of IHE.

The second part of this symposium deals with HEE and also clearly shows the need for test methods to produce design data. A review of the methods, analyses, and ideas of the experts presented during this symposium leads to the question of whether IHE and HEE are only different manifestations of the same thing. The closing comments at the end of the text discuss this possibility. Although it is not possible to present all the information available or to answer every question, this symposium volume fulfills the purpose of its organization. The symposium presents many approaches, illustrates the complexity of the subject, the wide interest in hydrogen embrittlement, and, most of all, the need to standardize testing.

Because the book is relevant to present and future problems in two areas of hydrogen embrittlement, it will be useful to metallurgists, researchers, plating and process engineers, testing laboratories, and designers. Everyone interested in the phenomena of hydrogen embrittlement, the causes, methods of controlling, detecting, and testing, will find this book of interest. F. P. Brennan of Douglas Aircraft, the Chairman of Committee F-7 on Aerospace Industry Methods ASTM, and Craig Susskind of the Aerospace Corporation were most helpful in the work involved in creating this symposium, and their efforts are gratefully acknowledged.

Finally, a word of gratitude must be expressed to the late Dr. J. K. Stanley of The Aerospace Corporation, to whom this publication is dedicated. He initiated the action required to organize the symposium, worked to bring the interested members together, but did not live to see the proceedings published.

Louis Raymond

The Aerospace Corporation,
El Segundo, Calif. 90245;
symposium chairman.

STP543-EB/Jan. 1974

H. R. Gray [1]

Opening Remarks

Hydrogen embrittlement of metals is an old, a frequently encountered, and often misunderstood phenomenon. Metals processing, chemical, and petrochemical industries have experienced various types of hydrogen problems for many years. More recently, however, the aerospace industry has experienced new and unexpected hydrogen embrittlement problems. There are many sources of hydrogen, several types of embrittlement, and various theories for explaining the observed effects. For purposes of this symposium, hydrogen embrittlement will be classified into three types:

1. Internal reversible hydrogen embrittlement (IHE).
2. Hydrogen environment embrittlement (HEE).
3. Hydrogen reaction embrittlement (HRE).

The definitions of these three types of embrittlement are as follows. If specimens have been *precharged* with hydrogen from any source or in any manner and embrittlement is observed during mechanical testing, then embrittlement is due to either internal reversible embrittlement or to hydrogen reaction embrittlement. If hydrides or other new phases containing hydrogen form during testing in gaseous hydrogen, then, for the purpose of the symposium, embrittlement will be attributed to hydrogen reaction embrittlement. For all embrittlement determined during mechanical testing in gaseous hydrogen other than internal reversible and hydrogen reaction embrittlement, hydrogen environment embrittlement is assumed to be responsible.

1. *Internal reversible hydrogen embrittlement* (*IHE*)—Internal reversible hydrogen embrittlement has also been termed slow strain rate embrittlement and delayed failure. This is the classical type of hydrogen embrittlement that has been studied quite extensively. Widespread attention has been focused on the problem resulting from electroplating—particularly of cadmium on high-strength steel components. Other sources of hydrogen are processing treatments, such as melting and pickling. More recently,

---

[1] Research metallurgist, Alloys and Refractory Compounds Section, National Aeronautics and Space Administration-Lewis Research Center, Cleveland, Ohio 44135.

the embrittling effects of many stress-corrosion processes have been attributed to corrosion-produced hydrogen. Hydrogen that is absorbed from any source is diffusable within the metal lattice. To be fully reversible, embrittlement must occur without the hydrogen undergoing any type of chemical reaction after it has been absorbed within the lattice.

Internal reversible hydrogen embrittlement can occur after a very small average concentration of hydrogen has been absorbed from the environment. However, local concentrations of hydrogen are substantially greater than average bulk values. For steels, embrittlement is usually most severe at room temperature during either delayed failure (static fatigue) or slow strain rate tension testing. This time-dependent nature (incubation period) of embrittlement suggests that diffusion of hydrogen within the lattice controls this type of embrittlement. Cracks initiate internally, usually below the root of a notch at the region of maximum triaxiality. Embrittlement in steel is reversible (ductility can be restored) by relieving the applied stress and aging at room temperature, provided microscopic cracks have not yet initiated. Internal reversible hydrogen embrittlement has also been observed in a wide variety of other materials including nickel-base alloys and austenitic stainless steels provided they are severely charged with hydrogen.

2. *Hydrogen environment embrittlement* (*HEE*)—Hydrogen environment embrittlement was recognized as a serious problem in the mid 1960's when the National Aeronautics and Space Administration (NASA) and its contractors experienced failures of ground based hydrogen storage tanks (Refs *1* and *2* of author's paper in text). These tanks were rated for hydrogen at pressures of 35 to 70 MN/m^2 (5000 to 10 000 psi). Consequently, the failures were attributed to "high-pressure hydrogen embrittlement." Because of these failures and the anticipated use of hydrogen in advanced rocket and gas-turbine engines and auxiliary power units, NASA has initiated both in-house (Refs *3* through *5* of author's paper in text) and contractural (Refs *6* through *14* of author's paper in text) research. The thrust of the contractural effort generally has been to define the relative suscepibility of structural alloys to hydrogen environment embrittlement. A substantial amount of research has been concerned with the mechanism of the embrittlement process (Refs *4, 5, 15* through *26* of author's paper in text). There is marked disagreement as to whether hydrogen environment embrittlement is a form of internal reversible hydrogen embrittlement or is truly a distinct type of embrittlement. Some background information regarding this controversy will be presented later in this publication.

3. *Hydrogen reaction embrittlement* (*HRE*)—Although the sources of hydrogen may be any of those mentioned previously, this type of embrittlement is quite distinct from that discussed in the previous section. Once hydrogen is absorbed, it may react near the surface or diffuse substantial distances before it reacts. Hydrogen can react with itself, with the matrix,

or with a foreign element in the matrix. The chemical reactions that comprise this type of embrittlement or attack are well known and are encountered frequently. The new phases formed by these reactions are usually quite stable and embrittlement is not reversible during room temperature aging treatments.

Atomic hydrogen (H) can react with the matrix or with an alloying element to form a hydride (MH_x). Hydride phase formation can be either spontaneous or strain induced. Atomic hydrogen can react with itself to form molecular hydrogen (H_2). This problem is frequently encountered after steel processing and welding and has been termed flaking or "fisheyes." Atomic hydrogen can also react with a foreign element in the matrix to form a gas. A principal example is the reaction with carbon in low-alloy steels to form methane (CH_4) bubbles. Another example is the reaction of atomic hydrogen with oxygen in copper to form steam (H_2O) resulting in blistering and a porous metal component.

Although HRE is not a major topic of discussion in this symposium, its definition is included for the sake of completeness and in the hope of establishing a single definition for each of the various hydrogen embrittlement phenomena in order to avoid problems with semantics.

INTERNAL HYDROGEN EMBRITTLEMENT (IHE)

Testing for Relative Susceptibility

T. P. Groeneveld[1] *and A. R. Elsea*[1]

Mechanical Testing Methods

REFERENCE: Groeneveld, T. P. and Elsea, A. R., "**Mechanical Testing Methods,**" *Hydrogen Embrittlement Testing, ASTM STP 543,* American Society for Testing and Materials, 1974, pp. 11–19.

ABSTRACT: An experimental approach and experimental procedures for evaluating the hydrogen-stress cracking (HSC) of steels as a result of hydrogen absorbed during processing or service are described. The procedures involve sustained loading of specimens while they are being charged with hydrogen under conditions that provide hydrogen-entry rates or result in hydrogen contents representative of those obtained from processing or service environments. The procedures can be used to evaluate the relative susceptibilities of various steels to HSC or to evaluate the tendencies for processing or service environments to cause HSC in steels.

KEY WORDS: hydrogen embrittlement, hydrogen stress cracking tests, test methods, cracking (fracturing), steels, environments, failure, evaluation, cathodic polarization

Hydrogen-stress cracking (HSC), or hydrogen-induced, delayed, brittle failure as it is sometimes called, is a failure mechanism that is only one of the many distinctly different undesirable reactions that can occur when hydrogen is dissolved in steel; it is the only reaction of concern in this discussion.

Although the mechanism of HSC has not been completely defined, there is general agreement that three conditions must be satisfied for such failures to occur. Those conditions are as follows:

1. The steel must be heat treated to a strength level above some minimum value. This minimum generally is about 100 000 psi.
2. The steel must be subjected to an applied tensile stress above some minimum value, which is dependent on the strength level of the steel.
3. The steel must contain atomic hydrogen that is free to diffuse through the lattice. The critical hydrogen content appears to be dependent on the

---

[1] Research metallurgist and manager, respectively, Ferrous Metallurgy Section, Battelle-Columbus, Columbus, Ohio 43201.

strength level of the steel and the applied stress, but the source of the hydrogen that enters the steel does not seem to be important.

If these conditions are satisfied, failure may occur after some period of time during which cracks nucleate and grow. The cracks that grow by this mechanism usually, but not always, follow grain boundaries, and there is no detectable plastic deformation in the regions of such cracks.

This paper describes the methods that have been used at Battelle's Columbus Laboratories to study factors that influence HSC and to evaluate the susceptibilities of steels to HSC.

Experimental Approach

Numerous test methods have been employed, both at Battelle and in other laboratories, to evaluate the susceptibility of materials to HSC or to determine whether they have become "embrittled" (experienced damage caused by hydrogen) during processing or in service. These tests have included various sustained-load (or static) tests, dynamic tests (such as impact tests, low-strain-rate tension or bending tests, and torsion tests), and, more recently, tests employing fracture-mechanics-type specimens. None of the test methods seems to be entirely satisfactory; the time of the test may be long, specimen preparation costly, interpretation of the data questionable, hydrogen may be lost from the specimens during the test, or the test conditions may not adequately simulate the service or processing conditions.

In view of these problems, any test procedure that is used must represent a compromise; at Battelle we have selected a sustained-load test (using either notched or unnotched tension test specimens) in which the specimen is under stress while it is being continuously charged with hydrogen under conditions that simulate the service or processing environment.[2]

For example, if, for the problem under study, the principal source of hydrogen is from a processing environment (pickling, cleaning, or electroplating) prior to placing the part in service, then the specimens to be evaluated are exposed to a charging environment that will introduce into the specimen (and cause to be retained in it) an amount of hydrogen equal to that which would be absorbed in processing. On the other hand, if the principal source of hydrogen in the steel is a surface reaction from a service environment (for example, cathodic-protection reactions; high-

---

[2] Studies conducted at Battelle and at other laboratories have shown that the sustained-load test is the most sensitive test for detecting HSC [*1, 2*].[3] We are currently investigating a test procedure that employs a wedge-opening, fracture-mechanics-type specimen to evaluate the susceptibility of steels to HSC, but there are reservations regarding the applicability of this test because hydrogen-stress interactions can cause cracks to initiate in "defect-free" steels as well as to cause crack growth from preexisting defects.

[3] The italic numbers in brackets refer to the list of references appended to this paper.

temperature, high-pressure hydrogen, as in reactor vessels; or corrosion in sour gas or marine environments) then the charging conditions are selected to provide a hydrogen-entry rate that is similar to that obtained from the service environment. In some studies, the actual processing or service environment may be used to introduce hydrogen into the steels. Considerable work at Battelle during the past ten years has been directed toward developing a group of charging conditions that will provide a broad range of hydrogen-entry, or absorption, rates and a range of equilibrium-hydrogen contents that simulate those obtained in various processing or service environments.

To more closely simulate the conditions that cause the problem, plate-type tension specimens may be charged on only one surface to represent conditions in the wall of the pressure vessel or pipeline that receives hydrogen from one surface only. Under these conditions, hydrogen enters the material at one surface, diffuses through the section, and leaves the material at the opposite surface, thus establishing a hydrogen-concentration gradient across the section. Round bars charged on their entire periphery simulate the conditions for parts that are pickled, cleaned, or electroplated. Either notched or unnotched, round, tension specimens charged on their entire periphery provide a very sensitive test for evaluating the relative susceptibilities of various materials to HSC. In some cases, studies are conducted to evaluate only the relative susceptibilities of steels to HSC, but, in other cases, studies are conducted to obtain data needed to solve actual production or operational problems. Thus, the experimental procedures, the specimens, and the charging conditions used are chosen to suit the particular circumstances.

Experimental Procedures

Sustained-Load Tests

One test procedure used at Battelle's Columbus Laboratories to study HSC consists of continuously charging specimens with hydrogen while they are subjected to a predetermined, static, uniaxial tensile stress and measuring the time for failure to occur. The data from a series of tests performed under different stresses are plotted to provide a curve that relates the time for failure to occur and the applied stress; the curve shows the stress level below which failure will not occur and the approximate time for failure to occur at a given stress level under the selected charging conditions. Figure 1 shows a typical HSC curve.

Peripheral Charging—One of the static-loading devices that was developed for these tests is shown in Fig. 2; it is a small, screw-loaded, tensile machine with the load on the specimen measured by means of strain gages attached to the shaft of the loading screw. Belleville springs under the loading nut reduce the load relaxation as the specimen cracks.

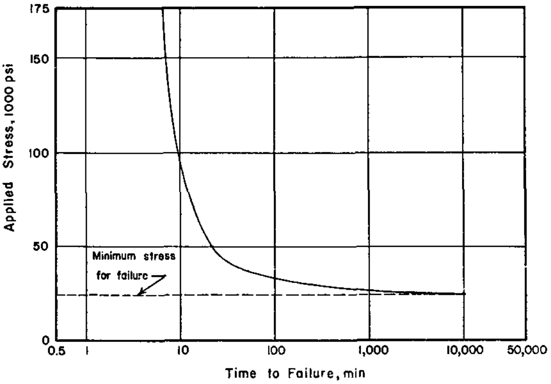

FIG. 1—*Plot of applied stress versus time to failure for SAE 4340 steel, ultimate tensile strength—230 000 psi, continuously charged cathodically with hydrogen under charging Condition A*[3].

An electrolytic cell, sealed to the specimen, is contained within the apparatus. The specimen is a button-end, unnotched tension specimen with a reduced section 0.250 in. in diameter, as is shown in Fig. 3.

The surface of the specimen is masked with pressure-sensitive electroplater's tape so as to leave a 1-in.-long (0.786-in.^{2}) exposed region in the reduced section. The electrolytic cell is then sealed around the specimen, the platinum anode is inserted in the cell surrounding the specimen, the specimen is placed in the loading apparatus, and the desired load is applied by turning the nut on the loading post. Electrical leads are then attached to the anode and the cathode (specimen), and the electrolyte is added to close the circuit. Thus, from the very start of the experiment, the specimens are protected cathodically. A timer is connected to the loading apparatus through a microswitch so that the timer stops when the specimen fails, thereby indicating the time required for failure to occur. The timer is started when the electrolyte is added. In experiments of long duration, the electrolyte is changed daily. This test procedure is repeated with specimens loaded to progressively lower stresses until a stress is reached at which the specimen does not fail within a predetermined runout time. The data obtained are plotted to obtain a curve of the type shown in Fig. 1.

Those specimens that do not fail during the experiments are baked (usually at 375° F for 24 h) to remove hydrogen absorbed during exposure. They then are pulled to failure in a conventional tension test to determine whether their properties were affected permanently as a result of the hydrogen absorbed during exposure. The fracture surfaces of the specimens are examined to determine whether a crack has initiated but not grown to a critical size during the experiment.

One-Side Charging—Another method for conducting the sustained-load tests under continuous cathodic charging involves loading of plate-type tension specimens (shown in Fig. 4) in a conventional, dead-load, creep-rupture apparatus. Such an apparatus is used when the specimens are to be charged from one surface only; in these experiments, the electrolytic cell is sealed to one surface of the specimen. The procedures used are essentially the same as those described previously, and the results are plotted to obtain a curve of the type shown in Fig. 1.

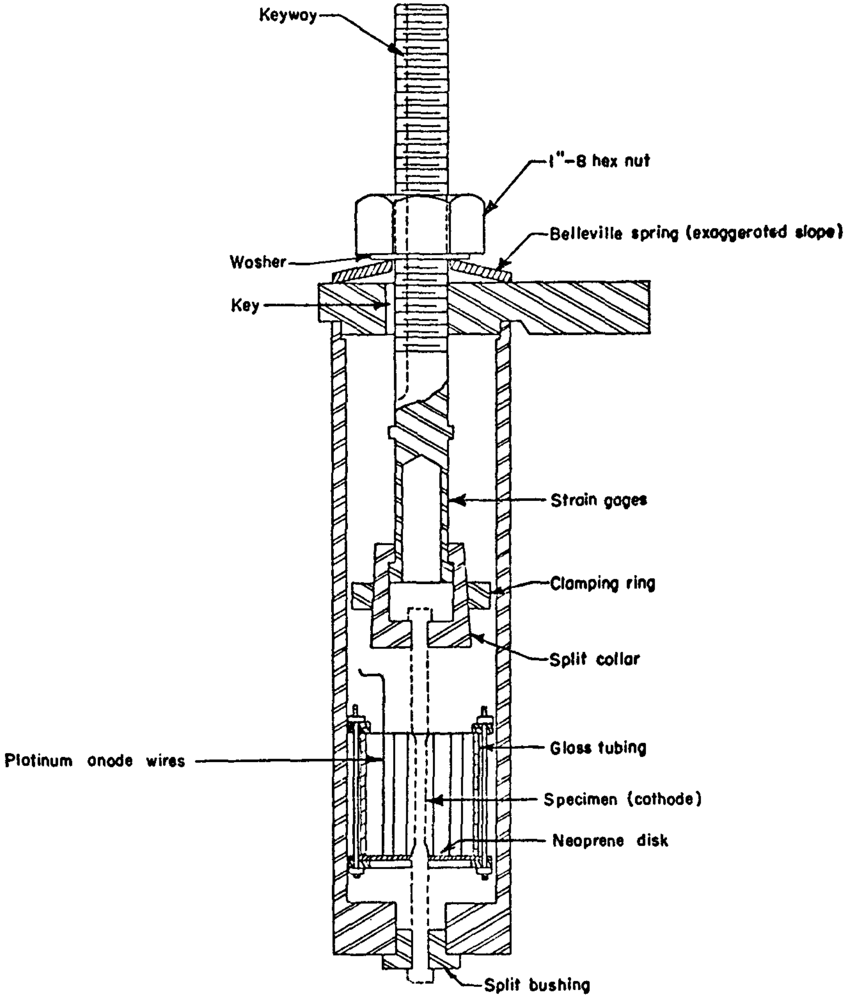

When cathodically precharged, cleaned, or electroplated specimens are evaluated, the glass cell is removed, since no electrolyte is required.

FIG. 2—*Apparatus used in the hydrogen-stress-cracking experiments.*

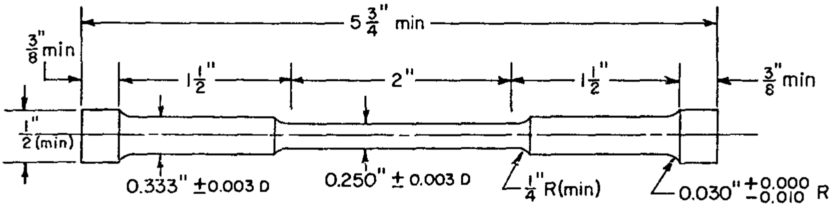

FIG. 3—*Unnotched tension specimen used in the hydrogen-stress-cracking experiments.*

Under one-side-charging conditions, the time for failure of specimens of a steel at a given stress generally is longer than for peripherally charged specimens. Also, the minimum stress for failure in a given environment is higher, as is illustrated in Fig. 5. This behavior is attributed to the difference in hydrogen content and distribution within the one-side-charged specimens, because the hydrogen can diffuse through the specimen and exit on the unexposed surface.

Precharged Specimens—The sustained-load test also is used to test notched tension specimens that have been precharged with hydrogen by cathodic charging, cleaning, pickling, or electroplating processes and to evaluate the effectiveness of bakeout treatments for preventing HSC. When cathodically precharged, cleaned, or pickled specimens are tested, hydrogen can leave the specimens during the test. If sufficient hydrogen leaves the specimen prior to crack initiation, the specimen will not fail; thus, the results obtained can be misleading. If an electroplate is applied to precharged specimens to prevent the loss of hydrogen, the hydrogen absorbed during plating can influence the results of the experiments. However, sustained-load tests of notched specimens are useful to evaluate the HSC behavior of electroplated specimens and to evaluate the effectiveness of bakeout treatments in alleviating HSC. The notched-specimen configuration is shown in Fig. 6.

When precharged, notched, tension specimens are used, the specimens are loaded to a predetermined stress level, such as 75 percent of the

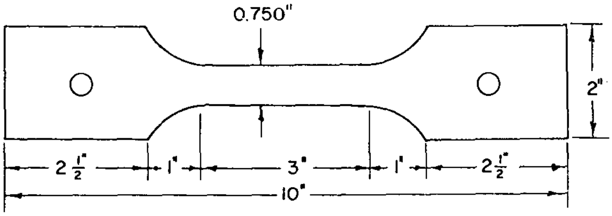

Specimen Thickness Variable

FIG. 4—*Flat-plate-type specimen used in the one-side-charging, hydrogen-stress-cracking experiments.*

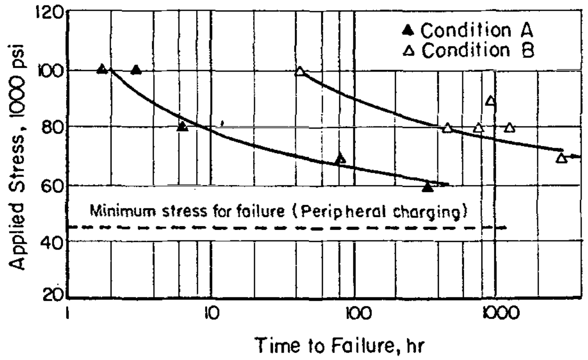

The minimum stress for failure for this steel peripherally charged under Conditions A and B is shown for comparison.

FIG. 5—*Curves showing time to failure as a function of applied stress for a steel, ultimate tensile strength—149 000 psi, continuously charged cathodically with hydrogen on one surface only, under charging Conditions A and B*[4].

notched-bar tensile strength; if failure does not occur within a predetermined runout time (such as 100 h), the test may be terminated or the stress may be increased to 90 percent of the notched-bar tensile strength. If failure does not occur within the runout time at either applied stress, the specimen is baked and pulled to failure to determine whether permanent damage has occurred. If no loss in notched-bar tensile strength is noted, the precharging process is considered to be "nonembrittling" for the steel used in the evaluation. When precharged specimens are used, it is desirable to test a large number of specimens and to evaluate the data statistically.

Hydrogen-Entry-Rate Measurements

As was discussed earlier, the charging conditions employed in these experiments are selected to duplicate an equilibrium hydrogen concen-

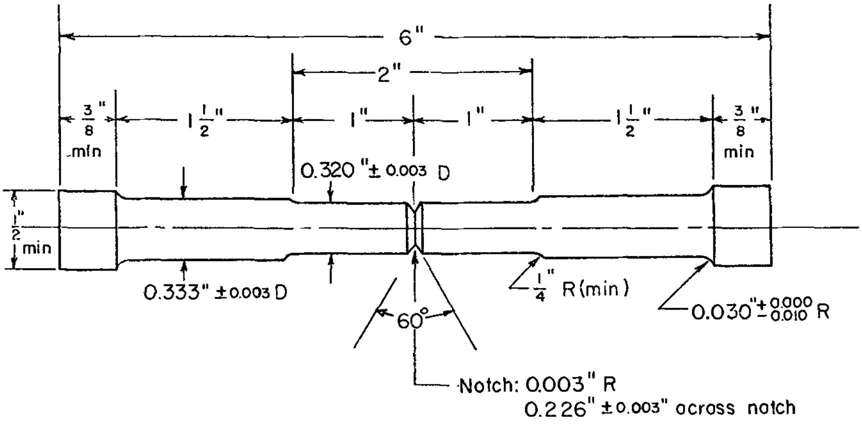

FIG. 6—*Notched tension specimen used in the hydrogen-stress-cracking experiments.*

tration or a hydrogen-entry rate representative of the environmental conditions under study. Consequently, a part of the experimental procedure involves measuring the hydrogen-entry rate from the environment under study and adequately simulating that entry rate with laboratory electrolytes that do not corrode the specimens and that are sufficiently stable to provide reproducible data. One of two methods is used to make these measurements. One method involves charging of small coupons of the steel under study for various periods of time and determination of their hydrogen contents by vacuum-fusion methods. The hydrogen content is plotted as a function of charging time to obtain the hydrogen-entry rate and equilibrium hydrogen content. Although this technique is useful for determining the hydrogen-entry rate from, and the hydrogen content at equilibrium with, an environment, research has shown that there often is not a good correlation between the average hydrogen content of the steel and the tendency for HSC to occur [*5*]. The other method involves determination of the hydrogen-entry rate by means of a permeation experiment. A thin diaphragm of the metal under study is charged with hydrogen on one surface, and the hydrogen that permeates the specimen is collected in an evacuated chamber of known volume. The amount of hydrogen permeating the specimen is determined by monitoring the pressure increase in the vacuum chamber. Under steady-state conditions, the amount of hydrogen leaving the specimen is proportional to the amount entering the specimen at the opposite surface.

A number of laboratory electrolytes have been developed for use in HSC experiments. Three of the frequently used electrolytic-cell conditions that provide a broad range of hydrogen-entry rates and equilibrium hydrogen contents are as follows:

Condition A—Severe Charging

The electrolyte is 4 percent by weight sulfuric acid in distilled water with a cathode poison,[4] the pH is about 1.0, and the current density is 8 mA/in.^{2}.

Condition B—Intermediate Charging

The electrolyte consists of 0.004 percent by weight sulfuric acid in distilled water with a cathode poison, the pH is about 3.2, and the current density is 0.625 mA/in.^{2}.

Condition C—Mild Charging

The electrolyte is five parts by volume lactic acid in 95 parts of ethylene glycol, and the current density is 0.125 mA/in.^{2}.

It is not possible to assign an actual value to the hydrogen-entry rate or hydrogen content obtained with these electrolytes, because the value

---

[4] The cathode poison consists of 2 g of phosphorus dissolved in 40 ml of carbon disulfide. Five drops of poison are added to a liter of solution. The cathode poison retards the recombination of hydrogen atoms to hydrogen molecules at the surface of the specimen (cathode) and, thus, promotes hydrogen entry into the steel.

depends upon the composition, strength level, microstructure, and surface condition of the steel or other metal under study. However, data obtained from studies of the rate at which hydrogen enters steels show that, frequently, the rate of entry from Condition A is about twice that from Condition B and about ten times the rate from Condition C [*6*].

In other studies, particularly those directed toward evaluating the HSC behavior of steels, charging conditions may be varied, depending on the environmental conditions of interest. For example, environments such as seawater, soil, groundwater, and aqueous hydrogen sulfide have been used. In other cases, the hydrogen has been introduced into specimens by a glow discharge in a rarified hydrogen environment, and the hydrogen-entry rates and hydrogen contents resulting from exposure to high-pressure, high-temperature hydrogen environments have been determined.

Concluding Remarks

The experimental approach and procedures described here can be used in several ways to evaluate the hydrogen-stress-cracking behavior of high-strength steels or other materials. They can be used to: (1) determine the behavior of a given steel heat treated to various strength levels, (2) determine the relative susceptibilities of several steels heat treated to equivalent strength levels, or (3) determine the tendencies for environments to cause HSC in steels. The procedures are used primarily as research tools rather than to control quality. However, the information acquired from such studies has been used successfully to guide selection of materials and processing procedures when HSC problems were anticipated.

References

[*1*] Elsea, A. R. and Fletcher, E. E., "Hydrogen-Induced, Delayed, Brittle Failures of High-Strength Steels," DMIC Report 196, Metals and Ceramics Information Center (formerly Defense Metals Information Center), Battelle-Columbus, Columbus, Ohio, 20 Jan. 1964.

[*2*] Carlisle, M. E., "Methods of Testing for Hydrogen Embrittlement," Northrup Report No. NOR-59-472, Aerospace Research and Testing Committee, Project W-95, Final Report, 21 Oct. 1959.

[*3*] Slaughter, E. R., Fletcher, E. E., Elsea, A. R., and Manning, G. K., "An Investigation of the Effects of Hydrogen on the Brittle Failure of High-Strength Steels," WADC Technical Report 56-83, Air Force Materials Laboratory, Wright-Patterson Air Force Base, Dayton, Ohio, June 1955.

[*4*] McEowen, L. J. and Elsea, A. R., "Behavior of High-Strength Steels Under Cathodic Protection: Part II," paper presented at the 21st Annual Conference, National Association of Corrosion Engineers, St. Louis, Mo., 15–19 March 1965.

[*5*] Groeneveld, T. P., Fletcher, E. E., and Elsea, A. R., "A Study of Hydrogen Embrittlement of Various Alloys," Final Report, NASA Contract NAS 8-20029, to National Aeronautics and Space Administration, George C. Marshall Space Flight Center, from Battelle-Columbus, Columbus, Ohio, 23 Jan. 1969.

[*6*] Groeneveld, T. P., "Fourth Symposium on Line Pipe Research," Report L30075, American Gas Association, New York, N. Y., Nov. 1969, pp. E1-E15.

D. L. Dull [1] and Louis Raymond [1]

Electrochemical Techniques

REFERENCE: Dull, D. L. and Raymond, Louis, "**Electrochemical Techniques,**" *Hydrogen Embrittlement Testing, ASTM STP 543*, American Society for Testing and Materials, 1974, pp. 20–33.

ABSTRACT: An electrochemical test method is proposed for determination of the susceptibility of materials to internal hydrogen embrittlement (IHE). The method is based on the assumption that the relative susceptibility of a material depends both on the specific aqueous environment to which the material is exposed and to the dissimilar materials to which it is coupled. Potentiostatic techniques are employed to impress potential on sustained loaded notched round-bar specimens. The result is a plot of impressed potential versus time to failure; superpositioning of the resultant curves provides a basis for rating the relative susceptibility of various materials to IHE.

KEY WORDS: hydrogen embrittlement, potentiostatic polarization, galvanostatic polarization, galvanic couplings, high strength steels, stress corrosion tests

Two electrochemical techniques have been used for the introduction of hydrogen into a tension specimen in a study of material susceptibility to internal hydrogen embrittlement (IHE). The more common technique is the galvanostatic technique in which a constant current is maintained in the circuit containing the tension test specimen and the counter electrode (Fig. 1). The test cell can also contain a reference electrode in the environment. An electrometer is then used to measure the electrode potential of the test specimen against a standard reference electrode. Either a d-c current supply (Fig. 1*a*) or a d-c voltage supply in conjunction with a load resistance (Fig. 1*b*) may be used as a constant current source. It should be realized that it is the electrode potential and not the current source that governs the electrochemical reactions occurring at the surface. In the galvanostatic technique, the constant current produces an electrode potential that changes with time as the concentration of the environment changes as the result of precipitation of reaction products and gas evolution.

By comparison, the potentiostatic technique (Fig. 1*c*) maintains the

---

[1] Member of technical staff and section manager, respectively, Metallurgy Department, Materials Sciences Laboratory, The Aerospace Corp., El Segundo, Calif. 90009.

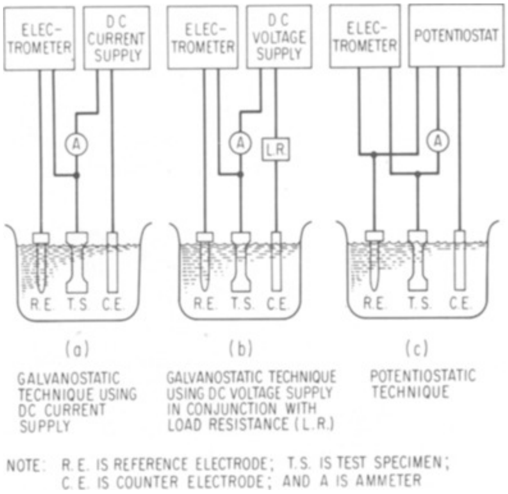

(a) GALVANOSTATIC TECHNIQUE USING DC CURRENT SUPPLY

(b) GALVANOSTATIC TECHNIQUE USING DC VOLTAGE SUPPLY IN CONJUNCTION WITH LOAD RESISTANCE (L.R.)

(c) POTENTIOSTATIC TECHNIQUE

NOTE: R.E. IS REFERENCE ELECTRODE; T.S. IS TEST SPECIMEN; C.E. IS COUNTER ELECTRODE; AND A IS AMMETER

FIG. 1—*Schematic of electrochemical techniques.*

electrode potential of the tension test specimen constant as referenced against a standard reference electrode during the test period. Again, the current path is maintained in the circuit containing the tension test specimen and the counter electrode, but it is not kept constant. Instead, the current is allowed to float and become the dependent variable. With the potentiostatic technique, it is imperative that a reference electrode be used in the electronic circuitry for continuous monitoring of the electrode potential of the test specimen.

The potentiostatic technique offers a method to control the electrode potential of the test specimen within a range that simulates the potentials produced by galvanic coupling of two dissimilar metals under actual service conditions. In contrast, the current densities produced by the galvanostatic technique can lead to electrode potentials that metals never see in service. This is an important consideration when determining the relative susceptibility to IHE under actual service conditions. For a more detailed review of the various electrochemical techniques, reference is made to the handbook edited by Ailor [*1*].[2]

Background

In 1958, Johnson et al [*2*] demonstrated the effect of hydrogen introduced into steel by galvanostatically charging unstressed SAE 4340 notched round bars in sulfuric acid solutions. The authors showed that the time to failure (TTF) and the threshold stress increased as the hydrogen concen-

---

[2] The italic numbers in brackets refer to the list of references appended to this paper.

tration in the steel decreased. It was shown also that the TTF increased as the stress decreased. Later, Brown [*3*] galvanostatically polarized smooth bar tension specimens while under stress and demonstrated that the TTF is a function of environment, while under cathodic or anodic polarization. Bhatt and Phelps [*4*] summarized the effects of electrochemical polarization on high-strength steels and identified the failures under cathodic polarization as those due to IHE.

In 1967, Smialowski and Rychcik [*5*] demonstrated the use of potentiostatic techniques to provide extremely reproducible TTF data. Every experiment was repeated at least six times with very little scatter in data. Uhlig and Cook [*6*] further demonstrated with the potentiostatic technique that the TTF is a function on environment and electrode potential. Leckie [*7*] in 1969 showed that the TTF and the threshold stress are functions of the impressed potential. The results were very sensitive also to a variation in heat treatment for 12Ni maraging precracked cantilever beam specimens.

In summary, a variety of specimen configurations have been used to demonstrate that materials are susceptible to IHE. The experimental variables are composition, state of stress, environment, electrode potential, and, most important, heat treatment. Specimens have been cathodically charged without stress in an environment and then had the load applied, while others have been cathodically charged while under stress. The former technique has been primarily applied to evaluation of the severity of hydrogen pickup during plating of those steels susceptible to IHE; the latter technique has been applied to evaluation of the susceptibility of steels to IHE. In the former, a material recognized to be susceptible, for example, SAE 4340, is used, and the emphasis is to avoid deleterious conditions during manufacturing and processing that can lead to IHE. Performance under service conditions is totally ignored, often leading to in-service failures.

The purpose of this study is to demonstrate the usefulness of the potentiostatic technique in generating a standard method to evaluate the relative susceptibility of materials to IHE which is typically related to cathodic polarization conditions. It has been generally accepted that crack growth resulting from anodic polarization conditions is to be termed stress corrosion cracking (SCC). This has implied that two different crack growth mechanisms are prevalent. It is our feeling that substantial evidence has been shown to clearly not warrant such a distinction between these mechanisms in steels.

For instance, anodic polarization does not totally eliminate cathodic reactions from occurring, it only suppresses them with increasing anodic polarization. Further, for materials which can be readily passivated, anodic polarization will enhance pitting corrosion where these pits can serve as nucleation sites for cracks. More important, the localized environment within a pit cannot be typified as the same as the bulk environment. It has been demonstrated by Brown et al [*8*] and Sandoz et al [*9*] that the pH within a crack is approximately 3.7 in steel in a 3.5 percent sodium chloride (NaCl) solution. Sandoz et al further show that the pH within the crack is essentially independent of the bulk pH of the environment. Thus, SCC is defined as any cracking process in an environment that requires the simultaneous action of the environment and stress. In this study, IHE is a particular SCC mechanism that is characteristic to steels and independent of the polarization direction, that is, cracking resulting from anodic polarization is attributed to IHE.

For the determination of the relative susceptibility, it is imperative that the metal environment system be included. The implication is that the relative susceptibility depends on a specified critical hydrogen concentration for failure, but, more important, the relative susceptibility is application sensitive. Thus, a given material can have a different rating depending on the specific environment; this environment includes not only the surrounding aqueous solution but also the metal to which it is coupled. A material might have a good rating with regard to performance in an aluminum structure but very poor in a titanium structure. For economical testing, short TTF may be obtained by the use of notched round bars at a high-stress level. The TTF results are monitored as a function of electrode potential of the tension test specimen in the environment.

Experimental Procedure

Materials and Mechanical Properties

The materials and their heat treatments used in this study are listed in Table 1. They have been categorically separated into three strength classes which are: Class I, below 220 ksi (1520 MN/m^2) ultimate tensile strength (UTS); Class II, 220 to 250 ksi (1520 to 1720 MN/m^2) UTS; and Class III, above 250 ksi (1720 MN/m^2)UTS.

The mechanical properties for each material are summarized in Table 2. A 20 000-lb (90 kN) Instron testing machine and a 60 000-lb (270 kN) Tinius Olsen testing machine were used for determination of the mechanical properties. The tension bar specimen and the notch bar specimen are shown in Fig. 2. The stress concentration factor for the notched bar specimen was 5.2.

Test Equipment and Environment

A schematic of the test setup is presented in Fig. 3. The potentiostat used was an Anotrol Model 4700 M. The impressed potential and corrosion potential were measured with a Keithley Model 610C electrometer against a saturated calomel electrode (SCE). A Luggin probe was used to reduce the voltage (IR) drop of the solution during measurement of the potential. A platinum wire served as a counter electrode during testing.

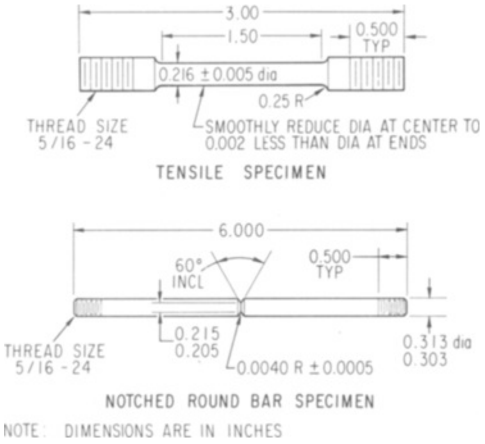

FIG. 2—*Specimen configurations used in this study.*

TABLE 1—*Heat treatment of materials used in the study.*

Material	Heat Treatment
Class I (below 220-ksi UTS):	
(*a*) 17–4 PH (H900–1 h)	solution treat 1038° C (1900° F), 1 h, oil quench + age 482° C (900° F), 1 h, air cool
(*b*) 17–4 PH (H950–4 h)	solution treat 1038° C (1900° F), 1 h, oil quench + age 510° C (950° F), 4 h, air cool
(*c*) A286	solution treat 954° C (1750° F), 1 h, oil quench + cold work 50% + age 677° C (1250° F), 8 h, furnace cool to 621° C (1150° F), 8 h, air cool
Class II (220 to 250-ksi UTS):	
(*a*) H-11	austenitize 996° C (1825° F), 1 h, air cool + triple temper (2 h + 2 h + 2 h) 579° C (1075° F)
(*b*) Inconel 718	solution treat 954° C (1750° F), 1 h, oil quench + cold work 19% + age 718° C (1325° F), 8 h, furnace cool to 635° C (1175° F), 8 h, air cool
(*c*) PH 13-8 Mo	solution treat 954° C (1750° F), 1 h, oil quench, + cold treat to −73° C (−100° F) 2 h, air warm + age 510° C (950° F), 4 h, air cool
Class III (above 250-ksi UTS):	
(*a*) H-11	austenitize 996° C (1825° F), 1 h, air cool + triple temper (2 h + 2 h + 2 h) 566° C (1050° F)
(*b*) Maraging 300	solution treat 816° C (1500° F), 1 h, oil quench + age 482° C (900° F), 3 h, air cool
(*c*) MP35N	cold work 48% + age 593° C (1100° F), 4 h, air cool

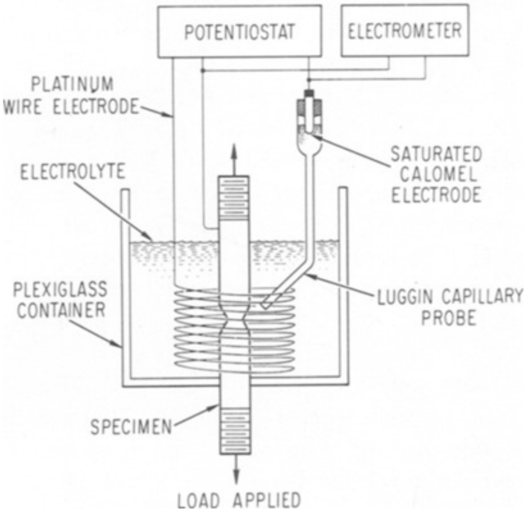

FIG. 3—*Potentiostatic stress corrosion test setup.*

TABLE 2—*Mechanical properties of materials used in the study.*

Material	Yield Strength (0.2% offset), ksi (MN/m²)	Ultimate Tensile Strength (UTS), ksi (MN/m²)	Notched Tensile Strength (NTS), ksi (MN/m²)	NTS/UTS
Class I (below 220-ksi UTS):				
(*a*) 17-4 PH (H900-1 h)	190 (1310)	205 (1410)	340 (2440)	1.66
(*b*) 17-4 PH (H950-4 h)	177 (1220)	185 (1280)	310 (2140)	1.68
(*c*) A286	204 (1410)	219 (1510)	320 (2210)	1.46
Class II (220 to 250-ksi UTS):				
(*a*) H-11	206 (1420)	248 (1710)	350 (2410)	1.41
(*b*) Inconel 718	231 (1590)	243 (1680)	350 (2410)	1.44
(*c*) PH 13-8 Mo	211 (1460)	227 (1570)	325 (2240)	1.43
Class III (above 250-ksi UTS):				
(*a*) H-11	235 (1620)	280 (1930)	370 (2550)	1.32
(*b*) Maraging 300	267 (1840)	273 (1880)	425 (2930)	1.56
(*c*) MP35N	270 (1860)	275 (1900)	340 (2440)	1.24

The environments used were a 3.5 percent NaCl solution and a 5.8 percent (1 *M*) NaCl solution acidified with concentrated sulfuric acid to a pH 1. All the chemicals were reagent grade; the water was deionized to >1 $M\Omega\cdot$cm before distillation with a Corning AG-1b distilling apparatus. The 3.5 percent NaCl solution was used initially for testing with all materials. If this environment did not cause failure under an impressed cathodic polarization condition, the more aggressive environment was used. The use of this environment was justified on the basis that, within a pit, the pH can be as low as 2 to 4, the Cl^- ion tends to break down the passive film, and the Cl^- ion concentration is higher [*8,10*].

Test Procedure

Notched round bars were painted with Mil-P-23377 epoxy-polyamide paint to within $\frac{1}{4}$ in. of each side of the notch. This was done to reduce the total current flow during polarization. Each specimen was cleaned with isopropyl alcohol and rinsed with distilled water. It was then mounted in a plexiglass container and placed in a 12 000-lb creep rupture frame, at which time the environment was added and the corrosion potential ϕ_{corr} was measured. The specimen was loaded to 0.9 notched tensile strength (NTS) and was potentiostatically polarized to a preselected impressed potential versus the SCE. These potentials were determined from two criteria, that is: (1) the measured corrosion potential ϕ_{corr} of the material in the environment and (2) the total potential range, which was from $+0.200$ to -1.250 V versus SCE. This potential range was felt to best represent the actual service potentials that a typical material would be subjected to if galvanically coupled in a 3.5 percent NaCl solution. Passivated titanium or stainless steel would represent the $+0.200$ V versus SCE for the more noble potentials, whereas the aluminum or magnesium would represent the -1.250 V versus SCE for the more active potentials.

It is important to realize that the corrosion potentials of most materials in 3.5 percent NaCl will fall within this range. Subjecting a material to potentials beyond this range is unrealistic in normal service conditions; thus, the TTF data have only academic significance.

Results

Results for each material are shown in Figs. 4 to 8. The abscissa is the TTF and the ordinate is the potential. The plotted curve is being referred to as a potentiostatic stress corrosion life curve (PSCLC). It should also be noted that a specimen without an impressed potential was loaded to 0.9 NTS. It is specifically indicated on the PSCLC with the corrosion potential symbol ϕ_{corr}.

In Fig. 4, the PSCLC for 17-4 PH materials in a 3.5 percent NaCl solution is presented. The effect of the overaging treatment (H950-4 h) of the 17-4 PH material shifts the PSCLC to the right approximately one order

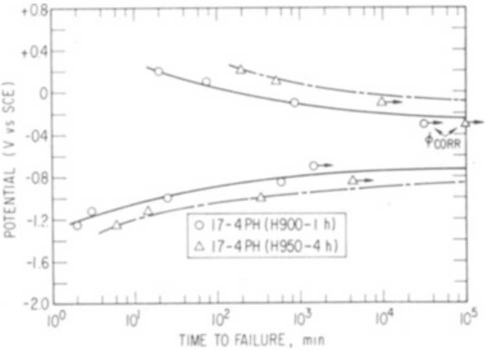

FIG. 4—*PSCLC for Class I materials, below 220 ksi (1520 MN/m^2) UTS, in 3.5 percent NaCl solution.*

of magnitude. This supports previous work [*11*] that shows that an overaging heat treatment reduces the susceptibility of 17-4 PH material to IHE. These curves emphasize the dependence of the time to failure on the impressed potential. This issue will be treated in more detail in the discussion.

In Fig. 5, the PSCLC for H-11 and PH 13-8 Mo materials in 3.5 percent NaCl solution is presented. The shape of the PH 13-8 Mo material PSCLC is similar to the 17-4 PH (Class I) material. The shape of the H-11 material for the potential range more noble than −0.800 V differs from the PH 13-8 Mo material. This behavior is attributed to the different types of corrosion behavior observed in these materials. The PH 13-8 Mo material tends to form pits, whereas the H-11 material uniformly corrodes with only slight pitting in the early stages of corrosion. In this region, the TTF is considered independent of the impressed potential.

In Fig. 6, the PSCLC for Maraging 300 and H-11 materials in a 3.5 per-

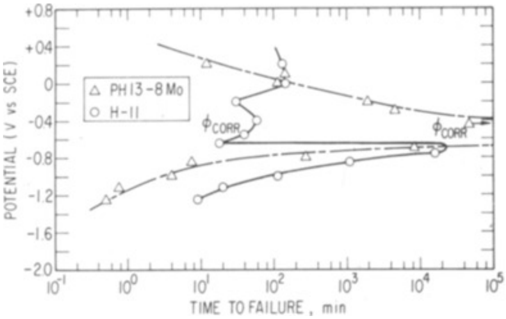

FIG. 5—*PSCLC for Class II materials, 220 to 250 ksi (1520 to 1720 MN/m^2) UTS, in 3.5 percent NaCl solution.*

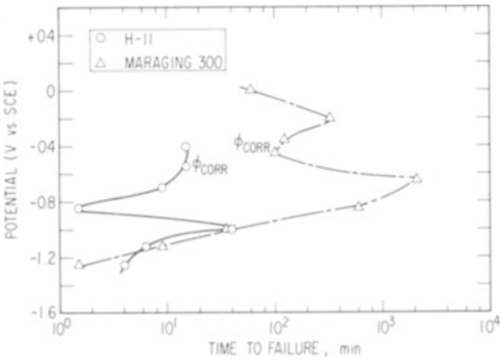

FIG. 6—*PSCLC for Class III materials, above 250 ksi (1720 MN/m²) UTS, in 3.5 percent NaCl solution.*

cent NaCl solution is presented. Under these stress conditions, it is not dependent on the impressed potential. The shape of the PSCLC for Maraging 300 material shows dependency on the TTF for potentials more active than −0.700 V. For potentials more noble than −0.700 V, the TTF is not dependent on the impressed potential, which is similar to the H-11 material already presented.

In Fig. 7, the PSCLC for H-11 material for Classes II and III are plotted together. Although the shape of the curves remains essentially the same, the shift of the PSCLC for H-11 Class II appears to be to the right, at least an order of magnitude and upwards, approximately 0.2 V. This shift is significant because it shows that tempering H-11 material to a lower strength level will improve its resistance to IHE at all selected potentials.

The PSCLC's for A286 (Class I), Inconel 718 (Class II), and MP35N (Class III) in a 5.8 percent NaCl solution acidified to a pH 1 are presented in Fig. 8. The A286 material is shown to fail only in the noble region. Fail-

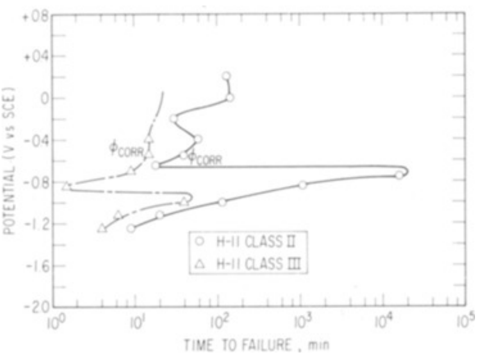

FIG. 7—*Effect of heat treatment on H-11 material.*

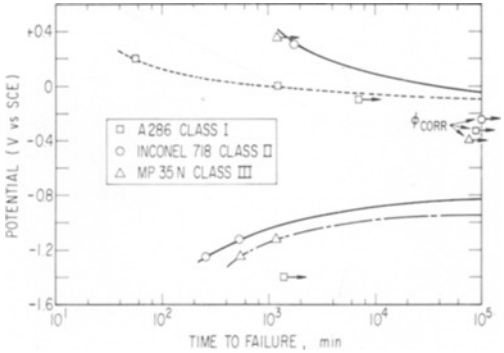

FIG. 8—*PSCLC of A286, Inconel 718, and MP35N in 1-M NaCl solution (pH = 1).*

ure is attributed to metal dissolution in the form of pitting with eventual tensile overload. Inconel 718 material is shown to be susceptible in both the noble and active regions. The MP35N material is shown to be susceptible only in the active region. Failures do not occur in the noble region due to its high pitting resistance.

Discussion

In a selection involving two or more materials for a particular application, difficulty arises because the TTF scatterbands from testing generally overlap. Laboratory results do not agree with actual service TTF. This makes it difficult to determine which material is really best. The problem is that TTF is dependent on the electrode potential of the test specimen. The galvanic couple potential ϕ_{gc}, which results when materials form a galvanic coupling and which can occur in structures, platings, and other such places, determines the TTF. This potential lies between the ϕ_{corr} of the materials to be coupled and is not easily predicted. The galvanic couple potential ϕ_{gc} depends on the coupling materials, the ratio and condition of the exposed areas, the kinetics of the reactants, and the temperature.

The test method presented in this study can be used to select the best IHE resistant material for a particular application, since all forseeable service potentials can be simulated. This is done in two steps. First, the PSCLC of specific materials in the selected environments are superimposed. Secondly, the anticipated potential range of the galvanic couple is partitioned. The material requiring the longest TTF is then selected. This is illustrated in Fig. 9 for two materials, A and B. With the PSCLC for each material, B is the obvious choice. The reason for the scatter is explained easily with a PSCLC for each material. The test results of this approach are summarized in Table 3. Although the results are not presented for A286, Inconel 718, and MP35N in a 3.5 percent NaCl solution, it is apparent that

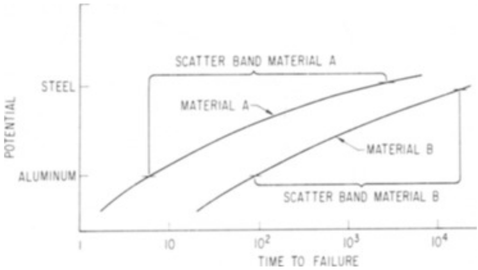

FIG. 9—*Selection of steel material to be used in an aluminum structure. Material B is the obvious choice.*

these materials, in the more aggressive environments, are still the best choice in each of the stress classes. When coupled to either an aluminum or a titanium structure, Classes I and III show no change in the order of selection of the most resistant material; however, Class II shows a change in the second and third choices. This change in position is a result of the corrosion resistance of these materials. In the noble region, PH 13-8 Mo material is more corrosion resistant than H-11. This gives it more resistance to nucleation of a pit and thus more resistance to IHE. In the active region, however, PH 13-8 Mo is quite susceptible to IHE, because the material surface now acts as an absorber of hydrogen without the need of an exterior

TABLE 3—*Summary of results of potentiostatic technique on* in situ *notched round bar specimens.*

Potentiostatically Simulated Couple to Aluminum[a]	Potentiostatically Simulated Couple to Titanium[a]
Class I:	
1. A286	1. A286
2. 17–4 PH (H950–4 h)	2. 17–4 PH (H950–4 h)
3. 17–4 PH (H900–1 h)	3. 17–4 PH (H900–1 h)
Class II:	
1. Inconel 718	1. Inconel 718
2. H-11	2. PH 13–8 Mo
3. PH 13–8 Mo	3. H-11
Class III:	
1. MP35N	1. MP35N
2. Maraging 300	2. Maraging 300
3. H-11	3. H-11

[a] Materials are rated 1, 2, and 3 in order of resistance: most resistant, next-most resistant, and least resistant, respectively.

nucleation site for the occurrence of the necessary reactions when notched bar specimens are used.

Another significant use for the PSCLC is that the effect of galvanic coupling can be determined; 17-4 PH (H900-1 h) Class I material and H-11 Class III material are two extreme cases. The failure of 17-4 PH material is shown to be dependent on the potential in both the noble and active regions. It should be noted that in a standard static test this material would be resistant to IHE in a 3.5 percent NaCl solution. However, a PSCLC would indicate failure if the 17-4 PH material were coupled galvanically to a different material. The PSCLC for this material in either of these regions indicates that the 17-4 PH material is quite susceptible to IHE. The effect of physically coupling 17-4 PH material to aluminum by placing an aluminum block next to a 17-4 PH notched round bar in a salt water environment has been demonstrated [*11*]. Failure by the IHE occurred only when the block was attached.

In the latter case, the failure of H-11 material is shown to be independent of the impressed potential in either the noble or the active region. This behavior is attributed to its extreme susceptibility to IHE in the NaCl solution. The combination of these effects has made the impressed potential only a secondary effect. The impressed potential plays an important part when the material is tempered to a lower strength level, as evidenced by H-11 Class II material (Fig. 7). In the active region, the TTF is dependent on the impressed potential.

For further emphasis of the usefulness of the potentiostatic technique, polarization curves were determined for PH 13-8 Mo, Inconel 718, and H-11 materials in an aerated 3.5 percent NaCl solution by use of standard electrochemical techniques. These results are shown in Fig. 10. If one was to select an anodic current density of 10^{-4} A/cm^2, the measured potential for the three materials would read 0.00 V for PH 13-8 Mo, −0.58 V for

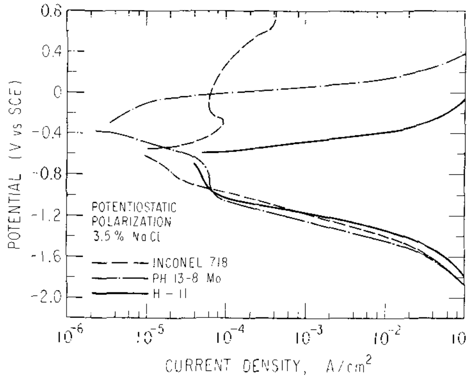

FIG. 10—*Polarization curves of Inconel 718, PH 13-8 Mo, and H-11 materials in aerated 3.5 percent NaCl solution.*

H-11, and +0.28 V for Inconel 718. The significance of these potentials is that Inconel 718 is being subjected to an impressed potential that would not occur in actual service conditions. Secondly, by comparing the TTF for the H-11 and PH 13-8 Mo materials from the PSCLC (Fig. 5), it can be shown that they are approximately equal (100 min). If they were compared at the same potential of −0.58 V, the PH 13-8 Mo material would be the better material.

In the case of applying cathodic currents for these materials, little difference is noted in the polarization curves in the 3.5 percent NaCl solution. However, in other solutions such as acids, bases, and organic solvents, the materials would be expected to exhibit definite characteristic differences. Such cases, as previously discussed for the noble potential region, would also be expected to occur.

Summary

It is well documented that TTF data of material susceptible to IHE can be influenced by impressing currents or potentials. The current electrochemical techniques employed are the galvanostatic and potentiostatic techniques. In this study, the use of the galvanostatic technique for determination of the relative susceptibility of materials to IHE is criticized because it offers no way of controlling the electrochemical reactions on the material surface with easy reproducibility; electrochemical reactions are potential dependent. It further allows materials to obtain potentials easily that are not found readily in actual service conditions. This leads to allowing reactions to occur that could result in erroneous conclusions when the susceptibility of two or more materials to IHE in a specific environment is rated.

In this study, stressed notched round bars were polarized potentiostatically and failed by an IHE mechanism in the case of steels and by a SCC mechanism in the case of Inconel 718 and MP35N. This led to the development of PSCLC for various materials. The significances of these curves are as follows: (1) experimental scatter obtained from either the standard specification methods or galvanostatic techniques can be explained; (2) the curves allow superpositioning of PSCLC from various materials, so that they may be rated for resistance to SCC, that is, IHE in steels; and (3) the curves show the effects of galvanic coupling. The advantages of using the potentiostatic technique on *in situ* specimens are as follows: (1) it allows electrode potentials of actual service conditions to be easily simulated; (2) it overrides the problem of the same current density not corresponding to the same potential; and (3) understanding the specific SCC mechanism to rate the various materials is not necessary. Though it was not performed in this study, it is not unreasonable to propose that a test data catalog could be generated for each material with the effects of different environments, temperature, stress, surface coating, and manufacture processing included. Of the electrochemical methods available, the potentiostatic technique is the most suited method for determination of the relative susceptibility of materials to IHE.

References

[1] *Handbook on Corrosion Testing and Evaluation*, Ailor, W. H., Ed., Wiley, New York, 1970, pp. 171–216.

[2] Johnson, H. H., Morlet, J. G., and Troiano, A. R., *Transactions*, American Institute of Mining, Metallurgical, and Petroleum Engineers, Vol. 212, 1958, pp. 528–36).

[3] Brown, B. F., NRL Report 6041, Naval Research Laboratory, Washington, D. C., Nov. 1963.

[4] Bhatt, H. J. and Phelps, E. H., "The Electrochemical Polarization on the Stress Corrosion Behavior of Steels with High Strength Yield Strength, "*Proceedings*, Third International Congress on Metallic Corrosion, Moscow, USSR, 1966, Buttersworth Scientific Publications, London.

[5] Smialowski, M. and Rychcik, M., *Corrosion*, July 1967.

[6] Uhlig, H. H. and Cook, E. W., Jr., *Journal of the Electrochemical Society*, Vol. 113, Feb. 1969, p. 173.

[7] *Proceedings*, Conference on Fundamental Aspects of Stress Corrosion Cracking, National Association of Corrosion Engineers, Houston, Tex., 1969, pp. 411–419.

[8] Brown, B. F., Fujii, C. T., and Dahlberg, E. P., *Journal of the Electrochemical Society*, Vol. 116, No. 2, Feb. 1969, pp. 218–219.

[9] Sandoz, G., Fujii, C. T., and Brown, B. F., *Corrosion Science*, Vol. 10, pp. 839–845.

[10] Fontana, M. G. and Greene, N. D., *Corrosion Engineering*, McGraw-Hill, New York, 1967, p. 51.

[11] Raymond, L. and Kendall, E. G., "Hydrogen Stress Cracking of 17–4 PH Stainless," Aerospace Report No. TR-0158(3250-10)-6, The Aerospace Corporation, El Segundo, Calif., Aug. 1967.

J.-P. Fidelle,[1] *R. Broudeur,*[1] *C. Pirrovani,*[1] *and C. Roux*[1]

Disk Pressure Technique

REFERENCE: Fidelle, J.-P., Broudeur, R., Pirrovani, C., and Roux, C., **"Disk Pressure Technique,"** *Hydrogen Embrittlement Testing, ASTM STP 543,* American Society for Testing and Materials, 1974, pp. 34–47.

ABSTRACT: This paper presents a method of evaluating the embrittling effect of hydrogen on metals by measuring the pressure required to burst a small metal disk. The metal disks are clamped, and the system is pressurized until failure occurs. Embrittlement is expressed by the inverse ratio of the rupture pressures of a hydrogen charged disk and the rupture pressure of an uncharged disk of the same material and processing procedures.

The disk pressure test (DPT) provides evidence of other causes of embrittlement and any synergistic effects with internal hydrogen embrittlement (IHE). Other advantages of the DPT are sensitivity, versatility, rapidity, simplicity, and low cost of specimens and equipment.

KEY WORDS: hydrogen embrittlement, pressure, biaxial stresses, plating, cathodic charging, thermal charging, high strength steels, austenitic steels, nickel, uranium, titanium, materials selection, quality control, field tests

The disk pressure test (DPT) was developed originally for hydrogen gas embrittlement (HGE) [*1, 2*][2] and permeation [*3, 4*] studies and has now been modified for internal hydrogen embrittlement (IHE) studies. The DPT consists of pressurizing small clamped disks until rupture. The environment can be helium, water, acid, or other fluids or mixtures, thereby providing versatility. A measure of the relative susceptibility to IHE is the ratio of the rupture pressures of the unembrittled disks to those of the embrittled material.

The test is essentially a bulge test and, therefore, is more sensitive to the embrittling effects of hydrogen than a smooth bar tension test because of the additional triaxial constraints in the clamped disks in attaining a bulged configuration.

Experimental Procedure

A schematic of the test line is shown in Fig. 1. The pressure source is a high-pressure tank filled under 2000 bars[3] by means of a two-stage mem-

---

[1] CEA, Centre d'Etudes de Bruyères-le-Châtel, France.

[2] The italic numbers in brackets refer to the list of references appended to this paper.

[3] 1 bar = 0.987 atm = 14.51 psi.

brane compressor. The tank is made of an age-hardened XN26 austenitic stainless steel, similar to A286. The line is evacuated and flushed by helium prior to each test.

Pressure is increased regularly at the desired rate by means of a sliding needle, fine-adjustment valve. Except when the influence of strain rate is being measured, experiments are carried out usually at a pressure increase rate of 65 bars/min. The rupture pressure is read on a maximum reading pressure gage, but this equipment gradually is being replaced by a pressure transducer, which allows recordings of the pressure variation versus time.

The test cell used is shown in Figs. 2 and 3. Although different disk sizes can be used, most specimens are 58 mm (2.28 in.) diameter. Thick-

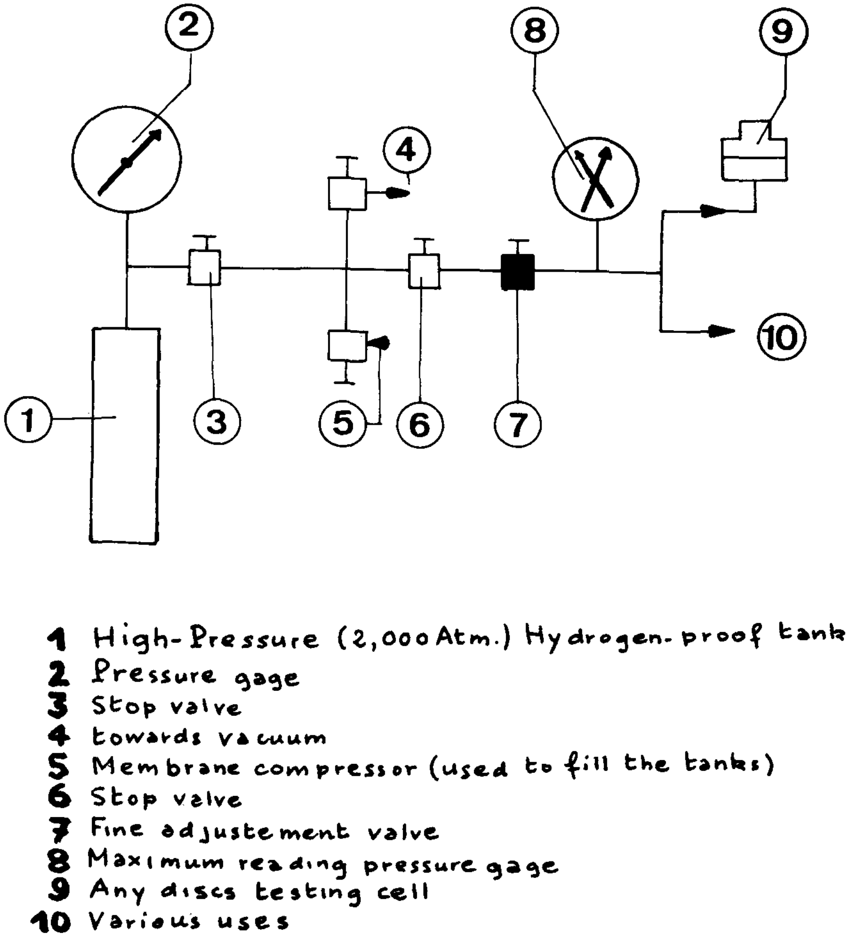

FIG. 1—*Test line.*

nesses range from 0.20 to 1.50 mm; a thickness of 0.75 mm (30 mils) has been used in the experiments described here.

The clamped area, which prevents the disks from slipping during bulging, is about three times the area under pressure. Disk slipping would decrease the sensitivity and reproducibility of the test; examinations of cross sections of bulged specimens can be used to establish the absence of slippage.

The maximum pressure used during the test is 1600 bars (23 200 psi). The upstream part of the disk cell is kept tight by means of perbunan (rubber) seals, but unwelded copper seals must be used for experiments at low and high temperatures [*5*].

The test is performed usually three times for each material under each set of conditions, and reproducibility is ±2 to 3 percent. This can reach

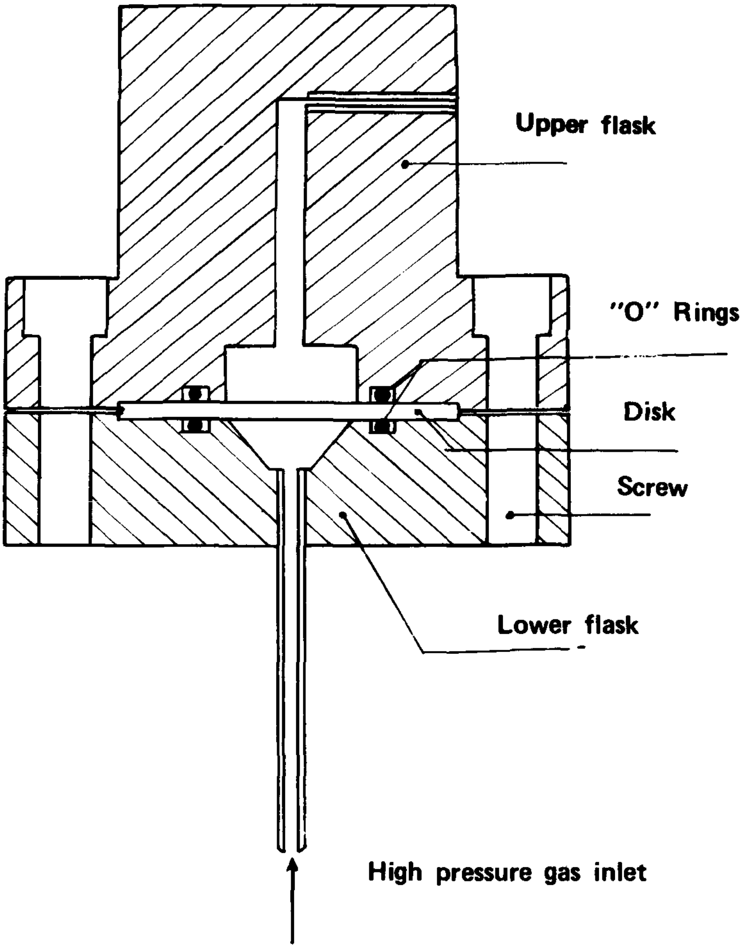

FIG. 2—*Cell for rupture tests under increasing gas pressure; regular model.*

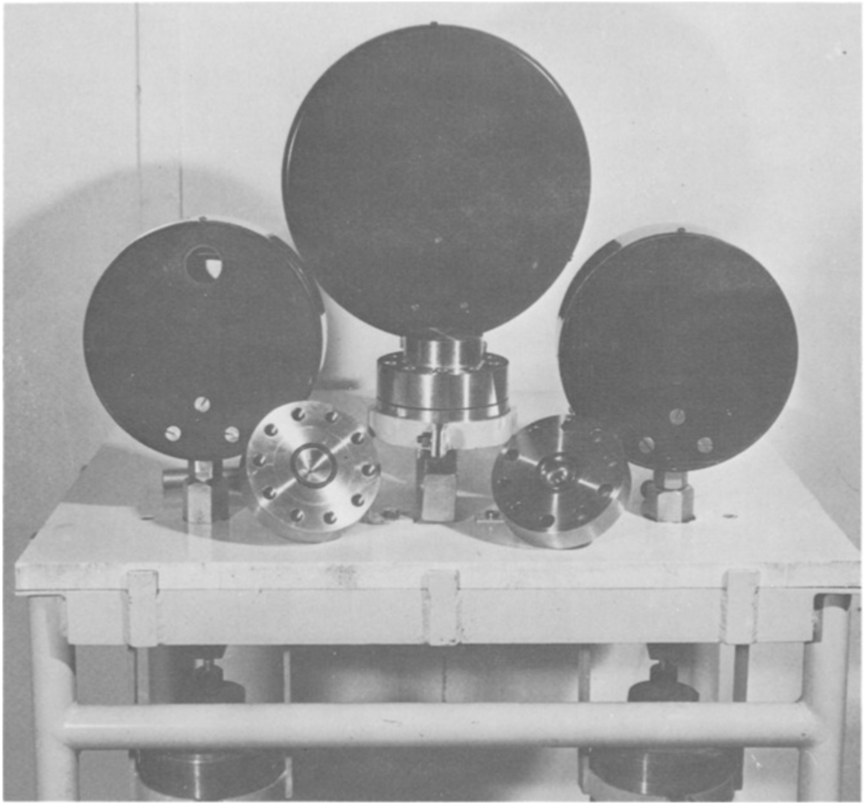

FIG. 3—*Setup and broken down cells in front of pressure gages.*

±1 percent or less for very precisely processed, high-quality materials. Generally, it becomes ±5 to 10 percent for ultrahigh-strength materials and can reach ±20 to 25 percent for inaccurately processed, low quality materials. This extreme is not due to the testing procedure but rather to the material itself and is also evident in less sensitive tests. In such instances, tests are performed at least five times for each condition.

Results

Cathodic Charging

Disks were made from two martensitic steels, Maraging 350 and 35NCD16;[4] the charged specimens were charged cathodically on both sides for 24 h in 10 percent hydrochloric acid (HCl) at a current density of 5 mA/cm^2 [*6*].

---

[4] 35NCD16 is a French alloy, 0.4C, 4Ni, 2Cr, 0.5Mo, and 0.3Si.

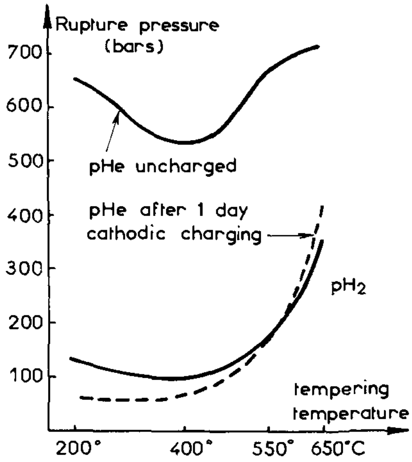

FIG. 4—*Influence of various conditions on the rupture pressures of 35NCD16 steel.*

The results obtained on charged and uncharged disks of 35NCD16 are shown in Fig. 4. The pressure to rupture uncharged specimen $p\mathrm{He}_u$, shows a decrease for specimens tempered at 400° C as compared to both lower and higher tempering temperatures. This indicates that DPT is sensitive to tempered martensite embrittlement (TME). Table I gives the mechanical properties of 35NCD16 for various tempering temperatures and shows the normal effect of decreasing strength with increasing tempering temperature. Ductility, as measured by percent elongation, increases only at high tempering temperatures, indicating some influence of TME, whereas the drop in helium rupture pressures indicates its sensibility more.

The helium pressure to rupture for cathodically charged disks is drastically lower than for the uncharged disks and agrees very closely with the pressure to rupture uncharged disks when hydrogen is used as the gas. The ratio of rupture pressures uncharged to charged ($p\mathrm{He}_u/p\mathrm{He}_c$), with helium is 10.5 for the 200° C tempered, high-strength condition.

TABLE I—*Mechanical properties of 35NCD16.*

Tempering Temperature[a]	200° C	230° C[b]	400° C	550° C	650° C
Yield strength, kg/mm^2	148	160	123	115	78
Tensile strength, kg/mm^2	198	193	163	133	121.5
Elongation, %	7	7.3	6.6	10.5	13.6

[a] Hardened at 875° C, helium cooled-chilled to −79° C for 2 h. Double tempered 2 h each.

[b] Those results were on a different heat of material.

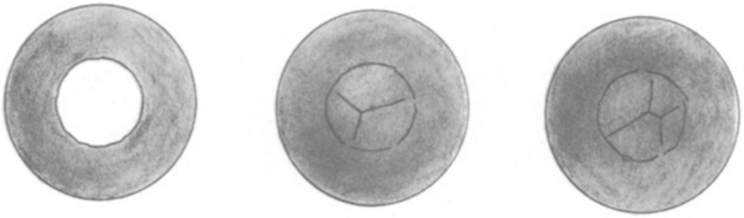

a. ASPECT B2
rupture under He gas

b. ASPECT Y
c. ASPECT X
cathodic charging + rupture under He gas

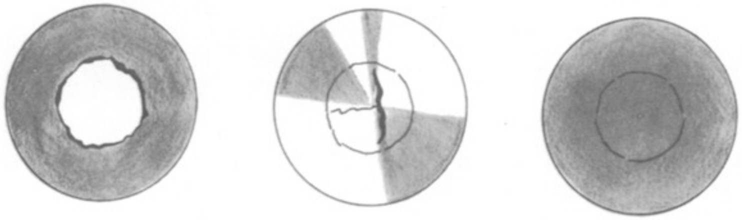

d. ASPECT B4
rupture under
pressurized HCl

e. ASPECT T3+E
rupture under He gas
after thermal charging H_2

f. ASPECT E
rupture under
H_2 . D_2 . T_2 gases

FIG. 5—*Aspects of Maraging 350 steel disks tested under various conditions.*

The pHe_c remains constant for disks tempered at 400° C and below, indicating that temper embrittlement is still effective [*2*, *7*].

The IHE not only causes a change in the rupture pressure but also changes the characteristics of the ruptured disks. Figure 5 shows the influence of various fluids and charged conditions on the rupture characteristics of Maraging 350 disks. Table 2 lists the rupture pressures of these various conditions.

TABLE 2—*Rupture pressures of 30 mil Maraging 350 disks under various conditions.*

Environment	Rupture Pressure Bars	Ratio, *Pu*/*Pc*
He	382	1.00
H_2O	288	1.32
HCl 10%	223	1.71
HCl 50%	173	2.21
He after cathodic charge 24 h 10% HCl 5 mA cm^{-2}	40	9.55
He after thermal charge 24 h in 20 bars GH_2 at 100° C	66	5.79
H_2	65	5.88
D_2	73	5.23

When tested under helium in the uncharged condition, Maraging 350 steel has a considerably lower burst strength than 35NCD16 despite the fact that the former is considerably stronger. The pHe is not related to tensile strength but, no doubt, is related to ductility. In both the charged and uncharged condition 35NCD16 disks rupture at a maximum in the lowest strength, maximum ductility condition.

The results listed in Table 2 also show that water is unsuitable as a fluid for high-pressure testing because it apparently embrittled the Maraging 350 steel.

Another case of IHE is illustrated by nickel plated U–1.5Mo alloy. Specimens in the polished condition, welded and polished, plated and welded, and plated condition were tested, and the results are shown in Table 3 [*8*].

Thermal Charging

Thermal charging has the following advantages over cathodic charging.

1. Hydrogen fugacity in the charging fluid is known.
2. It is better suited to materials where hydrogen diffusivity (D_H) is low at room temperature.
3. It better simulates industrial equipment operating under stress which may become embrittled near room temperature by hydrogen absorbed at higher temperatures.

Conversely the equipment for thermal charging is somewhat more complex than that used for cathodic charging. By modifying the regular cell with heating plates, as shown in Fig. 6, charging can be carried out in two ways.

1. By applying gaseous hydrogen (GH_2) on one side of the membrane, which makes it possible to simultaneously monitor hydrogen entry using the Daynes-Barrer's method. In this method hydrogen is not distributed homogeneously but rather obeys a concentration gradient. This represents, reasonably well, the case of many pressure vessels in the chemical, oil, and space industry.
2. By applying GH_2 on both sides simultaneously and using the information from Method 1, it is possible to know how long to charge to obtain a homogeneous concentration which can be related to the result of the rupture tests under helium.

When charging is completed, quenching to low temperatures takes place

TABLE 3—*Helium rupture pressures of U-1.5Mo disks in bars.*

(a) Base metal polished	745	(b) Welded polished	427	Ratio a/b 1.72
(c) Ni plated	553	(d) Welded Ni plated	277	Ratio c/d 2
Ratio	$\frac{a}{c} = 1.35$		$\frac{b}{d} = 1.54$	$\frac{a}{d} = 2.69$

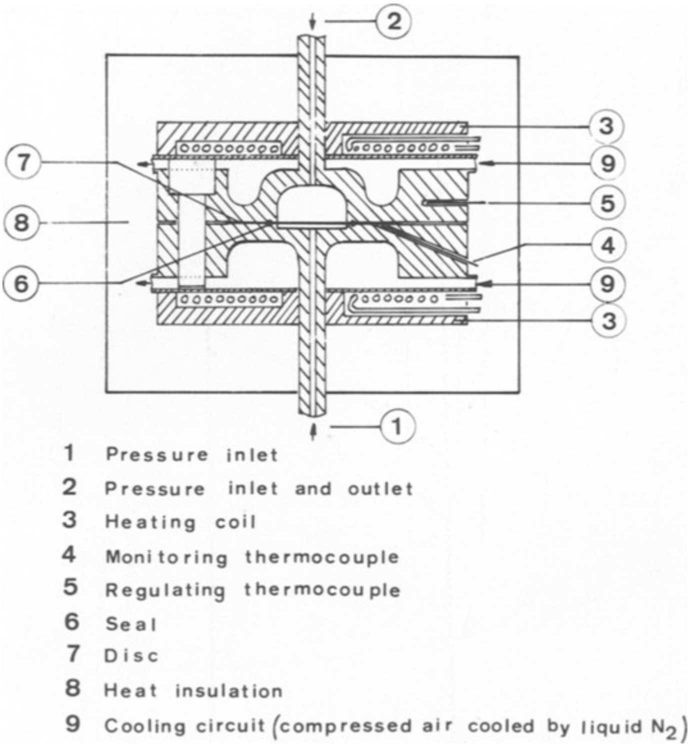

FIG. 6—*Disk cell for thermal charging under pressure.*

in situ with cold water and then a mixture of compressed air and liquid nitrogen. The rupture test is carried out as soon as the disk temperature has been raised again to the desired temperature. It can be done either in the charging cell or in another cell if helium contaminated by GH_2 has to be avoided.

Because of the low hydrogen diffusivity in alpha-titanium [*9*], cathodic charging proved unsuitable for hydrogen charging. Therefore, specimens were thermally charged for 30 min at 750° C, under various low GH_2 pressure to obtain different absorptions. These specimens were then treated for 5 h at 400° C to ensure a homogeneous distribution [*10*]. Prior to the thermal charging the Ti-40A specimens were heated for 60 h at 1000° C[5] and quenched, and had the following properties:

Yield point	31 kg/mm²
Tensile	39 kg/mm²
Elongation	30%
O_2	700 ppm

[5] This additional thermal cycle was used in order to duplicate a previous test involving this thermal cycle used to evaluate the role of O_2.

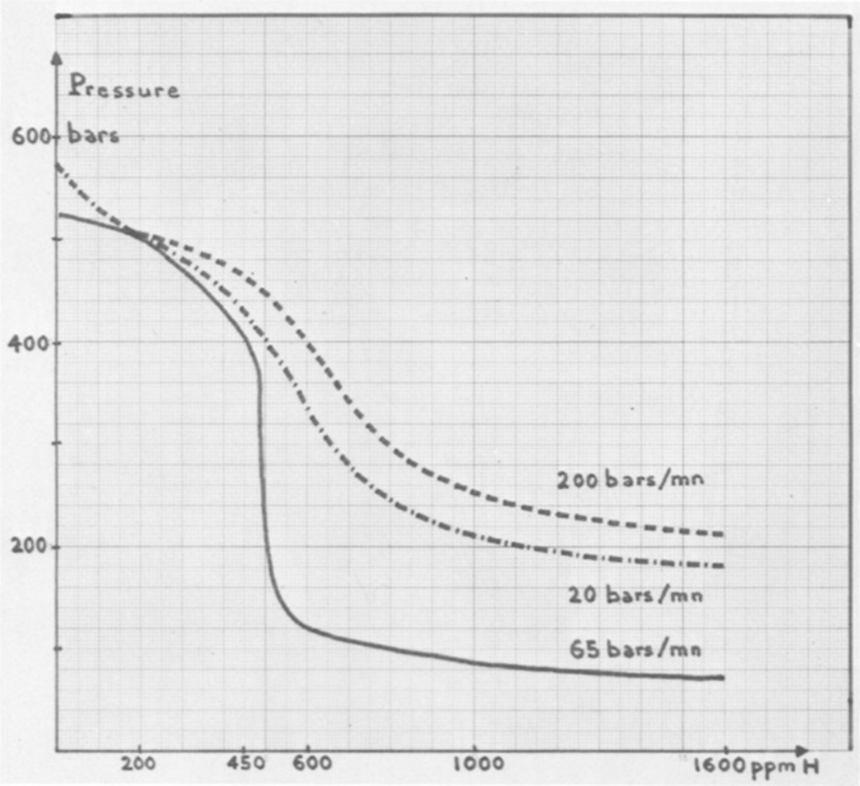

FIG. 7—*Embrittlement of hydrogen charged (hydrided) Ti-40.*

Figure 7 shows that the rupture pressure under helium decreases progressively with increasing hydrogen content and undergoes a transition between 400 and 900 ppm, depending on the rate of pressure increase during the test. The hybrided titanium is apparently strain rate sensitive, and the 65 bars/min rate increase curve shows a marked transition between 400 and 600 ppm. This 65 bars/min also decreases the burst pressure at all hydrogen content levels.

Table 4 shows that for 1000-ppm hydrogen level the 65 bars/min rate reduces the burst pressure precipitously.

Embrittlement due to hydrogen content is practically the same at 10 and 200 bars/min, which suggests that embrittlement of internally hydrided alpha-titanium is not only due to hydride embrittlement at high strain rates but also to slow strain rate embrittlement due to hydrogen in the solution (*1st effect*). The pHe decreases as thermally precipitated hydride concentration increases, which merely reflects the influence of the 1st effect on an increasingly precipitation-hardened material (*2nd effect*).

At higher rates—up to 200 bars/min—pHe increases as dissolved hydrogen embrittlement disappears. In contrast to steels, pHe greatly decreases at lower rates, presumably due to low strain-rate induced hydride precipitation, which does not significantly increase the gross hydride concentration but depletes the matrix from its hydrogen in the solution (*3rd effect*).

At 400 bars/min and above, pHe decreases steeply due to well-known "hydride embrittlement" occurring at high strain rates (*4th effect*).

Further experiments are worthwhile, since the foregoing preliminary data clearly indicate the span of the DPT to be large enough to encompass the complex situations most likely found in hydride forming materials.

Thermal charging was carried out at 100° C on Maraging 350 and at 400° C for XN26 (A286) age hardened austenitic stainless steel. From previous work on Maraging 250 the diffusivity D_H of this material at 100° C was determined to be 1.7×10^{-7} cm^2/s, and the hydrogen solubility at 100° C and 20 bars was determined to be 9 ppm assuming the same values for Maraging 350. From Crank [*11*], the time for nearly saturation, T_S, of a membrane with a thickness t is:

$$T_S = \frac{3}{8} \times \frac{t^2}{D_H} = 206 \text{ min}$$

For XN26 steel, previous work has determined the D_H at 400° C to be 10^{-6} cm^2/s. This rate allows permeation steady state T_{SS} to be established in:

$$T_{SS} = \frac{2}{3} \times \frac{t^2}{D_H} = 62 \text{ min}$$

for specimens charged on one side [*12*] and for specimens charged from both sides:

$$T_S = \frac{3}{8} \times \frac{t^2}{D_H} = 35 \text{ min}$$

In contrast with Maraging 350, XN26 has a very low sensitivity to hydrogen embrittlement (HE); therefore, charging experiments were carried out at higher temperatures and pressures.

Disks were charged on one side at 300 bars, and a thick plate on the downstream side prevented the disks from being stressed while being

TABLE 4—*Influence of the pressure increase rate* dp/dt *on embrittlement of hydrided Ti-40 (1000-ppm hydrogen).*

dp/dt, (bars/min)	10	20	65	200
*p*He (bars)	240	208	85	250

charged. Hydrogen uptake was found to be 19.3 to 22.3 ppm, with a maximum concentration of 38.7 to 44.6 ppm at the specimen skin exposed to GH_2. This noticeably decreased the rupture pressure under helium and gave a ratio of the ruptures = 810/400 = 2.02 [*13*].

During a second experiment, disks were saturated from both sides at the same temperature, 400° C, but under only 100 bars. According to Sievert's law, which is obeyed under these conditions, hydrogen pickup ranged from 22.3 to 25.3 ppm. However, the rupture pressures of charged specimens were only 1.16 times lower than of uncharged specimens.

The result obtained indicates that XN26 disks with 22.3 to 25.3-ppm hydrogen are noticeably less embrittled ($p\mathrm{He}_u/p\mathrm{He}_c = 1.16$) than others with a slightly smaller pickup (19.3 to 22.3 ppm) for which $p\mathrm{He}_u/p\mathrm{He}_c = 2.02$. This paradoxical result is due to a different hydrogen distribution within the material and points up the importance of knowing not only hydrogen concentration but also hydrogen distribution.

Table 5 summarizes the results of various tests on 282 ksi 35NCD16 and Maraging 350 steel.

If we compare these steels on the basis of similar absorptions (9 ppm for Maraging 350 steel and 10.5 for 35NCD16), the later appears more sensitive, and this is also true if we compare them on the basis of similar $p\mathrm{He}_u/p\mathrm{He}_c$ ratios. However, room temperature D_H's were measured and found to be 5.10^{-8} cm^2/s for 35NCD16 [*14*] $\simeq 3.10^{-9}$ cm^2/s for maraging.

After Crank [*11*], the time for nearly saturation of a 0.75-mm-thick disk is, at room temperature,

$$T_S = \frac{3}{8} \times \frac{t^2}{D_H} = 11\ \text{h, } 43\ \text{min}$$

for 35NCD16 and eight days for maraging, which indicates that only the first material was saturated.

This was confirmed by charging maraging for longer times. For example, after four days, hydrogen uptake became 43 ppm and $p\mathrm{He}_u/p\mathrm{He}_c$ was 70. Therefore, although maraging steel is more resistant than 35NCD16 to the effects of given amounts of hydrogen, since hydrogen solubility in the

TABLE 5—*Influence of charging times and conditions of IHE of high-strength steels.*

Conditions	Thermal Charging for 24 h		Cathodic Charging			
			for 24 h		for 4 days	
Results	uptake, ppm	$p\mathrm{He}_u/p\mathrm{He}_c$	uptake, ppm	$p\mathrm{He}_u/p\mathrm{He}_c$	uptake, ppm	$p\mathrm{He}_u/p\mathrm{He}_c$
35NCD16			10.5	10.48		
Maraging 350	9	5.88	15	9.55	43	70

first material is also much higher, the first characteristic is of little interest for field service, where times are long enough to get the materials saturated, even those where hydrogen diffusivity is small. Similar conclusions could be derived from HGE tests on H-11 and Maraging 250 steel conducted at various *dp/dt* rates. At faster rates, H-11 appeared more embrittled than maraging, but as *dp/dt* decreased, embrittlement quickly leveled for the first steel, but continued to increase for maraging and eventually surpassed that of H-11.

Discussion

In general, the results presented have pointed up the inadequacy of knowing only the overall hydrogen pickup of a material exposed under given conditions and, how ignoring the attainment of steady state and hydrogen distribution could lead to incorrect conclusions that could be highly detrimental if extrapolated to industrial conditions.

Of course, even without knowledge of hydrogen entry rate, solubility, and distribution, it is possible to compare: (*a*) various materials under given processing or service conditions, and (*b*) the effects of various processing or service conditions on a same material—provided that the experiments are carried out on actual specimens under actual conditions; one of the important conditions being time. Also, the tests have to be repeated a sufficient number of times to permit a statistical treatment. But, to follow this as a general policy would deny the interest of cost savings by means of less expensive laboratory experiments. IHE laboratory experiments are carried out for two practical purposes:

1. *Knowledge of the effects of hydrogen entered during processing* (thermal treatments, pickling, plating, etc.), either for materials selection, process selection, or quality control of both. Here it is not necessary to reach the steady state during laboratory charging experiments as this might represent a much more severe condition than reality. However, if the laboratory experiments cannot exactly duplicate reality, it is important to know hydrogen entry rate and distribution in order to simulate it adequately.

For instance, plating thin specimens during a limited time can induce more embrittlement than plating thicker ones, because a relatively larger section will be affected. Then, it might be inferred that baking thicker specimens for the time necessary to recover full ductility on thinner specimens will be enough to recover full ductility since the thicker specimens start with a lower embrittlement. However, this can be wrong since during baking, hydrogen diffuses two ways, through one side, or deeper inwards, then only after a sufficient time outwards, through the other side. Therefore, although starting from a relatively lower embrittlement level, thicker specimens may have to be baked for longer times than thinner laboratory specimens.

However, thin specimens should not be discounted because thinness accelerates the relative rate of impregnation and decreases test times, but it may mask the role of hydrogen motion kinetics, the knowledge of which is necessary to prevent HE of actual size specimens.

2. *Prediction of susceptibility of materials absorbing hydrogen during their service life.* This is tied to environmental hydrogen embrittlement but, while in the latter instance, HE occurs during the exposure conditions which allow hydrogen entry in the instance considered here, HE occurs under other conditions than those which favor hydrogen entry: For example, cracking of a shutdown ammonia synthesis reactor that had been cooled from elevated temperatures (where hydrogen enters) to lower temperatures (where cracking occurs). Hydrogen cracking of cathodically protected structures can be due to either hydrogen environment embrittlement (HEE) or IHE caused by prior bulk hydrogen absorption, this IHE being caused, for example, by an applied stress increase.

A safety approach to the problem implies that hydrogen entry steady state is established before conditions render absorbed hydrogen noxious. Then, in order to make useful predictions from laboratory specimens, these have to be placed under equilibrium conditions with the charging medium, after the suitable charging time has been determined.

Although it is certainly interesting for scientific purposes to compare materials on the basis of the same hydrogen uptake, materials selection for field service has to be made on specimens that are equilibrium-charged under equivalent service conditions.

Obviously these general statements are not limited to disks tested under pressure but can be applied to other kinds of specimens. However, disks are especially attractive because both hydrogen embrittlement and hydrogen entry can be sensitively tested with the same specimens. This avoids discrepancies that can occur when specimens have to be supplied from different sources or have to be heat treated, cold worked, or machined separately because of differing shapes. Moreover, in case of thermal charging, the permeation, charging, and embrittlement cells can be a single one. This represents more than a fringe benefit, because every time that IHE due to hydrogen pickup from gaseous hydrogen takes place, thermal charging appears better suited than cathodic charging, where hydrogen real fugacity has to be estimated tediously.

Summary

The advantage of the disk pressure test is summarized next:

1. Sensitivity: biaxial stresses.
2. Flexibility: possibility of being used under a variety of conditions in order to adjust to the needs of various industrial problems.
3. Control of hydrogen entry and distribution on the same specimens used for testing IHE.
4. Possibility of studying other kinds of embrittlement, such as HEE,

welding, or thermal treatment embrittlement and their synergistic effects with IHE.

5. Rapidity: it is possible to test up to 20 charged specimens a day.
6. Simplicity of operation and maintenance.
7. Simplicity of specimens.
8. Economy: specimens are easy to machine, and the equipment costs are relatively low compared with tensile equipment.

Acknowledgments

The authors would like especially to thank L. Bretin of Creusot-Loire, Le Creusot, for cathodic charging of specimens, A. Clauss of the National School of Chemistry, Strasbourg, for charging titanium specimens, and R. Bernardi for his valuable contribution to the disk tests.

References

[1] Fidelle, J.-P., Allemand, L.-R., Roux, C., and Rapin, M. in *Hydrogen in Metals*, J.-P. Fidelle and M. Rapin, Eds., Valduc, France, Sept. 1967, p. 131.
[2] Fidelle, J.-P., Allemand, L.-R., Deloron, J. M., and Roux, C., *Mécanique Electricité*, Vol. 52, 1969, p. 27.
[3] Fidelle, J.-P., Allemand, L.-R., Tanon, A., and Rapin, M., *Mémoires Scientifiques de la Revue de Métallurgie*, Vol. 65, 1968, p. 241, BISI Translation 6702, Jan. 1969.
[4] Fidelle, J.-P., Allemand, L.-R., Rapin, M., and Hocheid, B. in *Hydrogen in Metals*, J.-P. Fidelle and M. Rapin, Eds., Valduc, France, Sept. 1967, p. 209.
[5] Bernardi, R., Poirier, J., and Fidelle, J.-P., "Seals for Hydrogen Under Pressure," GMC 23–69–108, CEA, Bruyères-le-Châtel, France, 1969.
[6] Bretin, L. and Toitot, M. in *Hydrogen in Metals*, J.-P. Fidelle and M. Rapin, Eds., Valduc, France, Sept. 1967, p. 64.
[7] Fidelle, J.-P., Bernardi, R., Broudeur, R., Roux, C., and Rapin, M., this symposium, pp. 221–253.
[8] Poirier, J., Fidelle, J.-P., and Rapin, M., "Behavior of Uranium and Its Alloys Versus Hydrogen and Deuterium Under Pressure," GMC 18–69–103, CEA Bruyères-le-Châtel, France, 1969.
[9] Dexter, A. H., Derrick, R. G. and Louthan, M. R., Jr., *Corrosion*, National Association of Corrosion Engineers, Vol. 27, 1971, p. 466.
[10] Clauss, A., Schaller, B., and Arditty, J. P., National School of Chemistry in Strasbourg, French Atomic Energy Commission, Contract to Bruyères-le-Châtel, France, 1972.
[11] Crank, J., *Mathematics of Diffusion*, Clarendon, Oxford, England, 1956.
[12] Bastien, P. and Amiot, P., *Mémoires Scientifiques de la Revue de Métallurgie*, Vol. 55, 1958, p. 84.
[13] Legrand, J., Caput, M., Couderc, C., Broudeur, R., and Fidelle, J.-P., *Mémoires Scientifiques de la Revue de Métallurgie*, Vol. 68, 1971, p. 861.
[14] Bretin, L. and Fidelle, J.-P., "Study of Materials Behavior in the Presence of Hydrogen and Its Isotopes: Resistance of Specialty Steels to Embrittlement by Hydrogen and Deuterium, Introduced Cathodically or Under Pressure," Creusot-Loire Internal Report C.Ph.129, Aug. 1971, to appear as a French Atomic Energy Commission Report.

Testing for Hydrogen Pickup During Processing

Mechanical Delay-Time Test Methods

E. J. Jankowsky [1]

Notched C-Ring Test

REFERENCE: Jankowsky, E. J., "**Notched C-Ring Test,**" *Hydrogen Embrittlement Testing, ASTM STP 543,* American Society for Testing and Materials, 1974, pp. 51–57.

ABSTRACT: High-strength steel notched C-rings have proven to be useful specimens for studying the effects of hydrogen embrittlement, as well as screening plating processes, cleaning, and paint removal materials for use on naval aircraft parts. The specimen and some of its uses are described.

KEY WORDS: tests hydrogen embrittlement, high strength steels, cadmium coatings, plating, baking

Most of the first hydrogen stress cracking work conducted at the Naval Air Development Center employed a smooth C-ring specimen. Loading, measurement of stresses, and interpretation of results were simple. It was found, however, that results were very inconsistent when different heats of steel were used for making the rings. Addition of a notch corrected this inconsistency and generally made the specimens more sensitive.

Investigations conducted with notched specimens have involved mechanisms, electroplating processes, and material screening.

Experimental Procedures

Specimen

The notched C-ring consists of a 1¼-in. section cut from 2-in. outside diameter, ⅛-in. wall thickness tubing which is heat treated to the required strength level and finish ground to the dimensions shown in Fig. 1. Most of the Naval Air Development Center's work was conducted with AISI 4340 steel heat treated to a strength level of 260 to 280 ksi. A few experiments have been conducted with 6Al-4V titanium alloy, and it appears that it is a suitable specimen for almost any material if the necessary calibration equipment is available.

---

[1] Chemist, Air Vehicle Technology Department, Naval Air Development Center, Warminster, Pa. 18974.

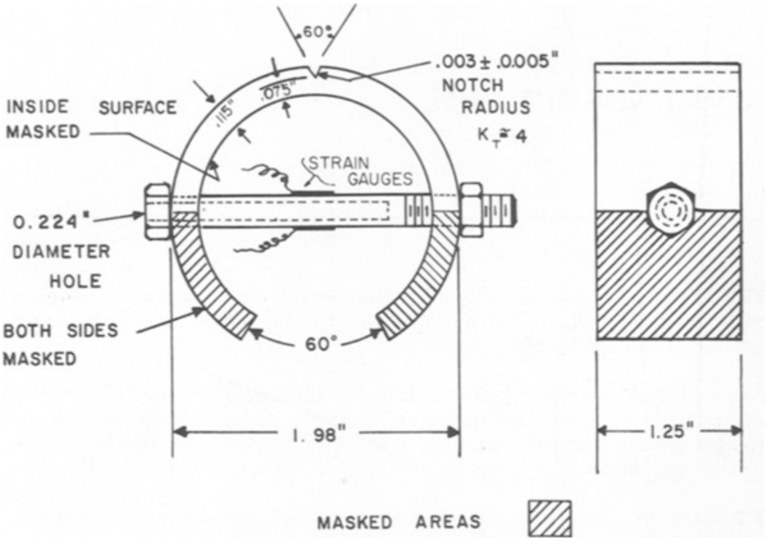

FIG. 1—*Notched C-Ring with instrumented loading bolt.*

Loading Based on Bolt Strain

Original work, which is fully described in a paper presented at the 1960 Annual Meeting of the American Society for Testing and Materials [*1*][2], was performed with a stressing bolt fitted with strain gages for measuring bolt strain. The bolt passed through the specimen diameter, and the load was applied by tightening a nut on the bolt. Strain was measured by means of a bridge circuit and a strain indicator as shown in Fig. 2. A recording oscillograph was used to make a continuous record of bolt strain from the beginning of loading to failure. The method was very sensitive and reproducible and could be used very well for measuring incubation time and crack progagation. The number of specimens that could be tested at one time was limited by the instrumentation available, however.

Loading Based on Ring Deflection

It was obvious that if a large number of tests were to be made a simpler stressing method had to be employed. The early work showed that there was no measurable yielding of high-strength AISI 4340 steel specimens prior to failure. A new stressing method based on deflection (reduction in diameter) of the specimens was devised based on the linear nature of the bolt strain versus nominal ring stress curve. The strain required to break several notched C-rings was determined using the instrumented bolt. Then the instrumented bolts were used to load several more specimens to 75

---

[2] The italic numbers in brackets refer to the list of references appended to this paper.

percent of the average breaking strain and the reduction in diameter measured. An average reduction in diameter could then be determined for 75 percent of the breaking stress. All subsequent tests were conducted with ordinary bolts for applying stress and a micrometer or the device shown in Fig. 3 for measuring deflection. A timing device employing microswitches and timers (Fig. 4) was then added, and many specimens could be tested at once. From this point on, the notched C-ring test became a go no-go test with a testing time of 200 h and an applied stress of 75 percent of the breaking stress.

Further Simplification

After considerable testing, it was observed that the deflection at 75 percent of the breaking stress was always very close to 0.100 in. A hydrogen embrittlement test using this stressing value is now included in military

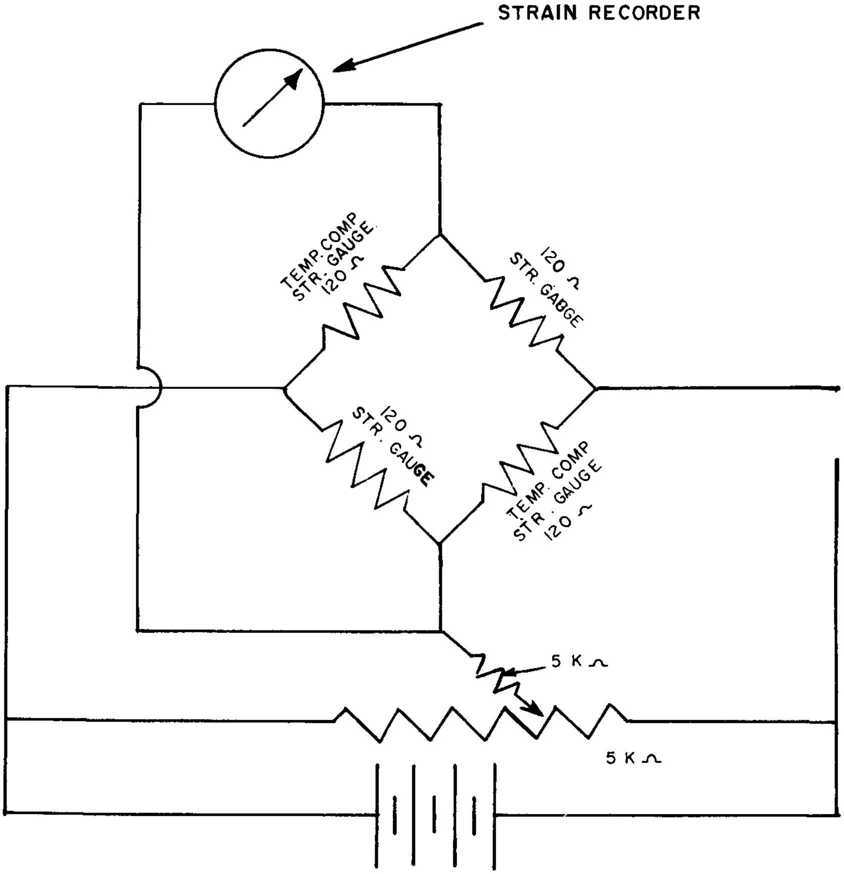

FIG. 2—*Strain gage wiring diagram.*

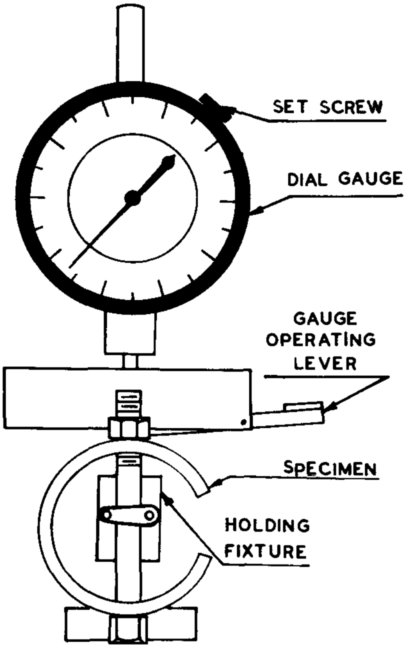

FIG. 3—*Deflection measuring device.*

paint remover specification MIL-R-81294 and federal specification TT-R-248.

Notched C-rings used for paint remover tests are generally flash cadmium plated (2 min at 50 amperes per square foot (ASF) in a nonbrightened bath) and baked 24 h at 375° F prior to stressing to simulate vacuum cadmium plated parts [2].

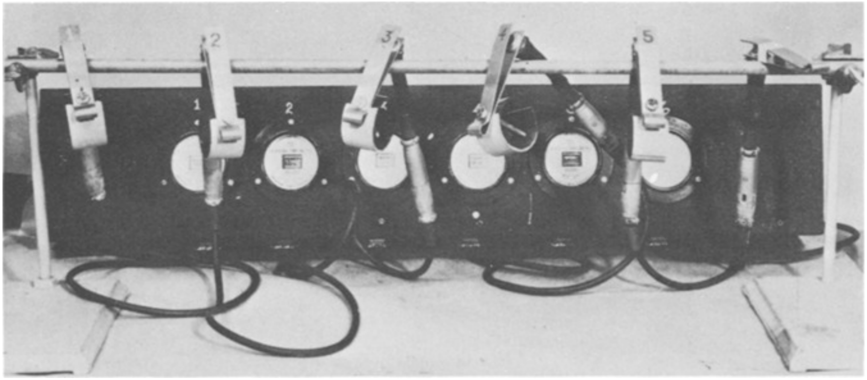

FIG. 4—*Notched C-rings with microswitches and timers.*

Test Methods

The notched C-ring can be used two ways. The stress can be applied prior to subjecting the specimen to the potentially embrittling medium to simulate parts containing high residual stresses, or the stress can be applied after the ring is treated to give a standard constant strain test.

Results and Discussion

The notched C-ring has been used for a number of years for both research investigations and screening tests. When used with the instrumented bolt and an appropriate strain indicator, cracking behavior can be monitored from a point remote from the testing environment. Figure 5 illustrates results of an investigation of cracking of plated specimens. The equipment required is no more expensive and certainly not as bulky as the sustained loading machines used for testing notched tension specimens.

In its simplest form, using a fixed deflection value for stressing, it still performs well as a critical screening specimen. The 200 h testing time is apparently sufficiently long to allow incubation, crack propagation, and failure even though this stressing method probably results in slight stress variations from one specimen to the next.

It is particularly useful for testing coatings which may be applied to high-strength steel parts without subsequent baking, such as selective cadmium plating ("brush" plating). It has been used satisfactorily for screening paint removers that may be applied to cadmium coated steel parts such as vacuum cadmium coated landing gear. Both of the latter tests are conducted with prestressed specimens. Failure times for one very embrittling paint stripper, for example, varied from 1.3 to 34.4 h for five

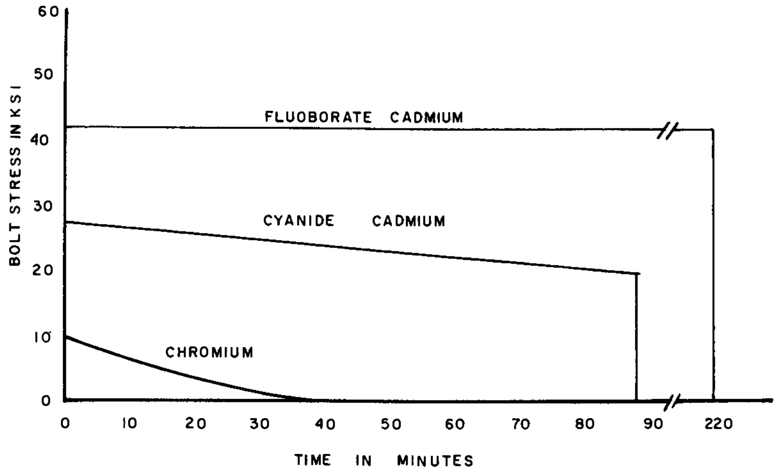

FIG. 5—*Crack progression in plated notched C-rings as indicated by decrease in loading bolt stress.*

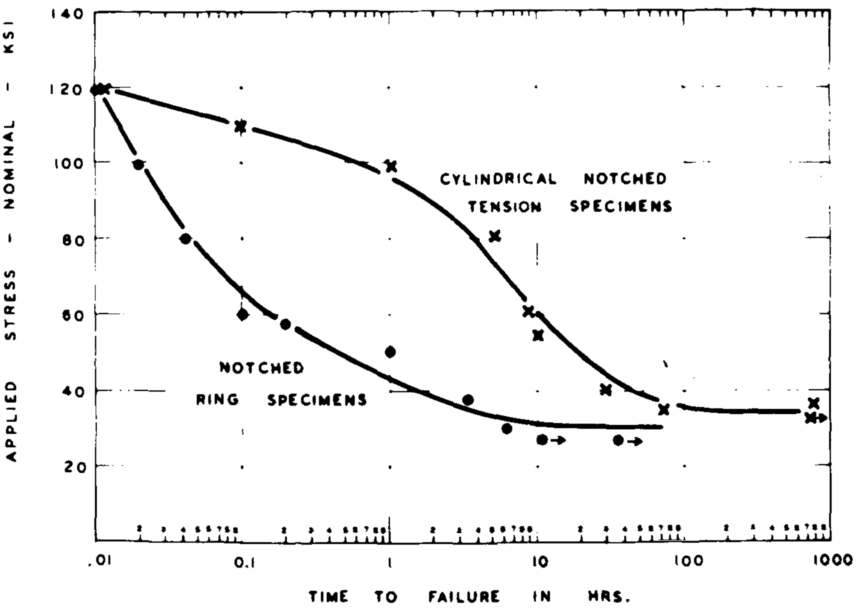

FIG. 6—*Comparison of two types of specimens plated with chromium to a thickness of 0.002 in.*

flash cadmium plated, baked, and prestressed specimens. Generally, failure times are less scattered.

Figure 6 is a comparison of sustained load curves for notched tension specimens and notched C-rings. Both curves reach approximately the same lower critical stress even though their incubation behavior is different.

Comparisons made with the Drilube notched bolt, the Lawrence hydrogen detection gage, and the HEP tester show that notched C-ring results compare well with other methods [*3*].

The principal disadvantages to the notched C-ring are that it is difficult to make and comparatively expensive. The equipment and experience needed to make good notched C-rings is apparently beyond that found in most job shops. When a machine shop capable of producing notched C-rings is found, the cost is about $25 per specimen for rings machined from solid bar stock. The cost for specimens fabricated from tubing would be slightly lower.

In summary, the notched C-ring is a reliable specimen for hydrogen embrittlement testing that can be used for either laboratory studies or material screening tests.

Acknowledgments

The author would like to express his sincere appreciation to Walter Beck and Forrest Williams of the Naval Air Development Center, for their technical advice and interpretation; Samuel Goldberg, Naval Air Systems Command, who sponsored the work, and Peter Sabatini, for his technical assistance. Thanks also to Sara Ketcham, who presented the paper and added so much to the work through her critical reviews and many useful suggestions.

References

[1] Williams, F. S., Beck, W., and Jankowsky, E. J. in *Proceedings*, American Society for Testing and Materials, Vol. 60, pp. 1192–1202.

[2] Jankowsky, E. J., "The Effect of Cleaning and Paint Stripping Compounds on Stressed High Strength Steels," Report No. NAEC-AML-1983, Naval Air Engineering Center, Philadelphia, Pa., July 1964.

[3] Jankowsky, E. J., "A Comparison of Various Test Methods for Detecting Hydrogen Embrittlement," Report No. NADC-MA-7066, Naval Air Development Center, Warminster, Pa., June 1971.

W. H. Hyter [1]

Stressed O-Ring Test

REFERENCE: Hyter, W. H., "**Stressed O-Ring Test,**" *Hydrogen Embrittlement Testing, ASTM STP 543,* American Society for Testing and Materials, 1974, pp. 58–63.

ABSTRACT: A stressed steel O-ring is used by the Douglas Aircraft Company to determine the hydrogen embrittling tendency of various processes. The use of the Douglas stress ring is described for testing processes, such as plating, cleaning, deoxidizing, and paint stripping. The method of selecting the hydrogen sensitivity of the steel used to make the ring is included.

KEY WORDS: hydrogen embrittlement, high strength steels, cadmium coatings, stresses, plating, baking

Method Used to Select the 4340 Steel

Douglas ring specimens for detecting hydrogen embrittlement are machined from AISI 4340 steel. Since some heats of 4340 steel are less sensitive to hydrogen embrittlement than others, a special test is conducted on the steel before it is chosen for manufacture of the ring specimens. To assure the sensitivity of a heat of steel, six trial ring specimens are machined from the steel according to a standard Douglas drawing (P/N S 4776683). The machined rings are heat treated 260 to 280 ksi ultimate tensile strength. Following magnetic particle inspection, the rings are lightly dry blasted with aluminum oxide (150 mesh or finer) and shot peened to an intensity of 0.006 to 0.010-in. Almen "A". After dimensional inspection, three of the rings are plated in a brightened cadmium cyanide bath at 10 amperes per square foot (ASF) for 30 min and baked for 8 h at 375° F. The plated rings are then stressed to 90 percent ultimate (240 000 psi). These rings must fracture within 24 h after stressing.

The other three rings are plated in our DPS 9.28 low embrittlement cadmium bath at 60 ASF for 6 min, baked at 395° F for 23 h, and stressed to 90 percent ultimate (240 000 psi).

All three rings must remain stressed for 168 h without failure. When a

---

[1] Section manager, Inorganic Coatings, Materials and Process Engineering, Douglas Aircraft Div., McDonnnell Douglas Corp., Long Beach, Calif. 90801.

heat of steel passes these tests it is then selected to be used to manufacture ring specimens.

Method Used to Produce Stress Level

The desired stress is applied to the ring by inserting the ring specimen into a vise and distorting it to allow insertion of the stress bar.

Details for manufacture of the test ring and stress bar are given in Fig. 1, Douglas Drawing No. S4776683 for the hydrogen embrittlement test ring. The ring, stress bar, and deflection data are shown in Figs. 2-5.

The stress values shown in Fig. 5 have been determined by calculation, photostress measurements, strain gage data, and X-ray diffraction determinations. These stress values are believed to be accurate within 15 percent.

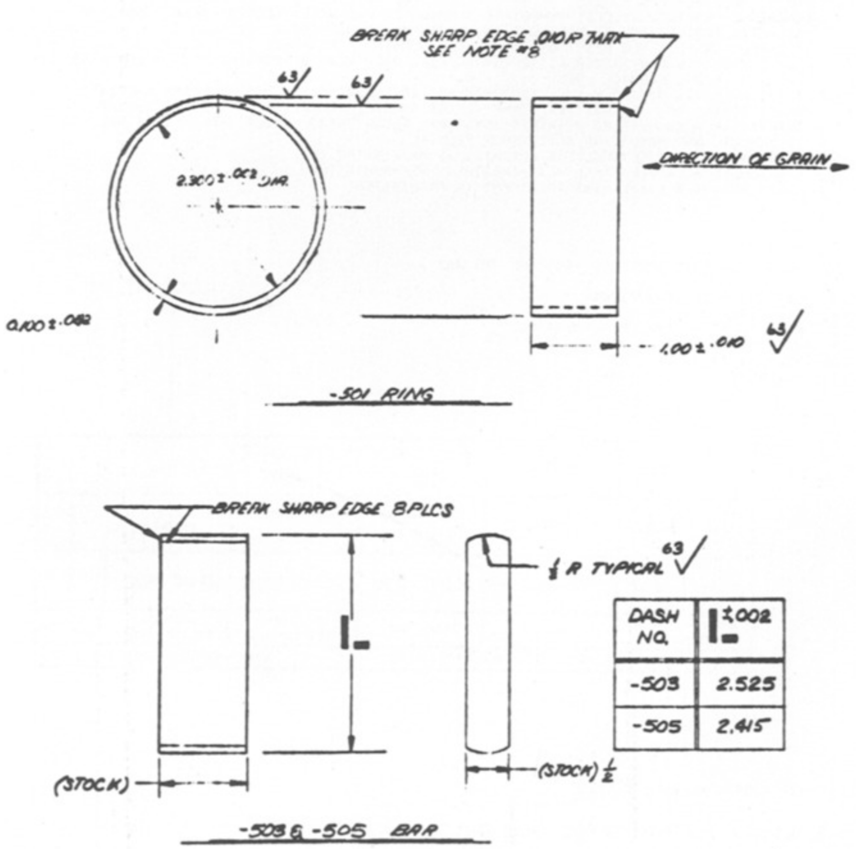

FIG. 1a

FIG. 1—*Ring hydrogen embrittlement test.*

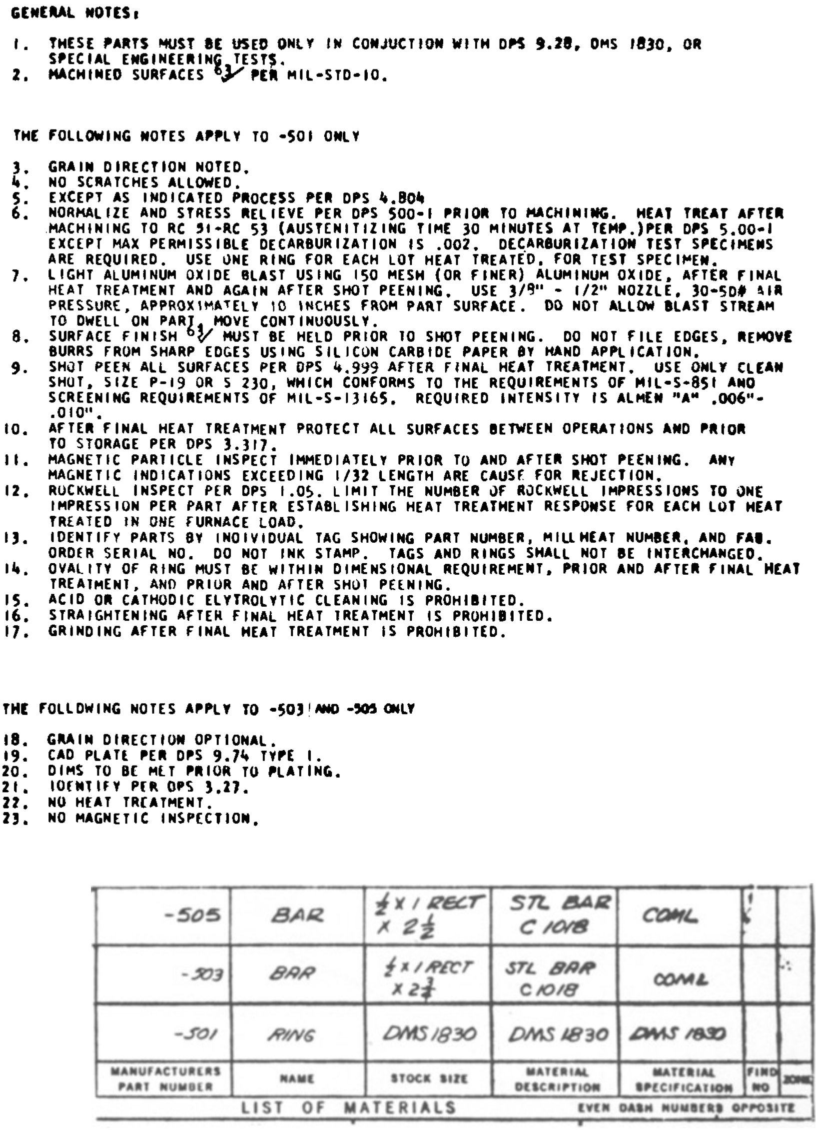

GENERAL NOTES:

1. THESE PARTS MUST BE USED ONLY IN CONJUCTION WITH DPS 9.28, OMS 1830, OR SPECIAL ENGINEERING TESTS.
2. MACHINED SURFACES 63√ PER MIL-STD-10.

THE FOLLOWING NOTES APPLY TO -501 ONLY

3. GRAIN DIRECTION NOTED.
4. NO SCRATCHES ALLOWED.
5. EXCEPT AS INDICATED PROCESS PER DPS 4.804
6. NORMALIZE AND STRESS RELIEVE PER DPS 500-1 PRIOR TO MACHINING. HEAT TREAT AFTER MACHINING TO RC 51-RC 53 (AUSTENITIZING TIME 30 MINUTES AT TEMP.)PER DPS 5.00-1 EXCEPT MAX PERMISSIBLE DECARBURIZATION IS .002. DECARBURIZATION TEST SPECIMENS ARE REQUIRED. USE ONE RING FOR EACH LOT HEAT TREATED, FOR TEST SPECIMEN.
7. LIGHT ALUMINUM OXIDE BLAST USING 150 MESH (OR FINER) ALUMINUM OXIDE, AFTER FINAL HEAT TREATMENT AND AGAIN AFTER SHOT PEENING. USE 3/9" - 1/2" NOZZLE, 30-50# AIR PRESSURE, APPROXIMATELY 10 INCHES FROM PART SURFACE. DO NOT ALLOW BLAST STREAM TO DWELL ON PART, MOVE CONTINUOUSLY.
8. SURFACE FINISH 63√ MUST BE HELD PRIOR TO SHOT PEENING. DO NOT FILE EDGES, REMOVE BURRS FROM SHARP EDGES USING SILICON CARBIDE PAPER BY HAND APPLICATION.
9. SHOT PEEN ALL SURFACES PER DPS 4.999 AFTER FINAL HEAT TREATMENT. USE ONLY CLEAN SHOT, SIZE P-19 OR S 230, WHICH CONFORMS TO THE REQUIREMENTS OF MIL-S-851 AND SCREENING REQUIREMENTS OF MIL-S-13165. REQUIRED INTENSITY IS ALMEN "A" .006"-.010".
10. AFTER FINAL HEAT TREATMENT PROTECT ALL SURFACES BETWEEN OPERATIONS AND PRIOR TO STORAGE PER DPS 3.317.
11. MAGNETIC PARTICLE INSPECT IMMEDIATELY PRIOR TO AND AFTER SHOT PEENING. ANY MAGNETIC INDICATIONS EXCEEDING 1/32 LENGTH ARE CAUSE FOR REJECTION.
12. ROCKWELL INSPECT PER DPS 1.05. LIMIT THE NUMBER OF ROCKWELL IMPRESSIONS TO ONE IMPRESSION PER PART AFTER ESTABLISHING HEAT TREATMENT RESPONSE FOR EACH LOT HEAT TREATED IN ONE FURNACE LOAD.
13. IDENTIFY PARTS BY INDIVIDUAL TAG SHOWING PART NUMBER, MILL HEAT NUMBER, AND FAB. ORDER SERIAL NO. DO NOT INK STAMP. TAGS AND RINGS SHALL NOT BE INTERCHANGED.
14. OVALITY OF RING MUST BE WITHIN DIMENSIONAL REQUIREMENT, PRIOR AND AFTER FINAL HEAT TREATMENT, AND PRIOR AND AFTER SHOT PEENING.
15. ACID OR CATHODIC ELYTROLYTIC CLEANING IS PROHIBITED.
16. STRAIGHTENING AFTER FINAL HEAT TREATMENT IS PROHIBITED.
17. GRINDING AFTER FINAL HEAT TREATMENT IS PROHIBITED.

THE FOLLOWING NOTES APPLY TO -503 AND -505 ONLY

18. GRAIN DIRECTION OPTIONAL.
19. CAD PLATE PER DPS 9.74 TYPE I.
20. DIMS TO BE MET PRIOR TO PLATING.
21. IDENTIFY PER OPS 3.27.
22. NO HEAT TREATMENT.
23. NO MAGNETIC INSPECTION.

-505	BAR	½ X 1 RECT X 2½	STL BAR C 1018	COML		
-503	BAR	½ X 1 RECT X 2¾	STL BAR C 1018	COML		
-501	RING	DMS 1830	DMS 1830	DMS 1830		
MANUFACTURERS PART NUMBER	NAME	STOCK SIZE	MATERIAL DESCRIPTION	MATERIAL SPECIFICATION	FIND NO	ZONE

LIST OF MATERIALS

EVEN DASH NUMBERS OPPOSITE

FIG. 1b

Use of the Stress Ring

A unique feature of the ring specimen is the fact that it can be used to test many types of hydrogen producing materials and processes under varying environmental conditions. In contrast to a notched tension specimen, the ring has an appreciable area that is exposed to the test medium. The thickness of the plating on this area can be accurately determined.

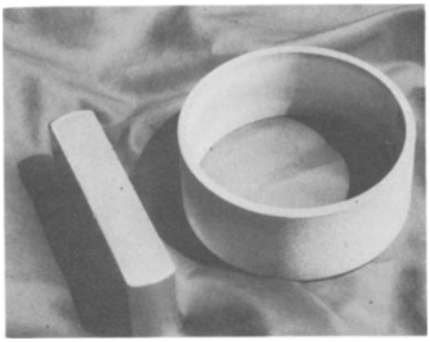

FIG. 2—*Ring specimen before stressing.*

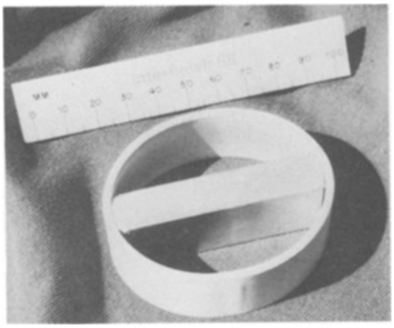

FIG. 3—*Ring with stress bar inserted.*

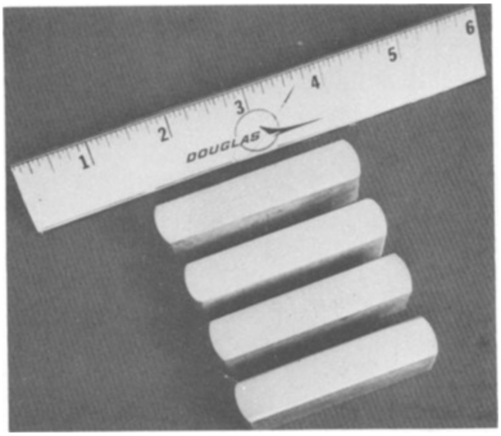

FIG. 4—*Stress bars of various lengths.*

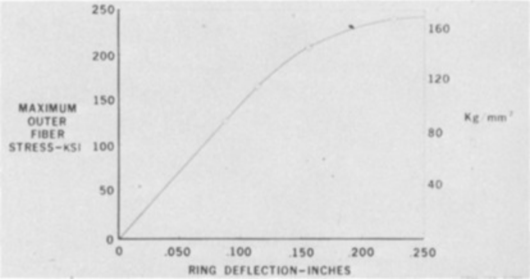

FIG. 5—*Chart showing stress and ring deflection.*

Aircraft Cleaners and Paint Strippers

Since high-strength steel parts can contain residual tensile stresses as a result of heat treating, machining, grinding, or service loads or all four, testing of aircraft cleaner and paint strippers are conducted while the rings are under a sustained load of 176 000 psi. This load, which is 80 percent of the yield strength of the ring material, was established by using water as a standard. This stress level will cause failure when testing materials that are more embrittling than water but will not fracture in water. Because the high-strength steel parts are cadmium plated, the ring specimens are also cadmium plated per DPS 9.28 and embrittlement relieved before stressing and testing the cleaner or stripper materials.

Hydrogen Embrittlement Testing of Plating Processes

The initial use of the Douglas stress ring was to determine the hydrogen embrittlement characteristics of the low embrittlement cadmium plating process.

Initially it was required that three rings be processed with each load of parts plated per DPS 9.28. Since for many years we had no ring failures after plating rings with the DPS 9.28 cadmium this requirement was reduced to embrittlement testing on initial qualification and once every three months.

1. *Hydrogen Embrittlement Test Procedure for DPS 9.28 Cadmium Plate*—Four rings are processed through the entire production cleaning and plating processing cycle, baked for 23 h, and then stressed to 90 percent ultimate, using a cadmium plated 2.525-in. stress bar. These rings must remain under stress for 168 h without failure.

If the production plating facility is properly maintained these plated and stressed rings will remain intact in air for several months.

2. *Hydrogen Embrittlement Testing of Other Plating Processes*—Ring tests have been used to establish the hydrogen embrittlement requirements for many other plating processes such as: (a) sulfamate nickel plating, (b) mul-

tiple step chromium plating, and (c) brush plating (cadmium, nickel, nickel-tungsten, etc.).

Stress Corrosion Testing with Inorganic and Organic Coatings

As mentioned before, a ring specimen properly plated per DPS 9.28 or an unplated ring stressed to 240 000 psi (90 percent ultimate), will remain intact normally for several months in air. However, fracture will occur within a few hours if the stressed rings are placed in a salt spray cabinet.

This provides a basis to determine the relative ability of inorganic and organic coatings to prevent failure due to stress corrosion.

Evaluation of the Ring Test by Other Investigators

A. G. B. Wadsworth and B. G. Johnson, APTC Project No. 13-59, *Boeing Wichita Report D-3-3655 Standardization of Methods of Testing for Hydrogen Embrittlement,* 29 May 1961, stated, "The sustained load specimens with 0.001, 0.003, and 0.005-in. notch radii and the Douglas ring specimen all indicated a high degree of embrittlement with a reasonable scatter in test results."

B. Theodore G. Kozan, The Boeing Co., MASD, Wichita Branch, *Evaluation of Cadmium Plating System for Hydrogen Embrittlement,* stated, "In comparing the results of the 0.003-in. notch tensile specimens and the Douglas ring specimens, it should be noted that the ring specimens correctly indicated the most embrittling plating systems but were not as sensitive as the 0.003-in. notch tensile specimens."

The results of ARTC 13-59 indicated the ring specimen to be less sensitive than the 0.003-in. notch but more sensitive than the 0.005-in. notch.

R. C. Movich [1]

Notched Bar-Bending Test

REFERENCE: Movich, R. C., "**Notched Bar-Bending Test,**" *Hydrogen Embrittlement Testing, ASTM STP 543*, American Society for Testing and Materials, 1974, pp. 64–73.

ABSTRACT: A new method of testing for hydrogen embrittlement of high-strength steels is described. Results of tests conducted to compare the ability of the new method and the stress-rupture machine to detect detrimental absorbed hydrogen are given. The new method was found to provide reliability, simplicity, and low cost for hydrogen embrittlement testing and compared directly with the stress-rupture machine in both sensitivity and variability. Results of tests conducted to determine the ability of the new method to detect varying amounts of hydrogen obtained by cadmium plating using three different processes with and without baking are given. The new method is well suited for periodic quality control tests of cadmium plating processes, selective plating tests, testing of cleaners and paint strippers, and stress corrosion testing.

KEY WORDS: hydrogen embrittlement, high strength steels, cadmium coatings, stresses, plating, heat treatment, notch tests

High-strength steels having an ultimate tensile strength of 260 000 to 280 000 psi are used extensively for structural components in modern aircraft and other products. One of the best methods for protecting these components from corrosion is by cadmium plating followed by the application of an organic coating. A characteristic of cadmium plating and its associated cleaning and pickling processing is that hydrogen can be generated and absorbed into the steel. Even very small amounts of hydrogen absorbed into the lattice of high-strength steels can cause catastrophic failure of these components during service at sustained static stresses much below the stress level which the components would withstand if they were free from absorbed hydrogen. Therefore, special precautions must be taken to prevent absorption of hydrogen or eliminate absorbed hydrogen when cadmium plating high-strength steels. A good method of testing to determine whether or not parts are free, in fact, from detrimental absorbed hydrogen has been a prime requirement for quality assurance.

---

[1] Manufacturing research specialist, Lockheed-California Co., Burbank, Calif. 91503.

Failure Mechanism and Test Methods

Hydrogen embrittlement failure occurs when the steel is subjected to a static tensile load for an extended period of time. Failure occurs by the migration of hydrogen to areas of high-stress concentration, resulting in localized concentrations of hydrogen sufficient to cause brittle fracture. The time required for failure of the steel is dependent upon the absorbed hydrogen concentration, the magnitude of the stress concentration, and the magnitude of the applied stress.

In order for a hydrogen embrittlement test method to be valid it must detect small amounts of absorbed hydrogen which can cause catastrophic failure of parts according to the mechanism just described. A destructive mechanical test generally is accepted to accomplish this purpose. The test most commonly used employs a notched tensile coupon which is statically loaded in tension in a stress-rupture machine at 75 percent of its ultimate strength until failure occurs or 200 h has elasped. The disadvantages of using the stress-rupture machine for hydrogen embrittlement testing are the high cost of the machine and the necessity of a coupon with threads or shoulders for gripping.

Notched tensile coupons used for hydrogen embrittlement testing are required to be of the same alloy and heat treated to the same ultimate tensile strength as the parts which are to be plated. In order to fabricate a notched tensile coupon, material must be rough machined, heat treated, and then finish machined, including machining of the notch when the material is in its hardened condition. Conventional grinding of the notch is not satisfactory due to a propensity to overheat the steel causing the formation of untempered martensite or retempered, tempered martensite in the vicinity of the notch. Therefore, final machining of the coupon must be accomplished on a lathe using sharp cutting tools. Proper tolerance, concentricity, and notch configuration are difficult to obtain using this method; thus, the cost of acceptable coupons is necessarily high.

New Testing Method

A new method of testing for hydrogen embrittlement has been developed. This method combines a unique coupon with a new method of loading to provide a complete system with high reliability and low cost. In this method, a notched coupon is loaded in tension by bending. Since the coupon is not loaded in tension axially, threads or shoulders for gripping are not necessary, and the coupon can be easily slipped into the testing device for loading. Due to the advantage gained by the bending moment, the load required is only a fraction of that required for loading in tension axially as done by the stress-rupture machine. The cost of the testing device is a small fraction of the cost of a stress-rupture machine. The notched coupon used is fabricated by crush grinding after the steel is heat treated to its desired level of strength. This method produces a coupon with proper tolerances, concentricity, and notch configuration at a fraction of the cost of machining and without the overheating associated with conventional grinding.

Two types of testing devices have been developed. The first, shown in Figs. 1 and 2, is used for testing of processed coupons and incorporates a timer for exact determination of time to failure. Figure 1 shows a four station module and the loading sequence as follows: (1) coupon is slipped into hole in base, (2) loading bar is slipped onto free end of coupon, (3) yoke is positioned over loading bar, (4) loading screw is turned down by hand to zero position (point at which loading bar just begins to move), (5) wrench is inserted into the screw and a predetermined number of turns applied (number of turns represents a percentage of the ultimate strength), and (6) timer switch is activated. The light and timer remain activated until the coupon fails or is unloaded. An installation of 20 testing devices, which were used to perform the tests described in this paper, is shown in Fig. 2.

The other type of testing device, shown in Fig. 3, accomplishes the same purpose as the more sophisticated device and stresses the coupon in exactly

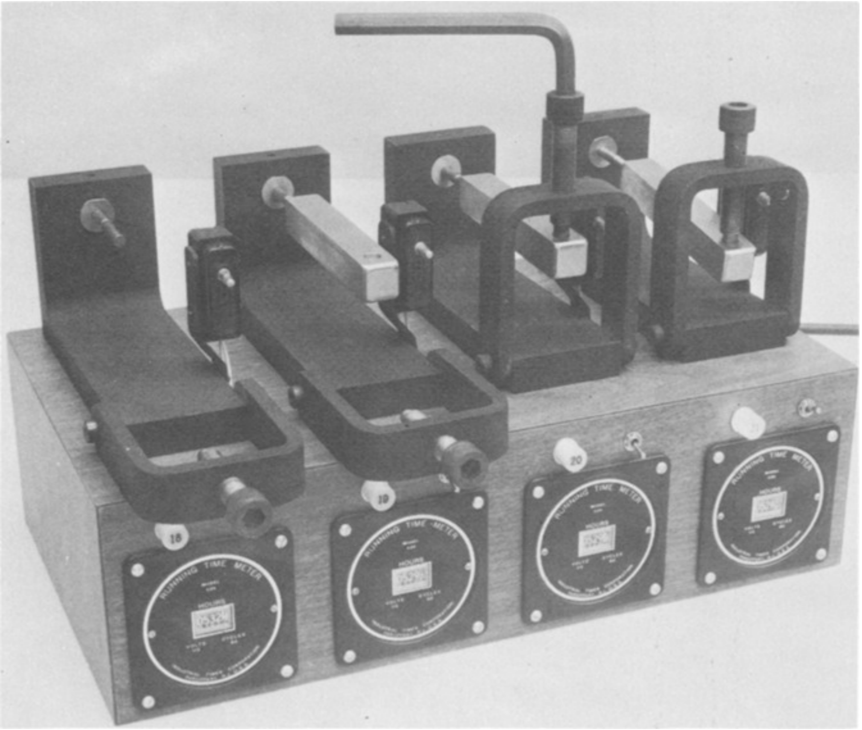

FIG. 1—*Four station testing device showing loading sequence.*

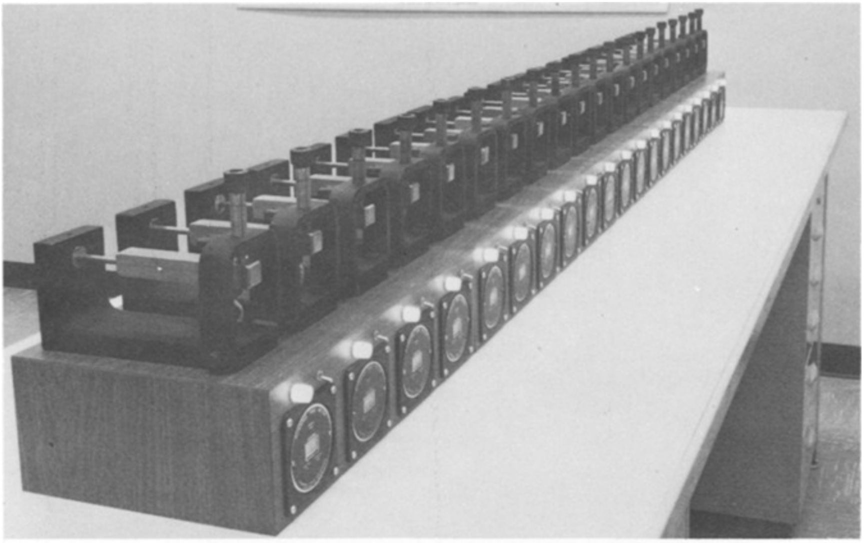

FIG. 2—*Bank of 20 testing stations used for experimental program.*

the same manner. It is ideal for go no-go quality assurance testing where the time to failure is not important and the most economical device is desirable. This device is also useful for exposure to potential hydrogen embrittling processes while the coupon is under stress such as for selective plating tests, testing of cleaners and paint strippers, and stress corrosion testing. Dimensional details for the device are shown in Fig. 4.

The coupons used in both devices are fabricated from $\frac{5}{16}$-in.-diameter rod of the desired alloy which is cut into coupon lengths and heat treated to the desired strength level. After heat treating the diameter is reduced to 0.250 in. The notch is then produced by crush grinding. This produces a

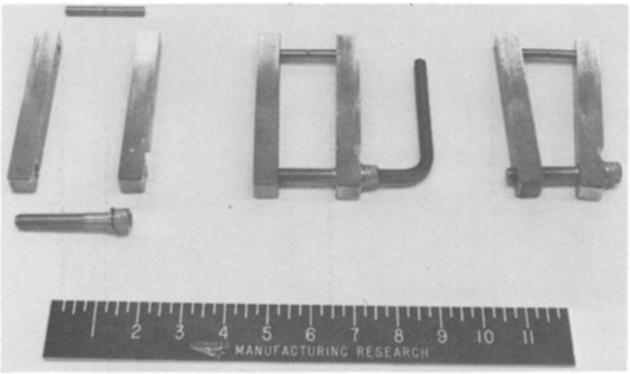

FIG. 3—*Portable testing devices and coupons with loading sequence shown.*

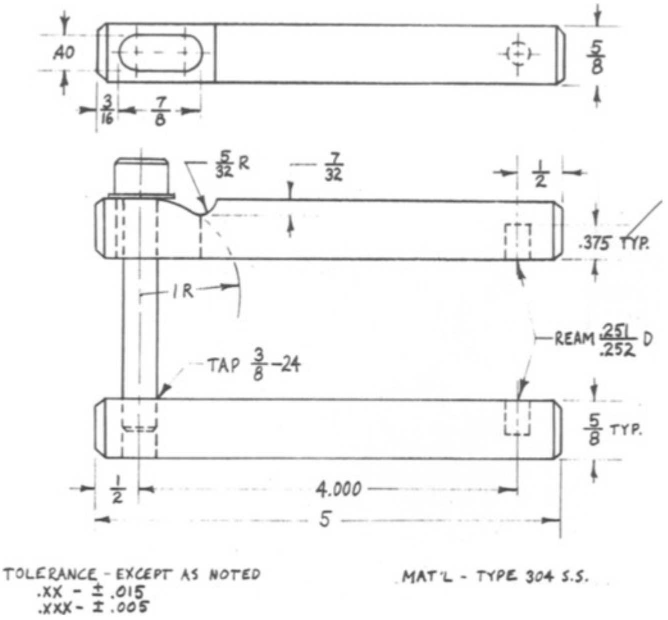

FIG. 4.—*Drawing of portable testing device.*

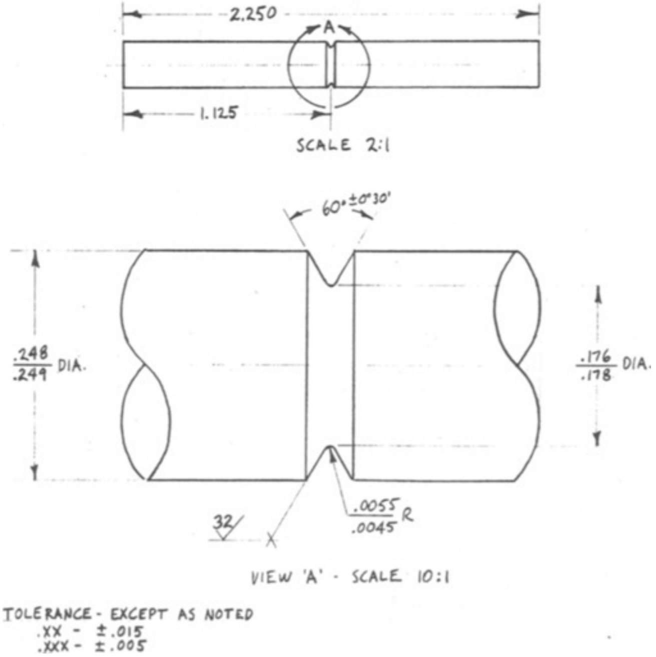

FIG. 5—*Drawing of test coupon which is fabricated by crush grinding.*

notch with close tolerances and with no metallurgical damage to the alloy in the vicinity of the notch. Figure 5 shows the dimensions and tolerances of the coupon.

Test Procedure

Tests were conducted to compare the ability of the new testing method and the stress-rupture machine to detect detrimental hydrogen embrittlement. Coupons were fabricated from $\frac{5}{16}$-in.-diameter air melted 4340 steel rod heat treated to 260 000 to 280 000 psi ultimate tensile strength. For the purpose of this test program, threaded notched coupons were used so that they could be loaded axially in tension in the stress-rupture machines. The first step in the test procedure was to determine the ultimate strengths of the coupons since sustained load tests for hydrogen embrittlement are conducted at various percentages of notched coupon ultimate strength. Coupons were degreased and dry blasted with 180 grit aluminum oxide. Ultimate strengths were determined by loading coupons to failure using a tension testing machine. The averages of these notched coupon ultimate strengths were used to determine the various percentages of ultimate strength for sustained load tests using the stress-rupture machines. Coupons were also loaded to failure in the new testing devices. The number of turns of the loading screw at failure was the coupon ultimate strength. The averages of these notched coupon ultimate strengths were used to determine the various percentages of ultimate strength for sustained load tests using the new testing devices. Figure 6 shows the ultimate strengths obtained and the curve used to determine the number of turns of the load-

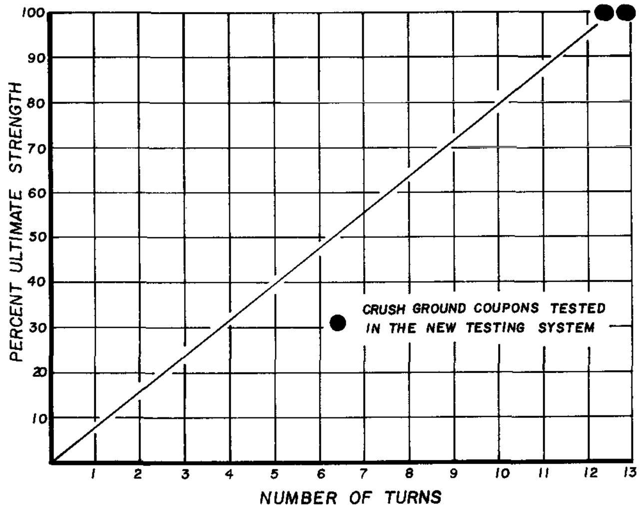

FIG. 6—*Loading curve for use with the new testing system.*

ing screw required to obtain various percentages of coupon ultimate strength.

For the purposes of the test program, coupons containing absorbed hydrogen were required. These coupons were obtained by plating in a bath made up of 3.5-oz/gal cadmium oxide and 12-oz/gal sodium cyanide. Coupons were degreased, dry blasted with 180 grit aluminum oxide, plated at 20 amperes per square foot (ASF) for 15 min, and held at room temperature for 60 min before application of the load. The coupons were not baked. All of the coupons in each set of results obtained were plated simultaneously.

Tests were also conducted to determine the ability of the new testing method to detect varying amounts of hydrogen obtained by cadmium plating using three different processes and baking at 375° F for 24 h. The plating processes used were unbrightened cadmium, bright cadmium, and titanium-cadmium.

Test Results

As stated previously, the most commonly used hydrogen embrittlement tests employs a notched coupon which is held at 75 percent of its ultimate strength until failure occurs or 200 h has elapsed. Sustained loading at one stress level, such as 75 percent of ultimate, is fine for quality control purposes. However, to obtain a complete characterization of the amount of embrittlement obtained from a plating process, sustained loading at several stress levels is necessary. Figure 7 shows the results of testing a group of 19

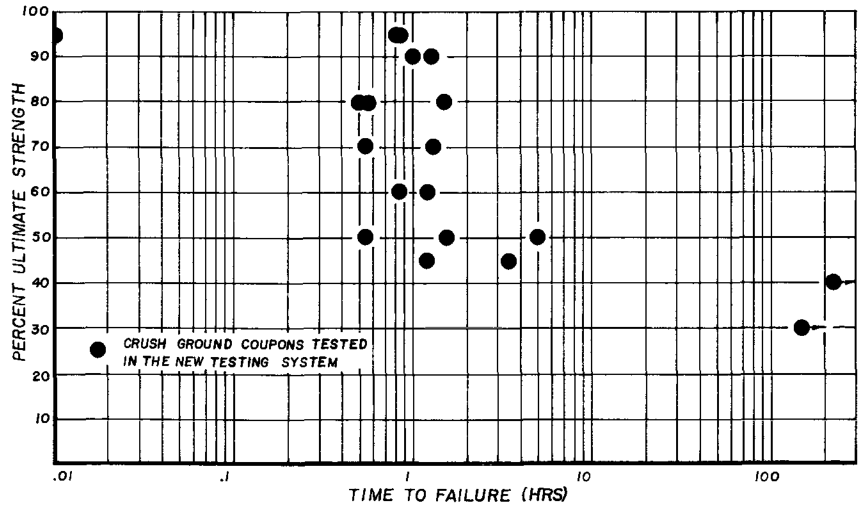

FIG. 7—*Typical hydrogen embrittlement test results for cadmium plated high-strength 4340 steel.*

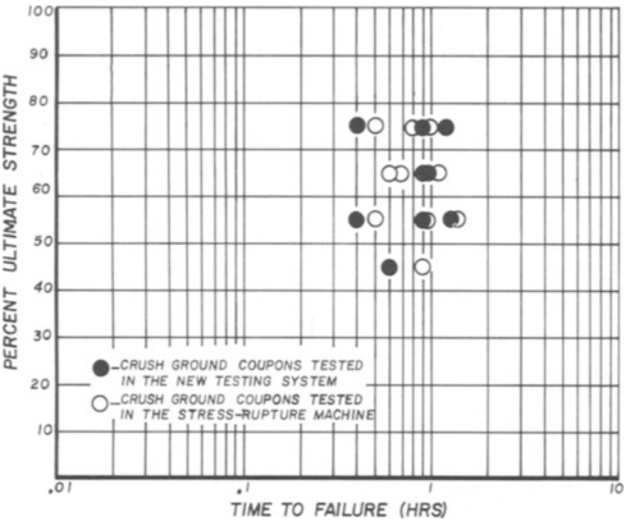

FIG. 8—*Test results comparing the new testing method with the stress-rupture machine.*

coupons using the new testing method. These results are typical of sustained load testing of high-strength 4340 steel containing absorbed hydrogen due to cadmium plating. If a curve was drawn through the points there would be a horizontal portion at 95 percent of ultimate, a vertical portion at 1 h, and another horizontal portion at 42 percent of ultimate. Both the vertical part

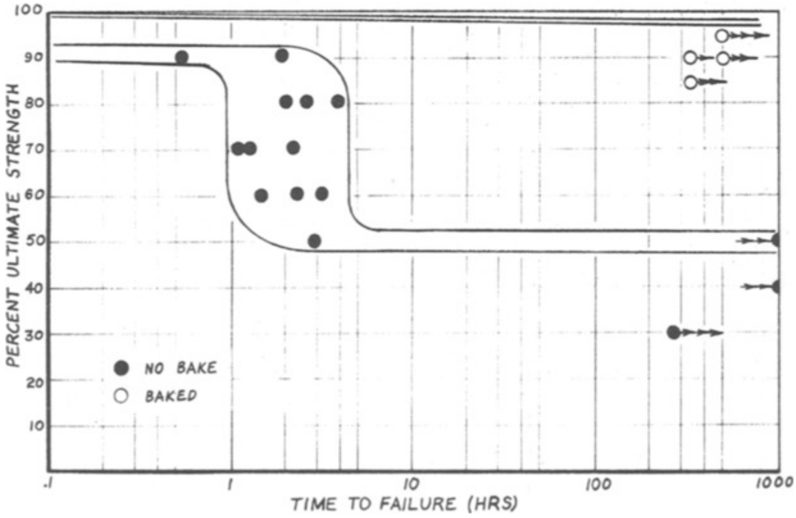

FIG. 9—*Test results of unbrightened cadmium showing the effect of baking in relieving detrimental hydrogen through the porous plate.*

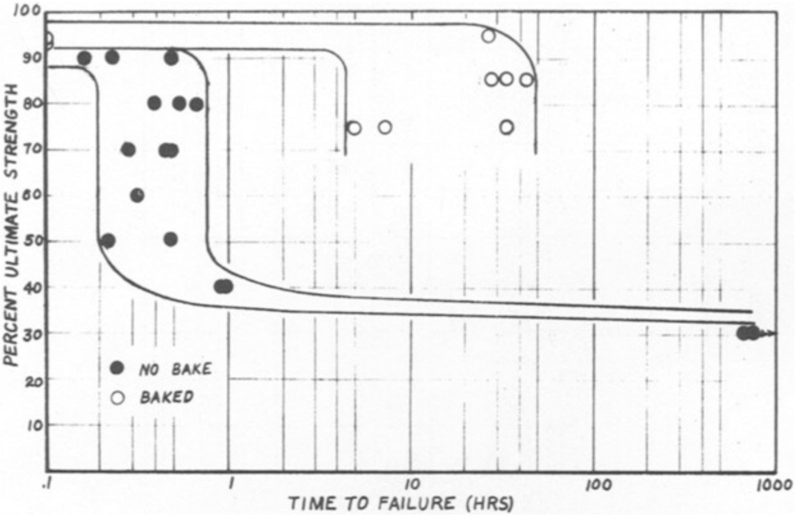

FIG. 10—*Test results of bright cadmium showing the inability of baking to relieve hydrogen through the dense plate.*

of the curve at 1 h and the horizontal part of the curve at 42 percent of ultimate are measures of the severity of hydrogen embrittlement caused by absorbed hydrogen.

Results of tests conducted to compare the ability of the new testing method and the stress-rupture machine to detect hydrogen embrittlement

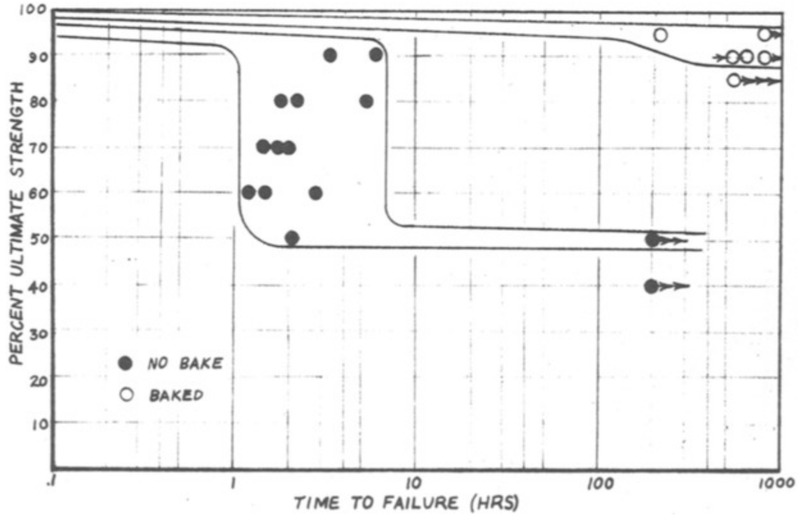

FIG. 11—*Test results of titanium-cadmium showing hydrogen relief by baking through a plate with excellent corrosion resistance.*

are shown in Fig. 8. Coupons stressed at 40 percent of ultimate strength by both methods did not fail within 200 h. As can be seen, the new testing method compares favorably with the stress-rupture machine in both sensitivity and variability.

Results of tests conducted with the new testing method using three different cadmium plating processes with and without baking are shown in Figs. 9 through 11. The effect of baking to relieve detrimental hydrogen is clearly shown in Fig. 9 where an unbrightened cadmium plating bath was used. A porous plate is produced by the unbrightened bath allowing the hydrogen to diffuse through the plate during the baking cycle. After baking, three coupons withstood 95 percent of ultimate load without breaking for 500 h at which time they were unloaded. The use of brighteners in cadium plating baths produces a dense, nonporous plate which hinders the relief of hydrogen by baking. This effect is shown in Fig. 10 where a bright cadmium bath was used. Test results using a proprietary cadmium plating bath containing a small amount of titanium are shown in Fig. 11. The advantage of this bath is that a plate with excellent corrosion resistance is produced which also is porous enough to allow relief of absorbed hydrogen by baking. As can be seen, baking relieved the detrimental hydrogen since failures after baking occurred only after long time periods at 90 percent of ultimate strength and higher.

W. C. Jones [1]

Notched Test Strips

REFERENCE: Jones, W. C., "**Notched Test Strips**" *Hydrogen Embrittlement Testing, ASTM STP 543,* American Society for Testing and Materials, 1974, pp. 74–80.

ABSTRACT: This paper describes a practical test that enables the metal finisher to detect changes in a standardized plating and baking procedure. Low-cost test strips are processed with the work through the complete cycle. Changes in their median time to fracture measures the degree of hydrogen embrittlement. A simple timing device is described that will automatically record the median breaking time for a set of five specimen. Median fracture times can be correlated to the hydrogen content of the strip.

KEY WORDS: hydrogen embrittlement, failure, cadmium coatings, metal finishing, plating, baking

Twelve years ago, the Forty-Seventh Annual Convention of the American Electroplaters' Society was held in Los Angeles, Calif. A portion of the technical program was a symposium on Hydrogen Embrittlement in Metal Finishing. Dr. Snavely, in his paper "Measurements pertaining to Hydrogen Embrittlement" concluded with the following statement. "Where some hydrogen permeation is allowable, but an effort is to be made to remove the embrittlement effects, a shop test might be based on some simple modification of the stress rupture test. Devising this simple test is a challenge to everyone interested in minimizing delayed failures caused by hydrogen."

This testing procedure, I will describe, was initiated by the Wallace Barnes Division of the Associated Spring Company and developed in conjunction with Luster-On Products, Inc. The method is the outgrowth of a procedure used for many years in the in-plant testing for adequate relief of hydrogen embrittlement. Test strips are cleaned, plated, and baked along with production lots of precision springs and the performance of the test strips used to assure compliance with the standard procedures for the control of hydrogen embrittlement. We feel that this practical test measures the embrittling effect of hydrogen directly and meets the challenge for a simple stress rupture test.

---

[1] Technical director, Luster-On Products, Inc., Springfield, Mass. 01109.

Test Specimens

The test specimen consists of a ½-in.-wide strip of spring steel, 0.70 to 0.80 percent carbon grade, 7½ in. long and 0.022 in. thick. In testing, these strips are held in a bent configuration with the ends between two fixed surfaces 3½ in. apart so that the strip assumes the shape of an arch. A static stress is created at the apex by this procedure, and the time delay to fracture of a plated spring is considered a measure of the degree of hydrogen embrittlement.

Experimental Procedures

To increase the sensitivity of the strip, a variety of stress raising devices were evaluated. These included a round punched hole, half round notches at the edge, a sharp V-notch across the width, a partially sheared out button, an extended button, an edge notch which simulated deep drawing folds or cracks, and a U-shaped cut sheared with the tab left in place. The partially sheared U-shaped tab was selected because of the adaptability to mass production as well as its sensitivity. The tab is made with slotting punch ground at a 6 deg angle, and the punch only partially enters the die. The test strips are manufactured under carefully controlled conditions with particular emphasis on minimum hardness variation. It was found that two of these tabs, arranged as shown in Fig. 1, improved the reproducibility of the test. The test strip must be bent so that the tabs project from the outside surface of the arch.

Figure 2 shows the general configuration of the strip during the test. Note that there is no movement of the ends of the strips. Figure 3 shows the breaking time plotted on the logarithmic ordinate for 100 individual strips from the same production lot that were cadmium plated and baked at the same time.

Conditions of Test

Rockwell Hardness C Scale, HRC 51 Plating Solution (barrel)

Cadmium metal	2.4 oz/gal
Sodium cyanide	13.0 oz/gal
Sodium hydroxide	2.9 oz/gal
Sodium carbonate	5.9 oz/gal
Metallic brightener	present
Temperature	75° F
Time	30 min
Average current density	10 ASF[a]
Baking temperature	375° F
Baking time	2 h

[a] ASF = amperes per square foot.

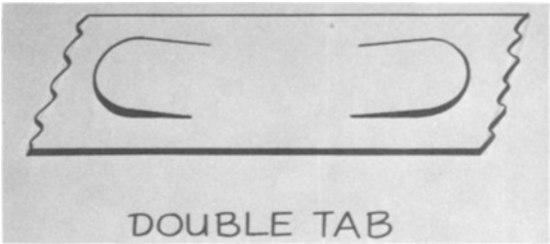

FIG. 1—*Tab configuration.*

The breaking times are arranged in ascending order. For these particular sets of specimens, the minimum time was 15 min, and three specimens did not break within 1000 min. The median time was 47 min. That is, 50 specimens broke before 47 min, and 50 broke after 47 min. There is a wide range of breaking times, and any individual value cannot be compared with another individual breaking time selected from another sets of specimens produced or processed under different conditions.

Repeated testing has indicated that the median breaking time of a set of specimens is significant and can be used for comparative purposes. It has been determined that five is the minimum number of strips that must be processed and tested at one time so that the median time to fracture is significant.

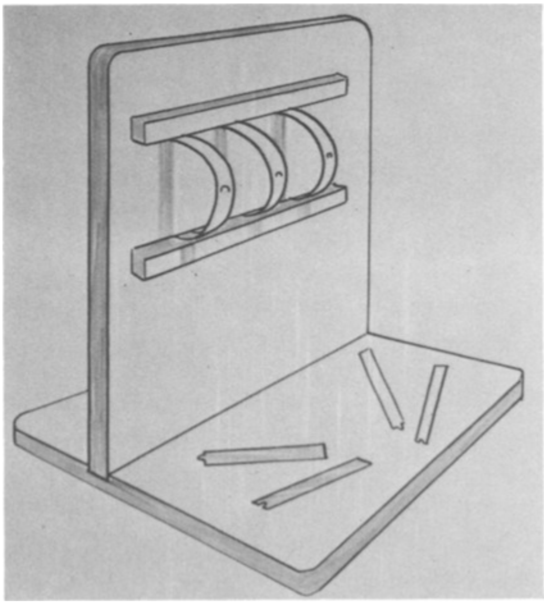

FIG. 2—*Configuration of strips under test.*

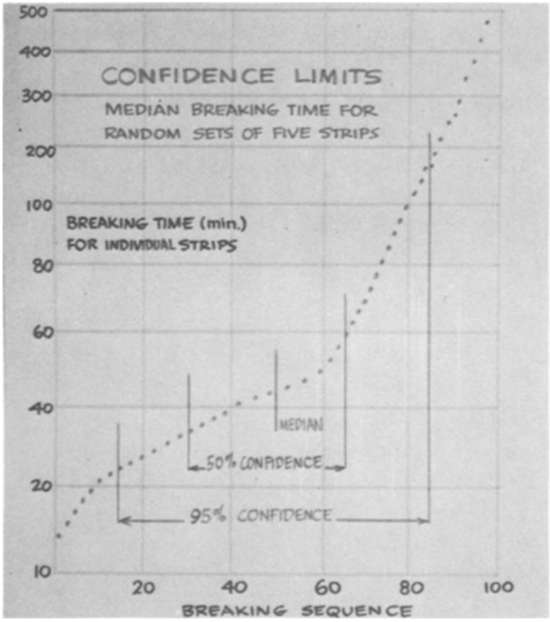

FIG. 3—*Breaking time of 100 individual strips processed at the same time.*

Let us for the moment consider 100 articles that are numbered 1 to 100. It can be shown from a table of random numbers that if we select a large number of sets of 5, the median number of the set will be between 32 and 69, 50 percent of the time and between 14 and 86, 95 percent of the time. Translating these values to those measured for the set of 100 strips, we find that if the true median time to fracture is 47 min, 50 percent of the time, the median of a set of five specimens will be between 33 and 70 min, and 95 percent of the time it will fall between 26 and 175 min. Any values outside these limits may be considered to be a significant change.

In other words, once a cleaning, plating, and baking process has been established and a median time to fracture determined, breaking times less than half or more than four times the median should be interpreted as measuring a definite change in the processing cycle.

Figure 4 shows a timing device that has been developed to record the median fracture time for a set of five strips. Various configurations are available that will test up to ten sets of five strips at one time. Each set is sensed electrically every minute to determine how many individual strips are unbroken. If the number is three or more, a counter adds one minute. This process continues until the third strip breaks regardless of the sequence. At this point, the counter will no longer count, and the median time to fracture of the set is recorded.

The strips are inserted into individual compartments with the apex innermost so that when they break, the specimens will be directed toward the rear of the enclosure. The median time to fracture can be correlated with the average hydrogen content of the set of strips tested. Each production lot of strips is evaluated for their sensitivity and a factor determined so that data from different lots of strips may be compared.

Figure 5 shows the median breaking time plotted on a logarithmic ordinate versus the average hydrogen content of the five strips of the set plotted on the arithmetic abscissa. The hydrogen values were determined by the hot extraction method.

All data shown are for barrel cadmium plated strips that had been baked for various periods of time to produce different hydrogen levels. Note that the median breaking time increases as the average hydrogen content decreases. There appears to be a straight line relationship between the log of the median breaking time and the average hydrogen content. The three sets of data shown were obtained from three different lots of springs. The harder springs exhibited a shorter median breaking time for the same amount of hydrogen present.

The right hand line is HRC 47, the center HRC 51, and the left HRC 54. Note that a 2 to 3 ppm change in hydrogen content produced a tenfold change in breaking time. At HRC 51, strips baked for 1 h at 375° F after cadmium plating showed an average time of 7 min, those baked for 2 h averaged around 20 min, and those baked for 3 h broke at around 100 min. By changing the hardness of the strip we can change the sensitivity of the strips and cover wider range of hydrogen levels.

The testing procedure described provides the plater with test strips that can be evaluated rapidly for their degree of hydrogen embrittlement. They represent a consistent and predictable metallurgical input to the

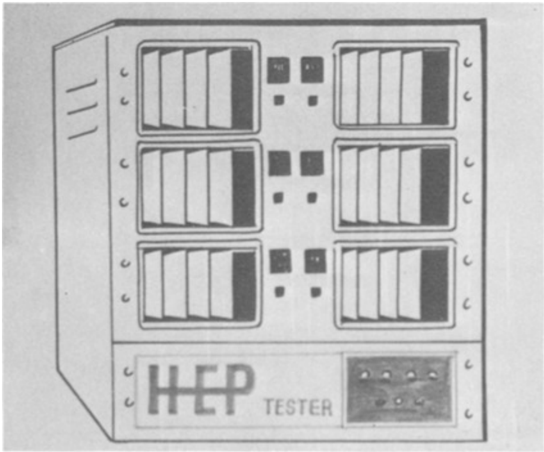

FIG. 4—*Automatic timing device.*

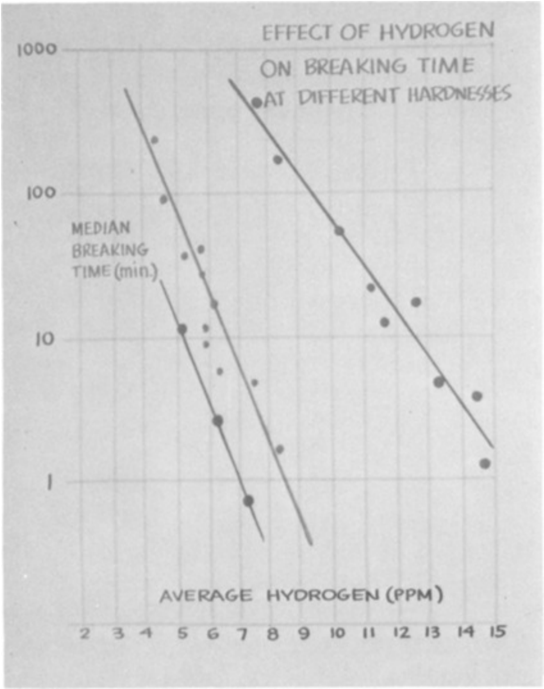

FIG. 5—*Relationship between hydrogen content and breaking time.*

metal finishing process, and changes in their breaking time can be used to detect changes in the processing cycle.

Results

In practice, the strips are utilized in the following manner. A metal finishing process is standardized, and the strips are processed through the complete cycle with the production work. This includes the cleaning, plating, and baking. The median breaking time is determined and recorded. Sets of test strips are then processed periodically along with the work and their median fracture times compared to the standard. Depending on the quantity of strips purchased at one time, the cost for a set of five strips will be between $1.00 and $2.00. Normal breaking times for production control seldom exceed the 3 h commonly specified for a baking time after cadmium plating. Thus, the tester is capable of keeping up with the batch baking process.

If the median breaking time for any one lot is less than half or more than four times the standard, then the plater knows that something has changed in his cycle that has an effect on hydrogen embrittlement. On the other hand, should hydrogen embrittlement be encountered in production parts, and the test strip results are normal, it may be surmised that the cause of the embrittlement is other than the plating process. For example, the hardness of that particular lot may be greater than normal, and a metallurgical examination of the basis metal would be indicated.

The median breaking time of these strips measures the degree of hydrogen embrittlement of the strips themselves, but these strips cannot predict the presence or absence of hydrogen embrittlement in any other part of the same or different composition; the same or different configuration; or the same or different hardness. However, they do represent a method for assuring consistency in the total metal finishing process and offer assistance in case of difficulty by indicating whether the problem is one for the plater or the metallurgist.

Testing for Hydrogen Pickup During Processing

Hydrogen Detection Test Methods

S. C. Lawrence, Jr.[1]

Hydrogen Detection Gage

REFERENCE: Lawrence, S. C., Jr., "**Hydrogen Detection Gage** " *Hydrogen Embrittlement Testing, ASTM STP 543*, American Society for Testing and Materials, 1974, pp. 83–105.

ABSTRACT: Hydrogen measurement systems for monitoring plating and corrosion embrittlement hazards are described, as is the new sensor for measuring molecular hydrogen levels at low partial pressures. Correlation between the first two and embrittlement thresholds of 260 to 280 ksi 4340 sustained load specimens of varying geometry are presented. Correlation measurements with the latter type have been shown feasible with salt spray, seawater acetic acid tests, field exposure, as well as exfoliation corrosion susceptability. Test procedures for both types of sensors and discussion of correlation data are given.

KEY WORDS: hydrogen embrittlement, reembrittlement, stress corrosion, surface activation, oxides, permeability, hydrogen poisons, palladium, steels, vacuum probes

Nomenclature

HP	Hydrogen pressure peak
λ	Time from *HP* to *HP*/2
γ	Time from probe in oven—oven on—to *HP*
HMG	Hydrogen measurement gage—electronic system used with steel probe
CMG	Corrosion measurement gage—electronic system used with palladium alloy window
H/CMG	Hydrogen/corrosion measurement gage—combines HMG and CMG features
HDP	Hydrogen detection probe—metal shelled vacuum hydrogen sensor with ion gage
GDP-H	Gas detection probe—hydrogen. HDP with palladium alloy hydrogen window
window	Hydrogen permeable section of probe

---

[1] President, Lawrence Electronics Co., Seattle, Wash. 98166.

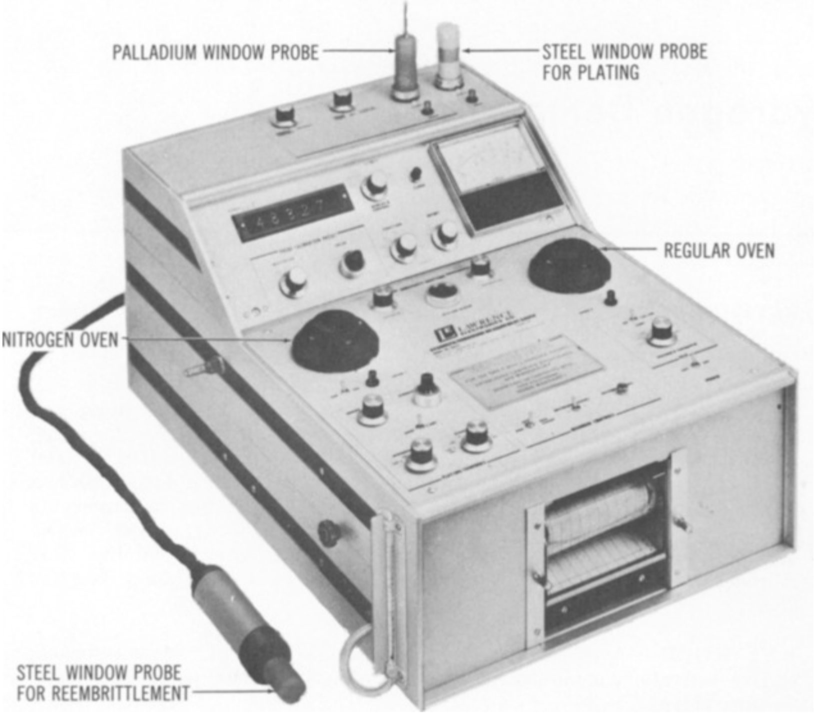

FIG. 1—*Lawrence hydrogen/corrosion measurement gage-5.*

LHE Cd	Low hydrogen embrittlement cadmium, a high current density cyanide cadmium bath
$I_{H/1}$ h	Hydrogen pressure/1 h
HP_c	Calibration $HP/100$
λ_c	Calibration $\lambda/40$
$I_{\gamma c}$	Calibration $I_{\gamma}/100$. Integral of hydrogen pressure to its peak value, divided by 100

This paper is a state of the art plus a feasibility one concerned with hydrogen measurement devices or gages using 1020 steel and palladium alloy vacuum probes as sensors. Some of the material presented, therefore, is old, while some of it is new. Measurement of probe sorbed hydrogen evolving from plating, corrosion, or from metals that have themselves absorbed hydrogen is discussed. All data presented have been derived from measurements made with Lawrence hydrogen/corrosion gages and probes (Fig. 1).

Early measurements and reports were qualitative only [*1–6*],[2] since the

---

[2] The italic numbers in brackets refer to the list of references appended to this paper.

probes were not calibrated for either their hydrogen pressure or permeation characteristics. The exact effects of exposure temperature were not known, and the ion gage pumping of the probe was ignored. Recent work has shown that this normal pumping rate is higher than 50 probe volumes of hydrogen per second and cannot be omitted from calculations if data are to become quantitative meaningfully. Temperature effects are known and included in calculations.

Successful correlations of probe hydrogen pressure signals with embrittlement thresholds of high-strength steels have been made using stressed 4340 O-rings, notched C-rings, and notched tension specimens [*3*, *5*, *7–10*, *17*]. Steel strength levels for the tests were in the 260 to 280 ksi range.

Low hydrogen embrittlement cadmium plating baths (LHE Cd) have been gage controlled to reduce embrittlement hazards since 1960 [*1–17*]. Also, reembrittlement of cadmium plated stressed high-strength steels by exposure to materials such as alkaline cleaners, carbon removers, paint strippers, deicers, and the like have been reduced by screening such materials with gage tests of LHE Cd plated probes since 1960 [*1–9*, *18–20*]. Many individual airline specifications require gage use for both application areas.

Development of an ultrasensitive molecular hydrogen detection probe has permitted detection of external hydrogen partial pressures in the 10^{-8} torr range. Reduction of effective probe ion pumping by a factor of 100 has improved the signal-to-noise characteristics of the gage significantly. Preliminary findings are that gage measurements of hydrogen evolving from short-term corrosion reactions in a aqueous media have been correlated with salt spray, seawater acetic acid tests, field exposure, and with exfoliation corrosion predictions of the EXCO test for aluminum alloys [*21*].

Limited additional tests have shown that the probe can also be used to detect hydrogen effusing from high-strength 4130 steel at 20° C after its exposure to corrosion and from titanium and zirconium at 300° C. New techniques for the differentiating of hydrogen in steel from that in the plate at the end of a plated probe's reembrittlement test are discussed. More meaningful probe correlation with stress rupture tests are, therefore, possible.

Scope

Application of hydrogen measurement system techniques for the reduction of plating and reembrittlement failures of similarly exposed high-strength steel parts is discussed. This indirect method of control uses signals from a steel shelled vacuum probe's ionization gage. While neither the precise hydrogen content nor the hydrogen permeability of parts coplated with the probe are determined, probe signals are being successfully used to prevent plating caused embrittlement of such parts. Further material on this is included in the discussion section.

When direct hydrogen in metal data is required, electronic signals from probes having a palladium alloy hydrogen window are used. Molecular hydrogen concentrations in metal corroding liquids are also measured.

Reproducible probe surface preparation is one of the keys to the obtaining of meaningful data. Precise timing of each measurement operation is another. Proper control of all pertinent thermal conditions is probably the single most important parameter. Measurement technology is detailed in Appendix I. Detailed procedures for calibration and use of both probe types are included in Appendix II.

Significance of Test

Tests with the steel probe have been used to rapidly measure embrittlement hazards to high-strength steels by plating or reembrittlement reactions [*1–22*]. This rapidity decreases work flow time in plating processes, since delayed sustained load failure no longer need be the sole criteria for acceptance or rejection of parts. Rework has been substantially reduced [*10*].

Probe hydrogen sensitivity is significantly greater than that of micromanometers sometimes used for corrosion or hydrogen-in-metal analysis. An additional probe advantage is that its window is permeable only by hydrogen and its isotopes, so that no manometric corrections are needed for other gases.

Time required to make embrittlement, reembrittlement, and corrosion tests is significantly less than that for stress rupture or salt spray tests and is comparable for hydrogen-in-metal tests. Cost per test, including straight line five year depreciation can be as low as $5.00 each for 400 tests annually. This compares favorably with the dollar cost of individual stress rupture specimens. Further cost advantage is gained since normally 2 gage tests rather than 3, 4, or 16 stress rupture tests are required (Fig. 2).

Experimental Procedures (see Appendix II)

Several critical parameters must be controlled in order to avoid measurement errors with either probe type. Primarily these are proper surface preparation, control of exposure temperature, control of oven heat level, and adherence to the time sequence specified for measurement, Appendix II.[3]

Surface Preparation

Steel Probe—Contaminants left on the probe hydrogen window from its last use must be removed. For ammonium nitrate cadmium stripping, 2 min rinsing in 2-gal/min spray at 50° C is adequate. Silicates remaining

---

[3] Instruction Manuals: HDG/HMG and CDG/CMG, available on request at Lawrence Electronics Co.

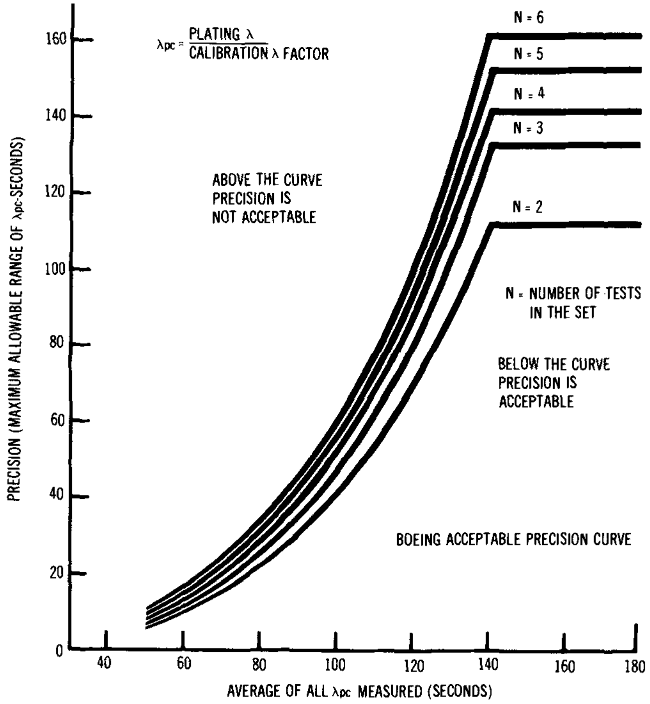

FIG. 2—*Hydrogen measurements—low-embrittlement cadmium or cadmium-titanium alloy plating.*

after reembrittlement testing of cleaners and the like are removed by immersing probe window in 40 percent sodium hydroxide (NaOH) at 90° C for 20 min. Acetone is used to remove certain organic residues. Cyanide levels are reduced satisfactorily by rinsing the probe in alternate hot (50° C)—cold (10° to 15° C)—hot water in 2-gal/min water spray.

During electronic outgassing, the window becomes oxidized. If these oxides are not all removed, a hydrogen entry blockage can be observed, for example, during calibration at 1 ampere per square decimeter (ASD). In this case, no change is observed in the measured *HP*-value, even though the probe shell is made thinner with each successive abrasion. However, during low embrittlement plating, at 6 ASD, the *HP*-value does increase. Thus when measured plating values are normalized by applying these calibration data, the normalized data are inconsistent.

It has been found necessary to abrasively blast the 12-cm^2 regular probe hydrogen window so that at least 50 mg of metal/oxide are removed. Where large window probes (Fig. 3) are used, as for reembrittlement tests, at least 140 mg should be removed. In best usage, the selected abrasive is used one time only; the nozzle is kept at a fixed distance from the probe which is rotated at 120 rpm during blasting. In our own system, we use

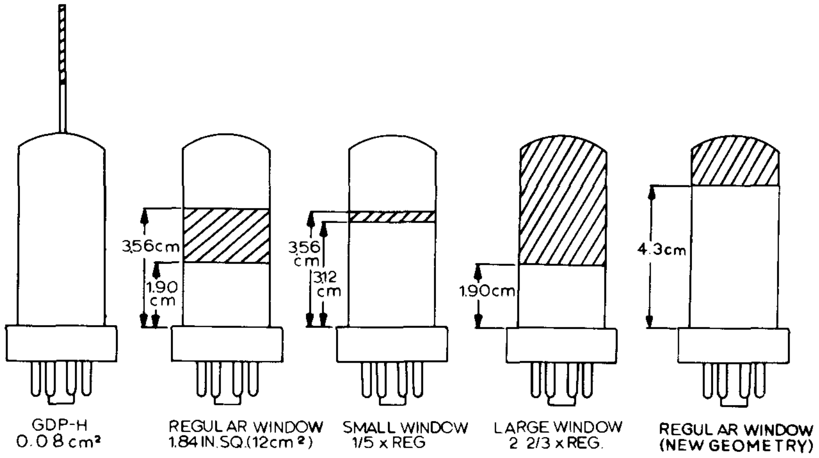

FIG. 3—*Probe window size.*

85 psi propellent pressure, 1 lb of aluminum oxide (Al_2O_3) 180 mesh grit, gravity fed into the blast gun during 60 s. Furthermore, nozzles are rotated 90 deg after each 10 uses and discarded after 40 to minimize nozzle variation due to erosion. For large window probes two 1-min blast cycles are used, the first at a 45 deg angle from the probe top edge; the second normal to cylindrical surface.

In our laboratory, when oil free, semidry air is used for blasting, hydrogen is introduced by the reoxidation of the steel. At pressures employed, the observed blast hydrogen is 10 percent of that introduced by the calibration. As shown earlier,[4] the total hydrogen introduced by blasting is not measured, since its highest concentration is on the probe shell outer surface. A more representative figure can be obtained by subtracting the hydrogen introduced during a single blast plus calibration from that measured for a double blast plus calibration.

Hydrogen introduced by abrasive cleaning can be reduced at least a hundredfold by using dry nitrogen as the abrasive propellant. However, the pneumatic tubing used in the blast system should be used only for nitrogen. When high pressure moist air is used, the tubing absorbs moisture, which is not removed even when continuously purged as much as 16 h with dry nitrogen at 85 psi delivery pressure.

Palladium Window Probe—The alloy used is soft, so that normal high pressure abrasive blast cleaning is impossible. Adequate activation has been, however, achieved by the technique of finger polishing with hypochlorite cleansers described in Appendix II.

[4] Lawrence, S. C., Jr., *Proceedings*, First Hydrogen Corrosion and Embrittlement Symposium, Vol. 1, 1967, p. 51. Available on request at Lawrence Electronics Co.

Oxygen access to the palladium surface after activation and test exposure must either be eliminated or kept to a minimum, since oxygen becomes tightly bound to active hydrogen absorption sites, blocking entry, or else will react at the catalytic palladium surface to form water with previously absorbed hydrogen. Oxygen access to the palladium prior to test immersion in aqueous solution can be limited by rapid transfer of the water wet palladium surface obtained after activation rinse and by rapid transfer from test solution to rinse, to the cold nitrogen stream oven. Probe insertion into a hot oven must be avoided for this accelerates the oxygen–hydrogen reaction.

In anaerobic gas test environments, however, the palladium probe tip should be dry to prevent oxidation reactions on the test specimen. In this case, a small amount of hydrogen is electrodeposited on the palladium window prior to the probe's insertion into the test cell to occupy active sorption sites. The cell is purged 20 times with 30-psi nitrogen before closure to reduce oxygen partial pressure. The probe is then electronically outgassed until hydrogen partial pressure in the cell is at 3×10^{-8} torr or less. Hydrogen partial pressures in the cell are measured by first heating palladium tip to 250° C and then introducing the hydrogen to be measured, either in gas mixtures or by heating a cell-enclosed test specimen.

Specimen Surface Effects

Whenever measurements of hydrogen desorption from metals are made, a limiting factor is often the surface of the specimen itself. Where this is occluded by oxides, little or no hydrogen effusion may be observed. We have observed this both in the case of low-alloy steels and titanium. A direct correlation between the degree of oxidation of steel after outgassing at 200° C and measured hydrogen effusion has been observed, with the heavier oxides yielding less hydrogen permeation. In the case of titanium, which oxidizes easily, no hydrogen effusion at all was observed until the 6Al-4V alloy was nickel plated. Where the plating was pinhole free, the hydrogen measured exceeded that from the nickel plate itself by a factor of greater than 1000. Where imperfect plating was used, hydrogen effusion was reduced significantly. Similar techniques for plating steel with nickel or palladium have been reported by König et al [*23*].

A large interference with measuring hydrogen in plated steel can be caused by permeability limitations of the plate itself. This, in turn, is changed by elevated outgassing temperatures [*24*]. Further blockages are observed in the presence of cadmium oxide when silicates, adsorbed on the cadmium plate during test immersion in alkaline cleaning materials, dehydrate and form a hydrogen impermeable "waterglass." Examples of measurement of corrosion hydrogen sorbed by 4130 steel during 11.5 min corrosion in 10 percent hydrochloric acid (HCl) are shown in Case 1.[5] The effects of plating on hydrogen transfer from base metal to atmosphere are described in Case 2.[5]

Solution Temperature Effects

When probe hydrogen sorption from the standard 5 percent NaOH + 5 percent sodium cyanide (NaCN) solution is measured at 1 ASD, *HP*-values double with each 20° C rise in solution temperature.[6] These data parallel that reported by Beck et al [*25*], where it is shown first that a rapid increase in hydrogen embrittlement occurs with increasing surface coverage of CN^- groups, and second that CN^- coverage also increases exponentially with increasing temperature when specimens are polarized cathodically at 10 mA/cm^2 in a 0.02 *M* NaCN + 0.1 *M* NaOH solution.

The Arrhenius plot obtained for probe hydrogen sorption in cyanide solutions suggest a diffusion controlled process. It is suggested that the reaction observed with temperature is controlled by the rate at which hydrogen diffuses into the steel from active sorption sites. Where the diffusion rate is low, more time is available for a recombination reaction to occur at the site, thus limiting hydrogen sorption.

Most, but not all, corrosion reactions increase with temperature. Details of one variation from the norm are given in Case 3.[5]

As had been shown, temperature affects hydrogen sorption greatly. It is not possible to maintain probe hydrogen window temperature constant with the probe turned on, because power dissipation within the probe heats it. Best control is achieved by first thermalizing the probe in dry spectrophotometric acetone to test the temperature and then exposing it at that same temperature to calibration, plating, or reembrittlement test conditions.

Oven Heat Level Effects

To quantify probe hydrogen sorption, hydrogen in the shell is driven into (and out of) the probe at a net input greater than the probe hydrogen pumping rate (Appendix I). When the hydrogen flow into the vacuum equals the removal rate from it, a plateau or hydrogen pressure peak (*HP*) is observed, followed by a pressure decrease (Figs. 4 and 5).

If the oven temperature is increased, and the cavity housing the oven is kept at the same temperature, the *HP*-value increases, and the time between *HP* and *HP*/2, (λ), is shortened proportionately. Their product remains essentially constant.

On the other hand, if the oven cavity temperature is reduced, the oven, following Newton's law of cooling, loses heat more rapidly. Since the oven

---

[5] Hydrogen case histories. Available on request at Lawrence Electronics Co.

[6] Lawrence, N. K., *Proceedings*, First Hydrogen Corrosion and Embrittelment Symposium, Vol. 1, 1967, p. 21. Available on request at Lawrence Electronics Co.

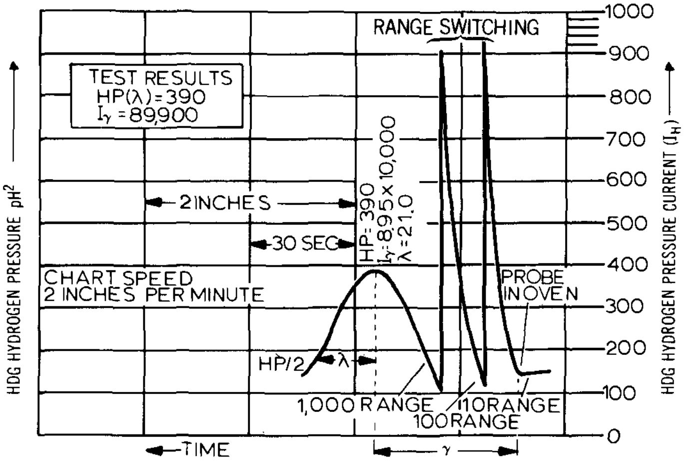

FIG. 4—*Probe* HP (λ) *curve.*

is temperature controlled, this extra heat loss rate causes little change in metered temperature. However, the oven can lose heat more rapidly in this state when a probe is inserted, since more of the additional energy required is lost to the surrounding cavity than to the probe. The net result observed is a decrease in *HP*-value and increase in λ.

This effect is important and can cause like exposure measurement differences of *HP* as much as 300 percent. The result is controlled effectively, either by using the integral of hydrogen pressure to its peak rather than either *HP* or λ, Case 4,[5] or (1) by leaving the oven and associated equipment on in the cavity at all times and (2) by cycling the oven at predetermined times before probe insertion into the oven to establish reproducible oven heat levels. With older gages, cycling is accomplished by removing the oven plug for 10 s. With newer ones, programmed full power is applied. The cycling found satisfactory is:

1. 30 min prior to probe insertion into oven.
2. 390 s prior to probe insertion into oven.
3. 10 s prior to probe insertion into oven.

These effects are observed primarily with the steel probe because with the palladium window probe, the measurement oven cycle starts at 25° C, rising to 250° C in 2 min. There, when the gage is left on continuously, the palladium window probe measurement reproducibility is good [*21*].

Time Effects

Hydrogen is being continually lost from either probe type following its sorption. Losses greater than 90 percent have been observed if 16 h elapse between charging and measurement on bare steel. These effects are multiplied manyfold with the palladium window probe where the catalyzed

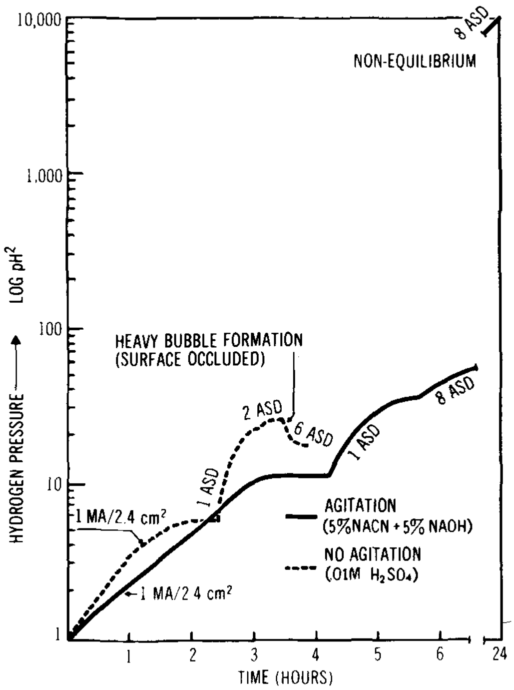

FIG. 5—*Probe hydrogen plateaus.*

hydrogen plus oxygen make water and the reaction rapidly pumps hydrogen from the probe. For example, doubling the transfer time in air between test solution and oven from 20 to 40 s reduces measured hydrogen by one half. For reproducible results, close control of time sequences is, therefore, imperative.

This time control also includes, for example, the length of time a steel probe is left on prior to oven insertion. Shorter times reduce hydrogen losses due to ion pumping, make the probe cooler at oven insertion time, and produce significantly longer λ values, Case 5.[5]

Discussion

Stress rupture tests determine only embrittlement tolerance of the specially selected sensitive stress rupture specimen itself, provided, of course, that the specimen has been properly machined, heat treated, activated prior to hydrogen charging, baked after exposure, and loaded to establish desired triaxial stress levels in it. As mentioned by Hyter at this meeting on "Standardization of Test Methods for Hydrogen Embrittlement," different heats as well as different pours from a given heat have different hydrogen embrittlement sensitivities. Particular care is taken to select the most sensitive lots of steel for making the stress rupture specimens.

In addition, time and costs required for such tests are both large. Nevertheless, in spite of all these adverse parameters, stress rupture tests have been used for many years for embrittlement control purposes. Less sensitive heats of steel and less severely stressed production parts are assumed to be safely processed if the process does not cause failure of the stress rupture specimens. No assumption, of course, is made that each part being so controlled has the same embrittlement sensitivity as the specimen, nor that it will receive precisely the same hydrogen or plating per square centimeter in all areas as the specimen, either.

Hydrogen gage signals have been correlated with embrittlement thresholds of stressed, sensitive high-strength steel rupture specimens. Two factors are measured: the hydrogen sorption per square centimeter of the probe's hydrogen window and the hydrogen permeability of plating applied to that window. These correlation studies have determined gage signals for embrittlement [*5–10*].

If the process produces gage signals that are below those known to cause stress rupture failures of similarly exposed sensitive test specimens, then the process is assumed to be also nonembrittling to less sensitive steel parts. This is analogous to criteria applied to stress rupture test controls. It should be observed, however, that probe data cannot be extrapolated upwards to higher strength levels than those tested, or extrapolated sideways to other steel types at the same strength levels.

The degree of hydrogen embrittlement of steel parts properly manufactured and processed up to the actual plating is related to how much hydrogen is absorbed by the part during plating and how easily this hydrogen can be removed by post-plate baking. Regardless of metallurgical conditions, hydrogen sorption is increased when metallic contaminants are coplated, because of the freshly created galvanic cells [*26*]; by the presence of certain "poisons," such as cyanides, arsenites, etc. [*9, 27*] by temperature [*25*]; by decreased current density [*6*]; and lowered plating efficiencies [*28*]; to name but a few. On the other hand, oxides on a surface reduce hydrogen sorption during low current density platings, while at the same time providing better plating permeability due to the noncomplete surface coverage of the steel by the plate. Certain organic impurities cause the crystal structure of the deposit to become finer grained, limiting hydrogen desorption during baking (Fig. 6).

All of these factors which can have adverse effects on processed parts produce significant changes in probe signals, when the probe is similarly exposed. Because of the extra hydrogen released by galvanic cells, due to the coplating of metallic impurities, the *HP*-values increase. Nickel contamination in a low embrittlement cadmium bath (as low as 15 ppm)

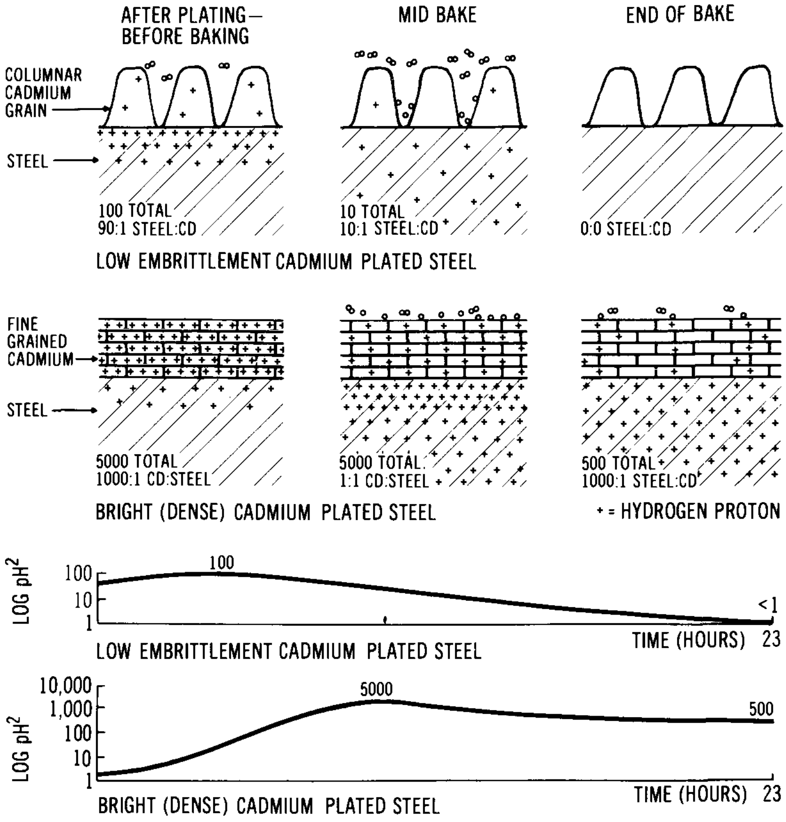

FIG. 6—*Hydrogen distribution in cadmium plated steel.*

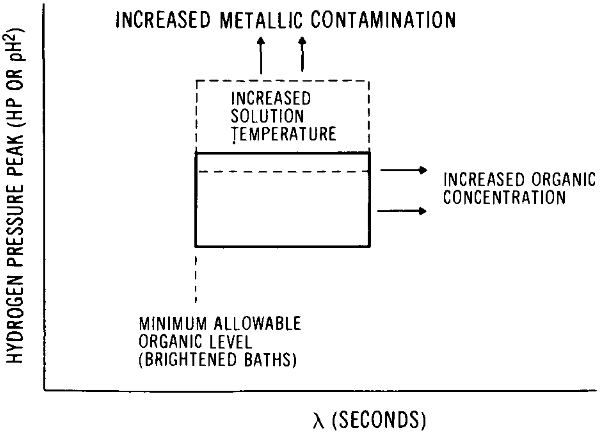

FIG. 7—*Organic, metallic, and temperature* HP (λ) *effects.*

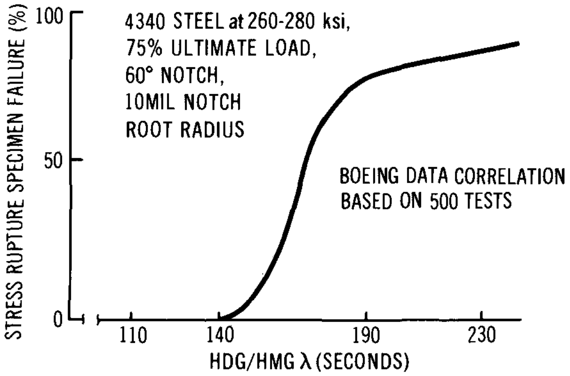

FIG. 8—*HDG/HMG* λ *(seconds) versus rupture percentage.*

introduces enough extra hydrogen to fail stress rupture tests [*29*]. Hydrogen levels three times normal, for 28 percent normal plating thickness, are introduced by aluminum [*30*]. The effects of both metallic and organic impurities on plating bath performance is shown in Fig. 7.

Surface roughness affects both hydrogen sorption and desorption by the probe and higher strength steels as well. The effects, of course, are magnified in the soft steel of the probe hydrogen window, but, nevertheless they have been correlated with variations in the stress rupture behavior of like-processed high-strength steel specimens, Case 6.[5]

Because the hydrogen measurement system can measure quantitatively and rapidly (Appendixes I and II) variations in sorbed hydrogen due to changes in the plating bath or process or both, it, therefore, can indicate the relative susceptibility of sensitive stress rupture specimens to these changes. The 500 tests by The Boeing Company [*10*] (Fig. 8) clearly show that variations in the permeability of plating applied to probes affect the percentage failures of 10 mil (60 deg) notch tension specimens made from 4340 steel of 260 to 280 ksi strength level, stressed to 75 percent of the ultimate. It would appear that the number of tests performed were statistically adequate enough so that The Boeing Company replaced stress rupture tests for LHE Cd plating control with their Boeing plating porosity meter (BPPM), whose mode of operation and use are roughly parallel to those described in this paper.

Airlines have used similar systems since 1962 for their overhaul plating of high-strength steel. Douglas has allowed hydrogen measurement gages to be used in lieu of stressed O-rings for low embrittlement cadmium plating control since 1963 [*11, 19*].

Results and Conclusions

Hydrogen measurement systems can be used to replace stress rupture tests for daily plating control and for reembrittlement testing after proper correlation has been obtained between steel probe signals and embrittlement thresholds of the selected type and strength level of this high-strength steel being monitored. In like manner, correlation has been demonstrated between palladium alloy probe signals and other methods used for determining corrosion rates or resistances to corrosion of metal systems.

As in the Federal Test Specification now under preparation, the hydrogen measurement systems should be accepted as an alternative to stress rupture tests for embrittlement and reembrittlement determination. The feasibility of using the gage for analysis of hydrogen in metals and prediction of corrosion resistance of "protected" steel fasteners has been shown. Standards for these latter two should be presented elsewhere than this particular volume as should those data relating to other plating baths [*22*, *31*, *32*].

APPENDIX I

Measurement Technology

Figure 9 is a schematic representation showing the operation of a hydrogen probe absorbing and desorbing hydrogen. Desorption occurs at an observable rate only when proper potentials are applied to the probe electrodes, ionizing the hydrogen present, and when the hydrogen concentration on the inner probe surface exceeds that on the outer. During hydrogen sorption, hydrogen permeates inward from the outer surface increasing the probe vacuum pressure.

These, however, are not the only significant parameters concerned with hydrogen measurement. Because during measurement the probe operates like an ion gage, hydrogen is pumped from the vacuum by sorption into the carbonized nickel

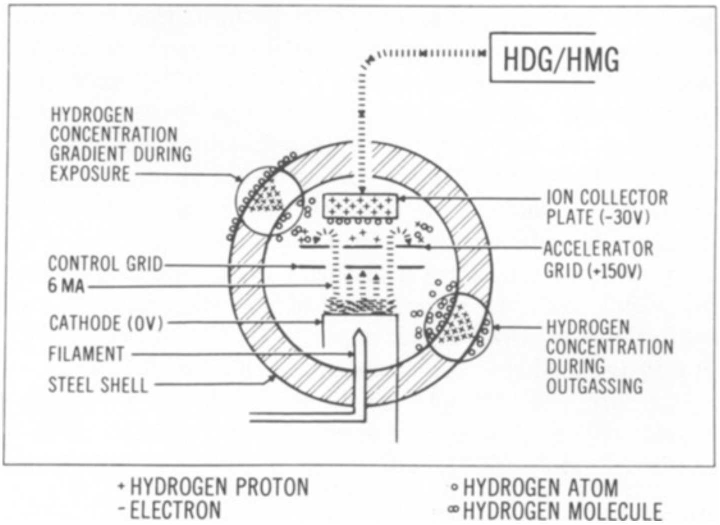

FIG. 9—*Hydrogen probe measurement schematic.*

ion plate at a rate directly proportional to pressure. This pumping rate is 50 probe volumes per second for the normal 6-mA ionizing electron current flow [*33*] and 750 volumes per second during 100-mA electronic bakeout, where the only hydrogen acceptor is the probe outer shell.

Additional effective hydrogen pumping is contributed by the barium getter, although this is reversible when the getter is heated above 200° C, as it is during electronic probe outgassing. It has been found that if two getters are used instead of one, the hydrogen sensitivity of the probe, as measured by calibration, is permanently cut in half, through the weight of hydrogen sorbed from all probe test exposures exceeds that of the barium itself.

Hydrogen adsorption on inner probe surfaces contribute additional pumping as does the outward permeation of hydrogen through the shell, discussed in the first paragraph. All of these effects can be expressed by the equation

$$\frac{dp}{dt} = \frac{dH}{dt} - \sum_{i=1}^{n} \frac{dg}{dt} \tag{1}$$

where

p = pressure,
H = hydrogen,
g = gettering (pumping), and
a = pumping constant.

The solution to Eq 1 is:

$$H = A\left[p + a\int_{t=0}^{t=t} pdt\right] \tag{2}$$

where A = scaling parameter.

Now while pressure, p, is normally measured in an analog manner, this analog signal can be converted to a digital one by an analog-to-digital type converter. Integration of the hydrogen pressure can be done in the same manner, yielding the further simplification

$$H = A(a + 1)\int_{t=0}^{t=t} pdt \tag{3}$$

By integrating the hydrogen pressure curve to its peak and multiplying the value obtained by appropriate constants, one has then a truly quantitative measure of hydrogen absorbed by the probe. This would then be presented mathematically

$$H = k\int_{t=0}^{t_{HP}} pdt \tag{4}$$

where

$K = A(a + 1)$ and
t_{HP} = time from probe insertion into oven to hydrogen pressure peak (HP).

This technique of course, does not measure all of the hydrogen initially deposited, since part of that will permeate outwards without ever entering the vacuum. Analogous behavior would be expected, for example, when plated high-strength steel parts are baked; through, of course, the ratios of hydrogen sorbed to desorbed would depend on parameters such as alloy, strength level, cold work, etc. for the latter.

APPENDIX II

Procedures

In all measurement procedures for systems using ovens to heat probes, it has been found necessary to "cycle the oven" at certain predetermined times before and during the measurement sequence. In older models this "cycling" consists of removing the oven plug for 10 s and then replacing it. In newer models an "activate" button turns oven full on for a programmed time, with the oven plug in place. In all procedures, the oven is cycled once at 20 min, 6½ min, and 10 s before the probe is inserted into the ovens. These maneuvers condition the oven so that its heat content is repeatable at the time the probe is inserted. They are not necessary with newer equipment, where the probe heats itself instead of being heated by an oven.

Calibration

Each probe has its own sensitivity to hydrogen pressure and permeability. Both change as the probe metal of the hydrogen window is activated and becomes thinner. The HP value increases with each use in a range between 4 to 8 percent. Smaller percentage decreases occur with the inverse partial permeability, λ, values. If these changes are not observed in successive calibrations, then there exists a strong possibility that the hydrogen access to the probe has been blocked by incomplete removal of window oxides or other contaminants. If changes greater than those just noted are seen, then it is probable that too much metal is being removed during activation.

Fortunately, the integral of the hydrogen pressure curve to its peak, I_γ, changes very little with time. Because of this, numerical comparisons of operator technique are made easily by comparing two successive calibration I_γ's.

Steel Window Probe

1. Probe window contaminants are removed.

2. Probe is heated electronically for 30 min by connecting plate and screen grid together at 180 V with respect to the cathode and by adjusting control grid potential so that a current of 100 mA flows. Total power dissipation is 21 W. Temperature at the probe top exceeds 220° C.

3. Probe is cooled to calibration temperature, masked, and the hydrogen window activated as follows:

Note—Probe can be weighed before and after activation to check metal removal.

(*a*) Rotate probe at 120 rpm with blast nozzle 6 in. from and normal to the hydrogen window center line.[7]

(*b*) Feed 1 lb of 180 mesh aluminum oxide (Al_2O_3) by gravity to blast nozzle.

(*c*) Blast at 85 lb pressure for 60 ± 10 s with nitrogen.[8]

(*d*) Blow off abrasion detritus with nitrogen (or air).

4. Connect probe to gage umbilical cord and make the base region water tight.

5. Spray rinse probe at a flow of 2 gal/min in 10° to 15° C water for 30 s.

---

[7] If larger hydrogen window than the regular 0.6-in.-high band is needed, then the whole probe surface beginning 0.75 in. and above the base flange may be used. This is commonly referred to as a large window probe. An additional blast but at 45 deg angle from probe center line and 6 in. from probe top edge is required.

[8] Moisture and oil-free air may be used, but extra hydrogen, roughly 10 percent of calibration total will be introduced. Oil will adversely affect surface cleanliness.

6. Electrodeposit hydrogen on the probe window at 1 ASD for 3 min from a standard calibration solution[9] at 25° C or other specified temperature.

(*a*) Use carbon arc rods (with any copper removed by immersion of the rods in concentrated nitric acid (HNO_3)) as anodes.

7. Spray rinse probe at a flow of 2 gal/min 30 s in 50° C water, 30 s in 10° to 15° C water, and 30 s in 50° C water.

8. Turn on probe for exactly 2 min before it is inserted into the gage oven.

(*a*) During this 2 min, dry the probe and check probe and gage electronic signals.

9. 110 s from step 8. The oven plug is removed (with newer equipment, apply full programmed power to oven also).

10. Insert probe into oven and turn hydrogen pressure integrator on.

11. Stop integration at HP. The integral valve is I_γ. Measure time from HP to HP/2.

By convention, an *HP*-value of 100 and λ of 40 s have been selected as standard. On the other hand, where I_γ values only are used for calibration, 100 has been chosen. The integration rate is 0.1 cpm at full-scale gage reading of 1, 1.0 cpm at 10, etc.

Example: Measured *HP* (λ) and I_γ: 187 (54) & 3.2874

Calibration factors: $HP_c = 1.87$

$\lambda_c = 1.35$

$I_{\gamma c} = 0.0329$

These factors are used to divide subsequent test results to normalize data obtained.

Palladium Window Probe

1. Remove probe window contaminants by finger scrubbing with an abrasive cleaner containing sodium hypochlorite, which chemically attacks the palladium.

2. Reduce probe vacuum pressure by electronically baking it in a 250° C heated air stream oven (2000 ml/min flow) until satisfactorily low measurement blanks are obtained.

3. Cool to immersion test temperatures.

4. Activate probe as in step 1, rinse with water.

5. Immediately insert it into calibration solution.[10]

6. Deposit hydrogen by making probe cathodic with respect to pencil "lead" anodes for 3 min at 1 mA.

7. Immersion rinse probe for 10 s in 70° to 80° C hot deionized water. Kimwipe dry.

8. Within 20 s from end of charging, insert probe into a nitrogen stream oven, initially at 25° C at 2000 ml/min flow.

9. Turn probe on for 2 min.

10. Apply programmed heat to the oven and turn on integrator.

11. Measure I_γ in the same manner as indicated for calibration of steel probe, step 11.[11]

Plating

The same general procedures are used as in Calibration, except:

6. Use appropriate plating solution.

---

[9] 50 g/l NaOH + 50 g/l NaCN in H_2O.

[10] Saturated K_2SO_4.

[11] The I_γ number obtained, divided by 100, is the calibration factor for the probe.

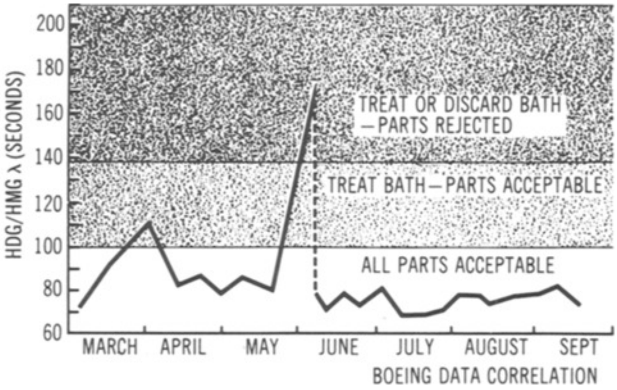

FIG. 10—*Control limits of low embrittlement cadmium plating.*

(*a*) Use appropriate anodes.
(*b*) Use appropriate temperatures.

Note 1—Plate to a minimum thickness of 10 μm (0.0002 in.) or to thickness required by specification being used (LHE Cd).

Note 2—Weigh probe before and after plating to determine bath efficiency.

Example 1: Safe plate

Calibration: $HP_c = 1.87$; $\lambda_c = 1.35$; $I_{\gamma c} = 0.033$

Plating: $HP_p = 273$; $\lambda_p = 60$ s; $I_{\gamma p} = 4.07$

Normalize: $HP_{pc} = \frac{273}{1.87} = 146$; $\lambda_{pc} = \frac{60}{1.35} = 44.4$ s; $I_{\gamma pc} = \frac{4.07}{0.033} = 123$

Note—Boeing control limits for λ_{pc} are shown in Fig. 10

Douglas control limits: λ_c (standard = 25 s) = 60 s max
λ_c (standard = 40 s) = 96 s max
$HP_{pc} = 1000$ max

Lawrence control limits: λ_{pc} as per Boeing

$HP_{pc} = 500$ max

Example 2. Embrittling plate

Calibration: $HP_c = 2.08$ $\lambda_c = 0.8$ $I_{\gamma c} = 0.02$

Plating: $HP_p = 780$ $\lambda_p = 240$ $I_{\gamma c} = 100$

Normalize: $HP_{pc} = \frac{780}{2.08} = 375$ $\lambda_{pc} = \frac{240}{0.8} = 300$ $I_{\gamma c} = \frac{100}{0.02} = 5000$

While normalized *HP*-values, HP_{pc}, are within limits, by all standards, normalized λ-values, λ_{pc}, exceed all limits. Probable cause of such results could be excess organic impurities in the bath, possibly coupled with too low current density. Low current density itself, by at least a factor of 6, will not affect measured λ, if the bath is laboratory clean, with minimum organic and metallic impurities.

Corrosion

General: The section is divided into two parts, one dealing with use of the steel shelled probe for reembrittlement testing of aircraft cleaning and maintenance materials, the other (dealing) with the use of the palladium window probe.

Reembrittlement

Large steel window probe is calibrated, electronically baked, low embrittlement cadmium plated, electronically baked, and thermalized in spectrophotometric grade acetone to avoid moisture containing air reacting with the active cadmium plate. This also avoids deposition on the cadmium surface of insoluble acetone residues found in commercial grades. Probe is then weighed to the milligram.

1. Attach probe to gage.
2. Turn probe on.
3. Integrate area under hydrogen pressure curve for 30 s from 2. The number obtained is the blank I_{30}. Larger numbers obtained later are proportional to hydrogen concentration in the steel portion of the cadmium steel corrosion cell. See Fig. 11. Record hydrogen pressure peak $I_{H/0}$ and integral value $I_{30/0}$.
4. Disconnect probe from gage and mask any nonplated areas with Teflon adhesive tape.
5. Immerse probe in solution to be tested and hold at 30° C for 1 h.[12]
6. Repeat step 3. Record hydrogen pressure peak, $I_{H/1}$ and integral value, $I_{30/1}$.[13]
7. Reimmerse probe in test solution for 5 more h.
8. Repeat step 3. Record $I_{H/6}$ and integral value $I_{30/6}$.[14]
9. Reimmerse probe in test solution for 18 h.
10. Cycle oven, rinse probe in warm water, with acetone if necessary to get a water-break-free surface.
11. Spray/rinse probe at a flow of 2 gal/min 30 s at 50° C, at 10° to 15° C, and at 50° C. Dry.

Note—All I_γ's used for these computations must be normalized, that is, divided by the probe calibration I_γ factor.

12. Repeat step 3. Record $I_{H/24}$ and integral value $I_{30/24}$.[15]
13. Rapidly turn probe on again for 80 s.
14. Pull oven plug (with newer equipment, apply full power to the oven).
15. 10 s after step 14, insert probe into oven.
16. Measure I_γ.[15]

Aqueous-Palladium Window Probe

1. Probe is calibrated, electronically baked, activated, and the I_{30} measurement is made to establish a blank.
2. 2.5 cm of the probe palladium tip is activated per step 1 in Calibration, Palladium.
3. Immerse specimen in test solution.[16]

---

[12] Paint strippers and other high vapor pressure corrosive materials should be tested at 20° C. Products used at temperatures higher than 30° C should be tested at use temperature.

[13] Boeing limits: $\Delta I_{30/0}$. $\Delta I_H = I_{H/1} - I_{H/0} \leq 0.05$.

[14] U. S. Navy limits: $\Delta I_H = I_{H/6} - I_{H/0} < 0.1$.

[15] Tentative limits (Lawrence) :$\Delta I_{30/24} = I_{30/24} - I_{30/0} = 1$. $I_\gamma = 100$.

[16] Specimen immersion in test is accomplished by hanging it with a Teflon cord through a masked hole.

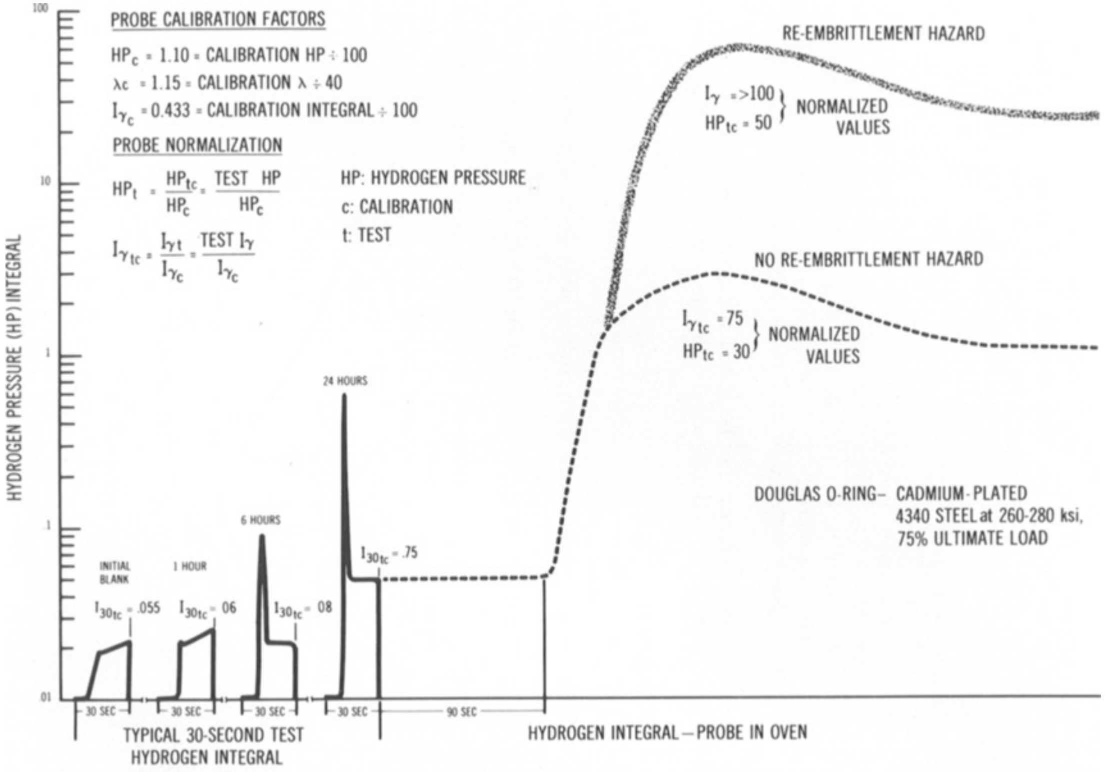

FIG. 11—*Hydrogen exposure integrals observed during probe exposure and subsequent heating.*

4. Connect probe to gage umbilical cord and immerse 2.5 cm of palladium tip in constant temperature corrodent solution[17] with metal system[18] to be measured.
5. Every 10 min, the I_{30} should be remeasured.
6. When $I_{30/10\ \mathrm{min}} \geq I_{30/0}$.
7. Remove probe and follow steps 7–11 of Calibration, Palladium.
8. Divide measured I_γ by Calibration I_γ factor. The number obtained is directly related to the corrosion which has occurred.

Hydrogen in Metals—Palladium Window Probe

General: Two measurement techniques are described briefly. One is a dynamic carrier gas test. The other is a static test.

Carrier Gas Technique

1. Probe is calibrated, electronically outgassed, activated, and placed in a nitrogen stream heated oven at 250° C.
2. Specimen to be tested is introduced into an anearobic test cell.
3. Input nitrogen flow is diverted to pass through test cell into nitrogen oven.
4. Test specimen is heated rapidly to desired temperature, producing hydrogen effusion.
5. This hydrogen is measured by integrating probe output signals to peak pressure and obtaining the I_γ-value.
6. Divide this value by the calibration I_γ (unless this has been already done electronically).

Static Test

1. Probe is prepared as in step 1 of Carrier Gas Technique but placed in a nitrogen charged hermetically sealed test cell with the specimen.
2. Probe palladium tip is heated to 250° C, with probe turned off.
3. Specimen may be heated or maintained at selected lower temperature.
4. I_{30} should be periodically checked until (as in step 6 of Corrosion—Aqueous Palladium) a suitable pressure increase is seen. Thereafter, the probe may be left on, and the increase in pressure should be integrated to its peak value, I_γ

Note—The high hydrogen pumping rate of 50 volumes per second of the probe may be reduced to 0.5/s by reducing the 6-mA ionizing cathode to screen electron current to 60 μA and increasing the gain of the electrometer ion current amplifier by a factor of 100. Different background pressures are observed when this low current technique is used, but these signals are reproducible for any one probe and may be electronically nulled out so that they do not mask pressure changes due to hydrogen.

References

[1] Lawrence, S. C., Jr. in *Technical Proceedings*, American Electroplaters' Society, 1960, p. 135.

[2] Lawrence, S. C. and Short, R., "Cadmium-Titanium Alloy Plating," Boeing Test Report T6-2404, The Boeing Company, Seattle, Wash., 1962.

[3] Lawrence, S. C., Jr., "The Hydrogen Detection Gauge for Use in Process Control and Corrosion Measurement," Boeing Document D6-8837, The Boeing Company, Seattle, Wash., 1963.

---

[17] Salt spray, immersion equivalent: 0.05 N H_2SO_4 + 3.5 percent NaCl solution. EXCO, immersion equivalent: 0.1 N H_2SO_4 + 7 percent NaCl solution.

[18] Specimen size, support hole diameter; surface cleaning prior to test, and edge masking should be made reproducible.

[*4*] Lawrence, S. C., Jr., U. S. Patent Nos. 3,241,056, 3,257,841, 3,258,683, 3,357,903, and 3,408,129.

[*5*] Hyter, W. H., "The Lawrence Hydrogen Detection Gauge," LR-AD-1575, Douglas Aircraft Div., McDonnell Douglas Corp., Long Beach, Calif., 1962.

[*6*] Sink, G. T., *Plating*, Vol. 55, 1968, p. 449.

[*7*] Fischer, P., "Evaluation of the Lawrence Hydrogen Detection Gauge for the Prevention of Hydrogen Embrittlement," Report No. NADC-MA-7151, Naval Air Development Center, Warminster, Pa., 1972.

[*8*] Jankowsky, E. J., "A Comparison of Various Test Methods for Detecting Hydrogen Embrittlement," Report No. AD-726165, Naval Air Development Center, Warminster, Pa., *Clearinghouse*, Announcements in Science and Technology, 1971.

[*9*] Beck, W., "Hydrogen Stress Cracking of High Strength Steels," Report No. NADC-MA-7140, Nos. 22, 23, 25, and 26, Naval Air Development Center, Warminster, Pa., 1971.

[*10*] Pritchett, L. D., "Hydrogen Control During Cadmium Plating of Steel," *Quality Progress*, Vol. 9, Dec. 1971.

[*11*] *DC-8 Overhaul Manual*, Douglas Aircraft Div., McDonnell Douglas Corp., Long Beach, Calif., 1963.

[*12*] "Special Cadmium Plating of High Strength Steel, DPS 9.28," Douglas Aircraft Div., McDonnell Douglas Corp., Long Beach, Calif., 1967.

[*13*] "Low Embrittlement Cadmium Plating," Specification BAC 5718, The Boeing Company, Seattle, Wash., 1969.

[*14*] "Low Embrittlement Cadmium Titanium Alloy Plating," Specification BAC 5804, The Boeing Company, Seattle, Wash., 1969.

[*15*] Jervolino, G. and Barndolini, F., "Control of Hydrogen Adsorption in Electroplating Processes," AGARD Conference Proceedings No. 64, Reference 9, AGARD-CP-64-70-NTIS, April 1970.

[*16*] Amano, R., *Jitsomu Hyomen Gigutsu*, Metal Finishing Society of Japan, Vol. 2, June 1972.

[*17*] Takada, K., *Jitsomu Hyomen Gigutsu*, Metal Finishing Society of Japan, Vol. 2, June 1972.

[*18*] Owens, C. E., *Soap and Chemical Specialties*, Vol. 51, Jan. 1970.

[*19*] 13-1 Service Bulletin, Douglas Aircraft Div., McDonnell Douglas Corp., Long Beach, Calif., 1963.

[*20*] "Qualification Testing of Airplane Maintenance Materials," Document D6-17487, The Boeing Company, Seattle, Wash., 1965.

[*21*] Fischer, P., "Applications of the Lawrence Corrosion Detection Gauge (CDG-2)," Report No. NADC-72251-VT, Naval Air Development Center, Warminster, Pa., 1972.

[*22*] Hyter, W. H., "Multiple Step Chromium Plating Hydrogen Embrittlement," LR-DAC-5322, Douglas Aircraft Div., McDonnell Douglas Corp., Long Beach, Calif., 1970.

[*23*] König, H. J., Lange, K. W., and Dahl, W., "Influence of Alloying Elements on the Diffusion of Hydrogen in Alpha Iron Between Room Temperature and 300 C," *L'Hydrogene dans les Metaux*, Ecole Centrol des Arts et Manufactures, Chatenay-Malabry, France, Vol. 1, 1972, p. 172.

[*24*] Rinker, J. G. and Hochman, R. F., *Corrosion*, Vol. 28, No. 6, June 1972, p. 231.

[*25*] Beck, W., Glass, A. L., and Taylor, E., *Journal of the Electrochemical Society*, Vol. 112, 1965, p. 53.

[*26*] Maja, M. and Spinelli, Pl., *Journal of the Electrochemical Society*, Vol. 118, 1971, p. 1538.

[*27*] Snavely, C. A. in *Technical Proceedings*, American Electroplaters' Society, 1960, p. 138.

[*28*] Kudzyartsev, V. N., *L'Hydrogene dans les Metaux*, Ecole Central des Arts et Manufactures, Chatenay-Malabry, France, Vol. 1, 1972, p. 253.

[*29*] Otto, Ed., personal communication, Air Canada, April 1973.

[30] Roth, H. P., *Plating*, Vol. 59, 1972, p. 765.
[31] Patterson, M., "A Study of the Lawrence Hydrogen Detection Gauge for Control of Production Electroplating Processes," WEPTASK RRMA 55 038/010 1/R1007 08 01, U. S. Navy Air Station, Alameda, Calif., 1964.
[32] Martin, R., "Hydrogen Gauge Control for Chromium Plating," Airlines Seventh International Plating Forum, 1971.
[33] Lange, W. J., *Physics Today*, Vol. 25, No. 8, 1972, p. 40.

K. B. Das [1]

An Ultrasensitive Hydrogen Detector

REFERENCE: Das, K. B., "**An Ultrasensitive Hydrogen Detector** " *Hydrogen Embrittlement Testing, ASTM STP 543,* American Society for Testing and Materials, 1974, pp. 106–123.

ABSTRACT: An ultrasensitive hydrogen detector is described which has a detection sensitivity of a few parts per billion in the gas stream. The detector's performance, range, and accuracy were evaluated by analyzing titanium standards from the National Bureau of Standards containing known amounts of hydrogen at the following levels: 32 ± 2 ppm, 98 ± 5 ppm, 215 ± 6 ppm. The fractional random error in the mean value of these standards at 95 percent confidence level was found to be ±5.01 percent, ±1.67 percent, and ±1.08 percent, respectively. Preliminary results of the hydrogen analysis of cadmium plated steel specimens heat treated to 260 to 280 ksi strength level when compared with the notched tension testing (failure) data show that the safe limit for (total or bulk) hydrogen concentration as measured by this technique is about 1 ppm. Results on forged steel specimens heat treated to 170 to 195 ksi level indicate that here the embrittlement failure can occur at levels exceeding 2 to 2.5 ppm. Testing costs are much lower compared to notched tension tests, and the results are reliable. The objective of this paper is to expose the readers to a new hydrogen detection system and (among its other applications) its use for studying the hydrogen embrittlement problem in high-strength structural materials.

KEY WORDS: hydrogen embrittlement, notch tests, cadmium coatings, plating, heat treatment, high strength steels, titanium alloys

The detrimental effects of hydrogen on various physical [*1*, *2*][2] and mechanical properties [*3*, *6*] of high-strength structural materials are well known to the scientific community. Once hydrogen enters high-strength steels and titanium alloys, these metals can lose their ductility and, depending upon the level of hydrogen, can suffer brittle failure when subjected to stress. This much studied but vaguely understood phenomenon is known to us as "hydrogen embrittlement" and is of primary concern to aerospace industries.

Hydrogen enters all metals in ionic form and diffuses interstitially in most metals. It may be absorbed by metals both during processing and

---

[1] The Boeing Company, Seattle, Wash. 98124.

[2] The italic numbers in brackets refer to the list of references appended to this paper.

when the finished products are in use. For example, it is well recognized that a plated steel part is embrittled as a result of being penetrated by the nascent hydrogen, produced during the plating operation as a side reaction at the cathode. Published literature [*6*] shows that few hydrogen determinations have been made on plated steel (for a specific plating) to correlate the quantity of hydrogen to the degree of embrittlement. In general hydrogen embrittlement and hydrogen determinations are still technological problems. The key to the solution of these problems depends in part on how reliably we can measure the hydrogen content in high-strength structural materials.

Based on several years of research effort, the Aerospace Group of The Boeing Company has been recently successful in developing an ultrasensitive hydrogen detector [*7, 8*], which can detect hydrogen concentrations of as low as a few parts per billion in a gas stream. This detector has proven its capability in successfully completing a number of National Aeronautic and Space Administration (NASA) programs which involved hydrogen measurements during welding of aluminum alloys [*9*], detecting trace amounts of surface hydrocarbon contamination (including contamination due to fingerprints) on specially treated aluminum alloy plates [*10*], and measuring hydrogen concentration gradients below the original surface of Ti8-1-1 alloys [*11, 12*]. In addition the detector has also been used on a variety of company research and development programs [*13, 15*] such as: (*a*) corrosion of substrate material of microelectronic components, (*b*) blistering on surfaces of alumium parts after certain fabrication operations [*16*], and (*c*) failure of pickled and anodized titanium parts after bonding [*17*].

This paper describes the results of a preliminary study of the hydrogen analysis of cadmium plated 4340 steel specimens heat treated to 260 to 280 ksi strength level. The results of the hydrogen analysis are compared with the notched tension testing and the Boeing plating porosity meter data. The porosity meter gage was used to control the porosity of plating and hence hydrogen introduction or retention in the test specimens.

Principle of Hydrogen Detector

A schematic of the hydrogen analyzer is shown in Fig. 1. The system essentially consists of an airtight specimen holder, an induction furnace for extracting hydrogen from the test specimen, a microquantitative gas metering system [*14*] (MGM system), or an electroysis cell which serves as hydrogen generator, a semipermeable membrane (from here on referred as SPM), a Vacion pump, high-purity argon gas source, and electrical signal conditioning system. Hydrogen, present as water, organic material, and elemental, is released from a metal in a suitable furnace. The hydrogen thus liberated is directed toward an activated SPM by the flowing argon gas (carrier gas). The SPM lets only hydrogen permeate through it while

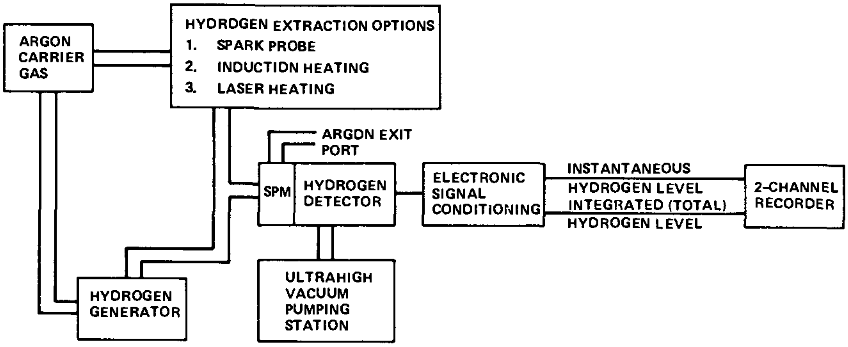

FIG. 1—*Schematic of hydrogen measurement system.*

remaining impermeable to other gases. On the other side of the SPM is a continuously pumped high-vacuum chamber. Thus, the SPM has a high vacuum on one side and about one atmosphere pressure on the other. The pressure in the high-vacuum chamber is measured by monitoring the ion pump current. Once the chamber is pumped down to its base vacuum ($\sim 10^{-9}$ torr), any permeation of hydrogen through the SPM will result in an increase in the pressure reading as seen by the ion pump. An increase in the ion pump current or pressure reading is, therefore, directly proportional to the amount of hydrogen (parts per million by volume) in the carrier gas stream. The linearity of the detector is checked by introducing known amounts of hydrogen in the vacuum chamber by the MGM system. This procedure also establishes a relationship (a calibration curve) between the concentration of hydrogen (by volume) in the gas stream and the ion-current readings, as shown in Fig. 2.

Experimental Approach

The experimental approach essentially consisted of extracting hydrogen from the test specimens using an induction (or muffle furnace) and then measuring the amount of hydrogen thus extracted with the hydrogen detector. Hydrogen, after permeating through the SPM, arrives in the detector housing which results in a proportional increase in the ion-pump current reading. This (instantaneous) electrical signal representative of the amount of hydrogen present is recorded on a two channel strip chart recorder. In practice when the specimen is heated, the time for complete extraction of hydrogen depends upon the rate at which hydrogen diffuses out of the specimen. This rate of effusion is proportional to the temperature of the specimen and as such the time required for complete extraction of hydrogen depends on how rapidly the temperature of the specimen is raised. In the case of bulk hydrogen analysis the instantaneous hydrogen signal generally traces out a Maxwellian type of curve representing complete extraction of

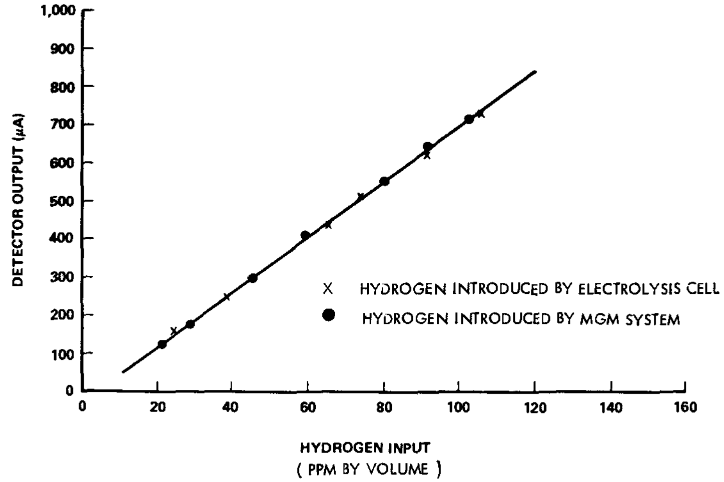

FIG. 2—*Calibration of hydrogen detector.*

hydrogen from the test specimen. When this curve is integrated electronically it results in an *S*-shaped curve giving a direct numerical value for the area under Maxwellian curve, (see Fig. 3). The sensitivity of the detector depends upon the flow rate of the carrier gas, the temperature of the SPM, and the pressure being measured by it. In order to maintain the same per-

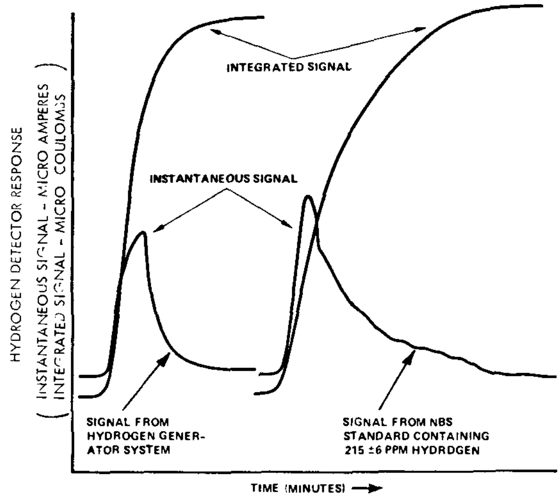

FIG. 3—*Hydrogen analysis of NBS Standard No. 354 containing 215 ± 6 ppm hydrogen.*

meating efficiency for hydrogen from the MGM system and the test specimen it is essential that the temperature of the SPM and the flow rate of the carrier gas be kept constant.

The design of the system is such that not all the hydrogen directed toward the SPM goes through the detector. Moreover, the diffusion of hydrogen through SPM itself is a time-dependent process. When using an induction furnace such factors are eliminated by following a special operating technique [*10, 14*]. Here the SPM is held at a constant temperature $T°$ C and a flow-rate of about 80 cm^3/min is set for the carrier gas. Thereafter, hydrogen is introduced into the detector from the MGM system for a given time "t". With a knowledge of the known leak rate of hydrogen, the time t, and the density of hydrogen gas, the amount of hydrogen m_1 (in grams) introduced into the detector is computed. As shown in Fig. 3 the instaneous current representative of m_1 g of hydrogen and its corresponding integrated signal I_1 is recorded. This implies that at a given SPM temperature ($T°$ C) and a flow-rate of carrier gas ($\sim$ 80 cm^3/min), I_1 is proportional to $m_1 = kI_1$, where k is the constant of proportionality. Without changing the temperature of the SPM and at the same carrier gas flow rate, hydrogen is extracted from the test specimen using an induction furnace. The unknown m_2 g of hydrogen extracted from the test specimen gives an instantaneous signal and a corresponding integrated signal I_2. Since the SPM temperature and the flow rate of the carrier gas is held constant, m_2 is related to I_2 by the relationship $m_2 = kI_2$. From the simple ratio between $m_1 = kI_1$ and $m_2 = kI_2$ the unknown m_2 is computed. Figure 3 shows typical curves of the analysis of a NBS standard containing 215 ± 6 ppm (by weight) of hydrogen.

The results of the hydrogen analysis of cadmium plated steel specimens heat treated to 260 to 280 ksi strength level, cadmium plated forged bolts heat treated to 180 ksi strength level, and titanium standards for hydrogen obtained from the National Bureau of Standards are described in the following sections.

Results and Discussion

Sensitivity and Minimum Detectable Limit of the Hydrogen Detector

Following the accepted definition of sensitivity as proposed by the "Mass Spectometer Subcommittee" of the American Vacuum Society, the sensitivity of the hydrogen detector is defined here as the output meter deflection of a given known amount of hydrogen input or the slope of the ion-pump current reading versus the hydrogen input in parts per million. A series of sensitivity determinations have yielded a value of 7.0 μA/ppm of hydrogen. The minimum detectable limit of the instrument, for hydrogen detection, was found to be five parts per billion in the gas stream. Although some reduction in sensitivity is observed with the aging of the SPM, the method of determining the hydrogen content in the test specimens is such that this variation in sensitivity does not affect the accuracy of the test results.

Hydrogen Content Analysis of the NBS Specimens

A number of standard specimens were procured from the National Bureau of Standards (NBS) to cross check the hydrogen content determinations of the hydrogen detector and establish the accuracy in the range studied. These specimens consisted of commercially pure titanium containing known amounts of hydrogen at the following levels: 32 ± 2 ppm, 98 ± 5 ppm, 215 ± 6 ppm. The method of preparation, analysis, and certification of these specimens is described by Sterling et al in an NBS publication [*18*].

The results of the NBS standard specimens as analyzed by the hydrogen detector are given in Table 1. The fractional random error in the mean value at 95 percent confidence level for Specimens 352, 353, and 354 is ± 5.01 percent, ± 1.67 percent, and ± 1.08 percent, respectively. In other words, at 95 percent confidence limit the uncertainty in the mean values for the three standards were 30.74 ± 1.54 ppm, 97.84 ± 1.64 ppm, and 220.26 ± 2.37 ppm.

TABLE 1—*Hydrogen content determinations of NBS standard specimens by hydrogen detector.*

	Specimen 352 NBS Certified Value 32 ± 2 ppm	Specimen 353 NBS Certified Value 98 ± 5 ppm	Specimen 354 NBS Certified Value 215 ± 6 ppm
	31.8	98.6	218.4
	27.8	98.6	218.3
	29.6	95.1	220.9
	31.1	97.5	222.8
	34.4	100.8	220.9
	28.1	97.6	
	34.5	96.7	
	31.6		
	31.1		
	29.3		
	28.8		
Total Number of Determinations	11	7	5
Mean (ppm)	30.74	97.84	220.26
Standard Deviation	2.289	1.775	1.908
Coefficient of Variance (%)	7.446	1.814	0.867
Range (ppm)	6.7	5.7	4.5
High Value (ppm)	34.5	100.8	222.8
Low Value (ppm)	27.8	95.1	218.3
Standard Error	0.690	0.671	0.853
95% Confidence Limits	1.54	1.64	2.37

The results of vacuum fusion analysis on similar NBS standard specimens as reported by others [*18*] were compared with those taken by the hydrogen detector and are summarized in Table 2. As can be seen, the hydrogen detector's data seems to agree remarkably well with those obtained by vacuum fusion analysis. Also, the mean values of hydrogen detector appear to fall well within the uncertainty limits established by the NBS.

Although vacuum fusion analysis for hydrogen is fairly accurate in ranges above 10 ppm, the uncertainty below 5 ppm is quite large. Furthermore, the analysis by vacuum fusion is time consuming and relatively expensive [*19*]. In the case of hydrogen detector the analysis below 5 ppm range is accurate (better than ± 10 percent), analysis time is short (since one does not have to break the vacuum to introduce test specimens into the furnace), and the hardware involved is relatively inexpensive.

Since NBS does not provide any hydrogen standards below 30 ppm range the accuracy in the 1 to 30 ppm range and in the overlapping range up to 50 ppm was determined by using an electrolysis cell or the MGM system or both.

The results of the hydrogen detector as described in Table 1 provide indirect traceability of the detector's measurements. The calibration of the detector by the MGM system is in terms of length and time measurements which are directly traceable to NBS. Thus, all the hydrogen measurements of the detector reported in this paper are absolute.

Comparison of Hydrogen Detector's Data with Notched Tension Testing (NTS) and Boeing Plating Porosity Meter Results on Cadmium Plated 4340 Steel Specimens

As said before, to date there is no cost effective method available to accurately measure low concentrations (5 ppm and below) of hydrogen in metals. As a result, establishment of a quantitative relationship between hydrogen concentration and fracture failure characteristics had been difficult. Today some processors still control hardware by relying on a time consuming mechanical testing which has proven to be less than adequate and overall an extremely expensive process.

This portion of the study was aimed at relating hydrogen content of test specimens which were processed through a set of typical production operations (with the exception of the process where hydrogen introduction was controlled) to NTS data by an indirect method. The processes to which the specimens were subjected included machining, heat treating, dry abrasive blasting, cadmium plating, vapor degreasing, and baking at 350° F for 24 h. All specimens were made out of 4340 steel, heat treated to 260 to 280 ksi strength level, and were processed in the same manner except in the cadmium plating process where they were plated to have a different degree of porosity to cause varying amounts of hydrogen retention in the material

TABLE 2—*Results of other laboratories as published in the Journal of Research of the NBS* [18].

Laboratory	Total No. of Detections	Mean	Standard Deviation	Coefficient of Variance	Range	High Value	Low Value
Specimen 352 (32 ± 2 ppm, NBS Certified Value)							
National Research Corp.	13	32.9	3.1	9.4	11.2	35.9	24.7
Watertown Arsenal	14	31.7	1.5	4.7	5.3	35.0	29.7
Battelle Memorial Institute	6	30.9	6.0	19.	1.8	31.8	30.0
DuPont Co.	5	30.2	3.1	7.7	6.0	34.0	28.0
Allegheny Ludlum Co.	6	33.8	0.6	1.8	1.7	34.4	32.7
National Bureau of Standards	44	31.0	2.2	7.1	8.0	35.0	27.0
Boeing Co.	11	30.7	2.3	7.4	66.7	34.5	27.8
Specimen 353 (98 ± 5 ppm, NBS Certified Value)							
National Research Corp.	14	100.8	8.1	8.1	30.7	113.8	33.1
Watertown Arsenal	15	99.7	3.4	3.4	13.6	106.2	92.6
Battelle Memorial Institute	6	96.4	2.7	2.8	6.8	99.5	92.7
DuPont Co.	5	93.8	5.2	5.5	13.0	101.0	88.0
Allegheny Ludlum Co.	6	103.0	1.7	1.7	4.0	105.0	101.0
National Bureau of Standards	107	95.0	3.1	3.3	14.0	102.0	88.0
Boeing Co.	7	97.8	1.8	1.8	5.7	100.8	95.1
Specimen 354 (215 ± 6 ppm, NBS Certified Value)							
National Research Corp.	13	219.0	5.4	2.5	19.6	228.3	208.7
Watertown Arsenal	15	215.3	3.0	1.4	9.6	221.2	211.6
Battelle Memorial Institute	6	209.0	5.9	2.9	16.0	217.0	201.0
DuPont Co.	5	212.0	3.4	1.6	8.0	215.0	207.0
Allegheny Ludlum Co.	6	222.3	3.3	1.6	8.0	227.0	219.0
National Bureau of Standards	103	211.8	4.3	2.0	31.0	221.0	190.0
Boeing Co.	5	220.3	1.9	0.9	4.5	222.8	218.3

[*20*, *21*]. The present tests were conducted after the final baking operation of the processing sequence.

The samples (diameter = 0.0333 in., length = 1.00 in.) were prepared per Boeing Airplane Company Specifications BAC 5718 and BAC 5701. A total of 10 specimens was obtained in two different batches of five specimens each. The porosity varied from being completely porous to almost a nonporous state. The two batches were prepared under identical conditions to test for the repeatability and accuracy of the results. The Boeing plating porosity meter (BPPM) was used in the cadmium plating bath to ascertain the level of porosity produced (for a given current density) for plating the test specimens. In a plating operation like this, nascent hydrogen generated as a side reaction at the cathode is introduced into the specimen. Thus a porous plating will permit this hydrogen to escape while a nonporous plating will retain the hydrogen inside the material, which of course, can lead to hydrogen embrittlement failure. By varying the degree of porosity in the plating, different amounts of hydrogen can be retained in the test specimens. A measure of the relative degree of porosity was indicated by a numerical index λ as read by the BPPM.

The BPPM essentially consists of a specially modified 6V6 metal vacuum tube (called the probe), an oven, and associated electronic hardware to measure the probe output. Prior to its use the exterior shell of the probe is painted, and a standard area is sandblasted for hydrogen permeation. The standard area is then electroplated and the probe placed in the oven. Hydrogen picked up by the probe during electroplating is then released at elevated temperatures which is measured as ion current (probe plate current) by the control unit. The plating porosity measurements begin when the probe is placed in the oven. At elevated temperatures hydrogen picked up during plating is driven both into and out of the probe. The hydrogen that enters into the interior of the probe builds up to a peak value (heat peak (HP)) and then decreases to a minimum value as time progresses. The measure of ion current in the probe from HP to the end of the test is half the HP reading. The decay time of the ion current signal from HP to half HP is designated as λ . Since λ is the time span where the probe response measures the ease of hydrogen removal, it is used in assessing the porosity of plating. A porous plate will allow rapid hydrogen diffusion from the shell and should give a faster decay time. Likewise a nonporous plate should result in a longer decay time.

Considerable effort had been devoted in the past by The Boeing Company to relate λ-values with the notched tension testing (failure) data from which statistical information on failure has been compiled [*20*, *21*]. This information was used to relate indirectly the hydrogen content of specimens (prepared with a given λ value) to the NTS failure data.

Hydrogen was extracted from the test specimens by hot extraction method. The test specimen was placed inside a furnace which was purged continuously with high-purity argon gas. The temperature of the furnace was raised in small increments. For the test specimens described here the maximum temperature for complete extraction of hydrogen was in the neighborhood of 800° C or 1472° F.

Based on the limited amount of data available at this time certain parts of the discussion presented next are speculative. In a cadmium plated specimen, hydrogen was observed to come out from three different areas as the temperature was slowly increased. These regions are as follows:

Region A—At low temperatures, between 72 to 300° F, hydrogen is desorbed from the volume of the plating only. This temperature range (and time span) is not high enough for complete extraction of hydrogen from the interior of the specimen. However, some subsurface hydrogen may be present in this region.

Region B—At intermediate temperatures, between 300 to 575° F (and the time span of test in this region) as the plating material gets soft, hydrogen in the region of the plating metal interface and from the subsurface is given off.

Region C—At higher temperatures, between 575 to about 1472° F, hydrogen is extracted from the interior of the specimen.

As just mentioned the specimens were prepared in two separate batches. Batch 1, contained five specimens coded C, D, E, V, and X. Batch 2 also contained five specimens coded 1, 2, 3, 4, and 5. Figure 4 shows the results of the analysis of all the specimens. Here the detector response (in microamps) is plotted against the time in minutes. The area under the curve (detector response versus time) gives a measure of the hydrogen concentration in the material. Regions A, B, and C, as described previously, can be easily identified in these figures. In some cases Regions A and B are difficult to identify because of the scale factor.

All the quantitative data on the test specimens are summarized in Table 3. The sequence of Batch 2 is changed when the specimens are lined up as per hydrogen concentration from Region A only. Specimens V and 5 were vacuum plated, whereas Specimens X and 3 had bright cadmium type plating on them, and as such these specimens represent extreme conditions.

As can be seen from Table 3, the lineup of Batch 1, agreed 100 percent with the λ-values of the BPPM and notch tension testing results. In Batch 2, with the exception of Specimen 4, all others agree with the BPPM data. However, when the lineup is arranged on the basis of hydrogen from Region A alone, the agreement between λ-values and hydrogen concentration is once again 100 percent. Figure 5 shows the regions (A + B + C) and λ-values from BPPM, respectively.

For the sake of discussion let us speculate upon the meaning of these data. In Region A the amount of hydrogen which comes out is either desorbed from the skin of the cadmium plating or from the outer surface or both because of some surface contamination and from the subsurface. The

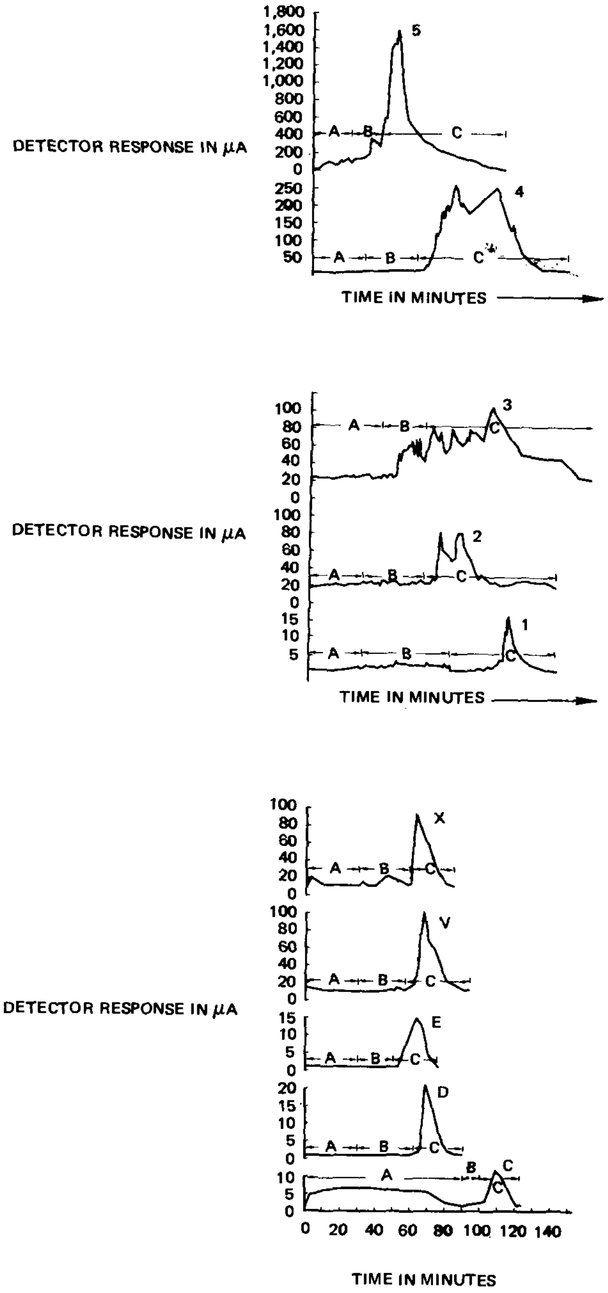

FIG. 4—*Hydrogen content analysis of cadmium plated 4340 steel.*

TABLE 3—*Quantitative results of the analysis of hydrogen concentration in 4340 steel specimens.*

Specimen Identification No.	Region A (up to 550° F) ppm of H_2	Region B (soon after Cd disappears) ppm of H_2	Region C (H_2 from bulk) ppm of H_2	Total H_2 in ppm from Regions A, B, and C	λ-Values from PMG	Percent Specimen Failed Under Tension Test
D	0.007	0.020	0.823	0.850	60 ± 5	0
E	0.025	0.015	0.946	0.986	163 ± 15	0 to 30
C	1.949	0.277	0.626	2.852	250 ± 40	85 to 98
V	0.352	0.181	4.322	4.855	vacuum plated	
X	0.541	0.819	4.451	5.811	1000	100
1	0.232	0.363	0.722	1.317	163 ± 15	0 to 30
2	0.243	0.057	1.419	1.719	250 ± 40	85 to 98
4	0.009	0.017	2.365	2.391	60 ± 5	0
3	0.126	0.565	4.432	5.123	1000	100
5	0.346	0.799	5.823	6.968	vacuum plated	

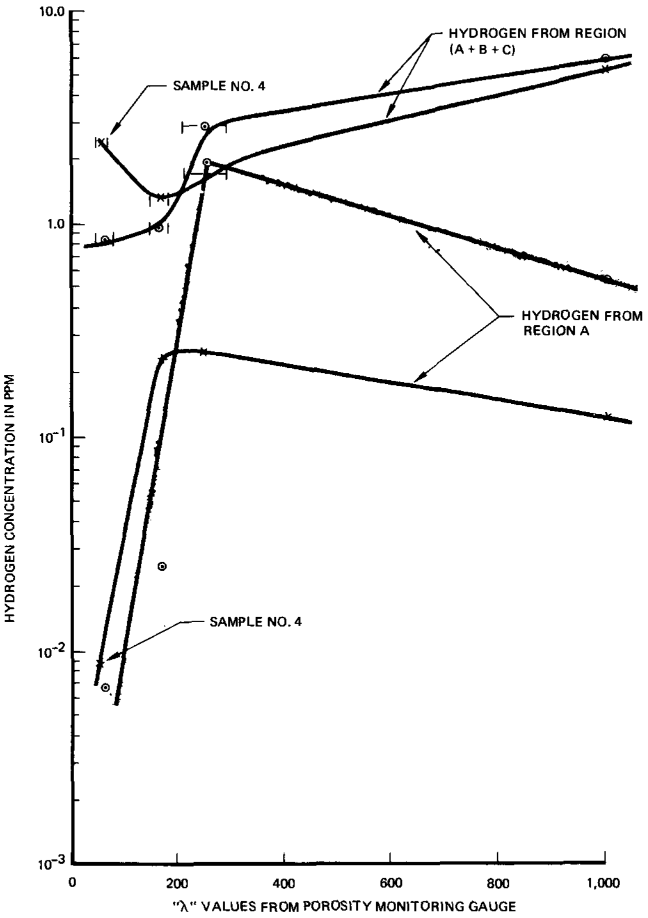

FIG. 5—*Hydrogen detector response versus λ-values of porosity monitoring gage.*

origin of this hydrogen content is not clearly known. It is unlikely that any hydrogen from the interior is coming out because the temperature is not high enough and the time duration of the test is relatively short. The actual amount of hydrogen desorbed in Region A depends on two factors: (*a*) true concentration of hydrogen and (*b*) porosity of the plating. If two specimens having identical structure are charged with equal amounts of hydrogen during a cadmium plating operation, the one which has less porous plating is liable to retain more hydrogen. Furthermore, a specimen which has almost a completely blind plating, like a bright cadmium specimen, is going to desorb much less hydrogen in Region A even though the total hydrogen content in the specimen (or plating) may be very high.

Thus both a completely blind plating and a highly porous plating are going to show a low level of hydrogen concentration in Region A. Since bright cadmium plating is not used on high-strength steel production parts, because of its undesirable effect of rendering a part highly susceptible to hydrogen embrittlement failure, it is concluded that for a normally plated specimen a high level of hydrogen from Region A could imply a less porous plating. The test results also show that the vacuum plated specimens have a low degree of porosity in the plating. From this discussion it appears that tests such as these may have the potential to nondestructively test the plated specimen for checking their porosity levels.

Let us consider Fig. 5 now. Here, the total hydrogen extracted from Regions A, B, and C is plotted against the λ-values of BPPM. With the exception of Specimen 4 in Batch 2 the hydrogen data for all other specimens seem to follow the λ-values. From the total hydrogen analysis it appears that Specimen 4 of Batch 2 is similar to Specimen C of Batch 1. However, the BPPM data show that Specimen 4 has the least amount of hydrogen among all the specimens in Batch 2 or Specimen C has a dense plating (least porosity) and Specimen 4 has a porous plating (most porosity). There could be several reasons for this apparent disagreement. The most obvious one could be that the hydrogen detector reading is in error or the λ-value of BPPM is in error. However, since 9 out of 10 specimens have shown excellent agreement, the likelihood of one of the two or both of these instruments being wrong is less probable. The less obvious, reasons include the following: (1) method of obtaining the specimen, (2) storage of the specimen until analysis, and (3) preparation of the specimen. As mentioned earlier, extreme care was exercised in handling and storing the specimens until analysis. Thus, the two most likely reasons appear to be the foregoing (1) and (3). It is quite possible that the structure of these two specimens prior to plating may be significantly different resulting in the observed discrepancy.

There is evidence in the literature [*22-25*] that the structure of the material prior to plating can have a significant effect on the hydrogen retention. For example, structural defects (like dislocations, vacancies, etc.) can act like trapping centers for hydrogen. A systematic, well-planned study is required to investigate various aspects of hydrogen absorption and its interaction with lattice defects. The conclusion is that, based on the porosity level alone, it may be difficult to predict whether a specimen is going to fail or not.

With regard to a relationship between hydrogen content readings, λ-values, and NTS data it can be said that there is a definite correlation between hydrogen concentration and susceptibility to failure of specimens. Based on the data presented here it appears that for this heat treat batch of material the safe limit of (total) hydrogen concentration is about 1 ppm. In the range from 1 to 1.5 ppm, depending upon the service conditions, it is estimated that up to 30 percent of the processed material can suffer embrittlement failure. These results are only preliminary, and as such no plus or minus limits could be established on the hydrogen content. It is important to note that a knowledge of λ-values of BPPM is desirable to control the plating process. However, the BPPM cannot be used to estimate how much hydrogen has actually gone into and is retained in the specimen. The results of the hydrogen detector presented here and of another comprehensive study in process in our laboratories thus far, show considerable promise for establishing reliable acceptance limits for hydrogen content in high-strength materials.

Hydrogen Analysis on Forged Bolts Heat Treated to 170 to 195 ksi Strength Range

Certain stud bolts that had failed in service were submitted for failure analysis. The objective of the test was to find whether the bolts failed because of hydrogen embrittlement or stress-corrosion cracking or both. Literature shows that several attempts have been made to distinguish stress-corrosion cracking from hydrogen embrittlement, where the cause of fracture is related directly to hydrogen that is already present or that enters the metal lattice through discharge of H^+ at the metal surface. Some features of hydrogen embrittlement are similar to those of stress-corrosion cracking, but it has been suggested that the causes differ at least in detail. However, from the data available in the literature it is far from certain whether a clear-cut distinction can always be made between stress-corrosion cracking and hydrogen embrittlement, which often occur in the same environment.

The bolts were forged, heat treated to 170 to 195 ksi strength range, and cadmium plated. From electron fractographic analysis it was concluded that the parts have failed because of hydrogen embrittlement or stress-corrosion cracking or both. Since the role of hydrogen in this failure remained speculative after such an analysis, one of the fractured bolt specimens was sectioned into four parts for hydrogen analysis. The hydrogen detector analysis showed that the section including the fractured surface had the maximum amount of hydrogen (4.67 ppm), while that at the extreme end had the least amount (1.85 ppm). The two specimens in between had 2.46 and 3.53 ppm, respectively. Literature shows *[22]* that the degree of embrittlement increases with increasing hydrogen content and the greater the strength level of steel (of a given composition and approximately the same structure) the greater the sensitivity to hydrogen embrittlement. A total of 18 sections from several unfractured bolts when subjected to bulk hydrogen analysis gave values ranging from 1.8 to 2.5 ppm. In the preceding sections we have seen that cadmium plated 4340 steel heat trated to 280 ksi level can suffer from hydrogen embrittlement if the hydrogen concentration exceeds about 1.5 ppm. In the present case since the bolt material has been heat treated to only 170 to 195 ksi strength level it is possible the bolt material has a higher tolerance limit for hydrogen concentration. However, a level of 4.67 ppm is considered high enough to cause hydrogen embrittlement failure. Since no detailed information was available with regard to the environment or the exact treatment the specimens were subjected to, it could not be concluded whether the parts have failed because of hydrogen embrittlement or stress-corrosion cracking. A detailed study is under way to investigate the limit of hydrogen concentration on steel heat treated to different strength levels.

Conclusions

In conclusion, the results of a newly developed ultrasensitive hydrogen detector can be summarized as follows:

1. The sensitivity of the hydrogen detector was found to be 7.5 μA/ppm, and the minimal detectable limit was measured as 5 ppb in the carrier gas stream.
2. The detector was calibrated by using a microquantitative gas metering system which employed a precision capillary leak. The measurements being in terms of length and time were absolute and traceable to NBS.
3. Three different titanium standards for hydrogen content were obtained from NBS to facilitate evaluation of detectors performance, range, and accuracy. This also provided a means for cross checking the results of this newly developed technique against the NBS's measurements. The fractional random error in the mean value at a 95 percent confidence level for specimens with 32, 98, and 215 ppm were found to be ±5.01 percent, ±1.67 percent, and ±1.08 percent, respectively.

From the hydrogen analysis of cadmium plated 4340 steel the following is concluded:

1. A testing technique is developed which can provide a reliable quantitative estimate of hydrogen in cadmium plated steel specimens. This technique also shows a potential to nondestructively test the plated specimens for their varying degree of plating porosity levels.
2. Two different batches of specimens treated in an identical manner prior to plating and having received similar plating treatment, as indicated by λ-values of BPPM, had considerably different amounts of hydrogen in them. This may mean that the structure of the material prior to plating could play a significant role in hydrogen absorption during the plating process.
3. For the material (heat treated to 260 to 280 ksi level) tested in this study the safe limit for hydrogen concentration appears to be about 1 ppm. Preliminary results thus far indicate that in the range 1 to 1.5 ppm (depending upon the service conditions) up to 30 percent of the processed material can suffer embrittlement failure. (The notched specimens were

tested at loads equivalent to 75 percent of their ultimate strength level).

4. The results of the hydrogen detector presented here and those obtained on another comprehensive study in process in our laboratories, thus far, show considerable promise for establishing reliable acceptance limits for hydrogen content in high-strength materials.

Preliminary results on forged steel specimens heat treated to 170 to 195 ksi level show that hydrogen embrittlement in this material can occur at hydrogen concentration levels exceeding 2 to 2.5 ppm.

References

[*1*] Buzzard, R. W. and Cleaves, H. E., Circular 511, National Bureau of Standards, U. S. Department of Commerce.

[*2*] Scott, T. E. and Troiano, A. R., *Journal of Metals*, Vol. 11, 1959, p. 619.

[*3*] Coe, F. R., *Applied Research in Industry*, Vol. 13, 1960, p. 323.

[*4*] Mehan, R. L., *Knolls Atomic Power Laboratory KAPL-M-RLM-8*, General Electric Co., March 1956, pp. 1–17.

[*5*] Rogers, H. C., *Transactions*, Metallurgical Society, American Institute of Mining, Metallurgical, and Petroleum Engineers, Vol. 215, 1959, p. 666.

[*6*] Beck, W., Jankowsky, E. J., and Fisher, P., "Hydrogen Stress Cracking of High Strength Steels," Center Report NADC-MA-7140, Naval Air Development, Warminster, Pa., 1971.

[*7*] Lebel, S. J. and Strobelt, W. E., U. S. Patent No. 3,426,579, 1969.

[*8*] Das, K. B. and Strobelt, W. E., patent pending.

[*9*] Lowry, N. M., "Study of Welding Defects–Saturn Joint Configuration," NASA Contract No. NAS8-24512, Final Report, National Aeronautics and Space Administration, Washington, D. C., 1970.

[*10*] Das, K. B., Boeing Quality Control Development Report No. 2–2505–70–111, The Boeing Company, Seattle, Wash., 1970.

[*11*] Das, K. B., "Hydrogen Concentration Gradient Measurement Beneath the Original Surface of Corroded/Ruptured Ti 8–1–1 Alloy," Final Report on NASA Contract PR No. 365916, National Aeronautics and Space Administration, Washington, D. C., 1971.

[*12*] Gray, H. R., *Corrosion*, Vol. 28, No. 2, 1972, pp. 47–54.

[*13*] Das, K. B., this symposium, pp. 106–123.

[*14*] Das, K. B., "An Ultrasensitive Hydrogen Detector and Its Applications," paper presented at the 19th National Symposium of American Vacuum Society at Chicago, Ill., Oct. 1972.

[*15*] Das, K. B., *Journal of Vacuum Science and Technology*, Vol. 10, No. 1, Jan.-Feb. 1971, p. 275.

[*16*] Das, K. B. et al, "An Investigation of Blistering in 2024-T6 Aluminum Alloy," paper to be presented at the International Conference on Hydrogen in Metals, Champion, Pa., Sept. 1973.

[*17*] Das, K. B. and Marceau, A., "Hydrogen Induced Damage in Pickled and Anodized Ti 6–4 Alloy Surfaces," paper to be presented at the International Conference on Hydrogen in Metals, Champion, Pa., Sept. 1973.

[*18*] Sterling, J. T. et al, *Journal of Research, A. Physics and Chemistry*, Vol. 66A, No. 6, 1962.

[*19*] Lank, P., masters' thesis, University of Wichita, Wichita, Kans., Feb. 1962.

[*20*] Forshee, A. G., Boeing QC Research and Development Report No. 312–23, The Boeing Company, Seattle, Wash., March 1968.

[*21*] Pritchett, L. D., "Hydrogen Control During Cadmium Plating of Steel," paper presented at the Aerospace Industries Association, Quality Assurance Committee, Denver, Colo., April 1971.

[*22*] Grant, N. J. and Lunsford, J. L., *Iron Age*, Vol. 175, June 1955, p. 12.

[23] Mills, R. L. and Edeskuty, E. J., *Chemical Engineering Progress*, Vol. 52, 1956, p. 477.

[24] Hudson, R. M., Riedy, K. J., and Stragand, G. L., *Corrosion*, Vol. 17, 1961, p. 334t.

[25] Amiot, P., "Contribution a l'Etude de la Fragilisation des Aciers de Structure Alpha par l'Hydrogene Introduit a Froid et a la Diffusion de l'Hydrogene dans les Memes Aciers," Germain-en-Laye, Series A., No. 158, April 1957.

[26] Fromberg, R. P., Barnett, W. J., and Troiano, A. R., *Transactions*, American Society for Metals, Vol. 47, 1955, p. 892.

S. M. Toy [1]

Neodymium Detection System

REFERENCE: Toy, S. M., "**Neodymium Detection System,**" *Hydrogen Embrittlement Testing, ASTM STP 543*, American Society for Testing and Materials, 1974, pp. 124–130.

ABSTRACT: A test method for assessing hydrogen embrittlement of high-strength steel parts in the field is described. It is applicable to both ferrous and nonferrous metals which evolve hydrogen when heated. The assessment of the hydrogen embrittlement of steel or other metal parts is dependent on the determination of the local hydrogen content and the stresses required to fracture them and the determination of the hydrogen pick-up rate by the metal part in the environment which it is exposed to. Local hydrogen analysis in the field is based on the application of a flexible neodymium hydrogen detection tape.

KEY WORDS: hydrogen embrittlement, hydrogen analysis, alloy steels, stress corrosion, field tests

Only a few parts per million (ppm) of embrittling hydrogen can damage 4340 steel metal parts [*1*, *2*].[2] A test method for assessing hydrogen embrittlement of high-strength steel parts in the field will be described. It is applicable to nonferrous metals which evolve hydrogen when heated. The assessment of the hydrogen embrittlement of steel or other metal parts is dependent on the determination of the local hydrogen content and stresses required to fracture them and the determination of the hydrogen pick-up rate by the metal part in the environment to which it is exposed. The local threshold hydrogen content and stresses required to fracture two high-strength alloy steels are given in Fig. 1. The alloy steels are safe if the combination of local hydrogen and stress are to the left of their respective threshold line and fail to the right of the threshold line. The two alloy steels, AISI 4340 and 300M, a 1.6 percent by weight silicon modification of 4340 steel, have the following mechanical properties: ultimate tensile strengths, 282 and 272 ksi, and yield strengths, 232 and 226 ksi, respectively. The tensile properties were within ±3 ksi. Notch

---

[1] Engineer, Palo Alto, Calif. 94306.

[2] The italic numbers in brackets refer to the list of references appended to this paper.

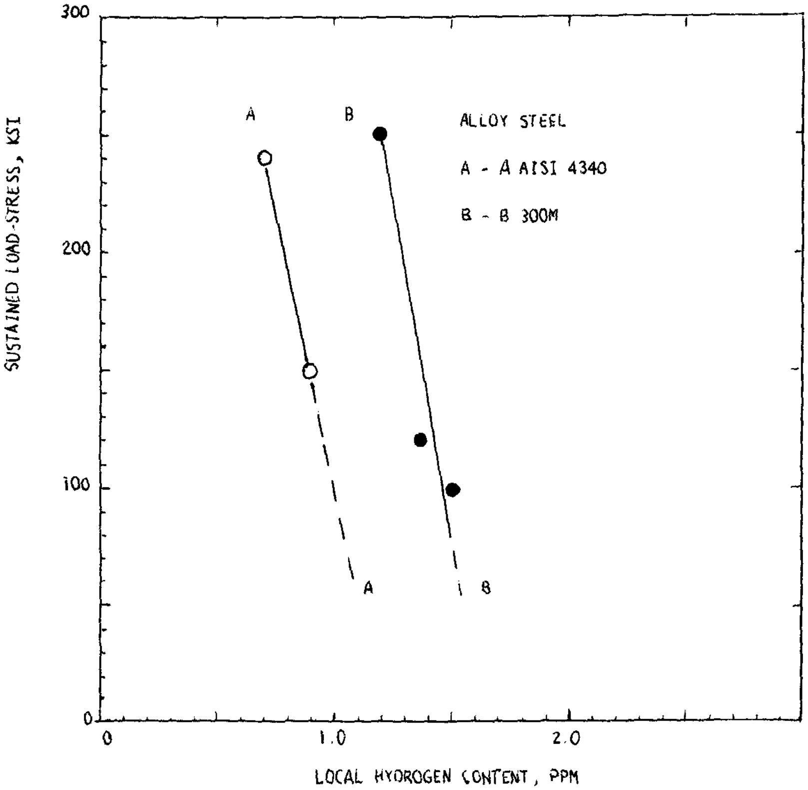

FIG. 1—*Sustained load-stress versus hydrogen content threshold failure lines for 4340 type steels, safe region left of lines and failure to right of line.*

tension specimens with a notch acuity of 0.014 to 0.016 were used. The strengths values were similar to Johnson et al [*2*].

The objective of this paper is to propose a tentative test method for assessing hydrogen embrittlement of metal parts in the field on the basis of calculated relative local hydrogen content with the neodymium hydrogen detection tape that has been correlated with sustained load, stress tests required to fracture the material.

Hydrogen Analysis by Application of Neodymium Hydrogen Detection Tape

The measurement of local hydrogen content of high-strength steel parts or other suitable metals used in the field can be made utilizing the following procedures [*2–4*]:

(*a*) Apply neodymium detection tape to the degreased surface of the part at the location to be analyzed for hydrogen. This is for removing hydrogenous surface contaminants. (If surface corrosion deposits are present, remove by suitable mechanical cleaning method before applying tape.)

(*b*) Place high-temperature pressure-sensitive adhesive tape over detection tape to seal the detector in position.

(*c*) Heat the local area of interest with a hot air heat source to a temperature of 300° F for 1 h. Temperature may be monitored with a heat sensitive temperature recording device such as Tempilstick or a contact thermocouple. (Higher temperatures may be required for materials that do not readily release hydrogen, for example, titanium and zirconium.)

(*d*) After the part has cooled, strip detection tape from the part and examine the detection tape for hydrogen reaction sites. The chemical reaction that occurs is neodymium plus two hydrogen reacts to form neodymium dihydride ($Nd + 2H \rightarrow NdH_2$). If the NdH_2 reaction sites are seen visually (eye), local hydrogen content will be greater than 150 ppm. Optical and electron scanning microscopic readout permits continuous determination from 150 ppm to below 1 ppm at 1-μm sites. (Optical to 0.01 ppm and electron to 0.001 ppm.) In the case of high-strength martensitic type steels, the absence of visible reaction sites on the tape indicate less than 1-ppm local hydrogen.

Flexible hydrogen detection tapes up to 2 by 12 in. have been produced in the laboratory. "Band aid" size tapes produced in commercial quantities could be in the range of five dollars per unit.

Specimen Calculation of Hydrogen Content for a Cadmium Plated 4340 Steel

Let subsurface embrittling (diffusible) hydrogen be evolved from the steel. The diffusion coefficient of alpha iron, D, = 5×10^{-5} cm^2/s at 300° F (149° C) [*6*].

Measured neodymium film thickness, T, = 945 Å ± 125 Å

Neodymium hydrogen reaction site diameter, d_s, = 0.1 cm

Area of site, A_s = $1/4\ \pi d^2$
= 0.0785 cm^2

Cadmium plate pore diameter, d_p = 0.1 cm

Diffusion length, X_L = $\sqrt{Dt}$
= $\sqrt{5 \times 10^{-5} \times 3600}$
= 0.43 cm

Weight of iron, W_{Fe}, = $(\rho X_L A_s)$
= (7.87) (0.43) (0.0785)
= 0.264 g

$$\begin{aligned}
\text{Weight of neodymium, } W_{\mathrm{Nd}}, &= (\rho_{\mathrm{Nd}})\ (\mathrm{T})\ (\mathrm{A}_s) \\
&= (6.8)\ (948 \times 10^{-8})\ (0.0785) \\
&= 5.05 \times 10^{-6}\ \mathrm{g} \\
\text{Weight of hydrogen, } W_{\mathrm{H}_2}, &= 5.05 \times 10^{-6}\ \frac{\text{mol weight } (\mathrm{H}_2)}{\text{mol weight } (\mathrm{Nd})} \\
&= 5.05 \times 10^{-6}\ (2/144) \\
&= 0.07 \times 10^{-6}\ \mathrm{g} \\
\text{Hydrogen content, H (ppm)}, &= W_{\mathrm{H}}/W_{\mathrm{Nd}} \\
&= (0.07 \times 10^{-6})/0.264 \\
&= 0.265
\end{aligned}$$

Triplicate hydrogen analysis steels by the neodymium hydrogen detection tape indicate a variation of ±0.01 ppm.

Figure 2 illustrates the application of a 1/2 × 1/2-in. neodymium detection tape to a large cadmium plated aircraft main landing gear part under shop conditions. A metal surface temperature of 300° F (149° C) was attained by heating the local area with a hot air gun for 1 h at temperature. If the hydrogen analysis indicated a local hydrogen content of 4340 steel to be 0.75 ppm, the critical tensile stress required to trigger failure would be 220 ksi (see Fig. 1). However, if the operating service stress did not exceed 100 ksi, then the part would have to pick up an additional 0.25-ppm hydrogen from some hydrogen source to trigger a failure (see Fig. 1). If the part was continuously exposed to an environment which resulted in the part accumulating 0.002 ppm hydrogen per hour (dC_{H}/dt) then one can predict the time to failure of the part at a sustained load-stress of 100 ksi to be $t = (C_f - C_i)/(dC_{\mathrm{H}}/dt) = 0.25/0.002 = 125$ h.

This type of information can then be used to formulate standards to assess the hydrogen embrittlement characteristics of different metals in the field or laboratory,

Discussion of Test Method

The relative hydrogen embrittlement of the material at a constant stress level can be compared on the basis of how far the calculated local hydrogen content is from the critical point on the sustained load-stress versus local hydrogen content curve in Fig. 1. It defines the critical parameters delineating the safe region (left) and the unsafe region (right) of the curve. Therefore, low initial local hydrogen content in conjunction with low hydrogen pick-up rate found when the material is exposed to a specific environment would suggest a low embrittlement index (that is, predicted service life) for this metal when assuming it is exposed constantly to the hydrogen generating environment.

If you compare the two curves in Fig. 1 of AISI 4340 and the silicon

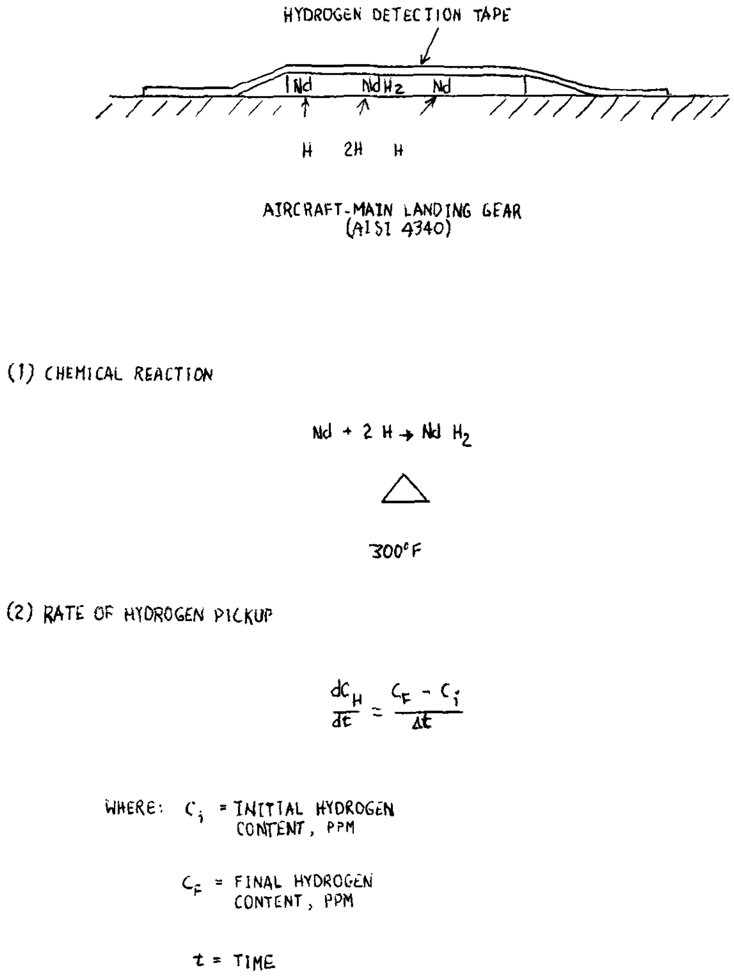

FIG. 2—*Principles for assessing hydrogen embrittlement of metal parts in the field.*

modified 4340, the shift of the modified 4340 to the right suggests it should, in general, better resist hydrogen embrittlement. This is consistent with its low susceptibility to hydrogen embrittlement in the aircraft industry for the design conditions investigated.

The sustained load test is used commonly in the aerospace industry for testing embrittlement of these type materials. Therefore, the correlating of this local relative hydrogen content with this type test is acceptable approach for assessing hydrogen embrittlement of the kind observed [7].

This test method was reduced to practice on different size aircraft parts under shop test conditions successfully. Aircraft components included commercial and military parts both from production and from service failures. In many cases, I foresee no serious technical problems which will prevent its direct use.

Permeation of hydrogen through surface protective coatings which are reported here have not interfered with the test. Correlation of our test with Lawrence permeation test indicates that our test detects hydrogen H_2 permeation below the H_2 sensitivity limit of that test method and some of the conventional test methods.

The diffusivity number used for the specimen calculation was selected from experimental reported values in Ref *6*. It gives a calculated local hydrogen content which is consistent with low critical hydrogen contents reported to cause failure of high-strength AISI 4340 steel and confirmed by agreement both with tape test method (that is, <1 ppm) hot extraction hydrogen analysis on the same steel (that is, 1 to 2 ppm). Scanning electron micrograph measurements of cadmium plated pores have been used to check the cadmium plate pore diameter and the pore diameter based on the smallest neodymium reaction sites observed on the tape. Both measurements were found to be in good agreement. An additional verification of the tape analysis performed was to remove the cadmium plate on an adjacent test area unaffected by the heat. Both calculations were found to give the same local hydrogen content value. In regards to other gases, we have not observed oxidation or nitriding of neodymium in our test. On rare occasions where a faulty seal was made, the distinct white neodymium oxide was observed and that particular test was disregarded. Electron diffraction of the thin hydrided neodymium film revealed no oxides or nitrides.

Hydrogen sensitivity test were also run on the neodymium hydrogen detection tape in 20 volume percent hydrogen + 80 percent argon at 300° F indicating no loss in original sensitivity from 3 to 17 weeks. Replica electromicrographs of evaporated neodymium thin film on hydrogen charged 4340 steel specimens appear to be completed reacted with some local film thicknesses estimated to be at least 50 percent reacted to NdH_2.

Acknowledgment

This report summarizes work performed at Douglas Aircraft Company under sponsorship of the Independent Research and Development Program (IRAD) of the McDonnell Douglas Corporation.

References

[*1*] Gray, H. R. and Troiano, A. R., *Metal Progress*, Vol. 90, No. 4, 1964, p. 77.
[*2*] Johnson, H. H., Morlet, J. G., and Troiano, A. R., *Transactions*, Metallurgical Society, American Institute of Mining, Metallurgical, and Petroleum Engineers, Aug. 1958, p. 531.

[3] Toy, S. M. and Phillips, A., *Corrosion*, Vol. 1, No. 7, 1970, pp. 200–207.
[4] Toy, S. M. and Phillips, A., *Welding Journal*, Vol. 49, No. 11, 1970, pp. 497s–504s.
[5] Toy, S. M., *Welding Design and Fabrication*, Vol. 44, No. 8, Aug. 1971, pp. 50–52.
[6] Fletcher, E. E. and Elsea, A. R., "Hydrogen Movement in Steel, Entry Diffusion and Elimination," DMIC Report 219, Defense Metals Information Center, Battelle Memorial Institute, June 1965, p. 41.
[7] Sink, G. T., "Hydrogen Embrittlement of High-Strength Steels," Douglas Paper 5377, presented to Fifth Airlines Plating Forum, Tulsa, Okla. 30 June 1969, Douglas Aircraft Co., McDonnell Douglas Corp., Long Beach, Calif.

HYDROGEN ENVIRONMENT EMBRITTLEMENT (HEE)

H. R. Gray [1]

Testing for Hydrogen Environment Embrittlement: Experimental Variables

REFERENCE: Gray, H. R., "**Testing for Hydrogen Environment Embrittlement: Experimental Variables,**" *Hydrogen Embrittlement Testing, ASTM STP 543*, American Society for Testing and Materials, 1974, pp. 133–151.

ABSTRACT: Hydrogen embrittlement is classified into three types: internal reversible hydrogen embrittlement, hydrogen reaction embrittlement, and hydrogen environment embrittlement. Characteristics of and materials embrittled by these types of hydrogen embrittlement are discussed. Hydrogen environment embrittlement is reviewed in detail. Factors involved in standardizing test methods for detecting the occurrence of and evaluating the severity of hydrogen environment embrittlement are considered. The effects of test technique, hydrogen pressure, gas purity, strain rate, stress concentration factor, and test temperature are discussed. Additional research is required to determine whether hydrogen environment embrittlement and internal reversible hydrogen embrittlement are similar or distinct types of embrittlement.

KEY WORDS: hydrogen embrittlement, metals, alloys, mechanical tests, pressure, purity, strain rate, temperature, notch tests

This paper is concerned exclusively with the more recently encountered form of hydrogen embrittlement—hydrogen environment embrittlement. The purpose of this paper is to review the factors in hydrogen environment embrittlement which must be considered in any effort to standardize test methods for detecting and evaluating this type of embrittlement. To do this, we must examine the characteristics of hydrogen environment embrittlement as well as the similarities and dissimilarities between hydrogen environment embrittlement and both internal reversible embrittlement and hydrogen reaction embrittlement. The effect of various experimental variables such as gas pressure, gas purity, test strain rate, stress concentration factor, and test temperature on hydrogen environment embrittlement will be discussed. The relative sensitivity of the

---

[1] Research metallurgist, Alloys and Refractory Compounds Section, National Aeronautics and Space Administration-Lewis Research Center, Cleveland, Ohio 44135.

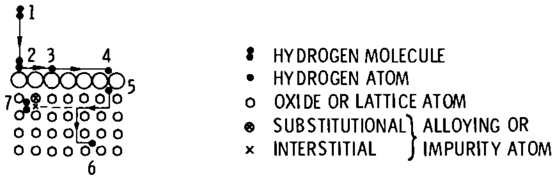

		OCCURRENCE OF EMBRITTLEMENT STEPS		
		TYPES OF EMBRITTLEMENT		
STEPS NECESSARY FOR EMBRITTLEMENT		HYDROGEN ENVIRONMENT	INTERNAL REVERSIBLE	HYDROGEN REACTION
1→2 MOLECULAR PHYSISORPTION	ADSORPTION	YES	NO	YES/NO
2→3 DISSOCIATION		YES	NO	YES/NO
3→4 CHEMISORPTION		YES	NO	YES/NO
4→5 SOLUTION (ABSORPTION)		YES	YES	YES
5→6 LATTICE DIFFUSION		?	YES	YES/NO
5/6→7 HYDROGEN REACTION TO FORM HYDRIDES AND/OR GAS BUBBLES		NO	NO	YES

FIG. 1—*Physical and chemical processes necessary for various types of hydrogen embrittlement* [5].

tension, fatigue, creep, fracture toughness, and disk pressure tests used by investigators will also be discussed. This paper will attempt to set the stage for subsequent papers in this Symposium which will present detailed descriptions of test specimens and test procedures for evaluating hydrogen environment embrittlement of materials.

Characteristics

Hydrogen environment embrittlement may occur when an essentially hydrogen-free material is mechanically tested in gaseous hydrogen [*1–26*].[2] It is well agreed among investigators that molecular hydrogen must dissociate to atomic hydrogen for embrittlement to occur. The physical and chemical steps necessary for hydrogen environment embrittlement, as well as the other types of hydrogen embrittlement, are illustrated in Fig. 1. For hydrogen environment embrittlement to occur, both adsorption (physisorption, dissociation, and chemisorption) and absorption probably take place (steps 1 through 5). The necessity for subsequent lattice diffusion (step 5 to 6) for hydrogen environment embrittlement has provoked marked disagreement. If it is shown eventually that hydrogen must diffuse through the lattice for embrittlement to occur during testing in gaseous hydrogen,

---

[2] The italic numbers in brackets refer to the list of references appended to this paper.

TABLE 1—*Characteristics of the types of hydrogen embrittlement.*

	Types of Embrittlement		
Characteristics	Hydrogen Environment Embrittlement	Internal Reversible Hydrogen Embrittlement	Hydrogen Reaction Embrittlement
Usual source of hydrogen	gaseous (H_2)	$\left.\begin{array}{l}\text{processing}\\ \text{electrolysis}\\ \text{corrosion}\end{array}\right\}$ (H)	gaseous or atomic hydrogen from any source
Typical conditions	10^{-6} to 10^8 N/m^2 gas pressure most severe near room temperature observed −100° to 700° C gas purity is important strain rate is important	0.1 to 10 ppm average H content most severe near room temperature observed −100° to 100° C strain rate is important	heat treatment or service in hydrogen, usually at elevated temperatures
Test methods	notched tensile unnotched tensile creep rupture fatigue (low, high cycle) fracture toughness disk pressure test	notched delayed failure slow strain rate tensile bend tests C-rings torqued bolts	can be observed visually or metallographically
Crack initiation	(surface or internal initiation)[a]	internal crack initiation incubation (reversible) slow, discontinuous growth fast fracture	usually internal initiation from bubbles or flakes
Rate controlling step	adsorption = transfer step $\left(\begin{array}{l}\text{absorption or}\\ \text{lattice diffusion}\end{array}\right)^a = \begin{array}{l}\text{embrittling}\\ \text{step}\end{array}$	lattice diffusion to internal stress raisers	chemical reaction to form hydrides or gas bubbles

[a] Unresolved.

TABLE 2—*Metals and alloys embrittled by hydrogen.*

Hydrogen Environment Embrittlement^{a,b}	Internal Reversible Hydrogen Embrittlement^{a,c}	Hydrogen Reaction Embrittlement
High-strength steels	High-strength steels	1. Hydrides (MH_x)
18Ni maraging	4340, 4140, H-11	(*a*) H reacts with matrix
410, 440C, 430F	17-4PH, AM 355	Ti, Zr, Hf, V, Cb, Ta
H-11, 4140, 1042 (Q&T)	18Ni maraging	Mn, Ni, Pd, U, Pu, Th
Fe-9Ni-4Co, 17-7PH	E8750, 17-7PH	Rare earths
Nickel and nickel alloys		Alkalies
Electroformed Ni		Alkaline earths
Nickel 200, 270, 301	Experimental Fe-Ni-Cr alloys	(*b*) H reacts with element in matrix
Inconel 625, 700, 706, 718		MgZr, MgTh alloys
René 41, Hastelloy X		
Udimet 700, Waspaloy	Experimental Fe-Cu alloys	
MAR M-200DS, IN 100		2. High-pressure gas bubbles
Low-strength steels		(*a*) H reacts with itself (H_2)
Armco iron, CK 22, CK 45, 1020	Ti, Zr, V, Cb, Ta	Steels, OFHC Cu
1042 Nor, HY-80, HY-100	Cr, Mo, W, Co, Ni	Ni, Al, Mg, Be
A302, A515, A517	Pt, Cu, Au, Al, Mg or some of their alloys	(*b*) H reacts with foreign element in matrix
Titanium alloys		
Ti-6Al-4V, Ti-5Al-2.5Sn		

Molybdenum TZM		CH_4—low alloy steels, Ni alloys
Cobalt alloys	Metastable stainless steels	H_2O—welded steels, Cu, Ni, Ag
HS-188, L-605, S-816	304L, 310	NH_3—molybdenum
Metastable stainless steels		
304L, 305, 310		
K-monel	K-monel	
Be-Cu alloy 25		
Pure titanium	High-strength nickel alloys	
Stable stainless steels	Inconel 718	
316, 321, 347, A286	René 41	
Armco 21-6-9, 22-13-5	Waspaloy	
Copper alloys, OFHC Cu		
Magnesium alloy HM21A		
Aluminum alloys	Stable austenitic steels	
1100, 2219, 6061, 7039, 7075	316, A286, U-212	

---

[a] Listed in approximate order of decreasing susceptibility at room temperature.

[b] Most alloys from Refs *14* and *23*.

[c] Most steels and nickel-base alloys from Ref *27*.

hydrogen environment embrittlement may then be considered equivalent to internal reversible hydrogen embrittlement.

The characteristics of hydrogen environment embrittlement are listed in Table 1. Hydrogen environment embrittlement has been observed over a wide range of gas pressures, temperatures, and in a variety of mechanical tests. Embrittlement appears to be most severe near room temperature. Gas purity and test strain rate can play significant roles in determining the degree of embrittlement. As will be discussed subsequently, the transfer step of surface adsorption has been shown to be the overall rate controlling step during hydrogen environment embrittlement [*4,5*]. However, if adsorption is bypassed, the rate controlling step for hydrogen environment embrittlement is either absorption [*5,23*] or subsequent lattice diffusion [*15,18,24*]. Analyses of substantial increases in the hydrogen content [*18, 20,22,24*] of embrittled alloys tend to support the necessity for lattice diffusion, since it is unlikely that such large quantities of hydrogen can be absorbed within the first atomic layer below the surface. Another important characteristic of hydrogen environment embrittlement that has not been conclusively resolved is the location of crack initiation—at the surface [*23*] or internally [*15,18,20*]. These characteristics can be compared with those observed for internal reversible hydrogen embrittlement and for hydrogen reaction embrittlement which are also listed in Table 1.

Hydrogen environment embrittlement has been observed in a wide variety of materials. The high-strength structural alloys such as steels and nickel-base alloys are particularly susceptible. Metals and alloys subject to all types of hydrogen embrittlement are listed in Table 2. Those affected by hydrogen environment embrittlement [*14,23*] and internal reversible hydrogen embrittlement [*27*] are listed in the approximate order of decreasing susceptibility at room temperature. The metals affected by hydrogen reaction embrittlement are also listed in Table 2, and the types of reactions are called out.

It is important to note that nickel alloys are very susceptible to hydrogen environment embrittlement, while they are relatively unsusceptible to internal reversible hydrogen embrittlement. This difference in sensitivity may be related to some undefined surface characteristic of nickel alloys. This marked difference in susceptibility exhibited by nickel alloys has been responsible for some of the controversy as to whether the mechanism of hydrogen environment embrittlement is the same as the mechanism for internal reversible hydrogen embrittlement. With this one major exception, the relative susceptibility of most classes of materials to both these types of embrittlement is remarkably similar.

Severity of embrittlement has also been observed to vary with both alloy form and annealing temperature. The degradation of notched tensile properties of Inconel 718 in bar, forging, and plate forms and in two solution annealed conditions is shown in Table 3 [*9*]. For example, bar and forgings

TABLE 3—*Degradation of notched tensile properties of Inconel 718.*

(Hydrogen pressure 35 MN/m² (5000 psi), 23° C, stress concentration factor (K_t) = 8 [*9*])

	Ratio of Property in Hydrogen/in Helium			
	Notch Tensile Strength		Notch Reduction of Area	
Material Form	940° C Anneal	1050° C Anneal	940° C Anneal	1050° C Anneal
Bar	0.54	0.71	0.31	0.34
Forging	0.59	0.76	0.37	0.39
Plate	0.86	0.77	0.67	0.62
Plate-weld metal	0.79	0.56	0.71	0.31
Plate-heat affected zone	0.63	0.72	0.39	0.29

annealed at the lower temperature are embrittled more severely than the same forms annealed at the higher temperature. For plate, the reverse ranking holds. These effects have been attributed to as-received and heat-treated precipitate (Ni_3Cb) morphology [*9*] and grain size [*9,10*]. The least embrittled structure is one which is fine grained with a uniform dispersion of the precipitate. The most embrittled structure is one which is large grained with intergranular precipitates.

Although these microstructural effects may be valid for Inconel 718, other severely embrittled nickel-base alloys [*12–14*] do not contain columbium (Udimet 700, René 41, and Hastelloy X). In fact, Nickel 270 does not contain any elements that are likely to form precipitates. Hence, it is unlikely that hydrogen environment embrittlement can be attributed exclusively to precipitated phases. The role of grain size and grain boundaries is also unresolved, particularly in light of the severe degree of hydrogen environment embrittlement recently reported for directionally solidified MAR M-200 [*13*].

Effect of Test Variables

Hydrogen Gas Pressure

Most of the materials listed in Table 2 were tested in a single investigation [*14,23*] at a hydrogen pressure of 70 MN/m² (10 000 psi) at room temperature. Notched tensile strength and both smooth and notched reduction of area were used as the embrittlement criteria. Subsequent research [*11, 14*] indicated that embrittlement can occur in hydrogen at much lower gas pressures. For example, tensile properties of A302-B steel and Inconel 718 determined over a range of hydrogen pressures from 0.7 to 70 MN/m² (100 to 10 000 psi) are compared with tensile properties in helium in Fig. 2. These investigations suggested that the degree of embrittlement was proportional to the square root of the hydrogen gas pressure.

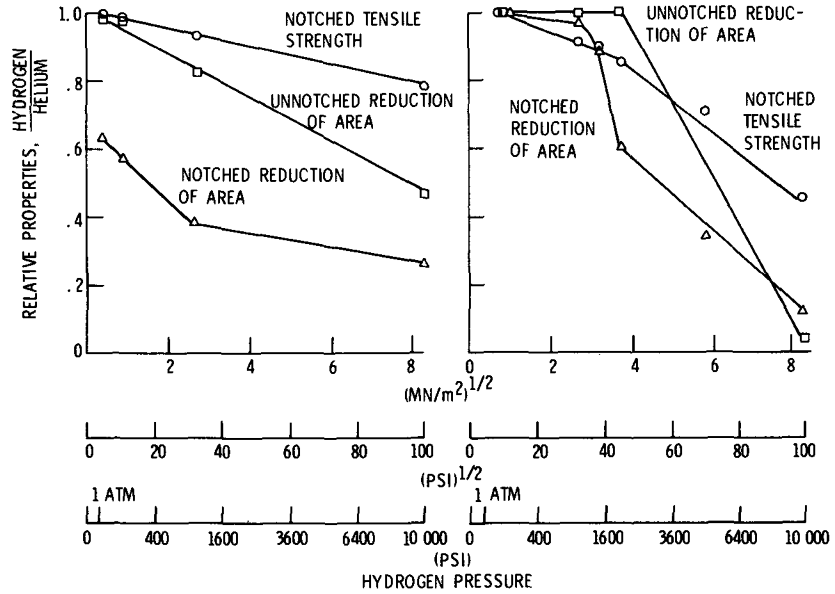

(a) A302-B STEEL.

(b) INCONEL 718 BAR.

FIG. 2—*Effect of gas pressure on tensile properties of A302-B steel* [14] *and Inconel 718* [9, 14] *at 23° C. Inconel bar annealed at 1050° C; notched specimens,* K_t = *8.*

More recent investigations [*4,25*] have demonstrated that hydrogen environment embrittlement occurs at gas pressures substantially below atmospheric pressure. Fatigue crack growth rates of Nickel 200 at room temperature increased by an order of magnitude over the pressure range 1 $\mu N/m^2$ to 20 kN/m^2 (10^{-8} to 150 torr) [*25*]. The threshold stress intensity factor (K_{th}) required for the initiation of measurable slow crack growth in 4130 steel in air decreased substantially in hydrogen at very low pressures [*4,5*]. For example, embrittlement was detected in molecular hydrogen at pressures of 17 kN/m^2 (127 torr), Fig. 3*a*, and in an atomic-molecular hydrogen mixture at a gas pressure of 1 N/m^2 (8×10^{-3} torr), Fig. 3*b*. As evident from the data presented in Fig. 3, embrittlement was a function of both test crosshead speed and test temperature. The significance of testing speed, testing temperature, and gas composition will be discussed in subsequent sections of this paper.

These same investigators [*4*] have also demonstrated that the degree of embrittlement is proportional to the square root of the gas pressure. However, they showed that such a relationship is true only in a relatively narrow temperature range near room temperature. They proposed that the transfer step of surface adsorption of hydrogen was the overall rate controlling step in the process of hydrogen environment embrittlement.

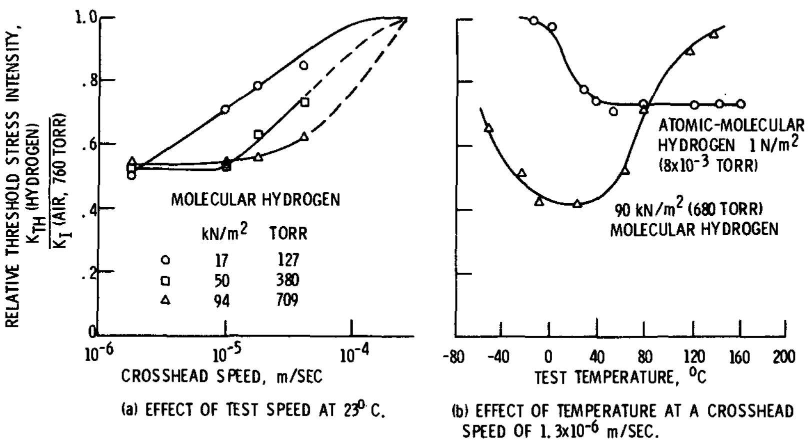

(a) EFFECT OF TEST SPEED AT 23° C.

(b) EFFECT OF TEMPERATURE AT A CROSSHEAD SPEED OF 1.3×10^{-6} m/SEC.

FIG. 3—*Effect of crosshead speed, test temperature, hydrogen pressure, and hydrogen composition on threshold stress intensity* (K_{th}) *4130 steel* [4, 5].

Hydrogen Gas Composition

The influence of gas purity is dramatically illustrated by the crack extension data shown in Fig. 4. Crack extension in a stressed precracked sheet specimen of H-11 steel could be started by the introduction of pure hydrogen, and a running crack could be literally stopped by the introduction of oxygen-doped hydrogen [17]. These investigators reported that crack propagation rates were not affected by an atmosphere of hydrogen containing less than 200-ppm oxygen at a total gas pressure of 0.1 MN/m^2

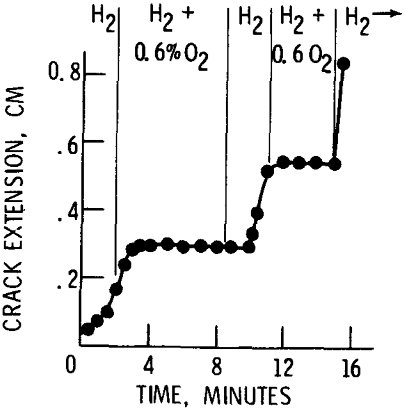

FIG. 4—*Effect of hydrogen purity on crack growth in H-11 steel at 23° C and a hydrogen pressure of 0.1* MN/m^2 *(15 psi)* [17].

(15 psi). However, at higher gas pressures, even lower concentrations of oxygen impurities inhibit embrittlement in gaseous hydrogen [*16,17,24*]. This inhibiting effect of oxygen is related probably to the preferential adsorption of the oxygen at freshly generated crack tips [*17*].

It is interesting to note that hydrogen environment embrittlement is not eliminated by dilution of hydrogen with inert gases. For example, measurable reductions of notched tensile properties were reported for both steels and nickel-base alloys for tests conducted in 70 MN/m^2 (10 000 psi) helium containing only 44-ppm hydrogen [*14*].

Some recently reported crack growth tests were conducted in an atomic-molecular hydrogen mixture achieved by a clever experimental procedure [*5*]. An atomic-molecular hydrogen gas mixture was created near the crack tip by dissociating molecular hydrogen on a hot filament. At a gas pressure of only 1 N/m^2 (8×10^{-3} torr), crack growth rates were several orders of magnitude greater in the atomic-molecular mixture than predicted rates in molecular hydrogen [*4*]. As shown in Fig. 3*b*, crack growth persisted to the limit of their experimental temperature capability (164° C), whereas crack growth diminished in molecular hydrogen as the test temperature was raised above room temperature. These test results confirmed that hydrogen adsorption is a transfer step which is the overall rate controlling step in the process of hydrogen environment embrittlement. When this slow reaction step is bypassed by creating atomic hydrogen near the crack tip, then the rate controlling step for embrittlement is either absorption of hydrogen into solution or lattice diffusion of hydrogen.

These results also suggest that, if sufficient atomic hydrogen were available, embrittlement might occur to a greater degree and over a broader range of temperatures and pressures than determined in laboratory tests to date. Such a phenomenon is particularly significant in regard to advanced engine applications that may use hydrazine or other fuels which decompose to atomic hydrogen.

The effect of an environment of water saturated hydrogen on the tensile properties of Udimet 700 has also been determined [*12*]. All tensile properties over the temperature range 150° to 305° C were essentially identical to those determined in dry hydrogen, as will be shown later in the section on the effect of test temperature. These results are not consistent with the crack growth inhibiting effects reported for both wet hydrogen [*21*] and oxygen plus hydrogen (Fig. 4). It is possible that contaminants in hydrogen readily inhibit embrittlement when testing precracked specimens, while the gross plastic deformation which occurs when testing smooth tension specimens may negate such an inhibiting effect.

Test Strain Rate

Some of the initial investigations of hydrogen environment embrittlement were concerned with the influence of test strain rate [*16,22*]. These tests demonstrated that embrittlement was more severe at low strain rates than at high strain rates. Such strain rate sensitivity is a well-known characteristic of internal reversible hydrogen embrittlement and implies that hydrogen diffusion through the metal lattice during mechanical testing controls the degree of embrittlement. An identical effect may be occurring during hydrogen environment embrittlement, or it is possible that the observed strain rate sensitivity is simply a manifestation of the time that freshly created surfaces are exposed to hydrogen.

The more recent experimental investigations have been concerned with screening numerous materials for relative susceptibility to hydrogen environment embrittlement [*10,12,14*]. None of these programs have investigated the potential influence of strain rate on the degree of embrittlement. Fortunately, the tests conducted in these investigations were performed at relatively low strain rates. Unfortunately, since each of the three investigators used different strain rates for tension testing, direct comparison of their experimental results may not be possible. Test crosshead speeds used by these investigators ranged from 4×10^{-5} m/s (1×10^{-1} in./min) [*10*] to 3×10^{-7} m/s (7×10^{-4} in./min) [*14*].

Another investigation dealing with the influence of testing speed was discussed previously with respect to Fig. 3*a*. Fracture toughness tests were performed over a range of crosshead speeds. Embrittlement was more severe at lower crosshead speeds for each of the gas pressures used in the tests. The significance of these results is that test speed is an important experimental variable for tests utilizing precracked specimens as well as smooth bar tension specimens.

Stress Concentration Factor

A limited amount of research has been conducted on the influence of notch stress concentration factor on the severity of hydrogen environment embrittlement. The data shown in Fig. 5 comparing tensile properties in hydrogen and in helium demonstrate that embrittlement in hydrogen is more severe for a notched specimen of A302-B steel than for a smooth specimen [*11,14*]. The tensile strength of a smooth specimen (a stress concentration factor of 1) is relatively unaffected by hydrogen. Embrittlemnt increases as the stress concentration factor increases from 1 to the range 4 to 6, but there does not appear to be any increased sensitivity at higher concentration factors of 8 or even for precracked specimens. Similar results were reported for A517 steel [*11,14*], 4140 steel [*19*], and 304L stainless steel [*19*].

An even more sensitive measure of the severity of hydrogen environment embrittlement is the reduction of area of notched specimens. From the data presented in Figs. 2 and 5, it is apparent that significant decreases in notched reduction of area occur during testing in hydrogen. Once again it does not appear necessary to test specimens with extremely sharp notches

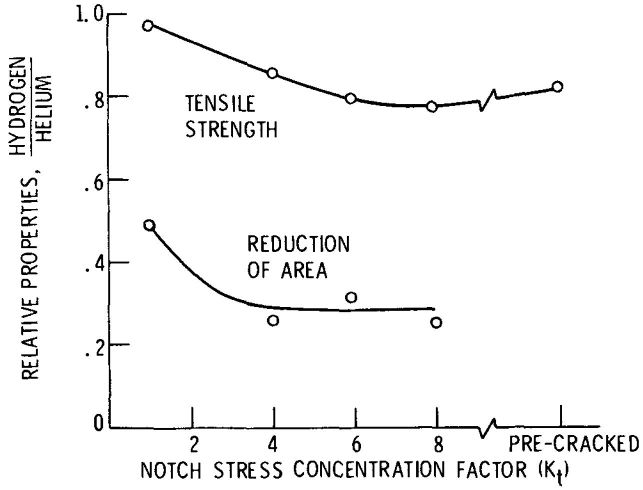

FIG. 5—*Effect of notch stress concentration factor* (K_t) *on tensile properties of A302-B steel at 23° C determined in hydrogen and helium at a pressure of 70 MN/m^2 (10 000 psi)* [11, 14].

Notch stress concentration factors in the range 4 to 8 appear to be sufficient for determining the severity of hydrogen environment embrittlement.

Test Temperature

A substantial amount of research has been conducted on the effect of test temperature on hydrogen environment embrittlement. The early data were determined over a relatively narrow range of test temperatures, −90° to 170° C, with CK 22 steel at a hydrogen pressure of 15 MN/m^2 (2200 psi) [*16*]. More recent research was performed over the temperature range −196° to 60° C with Inconel 718 and Ti-6Al-4V at a hydrogen pressure of 14 MN/m^2 2000 psi) [*14*]. In all cases reductions in unnotched tensile ductility or notched tensile strength were most severe in the vicinity of room temperature.

Increased interest in recent years in using hydrogen for advanced rocket and gas turbine engines has resulted in extensive investigations of the effect of hydrogen on structural materials over a much wider range of exposure temperatures. Materials of interest include steels [*3,10,12*], titanium alloys [*10,12*], refractory metals [*6*], and particularly, nickel- [*3,10,12*] and cobalt- [*3,13*] base alloys.

The tensile properties of Inconel 718 tested over the temperature range −196° to 525° C in hydrogen at 50 MN/m^2 (7500 psi) are presented in Fig. 6*a* and *b* [*12*]. It is apparent from these data that reductions in both notched tensile strength and unnotched ductility are most severe near room temperature. However, significant embrittlement is still evident at substantially higher temperatures. In particular, the reduction of area of Inconel 718 at 525° C in hydrogen is about 67 percent of the value determined in air (Fig. 6*b*).

The tensile properties of Udimet 700 determined from 23° to 680° C in hydrogen at 30 to 50 MN/m^2 (4500 to 7500 psi) are presented in Fig. 7*a* and *b* [*12*]. The extent of the embrittling effect of hydrogen on this alloy is far greater than for any other material reported to date. The notched tensile strength of Udimet 700 in hydrogen went through a minimum at about 200° C and gradually approached the notched tensile strength determined in air as the test temperature was increased to 680° C (Fig. 7*a*). Moreover, the tensile properties of smooth specimens (ultimate strength, reduction of area, and elongation)were reduced substantially by hydrogen and remained at these low values over the entire range of test temperatures. For example, the elongation of Udimet 700 in hydrogen was about 3 percent for all test temperatures, as compared to about 20 percent in air (Fig. 7*b*). As mentioned previously during the discussion on hydrogen purity, these investigators did not find any difference in the degree of embrittlement for Udimet 700 tested in dry hydrogen and water saturated hydrogen. Over the temperature range 150° to 305° C, there was also no effect of test temperature.

The results just discussed, determined in dry hydrogen, could not be reproduced in another investigation [*13*]. Neither the smooth nor the notched tensile properties of Astroloy (Udimet 700) were reduced by more than 10 percent by testing in dry hydrogen at both 3.5 and 35 MN/m^2 (500 and

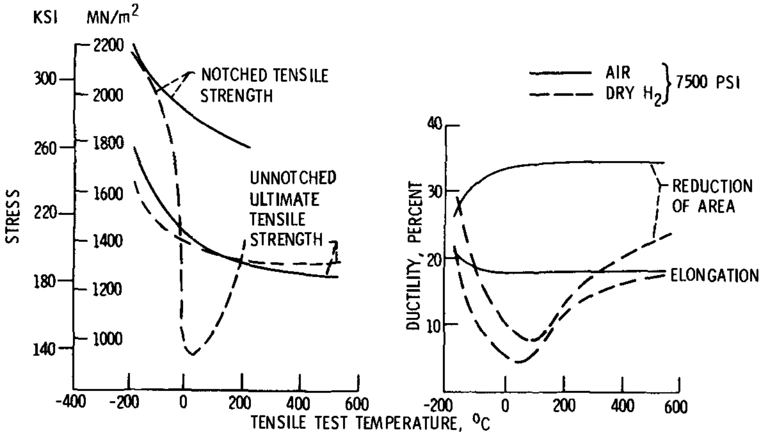

(a) STRENGTH. (b) UNNOTCHED DUCTILITY.

FIG. 6—*Effect of test temperature on tensile properties of Inconel 718 bar at a hydrogen pressure of 50 MN/m^2 (7500 psi)* [12]. *Alloy annealed at 950° C; notched specimens,* $K_t = 8$.

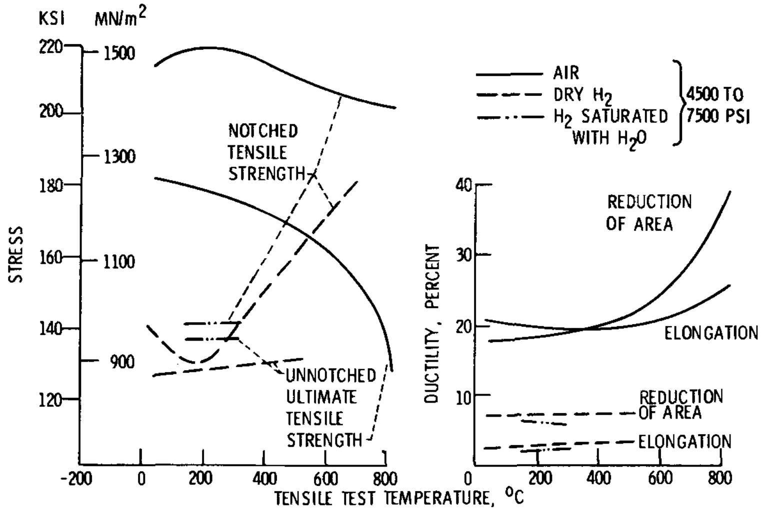

(a) STRENGTH. (b) UNNOTCHED DUCTILITY.

FIG. 7—*Effect of test temperature on tensile properties of Udimet 700 at a hydrogen pressure of 30 to 50 MN/m² (4500 to 7500 psi)* [12]. *Notched specimens,* $K_t = 8$.

5000 psi) and at 23° and 680° C. Such lack of reproducibility may be due to variations in alloy microstructure.

The effect of test temperature on the threshold stress intensity for crack initiation in Inconel 718 in hydrogen is shown in Fig. 8 [*12*]. Sustained load, plane-strain toughness test specimens were used to determine these data.

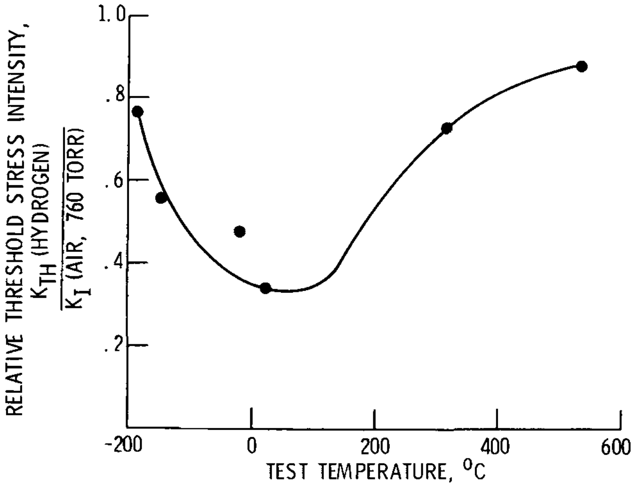

FIG. 8—*Effect of test temperature on threshold stress intensity* (K_{th}) *of Inconel 718 plate at a hydrogen pressure of 50 MN/m² (7500 psi)* [12]. *Alloy annealed at 1066° C.*

The effect of temperature on the threshold stress intensity of this alloy is almost identical to the effect determined for tensile properties (see Fig. 6). Embrittlement is most pronounced near room temperature (K_{th} = 33 $MN/m^2\sqrt{m}$ (30 ksi$\sqrt{in.}$)) and decreases at both lower and higher temperatures. A similar value of threshold stress intensity (K_{th} = 24 $MN/m^2\sqrt{m}$ (22 ksi$\sqrt{in.}$)) at room temperature has been reported by others for Inconel 718 annealed at 954° C [*7*,*9*].

Relative Sensitivity of Various Test Methods

From the data presented in the preceding figures, it is evident that tension tests have been frequently used to determine the extent of hydrogen environment embrittlement of metals. Large decreases in unnotched reduction of area, notched reduction of area, and notched tensile strength have been reported for various metals. Fracture toughness testing has also been shown to be a sensitive technique for determining the extent of hydrogen environment embrittlement. However, most investigators have utilized only one or two types of tests, and, frequently, experimental variables differ among investigators so that comparison of data is difficult.

A recent investigation [*10*] has used fatigue and creep testing in addition to tension and fracture toughness testing to determine the relative susceptibility of various alloys to hydrogen environment embrittlement. It is informative to evaluate the relative sensitivity of all of these test methods. The degradation of various mechanical properteis of Inconel 718 in hydrogen at a pressure of 35 MN/m^2 (5000 psi) is presented in Fig. 9. It is immediately evident that substantial decreases in both low-cycle (LCF) and high-cycle (HCF) fatigue lives occur during testing in hydrogen. Both LCF (2000 cycles in helium) and HCF (50 000 cycles in helium) lives were

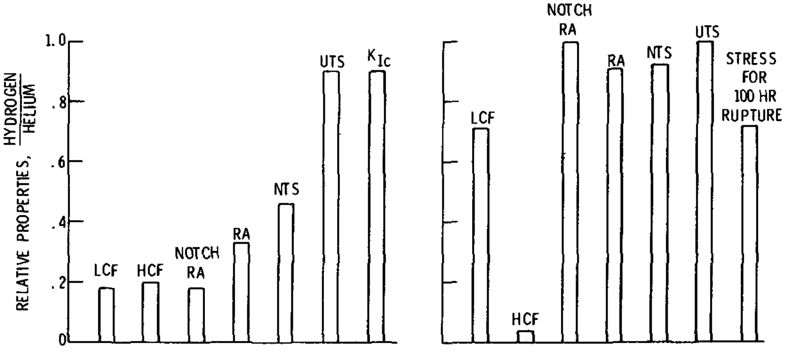

(a) TEST TEMPERATURE 26° C. (b) TEST TEMPERATURE 680° C.

FIG. 9—*Comparison of mechanical properties of Inconel 718 bar determined in hydrogen and helium at a pressure of 35* MN/m^2 *(5000 psi)* [10]. *Alloy annealed at 1038° C; notched specimens,* K_t = *8; LCF, 1 to 2 percent strain; HCF,* R = *0.1,* (a) *180 ksi,* (b) *140 ksi.*

reduced about 80 percent when tested at 26° C in hydrogen. At 680° C the LCF life (400 cycles in helium) was reduced about 30 percent, and the HCF life (20 000 cycles in helium) was reduced about 96 percent.

These same investigators also showed that notched tensile properties and unnotched reduction of area at 26° C are degraded substantially by hydrogen, as has been discussed in several previous sections of this paper. The stress for 100-h rupture life at 680° C also appeared to be reduced. All other properties were reduced by 10 percent or less. The negligible degradation of fracture toughness reported by these investigators is in marked contrast to the substantial decreases in the fracture toughness of Inconel 718 determined at room temperature by others (see previous section, Fig. 8 and Refs *7,9,12*). Such lack of reproducibility may be due to material variations or to slight differences in hydrogen pressure and purity.

A newly developed technique, the disk pressure test [*18*], has the appealing advantages of low cost, simplicity, and rapidity of testing. Small disks of sheet material are attached to a high-pressure chamber by restraint at their periphery and ruptured by introducing gaseous hydrogen into the chamber. Hydrogen pressure can be increased at a given rate until failure occurs or held constant at very low pressures to determine the delayed failure characteristics of the material. For example, the delayed failure behavior of high-strength (2 GN/m^2 (300 ksi)) martensitic steel (4.3Ni, 1.9Cr, 0.5Mo, 0.4C, 0.37Mn, 0.3Si) is shown in Fig. 10 [*26*].

These results determined during hydrogen environment testing are identical to results commonly encountered during testing for internal reversible hydrogen embrittlement. Figure 10 exhibits all the characteristics of the classical delayed failure tests determined with cathodically hydro-

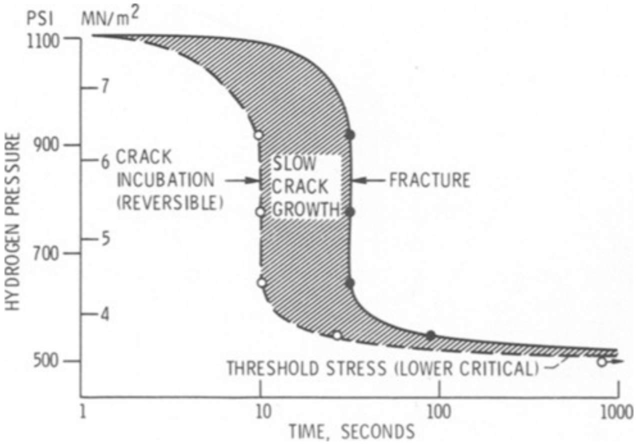

FIG. 10—*Effect of hydrogen pressure on the delayed failure of 35 NCD 16 steel at 23° C determined by the disk pressure test* [26].

genated steels—a crack incubation period which is reversible with respect to applied stress (pressure), a region of slow crack growth followed by catastrophic failure, and a threshold stress (lower critical stress) below which crack growth and failure do not occur in a reasonable test time. Such similarities between hydrogen environment embrittlement and internal reversible hydrogen embrittlement have been naturally used by these investigators [*18,26*] as evidence that these two types of embrittlement are analogous.

Concluding Remarks

In this paper the author has tried to lay the groundwork for subsequent discussions of mechanisms and the details of test specimens and test techniques for hydrogen environment embrittlement research. Both the effects of the experimental variables and test techniques used by previous investigators have been discussed. The results of both mechanistic and screening studies have been described.

It is important to determine the effects of several experimental variables before attempting to standardize either test specimens or test techniques. The results determined to date regarding the degree of susceptibility of metals to hydrogen environment embrittlement are not reproducible among investigators. The author feels that both experimental and material variables may account for this observed lack of reproducibility. Therefore, it is suggested that the effects of experimental variables such as test strain rate, gas purity, specimen surface condition, holdtime in the environment prior to testing, and baseline environment (air, helium, argon, or vacuum) be studied in more detail. The role of material microstructure, grain size, and grain boundaries is not well understood and requires additional research, possibly with directionally solidified alloys and single crystals. In addition to helping to resolve the lack of reproducibility of test results, greater knowledge of the precise influence of these variables would be invaluable in determining the mechanism of hydrogen environment embrittlement. Finally, in order to determine whether hydrogen environment embrittlement is distinct from internal reversible embrittlement, particular emphasis should be placed on the necessity for hydrogen diffusion through the lattice and the location of crack initiation during hydrogen environment embrittlement. It appears that the disk pressure and fracture toughness tests of various types have great potential for determining the influence of many of these experimental variables.

Both notched tensile and disk pressure testing appear to be sufficiently sensitive to determine the occurrence of and the relative susceptibility of materials to hydrogen environment embrittlement at pressures below about 7 MN/m^2 (1000 psi). At higher pressures, standard unnotched tension tests probably could also be used for screening purposes. All of these tests, however, should be conducted at low strain rates. Obviously, all mechanical testing should be conducted under simulated service conditions of gas pressure, gas purity, and temperature.

For more detailed investigations and prior to final design for service applications in hydrogen, it is suggested that fracture toughness, creep rupture, or fatigue tests be conducted. The choice of these tests should be dictated by the type of loading conditions that will be experienced in service. Once again it is extremely important for valid testing results that the hydrogen composition represent what is to be encountered in service. If precracked specimens are to be tested, then they should be precracked and tested in the simulated service environment without any intermediate exposure to other environments.

References

[*1*] McPherson, W. B. and Cataldo, C. E., "Recent Experience in High Pressure Gaseous Hydrogen Equipment at Room Temperature," Technical Report No. D 8–14.1, American Society for Metals, Metals Park, Ohio, Oct. 1968.

[*2*] Laws, J. S., Frick, V., and McConnell, J., "Hydrogen Gas Pressure Vessel Problems in the M-1 Facilities," NASA Report CR-1305, National Aeronautics and Space Administration, Washington, D. C., March 1969.

[*3*] Klima, S. J., Nachtigall, A. J., and Hoffman, C. A., "Preliminary Investigation of Effect of Hydrogen on Stress-Rupture and Fatigue Properties of an Iron-, a Nickel-, and a Cobalt-Base Alloy," NASA Report TN D-1458, National Aeronautics and Space Administration, Cleveland, Ohio, Dec. 1962.

[*4*] Williams, D. P. and Nelson, H. G., *Metallurgical Transactions*, Vol. 1, No. 1, Jan. 1970, pp. 63–68.

[*5*] Nelson, H. G., Williams, D. P., and Tetelman, A. S., *Metallurgical Transactions*, Vol. 2, No. 4, April 1971, pp. 953–959.

[*6*] Chandler, W. T. and Walter, R. J., "Hydrogen Effects in Refractory Metals," presented at the Symposium on Metallurgy and Technology of Refractory Metal Alloys, American Institute of Mining, Metallurgical, and Petroleum Engineers and National Aeronautics and Space Administration, Washington, D. C., 25–28 April 1968.

[*7*] Lorenz, P. M., "Effect of Pressurized Hydrogen upon Inconel 718 and 2219 Aluminum," Technical Report D2-114417-1, NASA CR-100208, The Boeing Company, Seattle, Wash., Feb. 1969.

[*8*] Campbell, J. E., "Effect of Hydrogen Gas on Metals at Ambient Temperature," Technical Report DMIC S-31, Battelle Memorial Institute, Columbus, Ohio, 1970.

[*9*] Walter, R. J., Hayes, H. G., and Chandler, W. T., "Influence of Gaseous Hydrogen on Metals," Technical Report R-8719, NASA CR-119917, Rocketdyne, Division of North American Rockwell Corp., Canoga Park, Calif., May 1971.

[*10*] Harris, J. A., Jr., and VanWanderham, M. C., "Properties of Materials in High Pressure Hydrogen at Cryogenic, Room, and Elevated Temperatures," Technical Report PWA-FR-4566, NASA CR-119884, Pratt and Whitney Aircraft Div., United Aircraft Corp., West Palm Beach, Fla., June 1971.

[*11*] Walter, R. J. and Chandler, W. T., *Materials Science and Engineering*, Vol. 8, 1971, pp. 90–97.

[*12*] Frick, V., Janser, G. R., and Brown, J. A. in *Space Shuttle Materials*, Vol. 3, Society of Aerospace Materials and Process Engineers, Azusa, Calif., 1971, pp. 597–634.

[*13*] Harris, J. A., Jr., and VanWanderham, M. C., "Influence of Elevated Temperature on Metals in Gaseous Hydrogen," Technical Report PWA-FR-5129, Pratt and Whitney Aircraft Div., United Aircraft Corp., West Palm Beach, Fla., June 1972.

[*14*] Jewett, R. P., Walter, R. J., Chandler, W. T., and Frohmberg, R. P., "Hydrogen-

Environment Embrittlement of Metals," NASA CR-2163, Rocketdyne, Division of North American Rockwell Corp., Canoga Park, Calif., 1973.

[*15*] Cavett, R. H. and Van Ness, H. C., *Welding Journal, Welding Research Supplement*, Vol. 42, July 1963, pp. 316s–319s.

[*16*] Hofman, W. and Rauls, W., *Welding Journal, Welding Research Supplement*, Vol. 44, May 1965, pp. 225s–230s.

[*17*] Hancock, G. G. and Johnson, H. H., *Transactions*, American Institute of Mining, Metallurgical, and Petroleum Engineers, Vol. 236, No. 4, April 1966, pp. 513–516.

[*18*] Fidelle, J.-P., Allemand, L. R., Roux, C., and Rapin, M. in *Hydrogen in Metals*, J. P. Fidelle and M. Rapin, Eds., Valduc Colloquim, Commissariat a l'Energie Atomique, France, Sept. 1967, pp. 131–172.

[*19*] Vennett, R. M. and Ansell, G. S., *Transactions Quarterly*, American Society for Metals, Vol. 60, No. 2, June 1967, pp. 242–251.

[*20*] Benson, R. B., Jr., Dann, R. K., and Roberts, L. W., Jr., *Transactions*, American Institute of Mining, Metallurgical, and Petroleum Engineers, Vol. 242, No. 10, Oct. 1968, pp. 2199–2205.

[*21*] Spitzig, W. A., Talda, P. M., and Wei, R. P., *Engineering Fracture Mechanics*, Vol. 1, 1968, pp. 155–165.

[*22*] Vennett, R. M. and Ansell, G. S., *Transactions Quarterly*, American Society for Metals, Vol. 62, No. 4, Dec. 1969, pp. 1007–1013.

[*23*] Walter, R. J., Jewett, R. P., and Chandler, W. T., *Materials Science and Engineering*, Vol. 5, No. 2, Jan. 1970, pp. 98–110.

[*24*] Fricke, E., Stuwe, H. P., and Vibrans, G., *Metallurgical Transactions*, Vol. 2, No. 9, Sept. 1971, pp. 2697–2700.

[*25*] Marcus, H. L. and Stocker, P. J. in *Specialists Meeting on Stress Corrosion Testing Methods*, Conference Proceedings No. 98, Advisory Group for Aerospace Research and Development, Paris, France, Jan. 1972, pp. 16–1 to 16–6.

[*26*] Jolly, N., LeGallo, P., Bretin, L., and Fidelle, J.-P., "Extensometric Measurements on 35NCD16 Steel Disks Ruptured by Hydrogen," TA-1336, Commissariat a l'Energie Atomique, France, 1970.

[*27*] Groeneveld, T. P., Fletcher, E. E., and Elsea, A. R., "A Study of Hydrogen Embrittlement of Various Alloys," Technical Report NASA CR-77374, Battelle Memorial Institute, Columbus, Ohio, June 1966.

H. G. Nelson[1]

Testing for Hydrogen Environment Embrittlement: Primary and Secondary Influences

---

REFERENCE: Nelson, H. G., "**Testing for Hydrogen Environment Embrittlement: Primary and Secondary Influences,**" *Hydrogen Embrittlement Testing, ASTM STP 543,* American Society for Testing and Materials, 1974, pp. 152–169.

ABSTRACT: The deleterious consequences of hydrogen on an engineering structure come about through an influence on either the crack initiation or the slow crack growth stage of fracture. Whether or not these two stages of fracture are affected by hydrogen will depend on a number of primary and secondary influences which severely complicate the embrittlement process. In this review we present a somewhat phenomonological overview of the hydrogen embrittlement process, both internal as well as external, in an effort to make more clear the type of parameters which must be considered in the selection of a test method and test procedure such that the resulting data may be meaningfully applied to real engineering structures. We consider what are believed to be the three primary influences on the embrittlement process: (1) the original location and form of the hydrogen, (2) the transport reactions involved in the transport of hydrogen from its origin to some point where it can interact with the metal to cause embrittlement, and (3) the embrittlement interaction itself. Additionally, a few of the large number of secondary influences on the embrittlement process are discussed, for example, the influence of impurity species in the environment, surface hydride films, and surface oxide films. Finally, specific test procedures are discussed in order to further elucidate the parameters which must be considered in the development of a standardized test method.

KEY WORDS: hydrogen embrittlement, crack propagation, parameters, engineering structures, voids, cyclic loads, tests

The capacity of an engineering structure to withstand an applied load is often degraded severely by the presence of hydrogen originating from its equilibrium position within the metal lattice, from a gaseous hydrogen environment in contact with the structure, or as the product of a hetero-

---

[1] Ames Research Center, National Aeronautics and Space Administration, Moffett Field, Calif. 94035.

geneous reaction between a hydrogen-containing molecule and the metal surface. The oldest and most extensively studied form of hydrogen embrittlement is that due to hydrogen within the metal lattice [*1–5*].[2] Hydrogen can enter a metal during production processes, such as pickling and electrolytic plating operations, where the hydrogen concentration at the metal surface can be very large [*6*]. The most recent form of hydrogen embrittlement to be recognized results from the direct exposure of a clean metal surface during deformation to a gaseous hydrogen environment. This form of embrittlement was first studied in detail in 1961 [*7*] and has since been regarded with increasing concern. Because of the usefulness of the hydrogen-oxygen reaction as a fuel cell to produce electric current [*8*] and as a source of energy for propulsion [*9*], this form of embrittlement will become more and more important and may, in the future if not today, control one phase of our technological growth.

The deleterious consequences of hydrogen on an engineering structure come about through an influence on its fracture behavior [*10*]. Under conditions of static loading, fracture in an inert environment occurs in two stages—crack initiation and rapid, unstable crack growth. An additional stage of fracture can be present in a structure under conditions of cyclic loading or in the presence of an active species such as hydrogen. This stage of fracture is termed the subcritical or slow crack growth stage and occurs following crack initiation but prior to rapid fracture. Under cyclic loading this stage of fracture is the result of the mechanical action of opening and closing the crack. When hydrogen is present, either internally or externally, this stage of fracture occurs because hydrogen embrittlement is a time dependent process—time dependent because time is required to transport hydrogen from its original location and form to some point on or within the metal where hydrogen can interact with the metal lattice [*11*].

The interaction between hydrogen and the metal may result in the formation of a solid solution of hydrogen in the metal, second phase hydride precipitates, molecular hydrogen within the metal lattice, products of the reaction between hydrogen and impurities, and others. From the numerous studies conducted on hydrogen embrittlement, the phenomenon can be classified into two distinct types according to its strain rate dependence. The first type of embrittlement is aggravated by increasing strain rate, while embrittlement of the second type decreases with an increase in strain rate. From an engineering standpoint, both forms of embrittlement are important. The first is due to the presence of a product of a completed reaction within the metal lattice and involves fracture theory as related to the crack initiation and crack growth processes within the second-phase precipitate and through the metal lattice. In the second

---

[2] The italic numbers in brackets refer to the list of references appended to this paper.

type, a kinetically controlled reaction occurs concurrently with embrittlement and, in fact, controls the degree of observed embrittlement. This form of embrittlement must then involve reaction kinetics as related to the transport of hydrogen or its interaction with the metal lattice as well as the mechanics of the fracture process itself. Additionally, the second type of embrittlement, unlike the first, need not involve a second phase reaction product.

In general, hydrogen embrittlement is a very complex phenomenon, and many times it can be further complicated by what appear to be unimportant secondary considerations. It is the purpose of this paper to present a somewhat phenomonological overview of the processes of hydrogen embrittlement, both internal as well as external, in order to make the type of parameters which must be considered in the selection of a test method and test procedure more clear, such that the resulting data may be meaningfully applied to real engineering structures. We will discuss what I believe to be the three common, primary influences on the embrittlement process, that is, (1) the original location and form of the hydrogen, (2) the transport reactions involved in the transport of hydrogen from its origin to some point where it can interact with the metal lattice to cause embrittlement, and (3) the embrittlement interaction itself. The implications of each and the potential influence of secondary considerations on each will be considered in some detail in an effort to elucidate the parameters which must be considered in the development of a standardized test method.

Origin of Hydrogen

After an engineering structure is processed, assembled, and in use, hydrogen can be present either externally (in contact with the metal structure) or internally (within the metal lattice). When it is present externally, hydrogen can exist as a molecule, as a dissociated molecule or atom, or as a component of a complex molecule such as hydrogen sulfide, water, or methanol. Internally, its form may be as an atom or screened proton within the metal lattice, as a molecule precipitated at a lattice defect, or as a precipitated metal hydride phase. The original location and form of hydrogen are of primary importance in that they establish the starting point and thus, the complexity of the overall transport process involved in embrittlement. For an example, if we are dealing with a metal that readily forms hydrides, such as alpha titanium, and hydrogen is present originally in the form of massive hydrides on the metal surface or within the metal lattice, the metal may be brittle because of the hydrides, and additional hydrogen transport is not required. This type of embrittlement is termed fast-strain-rate embrittlement, as previously discussed, and is a time independent form of hydrogen embrittlement. In this example it is the original location and form of the hydrogen within the metal structure that is the cause of embrittlement. If, however, hydrogen is present originally in solution within the metal lattice, hydrogen must be transported through the metal lattice under an activity gradient by lattice diffusion to a location where a sufficient concentration is developed to form a hydride and embrittle the metal. This process is time dependent because hydrogen transport is involved. Likewise, if hydrogen is present originally in the external environment, hydrogen transport will also be involved; however, the overall hydrogen transport reactions will be much more complex.

In the design of a standardized test method, it is imperative that the original location and form of hydrogen simulates that which will exist in or around the engineering structure. If tests are being conducted to qualify a plating procedure or to determine the hydrogen pickup in an engineering structure which potentially could be embrittled by the presence of hydrogen, tests are conducted on coupons processed along with the structure made of identical material and size to that of the structure or of material known to be more susceptible to embrittlement. If tests are being conducted to establish the influence of a working environment on an engineering structure, it is equally important that the form and contaminant level in the environment, the condition of the metal surface, and other such variables be duplicated in the greatest detail.

Transport of Hydrogen

If hydrogen is observed to influence the fracture behavior of a structure, hydrogen must have been at some critical location before the metal was stressed or have been transported to this location during deformation. As previously discussed, an example of the former is the embrittlement of a metal by the presence of massive precipitates on the metal surface or in the metal lattice; examples of the latter are forms of embrittlement identified by an inverse strain rate dependence. This inverse strain rate dependence is a result of an overall kinetic reaction involved in the transport of hydrogen from its equilibrium or quasi-equilibrium position in the system to some critical location where it can influence fracture. The rate in which a metal becomes embrittled, then, will depend on the reaction kinetics of the overall transport reaction.

The overall transport reaction involved in the embrittlement process will be very different depending on whether hydrogen originates in the environment surrounding the metal or is present within the metal lattice. When hydrogen originates in the metal lattice, lattice diffusion will be the primary transport reaction [*12*]; however, other reactions such as phase formation, dissolution or chemisorption or both onto an internal surface (of a void perhaps), and desorption into the void cavity may also be involved, depending on where and how hydrogen influences fracture. Even though these transport processes are relatively simple, they can

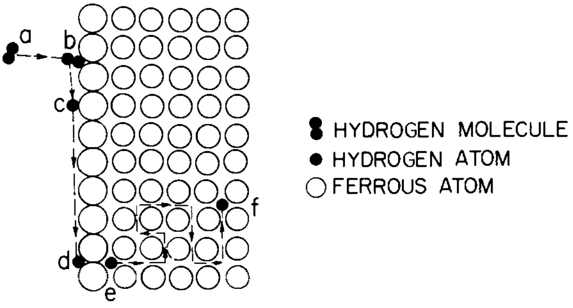

REACTION STEPS

a → b	GAS-PHASE DIFFUSION
b → c	PHYSISORPTION AND DISSOCIATION
c → d	ADATOM MIGRATION AND CHEMISORPTION
d → e	SOLUTION
e → f	LATTICE DIFFUSION

FIG. 1—*Schematic of possible elementary transport reactions involved in external hydrogen embrittlement.*

still be influenced by a number of secondary considerations. For example, alloy composition, microstructure, and grain size can have a significant influence on hydrogen diffusivity [*13*]. Additionally, the presence of plane strain as contrasted to plane stress or the existence of a notch can have a significant influence on the activity gradient for lattice diffusion [*14*].

When hydrogen originates in the environment, the overall transport reaction will be much more complex reflecting the form of the species in the environment, the purity of the environment, and the nature of the metal surface. For the simple case of embrittlement caused by a very high-purity gaseous hydrogen environment where the interaction influencing fracture occurs well within the metal and does not involve a phase precipitation, the elementary reactions may be as shown schematically in Fig. 1 and are:

1. Gas-phase diffusion of molecular hydrogen to the crack surface

$$r_1 = k_1 P \qquad (1)$$

where k_1 is the rate constant and P is molecular hydrogen pressure.

2. Molecular hydrogen strikes the metal surface, dissociates, and is adsorbed as atoms

$$r_2 = k_2 P^{1/2}(1 - \theta) \qquad (2)$$

where θ is the hydrogen surface coverage.

3. An absorbed atom migrates across the metal surface and chemisorbs

$$r_3 = k_3 \operatorname{grad} u \qquad (3)$$

where grad u is the gradient in surface hydrogen concentration.

4. An adsorbed atom dissolves into the metal

$$r_4 = k_4\theta[1 - (u/u_s)] \tag{4}$$

where u is the hydrogen concentration just inside the metal surface and u_s is the saturation concentration of hydrogen in the metal.

5. A hydrogen atom near the metal surface diffuses to the critical location to cause embrittlement

$$r_5 = D[(u - u_l)/l] \tag{5}$$

where D is the diffusion coefficient and u_l is the hydrogen concentration at the critical location l distance from the metal surface. The overall transport reaction will be the sum of the individual reaction and can involve reactions occurring in opposite directions, consecutively, and in parallel [*11*].

The exact form of the overall transport reaction will be very complex reflecting the original location and form of the hydrogen, the pressure and temperature of the test, as well as secondary considerations such as impurities present in the environment. For example, hydrogen-induced slow crack growth of hardened AISI SAE 4130 steel in high-purity molecular hydrogen has been observed to exhibit the temperature dependence shown by the dashed curve in Fig. 2 and obeys the equation [*15*];

$$\overset{\circ}{R} = C_1 \frac{C_2PT^{-1/2} \exp[-\Delta H/RT]}{C_3 + C_2PT^{-1/2} \exp[-\Delta H/RT]} P^{1/2} \exp(-E_m/RT) \tag{6}$$

where

C_1, C_2, and C_3 = constants;
P = molecular hydrogen pressure;
T = absolute temperature;
$-\Delta H$ = heat of adsorption; and
E_m = energy for surface migration of hydrogen on steel.

When atomic hydrogen is present in the environment, the temperature dependence obeys a simple exponential relationship, and crack growth rate increases in orders of magnitude as shown by the solid curve in Fig. 2 [*16*]. The interpretation of these observations is that the process involved in the dissociation of the molecule on the steel surface is the slowest transport process and controls crack growth in molecular hydrogen. In atomic hydrogen the dissociation reaction is no longer required in the overall transport process, the transport of hydrogen is more rapid, and the rate of slow crack growth is increased.

The importance of transport reactions to embrittlement, particularly

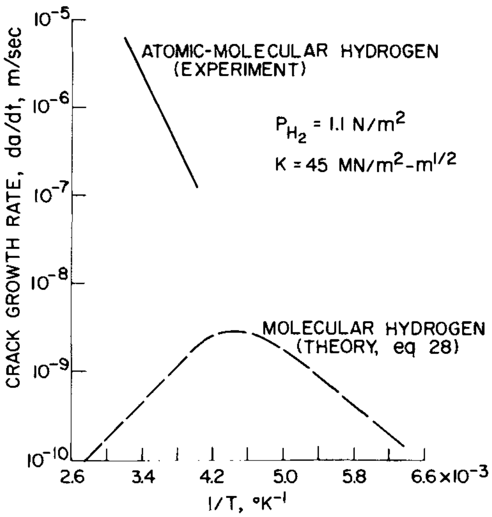

FIG. 2—*Temperature dependence of slow crack growth in atomic-molecular hydrogen compared with that predicted for a molecular hydrogen environment at the same pressure* [15, 16].

external hydrogen embrittlement, cannot be overemphasized. If any one of the reaction steps is hindered or eliminated, the structure will be less susceptible to embrittlement and, in fact, may not exhibit embrittlement at all. The influence of hydrogen pressure and test temperature on embrittlement come about primarily through their involvement in the overall transport process. In general, there is no real difference between high-pressure hydrogen embrittlement [*17*] and low-pressure hydrogen embrittlement [*18*] except that the higher the hydrogen pressure, the more rapid will be the rate of hydrogen transport [*11*].

Secondary influences are of extreme importance to external hydrogen embrittlement in that they can have significant effects on the reaction steps involved in transport. For example, contaminates in the external environment such as small amounts of oxygen [*19*] can slow down or can even eliminate the adsorption reaction (Eq 2). The presence of oxide films on the metal surface many times will not permit the dissociation of molecular hydrogen [*20*] (Eq 2). Hydride films present on metal surfaces can slow down hydrogen entry into the metal lattice [*21*] (Eq 3). Because there are so many required transport steps, each of which are capable of being influenced by so many secondary considerations, it is somewhat amazing that environmental hydrogen embrittlement is ever observed. Likewise, it is easily understood how selective embrittlement occurs in seemingly compatible systems after years of successful operation. For example, the classic gaseous hydrogen-steel storage tank failures of the

60's [*22*], the nitrous tetraoxide (N_2O_4) [*23*], and methanol [*24*] embrittlement of titanium, and the hydrazine embrittlement of stainless steel [*25*]. In each of these examples embrittlement occurred because of what was originally thought to be unimportant, secondary changes made to the originally compatible system.

Some metals such as aluminum, copper, and others do not adsorb molecular hydrogen at room temperature [*26*]; thus, hydrogen cannot be transported to the metal lattice. Under normal conditions, these metals and some of their alloys would never be expected to exhibit environmental hydrogen embrittlement. This is not to say that environmental hydrogen embrittlement may not some day be observed in these systems. Presently, we cannot be assured that these systems, too, will not be embrittled if a catalytic adsorption reaction develops from some unforeseen circumstance and permits hydrogen transport.

Hydrogen Embrittlement Interaction

A number of theories have been proposed to describe the potential interaction of hydrogen with metals. In general, they fall into one or more of the following categories; pressure formation [*27–30*], surface interaction [*31–33*], lattice decohesion [*34–36*], dislocation interaction [*37–41*], and hydride precipitation [*42–43*]. Each category has a strong experimental base, and the occurrence of each really cannot be denied under some specific set of conditions. Which of these interaction mechanisms results in the embrittlement of a structure depends on the conditions which exist in that structure.

Under some condition or another, hydrogen has been observed to influence the fracture behavior of all metals investigated to date. In a few metals, however, these effects are seen only when the lattice contains a supersaturated concentration of hydrogen with respect to the lattice equilibrium solubility or terminal solubility. Under this condition, hydride forming metals such as titanium, zirconium, and vanadium will precipitate a brittle hydride phase; metals such as iron, copper, and aluminum will precipitate molecular hydrogen; while metals such as nickel, magnesium, and palladium can precipitate either molecular hydrogen or a hydride phase depending on the degree of supersaturation [*37, 44–46*]. If second phase precipitation is extensive, all metals can fail even without an applied load because of pressure buildup of molecular hydrogen at internal defects [*10*] or the stresses developed around the less dense hydride precipitate [*37*].

Precipitation of a hydrogen-rich second phase in metals need not be associated only with precipitation from a supersaturated *bulk* lattice. It can also occur as the result of a *localized* supersaturation. The conditions for localized precipitation are: (1) if a localized saturation originally exists, transport within the metal lattice must be sufficiently slow to maintain the localized saturation during precipitation; or (2) if saturation is not originally present, transport must be sufficiently rapid to develop this saturation. An example of the former is the formation of titanium hydride on the surface of alpha-titanium when exposed to a gaseous hydrogen [*47*] and, of the latter, is the formation of hydride at the alpha-beta titanium boundaries by rapid transport of hydrogen in the nonhydride forming beta-titanium phase [*48–50*].

Second-phase precipitation is a sufficient but not a necessary condition for the occurrence of hydrogen embrittlement. Embrittlement is observed in many metals under conditions where a supersaturation probably could not exist. Most notably is, of course, the failure of many metals in a low-pressure gaseous hydrogen environment. Under these conditions, applied load acts to concentrate the hydrogen at areas of lattice distortion, for example, at areas of triaxial stress ahead of a crack tip or at a grain boundary. Hydrogen in these areas may affect lattice cohesion deleteriously to the extent that crack nucleation and propagation is possible. For steel in a hydrogen environment, the hydrogen-lattice interaction appears to occur on or just below the crack tip [*15, 16*] and can be considered the limiting case of lattice decohesion, that is, surface decohesion. Embrittlement as the result of a hydrogen-lattice interaction, unlike embrittlement by second-phase precipitation, is always associated with a brittle mode of failure; whether this mode is transgranular or intergranular, apparently depends on the site of crack initiation and the relative strength of the grain boundaries.

The contribution of the hydrogen-dislocation interaction to the embrittlement of metals in most cases, appears to be of secondary importance; however, under the right conditions, this mechanism could conceivably play an important role [*40*]. Hydrogen can combine with dislocations and influence their motion in iron [*51, 52*], molybdenum [*53*], vanadium [*54*], columbium [*55*], and nickel [*56*]. The rate of hydrogen transport within the lattice can be increased by its association with the dislocation movement [*41*]. In general, however, these effects require large hydrogen concentrations. Such hydrogen concentrations are not normally obtainable, say from a gaseous hydrogen environment at room temperature. Additionally, the effects of fatigue crack growth and gaseous hydrogen-induced crack growth in titanium appear to be independent processes; the former, of course, associated with deformation (dislocation motion), thus eliminating any significant contribution of dislocation motion to the latter.

From the above discussion it should be obvious that the hydrogen-metal embrittlement interaction is a specific interaction depending on many secondary influences. If conditions are not correct for a precipitation type interaction, they may be correct for a decohesion or a dislocation interaction. The relative importance of each depends on the original location and form of the hydrogen, the transport reactions, as well as the stage of fracture most important to the failure of the particular structure.

Testing for Hydrogen Embrittlement

The deleterious effects of hydrogen on the failure of an engineering structure comes about through its influence on either the crack initiation stage or the subcritical, slow crack growth stage of fracture. Most engineering structures contain preexisting cracks because of various processing procedures so the crack initiation stage of fracture is of little or no importance to the failure process. This may not be the case, however, for some structures and more importantly for many test specimen configurations such as the tensile bar [*17*] and rupture disk [*59*], particularly when evaluating environmental hydrogen embrittlement. In these the crack initiation stage can dominate the failure process.

When hydrogen is present originally within a structure, the crack initiation stage of fracture can be readily influenced. All engineering metals contain internal defects which can act as internal surfaces for molecular hydrogen precipitation or contain locally strained regions which can induce hydride precipitation. These areas are sites for crack initiation. The propensity of a metal to "precipitate" a crack is dependent on the degree of hydrogen saturation, or, in other words, the amount of hydrogen and distance hydrogen must be transported to the site of nucleation. If the level of hydrogen is high and the metal lattice is supersaturated, crack initiation will be virtually spontaneous [*60*]; if it is low, however, crack initiation will be time dependent with its rate controlled by the rate of hydrogen transport [*61*]. When hydrogen is present in the environment, the influence of hydrogen on this stage of fracture becomes more random and is dependent on the development of a surface site for crack nucleation where the environment can interact. In metals which do not form hydrides, crack initiation is more or less random because of the probability of an initiation site occurring on the metal surface [*11*], whereas in hydride forming metals, such as alpha-titanium, crack initiation is more predictable because a surface hydride can form in which crack initiation can occur more easily [*11*].

The subcritical crack growth stage of fracture occurs at values of stress intensity below some critical value for rapid fracture. In a very simple manner, crack growth will occur in an engineering structure at some level of applied stress when the applicable criteria are met, such as that proposed by Griffith for brittle materials [*62*]. Crack growth will occur at a lower applied stress, however, if hydrogen can influence the variables in the criteria in such a way as to reduce the stress intensity value determined by the criteria. If the influences of hydrogen on variables in the criteria were instantaneous and if hydrogen was present originally within the structure at sufficiently high concentrations and was homogeneous throughout, the new value of stress intensity would be the critical value, and unstable crack growth would immediately result. However, the influence of hydrogen is localized at or near the tip of a nucleated or existing crack, and continued crack growth is dependent on the rate of hydrogen transport to this localized area. These conditions are easily understood for hydrogen-induced crack growth by the interaction with a crack propagating from a surface; however, the same conditions apply to the propagation of a crack from an internal surface (void) as the result of the interaction of hydrogen within the void. Under the latter condition the additional force applied to the crack tip by the hydrogen pressure within the void must be considered [10]. Other mechanical factors which influence hydrogen-induced crack growth include mode of loading, state of triaxial stress about the crack tip, amount and form of plastic deformation associated with the crack tip, etc.

As we have seen, the process of hydrogen embrittlement can be a very complicated phenomenon. Figure 3 is a montage meant to better illustrate this point. Underlined in this figure are what I consider to be the primary steps in the embrittlement process and include origin of the hydrogen, transport of the hydrogen, and the interaction processes of hydride formation, lattice decohesion, dislocation interaction, and pressure formation. Also shown are a few of the secondary considerations which can influence one or more of the primary steps and include impurity species in the

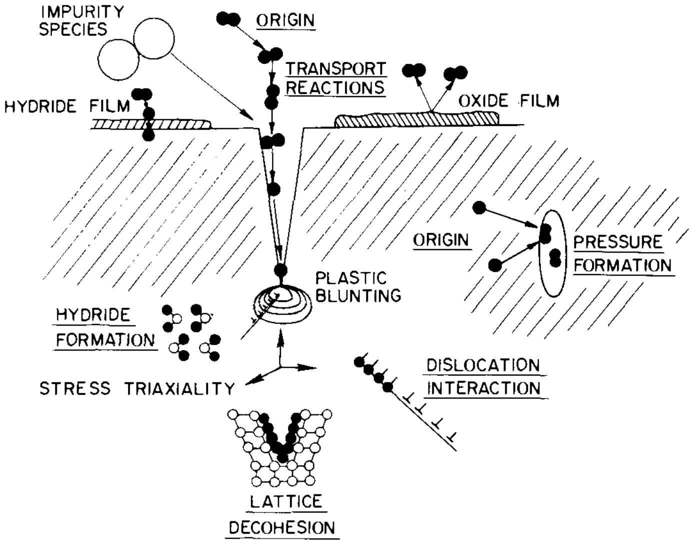

FIG. 3—*Montage of primary and some secondary effects involved in the embrittlement of a metal by hydrogen.*

environment, surface hydride films, surface oxide films, plastic blunting of the crack tip, and the level of stress triaxiality. Let us next consider specific test procedures in order to further illustrate the parameters which must be understood in the design of a standardized specimen and test procedure, if their results are to have meaning when applied to an engineering structure.

Internal Hydrogen Embrittlement

Probably the most usual cause of hydrogen within an engineering structure is a production process such as pickling or electroplating. Hydrogen pickup is the result of a high hydrogen fugacity developed during processing and is dependent on process-variables of bath composition, current, time, temperature, etc. When a potentially susceptible structure is processed, it is imperative that the degrading effect of the process be established in order to ensure the integrity of the structure. This is done either by qualifying the process with the use of test coupons or by processing test coupons along with the structure or both. All process variables must be duplicated on the test coupons including such variables as material, surface condition, potential susceptibility, etc. Following processing, the coupons are tested to establish any degrading influences of hydrogen pickup during processing.

In the selection of coupon design and test method, consideration must be given to: (1) the original location and form of the hydrogen picked up during processing, (2) the transport of the hydrogen from its original location to the site where it can interact with the metal to cause a degrading effect, and (3) the interaction process itself. Design parameters which can affect these variables include presence, location, and severity of a stress concentrator and level and form of loading. A test coupon should contain a stress concentrator such as a notch as near to the original location of hydrogen as possible to shorten the required transport path, as severe as possible to increase the rate of hydrogen transport by stress enhanced diffusion, and at the point of maximum tensile load to concentrate the hydrogen-metal interaction at the point of maximum stress. The coupon should be statically loaded to some level for some period of time reflecting the used condition of the engineering structure to permit the transport of hydrogen from its origin to the point where it can interact with the metal lattice to cause embrittlement. A number of current coupon designs fit these considerations [*63–65*]. Which one of these is optimum for the particular production process will depend on the particular metal tested as well as the suspected location and form of hydrogen within that metal.

External Hydrogen Embrittlement

Hydrogen in an external environment can degrade the properties of an engineering structure by interacting with the structure while it is being loaded or is under load. This form of embrittlement is much more complicated than internal hydrogen embrittlement because of the variety of external species which can supply hydrogen to the structure (molecular hydrogen, dissociated or ionized hydrogen, complex hydrogen containing gases such as hydrogen sulfide, and complex hydrogen containing liquids such as water and organics) and because of the large number of reaction steps required to transport the hydrogen from its equilibrium form in the environment to the metal lattice. Small amounts of contaminants can have a large influence on the transport process and thus on the potential embrittling effect of the particular environment. For example, small amounts of oxygen can eliminate the degrading effect of a hydrogen environment in some systems [*18*], whereas small amounts of carbon dioxide in a hydrazine environment can induce severe embrittlement in a normally passive system [*25*]. When testing for the potential embrittling effects of an environment, it is of extreme importance that either the influences of all species in the environment be understood or the environment be *exactly* duplicated.

Although both the initiation and growth stages of fracture can be influenced by hydrogen, in general, the greatest influence will be on the crack growth stage of fracture. When testing for external hydrogen embrittlement, it is imperative that the relative influence of the initiation and growth stages of fracture in the failure of a structure be understood such that the selected specimen design will yield data that can be meaningfully applied to the engineering structure.

Test specimen configurations which do not contain a preexisting crack (the smooth and notched tensile bar, the smooth and notched bend bar, and the rupture disk) must involve the crack initiation stage in the fracture process. The extent of involvement will be dependent on specimen configuration and method of loading as well as its sensitivity to the influence of hydrogen. If crack initiation occurs early in the deformation process, say because of its sensitivity to hydrogen, the crack growth stage may be the primary stage governing failure. However, if the material tested is extremely notch sensitive, failure may occur immediately upon the initiation of a crack [*11*]. In general, it is difficult if not impossible to separate the initiation stage and the crack growth stage in specimen configurations which do not contain preexisting cracks, and thus the application of data obtained from these types of specimens can only be applied to engineering structures with reservation. These problems are not always eliminated by the use of precrack specimens. Even in these types of specimens the crack initiation stage may contribute to the failure process, if the precrack is not sharp but is blunted by plastic deformation or if the precrack surface is contaminated.

The influence of hydrogen on the subcritical crack growth stage of fracture can be determined precisely in high-strength materials by the use of the correct specimen design and test method. Specimen design should, whenever possible, conform to the guidelines put forth by ASTM for plane strain fracture toughness testing. Precracks should be introduced in the specimen by cyclic loading or other methods at stress intensity values below those expected to be required for hydrogen-induced, slow crack growth. Additionally, if precracking is done in air, the oxide film normally formed at the crack tip must be ruptured in the test environment before hydrogen-induced, slow crack growth will be observed. One of the many acceptable test techniques applicable to high-strength materials will be outlined next [*49*].

The following test procedure is presented to illustrate one of many acceptable techniques used to determine the rate of hydrogen-induced, slow crack growth in high-strength materials. Specimens are wedge-opening-loaded, double-cantilever-beam (DCB) type originally discussed by Mostovoy [*66*], Fig. 4. The side grooves are added to ensure that the crack would propagate in a direction normal to the applied stress. This fracture mechanics type specimen has several features that are extremely useful when investigating hydrogen-induced cracking. For any fixed crack-opening displacement (COD), the stress-intensity level decreases as the crack grows, thus permitting a high degree of control of crack growth. Crack-growth rates can be easily determined by either optical-measurement methods [*67*] or by measurement of compliance changes [*49*]. The specimen is also easy to precrack by either fatigue or overload procedures.

Tests can be conducted in any test chamber that can be evacuated and

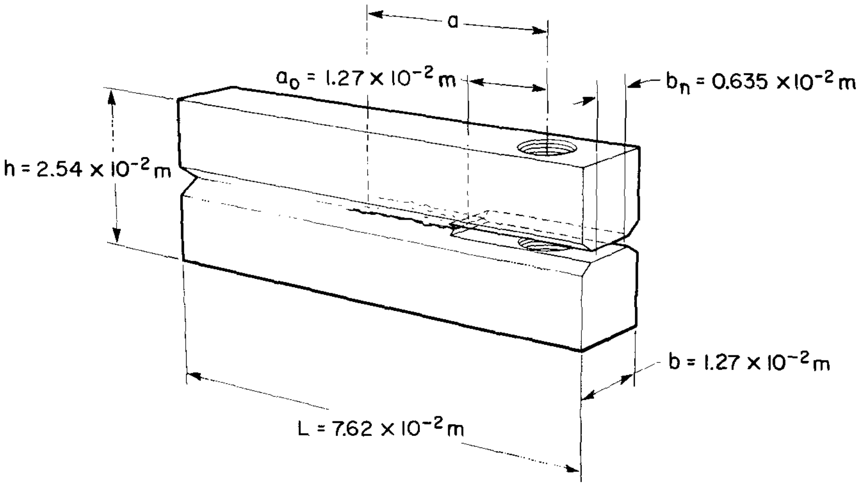

FIG. 4—*Double-cantilever-beam (DCB) specimen* [49].

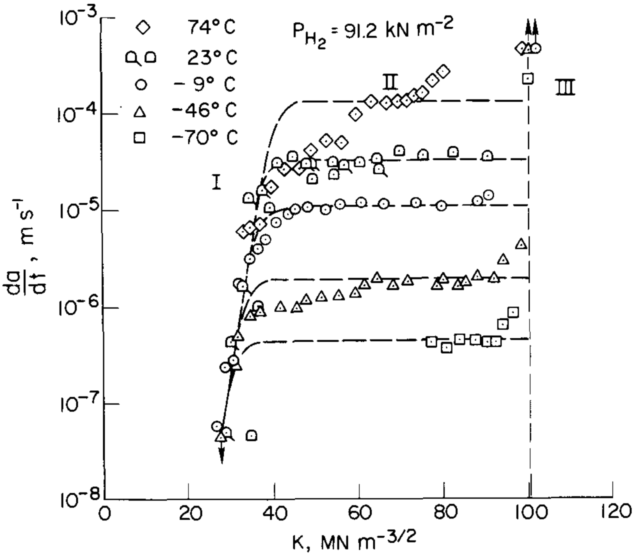

FIG. 5—*Experimentally determined relationship between hydrogen-induced crack growth and applied stress intensity in Ti-5Al-2.5Sn* [49].

then backfilled with hydrogen. The chamber should always be evacuated prior to backfilling with hydrogen to ensure that the total concentration of background gases will be lower than the concentration of active impurities in the test environment. Prior to testing, each specimen is precracked by fatiguing in the hydrogen environment. By this method, the original machined notches were extended and sharpened. After the desired environmental conditions (temperature, pressure, etc.) have been established, the specimen is loaded rapidly to a preselected COD value and held at that value while the corresponding load is measured continuously. As the crack grows, the continuously measured load (stress intensity) will decrease at a rate which is related to the crack-growth rate. Figure 5 shows typical results of tests conducted using the foregoing procedure [*49*]. In this figure the rate of hydrogen-induced, slow crack growth is shown as a function of stress intensity, *K*, at a hydrogen pressure of 0.9 atm and at five different temperatures. These data can now be applied to an engineering structure to estimate the life of that structure [*68*, *69*].

Summary

Hydrogen embrittlement has been shown to be a complex process which is many times further complicated by what could be termed secondary influences. Embrittlement, whether caused by internal or external hydrogen, involves three primary influences: (1) the original location and and form of the hydrogen, (2) the transport reactions involved in the transport of hydrogen from its origin to some point where it can interact with the metal to cause embrittlement, and (3) the embrittlement interaction itself. Of these, probably the most important is the hydrogen transport process—it is this process which controls the rate of hydrogen arrival at some critical location on or within the metal and thus controls the rate or severity of embrittlement in the structure. Further, if any one of the reaction steps involved in the transport process is hindered or eliminated, the structure will be less susceptible to embrittlement and, in fact, may not exhibit embrittlement at all. Besides these primary influences, a large number of secondary influences can be involved in embrittlement through their effect on the primary influences. Some secondary influences are impurities in the environment or within the metal, surface films of hydride or oxide, and state of stress triaxiality within the specimen or structure. From the preceding discussions it should be more clear the type of parameters which must be considered in the selection of a test method and test procedure such that the resulting data may be meaningfully applied to real engineering structures.

References

[1] Steigerwald, E. A., Schaller, F. W., and Troiano, A. R., *Transactions*, Metallurgical Society, American Institute of Mining, Metallurgical, and Petroleum Engineers, Vol. 215, Dec. 1959, pp. 1048–1052.

[2] Troiano, A. R., *Metal Process*, Vol. 77, Feb. 1950, pp. 112–117.

[3] Smialowsky, M., *Hyrogden in Steel*, Addison-Wesley, Reading, Mass., 1962.

[4] Schuetz, A. E. and Robertson, W. D., *Corrosion*, Vol. 13, July 1957, pp. 437t–458t.

[5] Tetelman, A. S., Wagner, C. N. J., and Robertson, W. D., *Acta Metallurgica*, Vol. 9, March 1961, pp. 205–215.

[6] Geyer, N. M., Lawless, G. W., and Cohen, B. in *Technical Proceedings of the American Electroplaters' Society*, 1960, pp. 143–151.

[7] Hofmann, W. and Rauls, W., *Archiv für das Eisenhüttenwesen*, Vol. 32, March 1961, pp. 169–173.

[8] Schwartz, J. H. and Ward, J. J., "Direct Energy Conversion," NASA SP-5057 National Aeronautics and Space Administration, Washington, D. C., 1968.

[9] Moeckel, W. E., "Propulsion Systems for Manned Exploration of the Solar System," NASA TM X-1864, National Aeronautics and Space Administration, Washington, D. C., 1969.

[10] Tetelman, A. S. and McEvely, A. J., Jr., *Fracture of Structural Materials*, Wiley, New York, 1967.

[11] Nelson, H. G., "The Kinetic and Mechanical Aspects of Hydrogen-Induced Failure in Metals," NASA TN D-6691, National Aeronautics and Space Administration, Washington, D. C., April 1972.

[12] Tetelman, A. S. in *Fundamental Aspects of Stress Corrosion Cracking*, National Association of Corrosion Engineers, Houston, Tex., 1969, pp. 446–460.

[13] Krishtel, M. A., *Diffusion Processes in Iron Alloys*, Israel Program for Scientific Translations (Translated from Russian), Jerusalem, 1970.

[14] Oriani, R. A. in *Fundamental Aspects of Stress Corrosion Cracking*, National Association of Corrosion Engineers, Houston, Tex., 1969, pp. 32–49.

[15] Williams, D. P. and Nelson, H. G., *Metallurgical Transactions*, Vol. 1, Jan. 1970, pp. 63–68.

[16] Nelson, H. G., Williams, D. P., and Tetelman, A. S., *Metallurgical Transactions*, Vol. 2, April 1971, pp. 953–959.

[17] Walter, R. J. and Chandler, W. T., ASM Report D8-14.2, American Society for Metals Report System, Metals Park, Ohio, 1968.

[18] Hancock, G. G. and Johnson, H. H., *Transactions*, Metallurgical Society American Institute of Mining, Metallurgical, and Petroleum Engineers, Vol. 236, April 1966, pp. 513–516.

[19] Harris, J. A., Jr., and VonWanderham, W. C., this symposium, pp. 198–220.

[20] Dushman, S., *Scientific Foundations of Vacuum Technique*, Wiley, New York, 1958.

[21] Johnson, D. L. and Nelson, H. G., "Determination of Hydrogen Permeation Through Alpha Titanium," accepted for publication in *Metallurgical Transactions*, 1972.

[22] McPherson, W. B. and Catalda, C. E., ASM Report D8-14.1, American Society for Metals, Metals Park, Ohio, Oct. 1968.

[23] Johnson, R. E., *The Science, Technology and Application of Titanium*, Pergamon, London, 1970, pp. 1175–1186.

[24] Boyd, W. K. in *Fundamental Aspects of Stress Corrosion Cracking*, National Association of Corrosion Engineers, Houston, Tex., 1969, pp. 593–602.

[25] Boyd, W. K., Berry, W. E., and White, E. L., DMIC Memo 201, Defense Metals Information Center, Battelle Memorial Institute, Columbus, Ohio, Jan. 1965.

[26] Hayward, D. O. and Trapnell, B. M. W., *Chemisorption*, Butterworth Washington, 1964.

[27] Zapffe, C. A. and Sims, C. E., *Journal of Metals*, Vol. 145, 1941, pp. 225–259.

[28] Dekazinczy, F., *Journal Iron and Steel Institute*, Vol. 177, 1954, pp. 85–92.

[29] Bilby, B. A. and Hewitt, J., *Acta Metallurgica*, Vol. 10, June 1962, pp. 587–600.

[30] Garofalo, F., Chou, Y. T., and Ambegaokar, V., *Acta Metallurgica*, Vol. 8, Aug. 1960, pp. 504–512.

[31] Coleman, E. G., Weinstein, D., and Rostoker, W., *Acta Metallurgica*, Vol. 9, May 1961, pp. 491–496.

[32] Petch, N. J., *Philosophical Magazine*, Vol. 1, 1956, pp. 331–337.

[33] Petch, N. O. and Stables, P., *Nature*, Vol. 169, May 1952, pp. 842–843.

[34] Troiano, A. R., *Corrosion*, Vol. 15, April 1959, pp. 207t–212t.

[35] Westwood, A. R. C., *Environment-Sensitive Mechanical Behavior*, Gordon and Breach, New York, 1966, pp. 1–65.

[36] Barnett, W. J. and Troiano, A. R., *Journal of Metals*, Vol. 209, April 1957, pp. 486–494.

[37] Kolachev, B. A., *Hydrogen Embrittlement of Nonferrous Metals*, Israel Program for Scientific Translations (translated from Russian), Jerusalem, 1968.

[38] Bastien, P. and Azou, P. in *Proceedings*, First World Metallurgical Congress, American Society for Metals, Metals Park Ohio, 1951, pp. 535–552.

[39] Bastien, P. and Azou, P., *Review Metallurgica*, Vol. 49, 1952, pp. 837–848.

[40] Beachem, C. D., *Metallurgical Transactions*, Vol. 3, Feb. 1972, pp. 437–451.

[41] Louthan, M. R., Caskey, G. R., Donovan, J. A., and Rawl, D. E., submitted for publication in *Materials Science and Engineering*, 1972.

[42] Wood, T. W. and Daniels, R. D., *Transactions*, Metallurgical Society, American Institute of Mining, Metallurgical, and Petroleum Engineers, Vol. 233, May 1965, pp. 898–903.

[43] Westlake, D. G., *Transactions*, American Society for Metals, Vol. 62, 1969, pp. 1000–1006.

[44] Hurd, D., *Introduction to the Chemistry of Hydrides*, Wiley, New York, 1952.

[45] Boniszewski, T. and Smith, G. C., *Journal of Physics and Chemistry of Solids*, Vol. 21, 1961, pp. 115–118.

[46] Wayman, M. L. and Smith, G. C., *Acta Metallurgica*, Vol. 19, March 1971, pp. 227–231.

[47] Williams, D. N. and Wood, R. A., NASA Contract NAS9-12044, National Aeronautics and Space Administration, Washington, D. C., May, 1972.

[48] Nelson, H. G., Williams, D. P., and Stein, J. E., *Metallurgical Transactions*, Vol. 3, Feb. 1972, pp. 469–475.

[49] Williams, D. P. and Nelson, H. G., *Metallurgical Transactions*, accepted for publication, 1972.

[*50*] Nelson, H. G., submitted to *Metallurgical Transactions*, 1972.
Metallurgical, and Petroleum Engineers, Vol. 239, Oct. 1967, pp. 1574–1585.

[*51*] Adair, A. M. and Hook, R. E., *Acta Metallurgica*, Vol. 10, Aug. 1962, pp. 741–745.

[*52*] Gibala, R., *Transactions*, Metallurgical Society, American Institute of Mining, Metallurgical, and Petroleum Engineers, Vol. 239, Oct. 1967, pp. 1574–1585.

[*53*] Lawley, A., Liebmann, W., and Maddin, R., *Acta Metallurgica*, Vol. 9, Sept. 1961, pp. 841–850.

[*54*] Eustice, A. L. and Carlson, O. N., *Transactions*, Metallurgical Society American Institute of Mining, Metallurgical, and Petroleum, Engineers, Vol. 221, April 1961, pp. 238–241.

[*55*] Wilcox, B. A., *Journal of Less-Common Metals*, Vol. 2, April–Aug. 1960, pp. 292–303.

[*56*] Boniszewski, T. and Smith, G. C., *Acta Metallurgica*, Vol. 11, March 1963, pp. 165–178.

[*57*] Latanision, R. M. and Staehle, R. W., *Scripta Metallurgica*, Vol. 2, 1968, pp. 667–672.

[*58*] Nelson, H. G., Tetelman, A. S., and Williams, D. P. in *Proceedings*, International Conference on Corrosion Fatigue, National Association of Corrosion Engineers, Houston, Tex., 1972.

[*59*] Fidelle, J.-P., Roux, C., and Rapin, M., *Memoires Scientifiques Metallurgica*, Vol. 66, 1969, pp. 833–844.

[*60*] Tetelman, A. S. and Robertson, W. D., *Transactions*, Metallurgical Society, American Institute of Mining, Metallurgical, and Petroleum Engineers, Vol. 224, Aug. 1962, pp. 775–783.

[*61*] Barth, C. F. and Steigerwald, E. A., *Metallurgical Transactions*, Vol. 1, Dec. 1970, pp. 3451–3455.

[*62*] Griffith, A. A., *Philosophical Transactions*, Vol. A221, 1920, pp. 163–198.

[*63*] Movich, R. C., this symposium, pp. 64–73.

[*64*] Jankowsky, E. J., this symposium, pp. 51–57.

[*65*] Hyter, W. H., this symposium, pp. 58–63.

[*66*] Mostovoy, S., Crosley, P. B., and Ripling, E. I., *Journal of Materials*, Vol. 2, 1967, pp. 661–81.

[*67*] Beck, T. R., Blackburn, M. J., and Speidel, M. O., NASA Contract NAS7-489, National Aeronautics and Space Administration, Washington, D. C., March 1967.

[*68*] Williams, D. P., "A New Criterion for Failure of Materials by Environment-Induced Cracking," accepted for publication in the *International Journal of Fracture Mechanics*, 1972.

[*69*] Wei, R. P., Novak, S. R., and Williams, D. P. in *Proceedings*, 33rd AGARD (NATO) Structure and Materials Panel Meeting, Brussels, Belgium, Oct. 1971.

W. T. Chandler [1] *and R. J. Walter* [1]

Testing to Determine the Effect of High-Pressure Hydrogen Environments on the Mechanical Properties of Metals

---

REFERENCE: Chandler, W. T. and Walter, R. J., **"Testing to Determine the Effect of High-Pressure Hydrogen Environments on the Mechanical Properties of Metals,"** *Hydrogen Embrittlement Testing, ASTM STP 543*, American Society for Testing and Materials, 1974, pp. 170–197.

ABSTRACT: Equipment and procedures used in performing tension, fracture mechanics, fatigue, and creep tests on metal specimens in high-pressure hydrogen are described. Important test parameters, in particular, hydrogen purity and methods of achieving high purity are considered. The interpretation and use of data obtained from the various tests in high-pressure hydrogen are discussed.

KEY WORDS: hydrogen embrittlement, fatigue tests, hydrogen environment effects, high pressure hydrogen testing, hydrogen purification, environmental effects, mechanical property tests, fracture mechanics tests

The term hydrogen environment embrittlement is used to signify the degradation of mechanical properties that occurs to a metal when it is exposed to a hydrogen environment as compared to inert environments; the term is quite descriptive. The effect is an environmental one, and, therefore, testing must be accomplished with the specimen in contact with the hydrogen environment. Susceptible metals are embrittled by hydrogen environments in the sense that: (1) the ductility of the metal (or more precisely, the ductility of the surface of the metal) is lower in hydrogen than in other environments, (2) surface cracking occurs in hydrogen, (3) subcritical crack growth occurs in hydrogen, and (4) crack growth rates for given cyclic or sustained stress intensities are faster in hydrogen than in inert environments. However, fractures in hydrogen may not always be completely brittle in nature.

---

[1] Manager and member of technical staff, Physical and Mechanical Metallurgy, Advanced Programs, Rocketdyne Division, Rockwell International, Canoga Park, Calif. 91304.

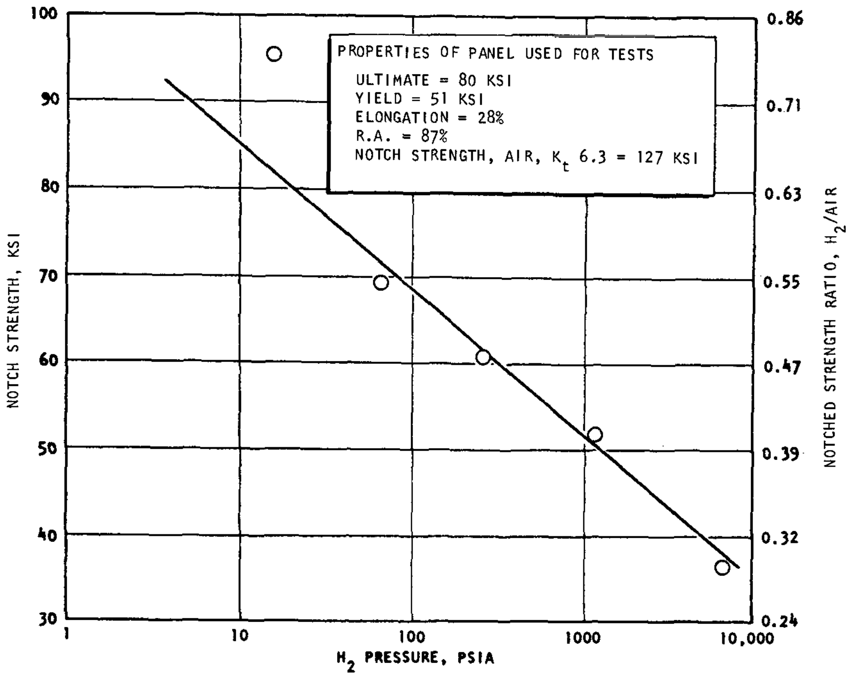

FIG. 1—*Notch strength versus hydrogen pressure for electroformed nickel at room temperature.*

The characteristics of hydrogen environment embrittlement set certain requirements for testing of this effect and result in some difficulties in interpretation and use of data obtained from "standard" tests, for example, tension tests. These areas will be discussed.

Environment

Since hydrogen environment embrittlement by gaseous hydrogen is an environmental effect, it is imperative in testing for this effect that the environment is well characterized. It has been found that this embrittlement increases with increasing hydrogen pressure (Fig. 1) [*1*][2] and occurs over a range of temperatures, but is most severe in the vicinity of room temperature. The change in embrittlement with temperature may be quite rapid in the vicinity of room temperature (Fig. 2) [*1*]. Thus temperature and pressure should be closely controlled and carefully reported for tests in hydrogen.

Hydrogen Purity

Most importantly, the purity of the hydrogen must be established, maintained, and reported for all tests. It has been found that oxygen in

[2] The italic numbers in brackets refer to the list of references appended to this paper.

hydrogen inhibits hydrogen environment embrittlement. The results of Hofmann and Rauls [2] are shown in Fig. 3. The embrittlement inhibiting effect of oxygen in 1500-psi hydrogen becomes noticeable above 0.1-ppm oxygen. On the other hand, Sawicki and Johnson [3] reported that embrittlement of high-strength steels by hydrogen at 14.7 psia pressure is not inhibited by oxygen contents of less than 200 ppm. An explanation of these seemingly contradictory results may be that the inhibiting influence of oxygen is a function of its absolute partial pressure regardless of the total pressure of the system. In such a case, the higher the hydrogen pressure, the lower the oxygen concentration required to inhibit the embrittling effect of hydrogen.

Surprisingly, Frick et al [4] found that saturating 4500-psi hydrogen with water vapor reduced very little the hydrogen environment embrittlement of Udimet 700 at temperatures from 300 to 580 F. The minimal inhibiting effect of water vapor on hydrogen environment embrittlement has been confirmed at Rocketdyne for temperatures up to 1250 F. Liu et al [5] tested cracked 4340 steel specimens at room temperature in one atmosphere pressure hydrogen to which additions of various gases were made. They found that small additions of sulfur dioxide (SO_2), carbon monoxide (CO), and carbon disulfide (CS_2) were very effective in stopping

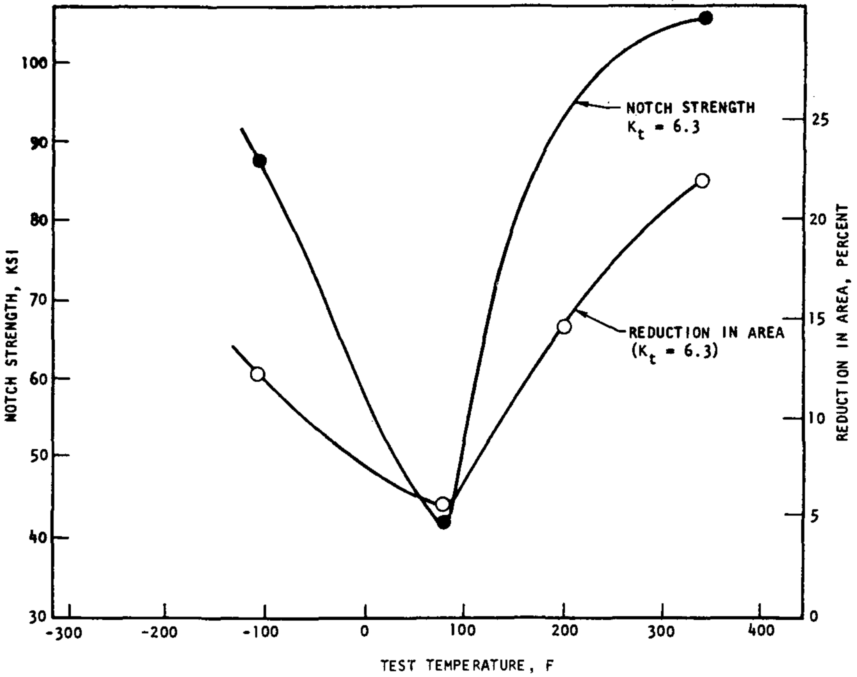

FIG. 2—*Notch ductility and strength versus test temperature for electroformed nickel in 1200-psi hydrogen.*

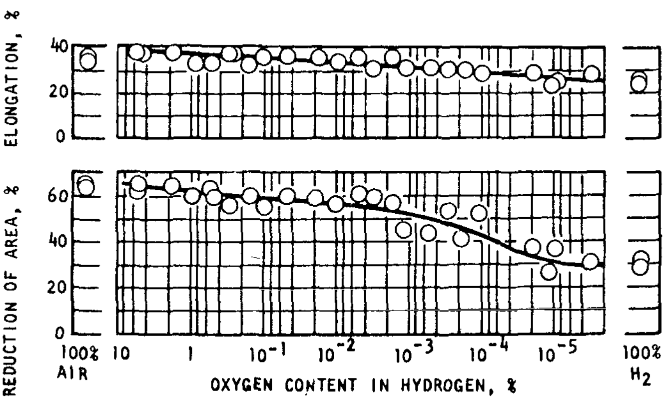

FIG. 3—*Effect of oxygen additions to 100-atm partial pressure hydrogen on the elongation and reduction of area of CK 22 N steel.*

a running crack, the inhibiting effect of carbon dioxide (CO_2) was moderate, and nitrogen (N_2) and argon had no noticeable effect.

Since relatively low concentrations of a number of impurities in hydrogen can inhibit hydrogen environment embrittlement, tests for this embrittlement should be performed in gaseous hydrogen of very high purity unless, of course, a specific purity level is chosen to simulate actual use conditions. A reasonable hydrogen purity specification to use for testing at this time (for other than simulation tests) is Marshall Space Flight Center specification, MSFC-SPEC-356A for liquid hydrogen. It might be noted that many aerospace system applications involve the exposure of metals to the gaseous hydrogen boiloff from liquid hydrogen. MSFC-SPEC-356A specifies a minimum total purity of 99.995 percent hydrogen by volume with the following maximum impurity levels (by volume): 1-ppm O_2 + argon, 1.0-ppm CO_2 + CO, and 9.0-ppm N_2 + H_2O + volatile hydrocarbons.

The usual source of hydrogen for tests is bottled hydrogen. It should be noted that the purity of the bottled hydrogen is considerably different for the different grades available. For the mechanical property tests performed in hydrogen at Rocketdyne, AIRCO Ultra Pure Grade No. 5 bottled hydrogen with a purity of 99.999 percent hydrogen, a dew point of −76°F, and a typical oxygen content of 2 ppm is used. Vendor analyses of hydrogen supplied to Rocketdyne has given the following impurity level ranges for this hydrogen: 1.2 to 2.0-ppm O_2, 2.6-ppm argon, 8 to 10-ppm N_2, <1 ppm each of total hydrocarbons, CO, and CO_2, and 0.9-ppm H_2O.

Hydrogen Purification

At Rocketdyne, the bottled hydrogen is further purified, first with a DeOxo unit, which is a pressure vessel containing a catalyst that catalyzes the $O_2 + 2H_2 \rightarrow 2H_2O$ reaction. The manufacturer [*6*] reports that the remaining oxygen impurity in gaseous hydrogen passed through the unit will be less than 1 ppm. Water vapor is removed downstream of the DeOxo unit by molecular sieve. Additional purification is achieved through the use of cryogenic adsorbers, that is, activated charcoal plus activated alumina and molecular sieve at −320°F. These cryogenic adsorbers reduce O_2, N_2, CO, and CO_2 levels to below 1 ppm [*7*]. One such adsorber is placed in the system before the compressor used to pressurize the hydrogen to high pressure and one after the compressor.

Other techniques are available for the preparation of high-purity hydrogen, for example, the use of hydrogen evolution from metals that absorb large quantities of hydrogen or the use of a palladium alloy purification tube, but these methods are limited as to pressures and purification rates.

Pressurization and System Purging

Experience has shown that contamination during pressurization and passage of hydrogen through pressure lines can be far in excess of the ordinary impurities present in bottled hydrogen unless considerable care is taken to avoid it. Oil lubricated piston compressors are the most common means of pressurizing. These compressors contaminate the pressurized gases with oil, and an oil trap (molecular sieve) downstream of the compressor is needed to remove the oil.

Nonlubricated piston compressors also are available. Air, however, may pass through the sliding seals into the pressurized gas. The mechanism involves air adsorption on the shaft during the extension cycle, and the air is transferred into the high-pressure cavity during the compression cycle. To prevent this form of contamination, the compressor can be enclosed inside a cavity filled with hydrogen or an inert gas [*8*].

In diaphragm compressors, the gas being compressed is isolated completely from air or hydraulic oil because there are no sliding seals in this type of compressor. The gases are compressed by metal diaphragms which are flexed by a pulsating hydraulic pump. A series of static O-rings prevents the oil from leaking around the diaphragm periphery into the gas side. Thus, of the three types of compressors, the diaphragm type used at Rocketdyne is preferred for maintaining purity during pressurization.

Air entrapment in high-pressure lines and test vessels is the main source of contamination in high-pressure systems. Unless air removal is systematic and thorough, the value of hydrogen purification is lost.

Methods used for removing air are: (1) flowing hydrogen through the lines, (2) pressurization/depressurization, and (3) evacuation. Purging lines with flowing hydrogen is quite inefficient because of the large momentum difference between hydrogen (the lightest of molecules) and the air. The pressure cycling method is capable theoretically of removing all contaminating gases entrapped in the lines. However, adsorbed gases are not removed effectively by this technique. Evacuation is the only method that can ensure adequate removal of air. Unfortunately, high-pressure valves and fittings are not designed for vacuum, and experience indicates that the best vacuum that is reasonably obtainable is about 20 μm. Even at this level, considerable effort is needed to maintain a vacuum/high-pressure, leak-tight condition.

The flushing procedure proved to be the most effective for high-pressure work is a combination of pressure and vacuum cycling. Greater embrittling effects were found with this procedure, which has been adopted at Rocketdyne [*8*]. The system is evacuated initially, then purged by a series of pressure-vacuum cycles between 100 psig and 20-μm hydrogen. This is followed by several pressurization/depressurization cycles between the test pressure (3000 to 10 000 psi) and approximately 1 atm pressure. For tests conducted below 3000 psi, several additional pressurization/evacuations are substituted for the higher pressure pressurization/depressurization purgings.

To be sure that the hydrogen purity is adequate, the hydrogen present in the test vessel must be analyzed. Also, precaution must be taken to ensure that the specimen represents the test environment. A specimen container (pressure vessel) is installed in the pressure system, the specimen container and pressure lines are evacuated several times as described previously, and then are filled with the test environment. The standard analysis technique is by gas chromatography [*9*]. The hydrogen impurities are collected in a cryogenic trap of molecular sieves or activated charcoal, then released into a gas chromatography column.

Analyses of hydrogen specimens taken at test location have yielded the following: $<$0.2-ppm O_2, $<$0.5-ppm argon, 0.6 to 0.9-ppm N_2, $<$0.5-ppm CH_4, $<$0.5-ppm CO, $<$0.5-ppm CO_2, and -85 F dew point ($\sim$1-ppm H_2O).

Specimen Preparation

Since hydrogen environment embrittlement is an environmental effect, the condition of the specimen surface is an important parameter in testing for this effect and care should be taken in characterizing, reproducing, and reporting surface condition. It should also be noted that hydrogen environment embrittlement is a function of the condition of the metal. For example, the ratio of notch strength in 7000-psi H_2 to notch strength in 7000-psi helium (N_{H_2}/N_{He}) for electroplated nickel can vary from 20 to 50 percent depending on electroplating conditions and can be increased from 20 to almost 70 percent by annealing at 600°F after electroplating. Also, as shown later in Table 5, the threshold stress intensity, K_{th}, was found to be approximately 35 ksi $\sqrt{\text{in.}}$ for Inconel 718 specimens that had been given a 1925, 1400, and 1200°F heat treatment but was only approximately 13 ksi $\sqrt{\text{in.}}$ for Inconel 718 specimens that had been given a 1725, 1325, and 1150°F heat treatment.

Mechanical Property Testing in High-Pressure Hydrogen

Cryogenic and Ambient Temperatures

Testing in high-pressure environments has its own unique problems. At high pressures, transmittal of the load from outside the vessel to the specimen is a major consideration. Bellows that can withstand high internal pressures are too stiff for attachment to a loading ram. Thus, sliding seals are required generally for high-pressure systems. The high pressure inside the vessel tends to force the loading ram back out of the vessel, and this load can be a significant percent of the total load applied to a specimen.

A simple method of performing tension tests in high-pressure hydrogen environments is to seal the specimen inside a small pressure vessel with the specimen extending out of the vessel through sliding seals at both vessel ends, as illustrated in Fig. 4. This test concept was developed initially at Rensselaer Polytechnic Institute [*10*] and has been used at Rocketdyne [*8*] with modification to the sliding seal design to eliminate metal-to-metal contact. Elimination of metal-to-metal contact at the sliding seals reduced the sliding seal friction, and electrical isolation between the specimen and vessel made it possible to follow crack growth during the test by electrical resistivity measurement. The test vessel can be placed in any mechanical testing machine.

The test specimens tested in this apparatus are 0.306 in. in diameter, 9 in. long, and are threaded for 1 in. on each end for gripping and have a 16-rms ground finish. Unnotched specimens contain a 1.25-in.-long, 0.250-in.-diameter gage section. Notched specimens have a 60 deg V-notch at the midplane. Unnotched specimens are crosshead paced usually at a rate of 0.005 in./min, and notched specimens are load paced at a loading rate that corresponds to 0.0007/min strain rate.

Calculation of the tensile load requires that the sliding seal friction and tensile load from the high-pressure gas be considered. The seal friction must be measured for the test conditions and must be maintained the same from test to test by using the same torque (for a given set of test conditions) on the seal plug (Fig. 4) for each test. The following equation is used to calculate the load at failure of unnotched specimens:

$$\text{Load} = \text{applied load} - \text{friction} + \text{pressure (specimen area at sliding seal} - \text{specimen area prior to necking)}$$

The maximum combined tensile load is assumed to occur prior to necking. For notched specimens, the final area at the base of the notch is used in place of the "area prior to necking" in the foregoing equation.

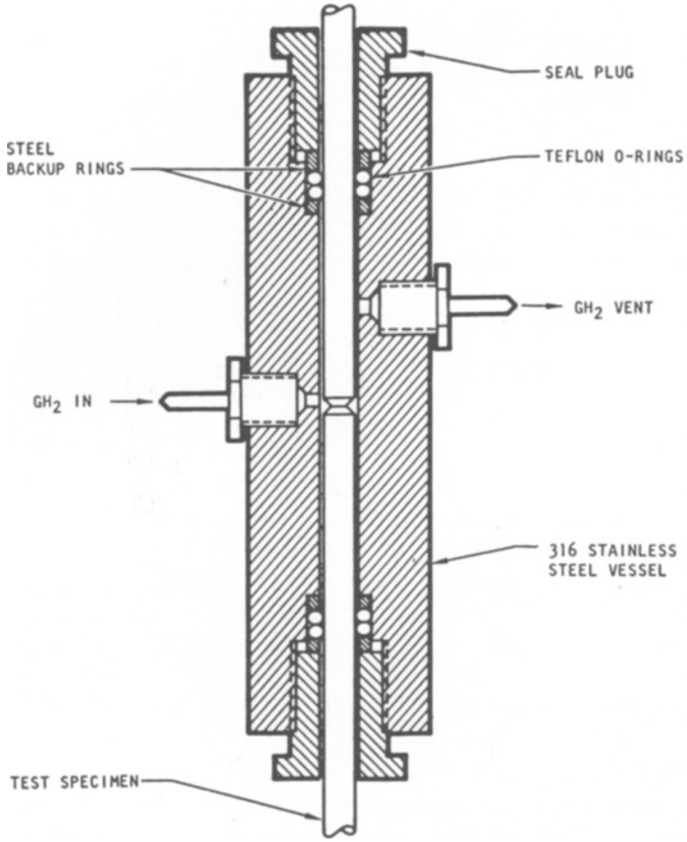

FIG. 4—*Specimen sealed to vessel for tension testing in high-pressure hydrogen at temperatures from cryogenic to ≈400° F.*

A second effect of extending the specimen ends outside the pressure vessel is an increase of shear stress from the hydrostatic forces that act in two of the three principal directions. It can be shown that the two-dimensional pressure component increases the shear stress on the 45-deg maximum shear stress plane to the same extent as the uniaxial applied tensile load. That is, the specimen should have a 10 000 psi lower yield strength in 10 000 psi pressure than in 1 atm pressure. This has been verified experimentally [*8*] in tests conducted on 35 various engineering alloys in air (1 atm), in 10 000-psi helium, and in 10 000-psi hydrogen.

The technique of gripping the specimen outside the vessel has also been used [*11*] for testing surface flawed sheet specimens. The vessel is clamped to the specimen as shown in Fig. 5 for a device in use at Rocketdyne. The center of the specimen is exposed to high-pressure hydrogen while the specimen ends are exposed to air. The same pressure and sliding seal

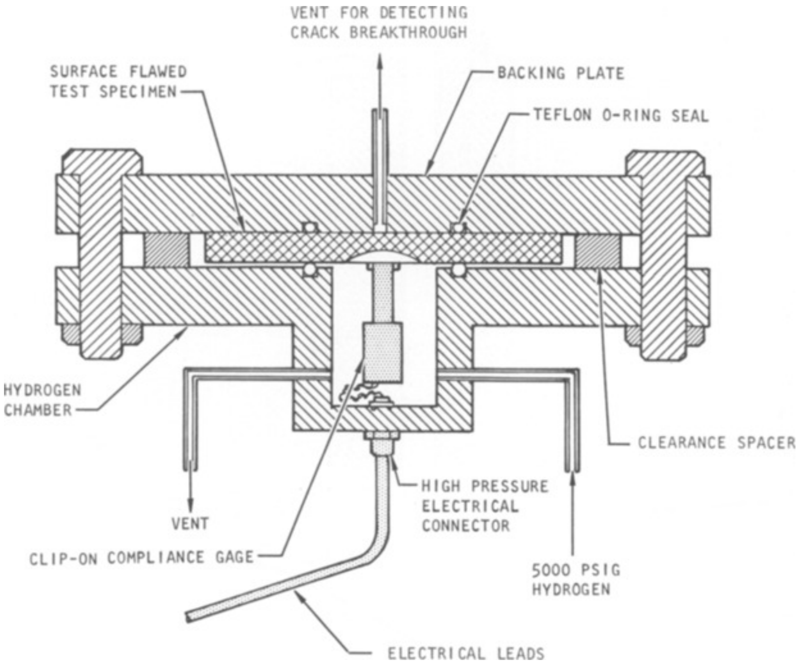

FIG. 5—*Apparatus for testing part-through-crack specimens with crack exposed to high-pressure hydrogen.*

effects discussed above on the cyclindrical specimens are also applicable. The O-ring area is considerably larger for the sheet specimen than for the cylindrical specimens; therefore, sliding friction is considerably higher during the sheet specimen tests.

Another technique used to simplify the testing of the effects of high-pressure hydrogen on properties is the use of hollow specimens with the high-pressure hydrogen on the inside and an inert (low pressure) environment on the outside. A specimen in use at Rocketdyne to determine the effect of high-pressure hydrogen on low-cycle fatigue properties is shown in Fig. 6. This specimen has the following advantages. The use of a pressure vessel is eliminated; thus, the complexity of test fixturing and procedures and the time and cost per test are reduced. Extensometry, particularly for diametral measurements, is simplified. Specimen heating is simpler, especially to heat to high temperatures, such as 1800°F, and to heat rapidly, for example, for thermal fatigue tests. The use of the hollow specimen with its small hydrogen volume reduces test hazards and thus facility costs. The hollow specimen has the following disadvantages: Solid specimens have been more extensively tested and analyzed. With hollow specimens, the surface in contact with the hydrogen is more difficult to control and inspect. It would be extremely difficult to form internal notches or precracks for testing in hydrogen or to test for the effectiveness of protective coatings. The hollow specimen has a small stress field caused by the internal pressurization, but this can be reduced to insignificant levels.

For other types of specimens or tests or both, it is generally necessary to design the pressure vessel so that the entire specimen is inside the vessel and the loading ram extends into the vessel through sliding seals. Thus, the vessel contains the specimen, loading ram and grips, and possibly a loading frame, and is comparatively large and expensive.

Figure 7 is a schematic of a vessel used at Rocketdyne to perform bend test fracture toughness measurements [*8*]. The specimens were 1 by 2½ by 14 in. and the vessel inside diameter is 6 in., while the inside length is 16 in. The load was applied by means of a 65 000-lb loading ram that extended into the side (top of figure) of the vessel through sliding seals. A load cell located inside the pressure vessel is attached to the loading ram. Thus, the exact load applied to the specimens is measured directly without the need to compensate for sliding seal friction or for pressure effects. This vessel has been adapted with grips suitable for compact tension (CT) (Fig. 8), wedge-opening loaded (WOL) (Fig. 9), and tapered-double-cantilever beam (TDCB) (Fig. 10) specimens. The specimen is mounted inside of and pinned to two yokes. The lower yoke, confined by the interior wall of the pressure vessel, forms a stable platform against which the upper yoke/hydraulic ram assembly can exert a tensile load on the specimen.

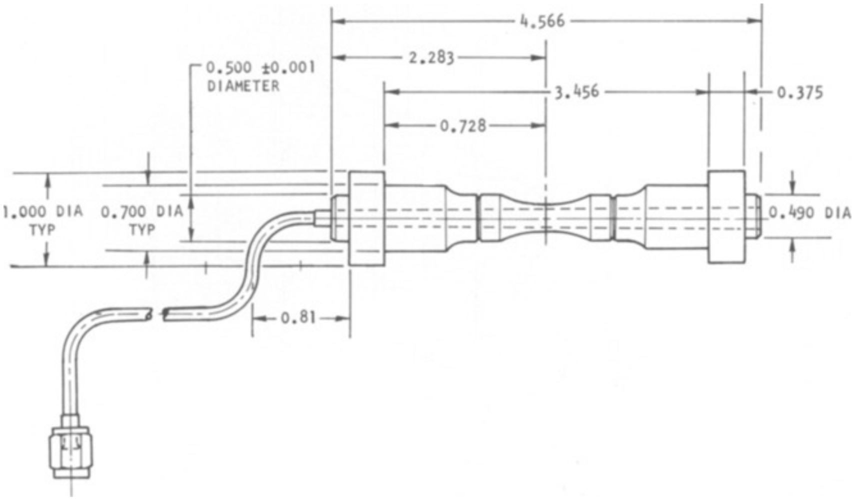

FIG. 6—*Hollow specimen for internal pressurization with* H_2 *for testing the effects of high-pressure hydrogen on mechanical properties.*

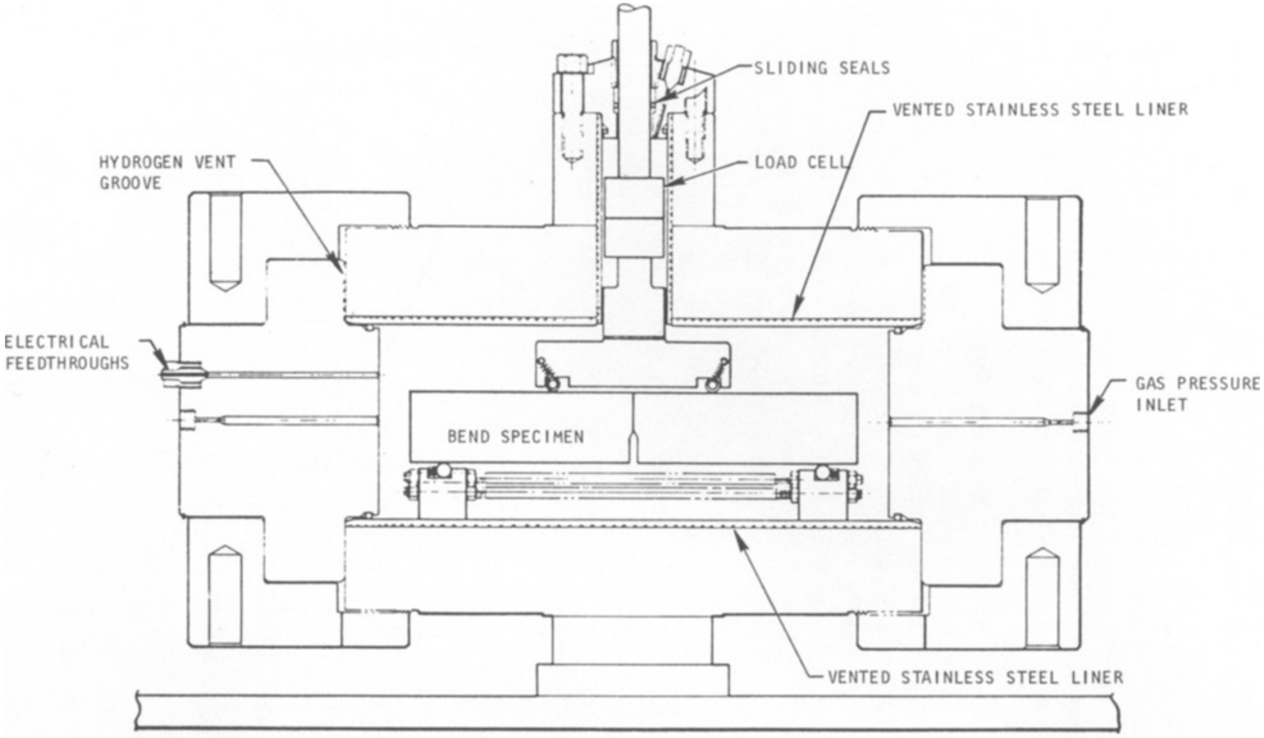

FIG. 7—*Schematic of vessel used for performing bend tests in high-pressure hydrogen (to 15 000 psi) at room temperature.*

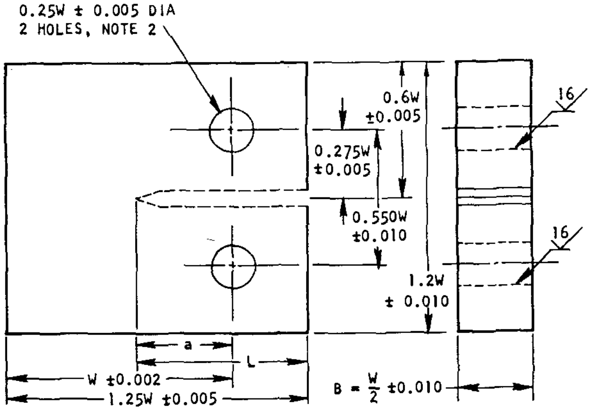

FIG. 8—*Compact tension specimen.*

The vessel shown in Fig. 11 is being used at Rocketdyne to measure sustained load threshold stress intensities of metals in high-pressure hydrogen. This vessel can be used at pressures up to 6000 psi at room and cryogenic temperatures. A modified WOL specimen (Fig. 10) is used. The specimen is loaded until the crack moves, then a crack opening displacement is established and held constant, and the crack is allowed to arrest.

The method for applying a constant displacement is shown in Fig. 12. By rotating the loading ram, a compressive force is extended across the load cells, and this force in turn acts as a tensile load across the specimen. From the load dropoff, the displacement at which crack growth initiates and the time at which the threshold has been reached can be ascertained. Thus, the specimen can be preloaded only to that level needed for crack growth, which is desirable for preventing excessive crack branching. Secondly, the load at threshold can be determined directly without subsequent reloading, which is usually required for obtaining the crack opening displacement (COD) at threshold. This is particularly important for tests conducted at other than room temperature, because the COD at the test temperature and the load to obtain this COD at that temperature must otherwise be measured.

The sliding seal friction is considerably higher at cryogenic temperatures, and this increased friction decreases the accuracy of the load measurements if a load cell is not located inside the test vessel. As an example of the magnitude of the sliding seal friction, the static friction on a 0.306-in.-(shaft) diameter specimen, illustrated in Fig. 4, was measured to be 36, 83, 566, and 300 lb at 140, 74, −109, and −320°F, respectively. The measurements were made while the vessel was pressurized with 2000-psi helium and with the sliding seals tightened sufficiently to hold this pressure

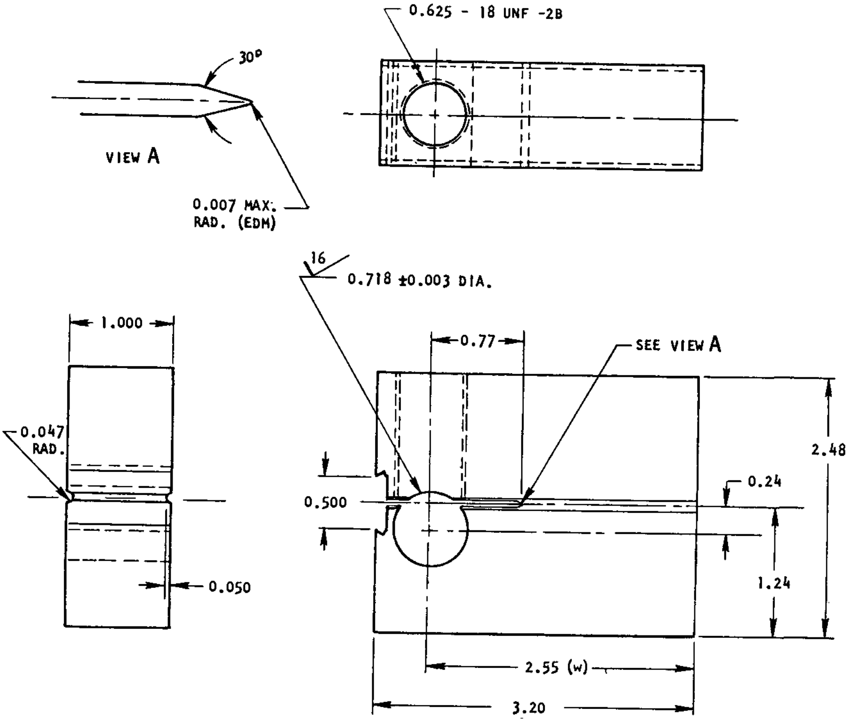

FIG. 9—*Modified WOL specimen.*

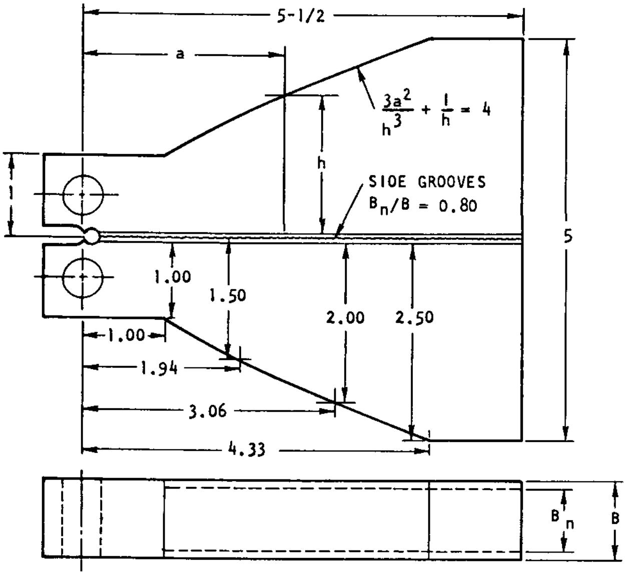

FIG. 10—*Tapered double cantilever beam specimen.*

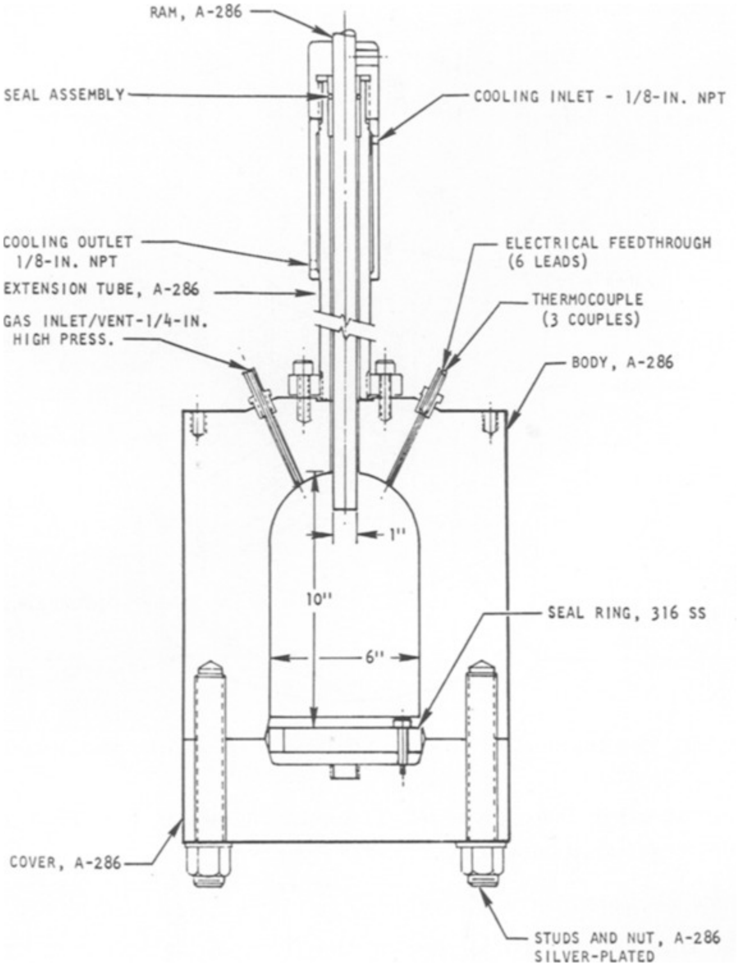

FIG. 11—*Pressure vessel used to perform tests on modified WOL specimen in high-pressure hydrogen.*

without measurable leakage. With increasing sliding seal area, the sliding seal friction would increase proportionately.

With large pressure vessels, the compatibility of the pressure vessel material with the high-pressure hydrogen is an important consideration. The materials that are not embrittled [*1*] by hydrogen are copper alloys, aluminum alloys, and the stable (will not transform to martensite during cold working) austenitic stainless steels. The smaller vessels, such as shown in Fig. 4, are constructed of AISI 316 stainless steel. The large vessel shown in Fig. 7 contains a vented AISI 316 stainless steel liner in contact with high-pressure hydrogen. The structural part of this vessel

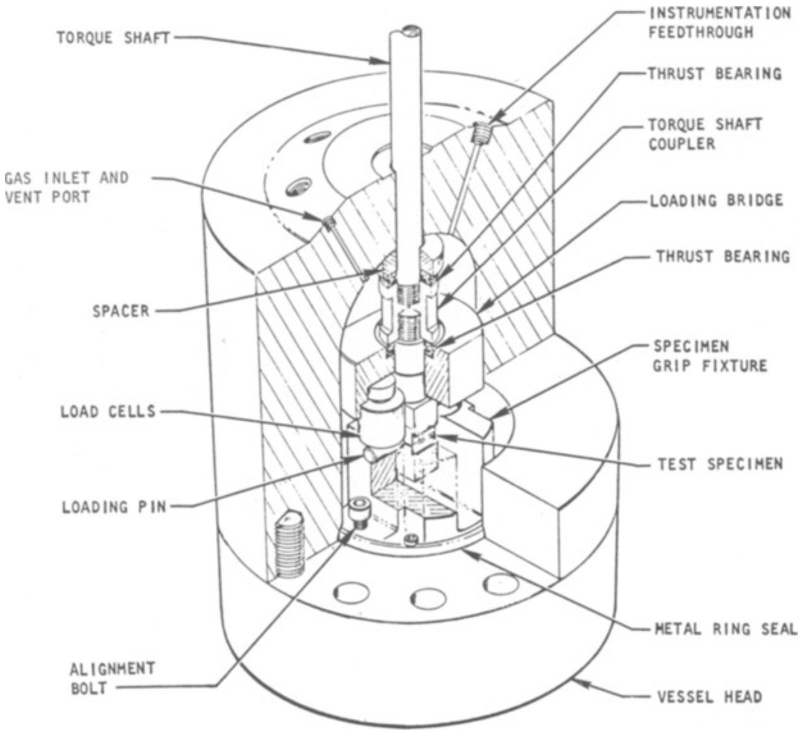

FIG. 12—*Apparatus for performing threshold stress intensity measurements.*

is constructed of low-alloy steel. The vessel shown in Fig. 11 is made of A286 precipitation hardening stainless steel.

Elevated Temperatures

The simplest method for testing the effect of high-pressure hydrogen on the mechanical properties of metals at elevated temperatures is to use pressurized, hollow specimens as described earlier. As noted earlier, such specimens have certain disadvantages, and in many instances it will be necessary to perform tests on specimens exposed to high-pressure hydrogen inside pressure vessels. Testing in high-pressure environments inside pressure vessels is considerably more difficult at elevated temperatures than at room temperature. Hazards are increased, of course, by the presence of a heater as an ignition source for any hydrogen released from the vessel. At elevated temperatures, O-ring materials for the sliding seals tend to soften and degas, making it ineffective as a sealant. Therefore, the sliding seal must be maintained near room temperature.

Material compatibility is also a problem. The strongest alloy tested thus far which is embrittled only slightly by high-pressure hydrogen (at least at room temperature) is A286, a precipitation hardenable austenitic stainless steel. A286 is not high strength (95 ksi yield and 140 ksi ultimate) at room temperature but does retain reasonable strength to elevated temperatures. However, it has been reported [12] that the creep properties of A286 are degraded by high-pressure hydrogen. Thus, the pressure vessel shown in Fig. 11, for example, is limited to moderate temperatures.

Materials limitations, therefore, place definite restrictions on the hydrogen pressure/temperature conditions at which pressure vessel materials can be used. There are two methods that can be used to extend this

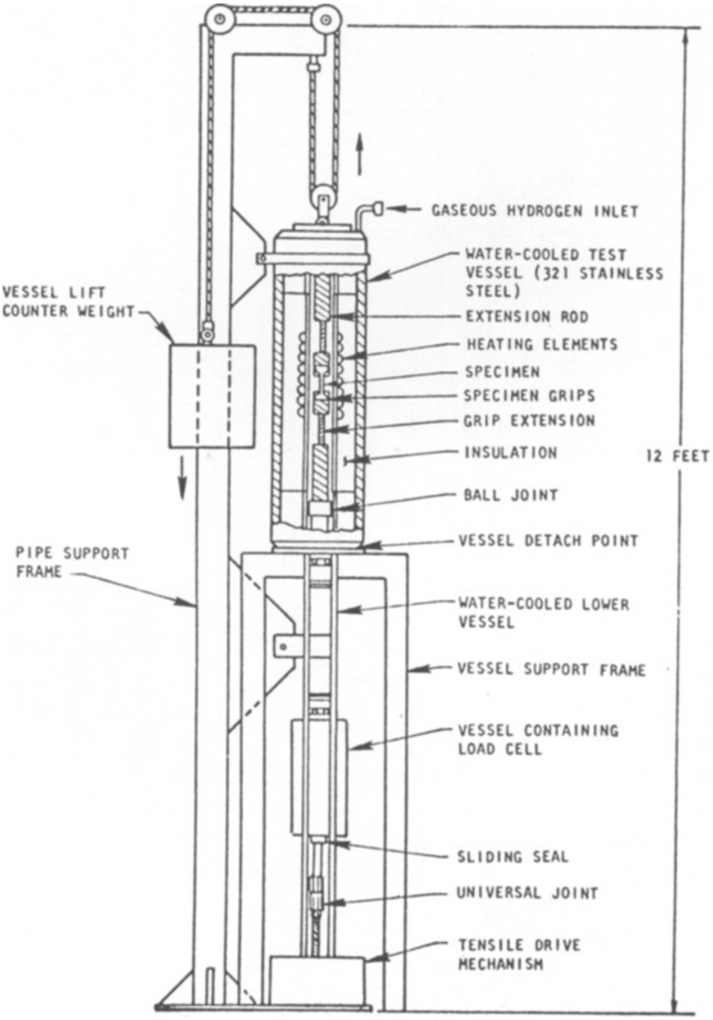

FIG. 13—*Schematic of apparatus for tension testing button head specimens in high-pressure hydrogen at elevated temperatures.*

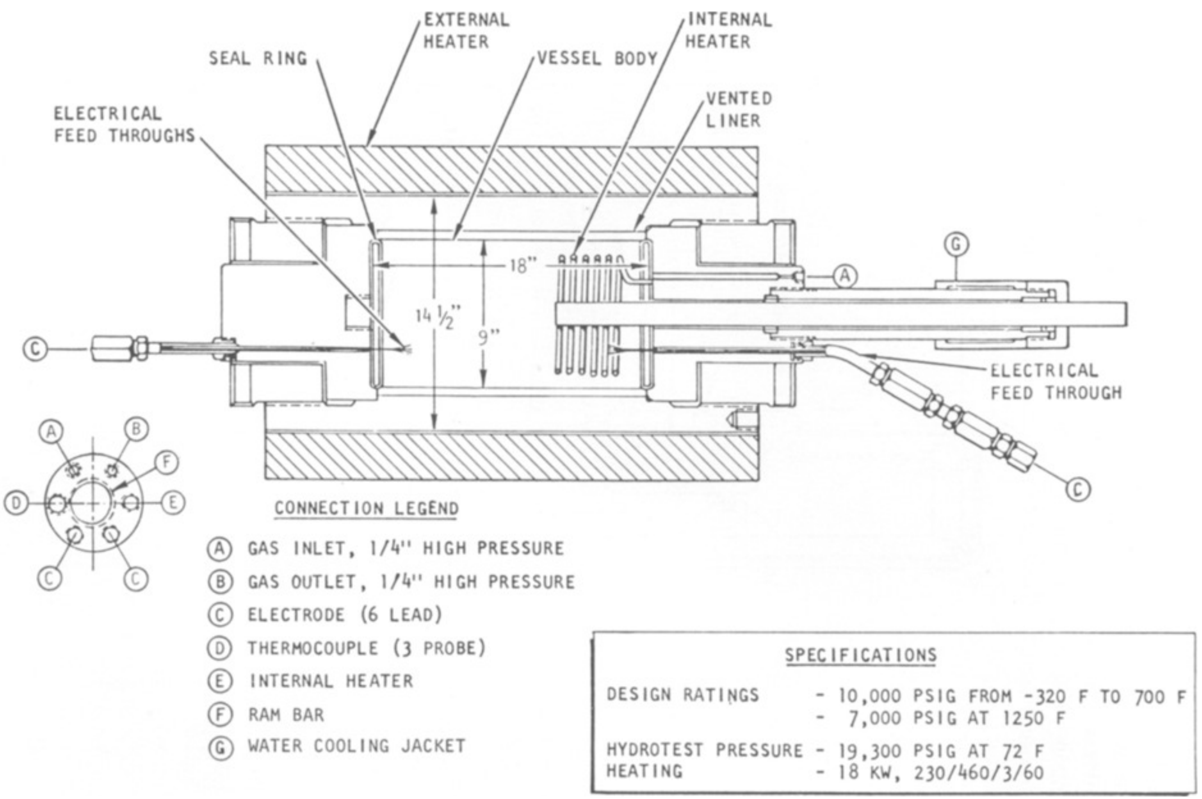

CONNECTION LEGEND

Ⓐ GAS INLET, 1/4" HIGH PRESSURE
Ⓑ GAS OUTLET, 1/4" HIGH PRESSURE
Ⓒ ELECTRODE (6 LEAD)
Ⓓ THERMOCOUPLE (3 PROBE)
Ⓔ INTERNAL HEATER
Ⓕ RAM BAR
Ⓖ WATER COOLING JACKET

SPECIFICATIONS

DESIGN RATINGS - 10,000 PSIG FROM -320 F TO 700 F
- 7,000 PSIG AT 1250 F
HYDROTEST PRESSURE - 19,300 PSIG AT 72 F
HEATING - 18 KW, 230/460/3/60

FIG. 14—*Vessel for testing fracture mechanics specimens in high-pressure hydrogen at elevated temperature.*

range. One method is for the vessels to contain an internal heater and water cool the vessel walls. A system of radiation shields is not effective in a high-pressure hydrogen system because of high-heat transfer due to high-thermal conductivity and rapid convection of hydrogen at high pressure. Outgassing from any ceramic insulation in the heater, however, would make it virtually impossible to maintain any degree of purity of the hydrogen unless the heater is isolated from the specimen. A cold-wall apparatus used at Rocketdyne for performing tension tests on cylindrical specimens at temperatures up to 2000°F is shown in Fig. 13. The test vessel has a double wall for water cooling, and includes a tube that separates the specimen cavity from the furnace cavity. A water-cooled lower extension contains a load cell. The specimen cavity, furnace cavity, and load cell cavity are separated from each other by Viton-A O-ring seals, and the same gas pressure is maintained in the three cavities during the tests to minimize gas passage across the O-rings and the stress on the inside tube. To minimize heat loss, the high-pressure gas in the heater cavity can be argon, and ceramic insulation can be used around the heater since it will not be in contact with the hydrogen. A disadvantage of this method is that the outside vessel is quite large to contain adequate size furnace and specimen chambers.

A second method for extending the temperature range of pressure vessels beyond the normal material compatibility is by using a vented liner. The liner is constructed of a material compatible with high-pressure hydrogen, and the vessel wall is constructed of a high-temperature alloy. Vented stainless steel liners are commonly used in ambient temperature hydrogen pressure vessels. For high-temperature service, the difference in thermal expansion between the vessel liner and structural material must be considered in the vessel design. The best match of thermal expansion apparently available is using A286 as a liner material and Inconel 718 as the vessel structural material.

A vessel of such hot-wall design, shown in Fig. 14, has been constructed for use at Rocketdyne for testing fracture mechanics specimens. It is designed for performing tests on specimens in 10 000-psi hydrogen at temperatures from −320 to 700°F and in 7000-psi hydrogen at temperatures up to 1250°F. The pressure vessel body is constructed of Inconel 718 and contains an A286 vented liner. For elevated temperature testing, it is heated from the outside and fine temperature control is obtained from an inside metal-sheathed (nonoutgassing) heater. The sliding seal is located inside a long-necked heat exchanger to maintain ambient temperature at the sliding seal.

Interpretation and Use of Test Results

The elastic properties, tensile yield strength, and, in many cases, the ultimate tensile strength of unnotched specimens are the same in hydrogen as in air or inert environments. The most significant effects of high-pressure hydrogen environments are on tensile ductility, notch tensile strength, and crack behavior. More precisely, the effect of the hydrogen environment is to embrittle the surface. The embrittled surface may be the immediate surface or a surface layer of some finite but limited thickness. The metal surface cannot undergo plastic deformation to the same degree in hydrogen as in air or inert environments or, for that matter, as can the interior of the metal whose surface is in contact with hydrogen. When a susceptible metal is stressed in tension in hydrogen to some critical amount of plastic deformation, the surface fractures (that is, a surface crack forms), while the interior of the metal is still capable of undergoing considerable additional deformation. This surface cracking provides some of the most dramatic visual evidence of hydrogen environment embrittlement. For a susceptible metal, an existing crack or one formed in the hydrogen environment will propagate at a lower stress intensity and at a more rapid rate for a given stress intensity in hydrogen than in air or inert environments.

The effect of the hydrogen environment is, for all practical purposes, immediate (that is, as soon as a susceptible metal is placed in the hydrogen it will behave in a brittle manner as just described). No holdtime in the hydrogen environment is required. This does not mean that failure is immediate. Time to failure obviously will depend on the type and rate of stress application and other factors.

The amount of hydrogen environment embrittlement of susceptible metals is highly influenced by the nature of the surface cracking and crack propagation in hydrogen. The greatest degree of embrittlement is associated with the formation of a sharp surface crack(s) and with the crack(s) remaining sharp during propagation. Lesser degrees of embrittlement are associated with the formation of surface cracks which are blunt or the blunting or branching of cracks during propagation.

Hydrogen environment embrittlement is an environmental effect, and occurs only while the metal is in contact with hydrogen. A metal that is exposed to hydrogen but then removed from the hydrogen is not subject to hydrogen environment embrittlement. Embrittlement due to previously absorbed hydrogen (internal hydrogen embrittlement) may add to, or synergistically interact with, hydrogen environment embrittlement.

Tensile Properties

A large number of alloys were investigated at Rocketdyne, and on the basis of tension tests on unnotched and notched specimens in 10 000-psi hydrogen at room temperature, the alloys were classified into four hydrogen environment embrittlement categories (that is, extreme, severe, slight, and negligible). Tables 1 through 4 show the reductions in some tensile properties caused by the hydrogen environment. The alloys are listed in order of decreasing effect of the hydrogen environment on notch strength, and

TABLE 1—*Materials extremely embrittled by 10 000 psi* H_2 *at 72° F.*

	Strength Ratio, H_2/He		Unnotched Ductility			
			Elongation, %		Reduction of Area, %	
Material	Notched (K_t = 8.4)	Un-notched	He	H_2	He	H_2
18Ni-250 maraging	0.12	0.68	8.2	0.2	55	2.5
410 stainless steel	0.22	0.79	15	1.3	60	12
1042 Q&T	0.22	...	...	...	...	...
17-7 PH stainless steel	0.23	0.92	17	1.7	45	2.5
Fe-9Ni-4Co-0.20C	0.24	0.86	15	0.5	67	15
H-11	0.25	0.57	8.8	0	30	0
René 41	0.27	0.84	21	4.3	29	11
Electroformed Ni[b]	0.31	...	...	...	...	...
4140	0.40	0.96	14	2.6	48	9
Inconel 718	0.46	0.93	17	1.5	26	1
440 C	0.50	0.40	...	...	3.2	0

[b] Tested in 7000-psi H_2.

they are grouped into the embrittlement categories. It should be noted that the names applied to the embrittlement categories are relative terms and that the reductions in properties shown in Tables 1 through 4 are for relatively severe embrittling conditions (that is, high-purity, 10 000-psi hydrogen at room temperature with severe (0.001-in.-radius)

TABLE 2—*Materials severely embrittled by 10 000 psi* H_2 *at 72° F.*

	Notch Strength Ratio, H_2/He (K_t = 8.4)	Unnotched Ductility			
		Elongation, %		Reduction of Area, %	
Material		He	H_2	He	H_2
Ti-6Al-4V (STA)	0.58	...	...	...	...
430 F	0.68	22	14	64	37
Nickel 270	0.70	56	52	89	67
A515	0.73	42	29	67	35
HY-100	0.73	20	18	76	63
A372 Class IV	0.74	20	10	53	18
1042 normalized	0.75	...	...	59	27
A533-B	0.78	...	...	66	33
Ti-6Al-4V (annealed)	0.79	...	...	...	...
AISI 1020	0.79	...	...	68	45
HY-80	0.80	...	...	70	60
Ti-5Al-2.5Sn ELI	0.81	...	...	45	39
Armco iron	0.86	...	...	83	50

notches in the notched specimens). The embrittlement categories have the following general characteristics:

1. *Extreme embrittlement*—High-strength steels and high-strength nickel-base alloys are in this category. Embrittlement is characterized by a large decrease of notch strength and some decrease of unnotched ultimate tensile strength. Large reductions are found for all three common measures of ductility (elongation and reduction of area of unnotched specimens, and reduction of area of notched specimens).
2. *Severe embrittlement*—The majority of the metals tested are in this category, including ductile, lower-strength steels, Armco iron, pure nickel, and the titanium-base alloys. Embrittlement is characterized by a considerable reduction of notch strength and ductility, but no reduction of unnotched ultimate tensile strength. The measure of ductility most affected by the high-pressure hydrogen environment is the reduction of area of notched specimens.
3. *Slight embrittlement*—The nonstable AISI 300 series stainless steels (AISI 304L and 305), beryllium-copper, and commercially pure titanium are in this category. Embrittlement is characterized by a small decrease of unnotched ductility.
4. *Negligible embrittlement*—The aluminum alloys, stable austenitic stainless steels, A286 (a precipitation-hardened austenitic stainless steel), OFHC copper, and the copper-base alloy NARloy-Z are in this category.

As noted, no significant effects of hydrogen environments at ambient temperatures on elastic properties or yield strength have been found. The deformation capability of the metal surface is lower in hydrogen than in air or inert environments. Thus, as the tension test proceeds, a critical surface deformation is reached at which the surface fractures in a brittle manner and a surface crack is formed. The most direct evidence for the environmental nature of the embrittlement in hydrogen is the brittle appearance of the fracture at the surface of unnotched and notched specimens and the cracks formed on the surface in deformed regions of unnotched specimens of susceptible metals. In notched specimens, the

TABLE 3—*Materials slightly embrittled by 10 000 psi* H_2 *at 72° F.*

Material	Notch Strength Ratio, H_2/He (K_t = 8.4)	Unnotched Ductility (reduction of area, %)	
		He	H_2
304 ELC stainless steel	0.87	78	71
305 stainless steel	0.89	78	75
Be-Cu alloy 25	0.93	72	71
Titanium	0.95	61	61

TABLE 4—*Materials negligibly embrittled by 10 000 psi* H_2 *at 72° F.*

Material	Notch Strength Ratio, H_2/He (K_t = 8.4)	Unnotched Ductility (reduction of area, %)	
		He	H_2
310 stainless steel	0.93	64	62
A286	0.97	44	43
7075-T73 Al alloy	0.98	37	35
316 stainless steel	1.00	72	75
OFHC copper	1.00	94	94
NARloy-Z[b]	1.10	24	22
6061-T6 Al alloy	1.10	61	66
1100–0 Al	1.40	93	93

[b] Rockwell International Corporation trademark; tested in 5800-psi H_2.

region of highest deformation is so localized at the base of the notch that surface cracks, other than those resulting in failure, are normally not found.

From the time at which surface cracking begins, the test is no longer a normal tension test but is a rather complex test of a cracked specimen; this must be considered in assessing the meaning and usefulness of the strength and ductility data obtained from these tests. In alloys that are placed in the extremely embrittled category (Table 1), the first surface crack to form propagates to failure, usually without the formation of additional surface cracks. This crack propagates at some finite rate that is more rapid in hydrogen than it would be in air or an inert environment. Because the test is being conducted as a tension test and the load is continuing to be increased, and because of the deepening of the crack, the stress intensity in front of the propagating crack is increasing rapidly during the test. The crack propagates until the remaining area fails due to tensile overload. The final failure is a ductile failure apparently unaffected by the hydrogen environment. It can be seen that the "ultimate tensile strengths" and "ductilities" determined from such tests on unnotched and notched specimens of metals that are extremely embrittled in hydrogen are determined by the load or strain rate, the time (plastic deformation) at which the surface crack is formed, and the rate of propagation of the crack in hydrogen. Thus, these properties are far more sensitive to load or strain rates than are tensile properties determined in air or inert environments.

For alloys in the severely or slightly embrittled categories (Tables 2 and 3), the first surface crack to form does not propagate to failure. The surface cracks in these alloys are blunt as formed or tend to blunt or branch during propagation in hydrogen. The first surface crack forms, propagates in a brittle manner to some extent, blunts or branches, and stops. A second crack forms, and the process continues until, finally, the remaining area has been reduced by the series of surface cracks so that ductile, tensile overload failure occurs. The properties determined from these tests will be a function of the same factors as listed in the preceding paragraph for the extremely embrittled metals and also will be a function of the extent of crack propagation before the crack is stopped by blunting or branching.

From the foregoing discussion, it can be inferred that the different tensile properties will show differing degrees of sensitivity to the hydrogen environments. The degrees of sensitivity in decreasing order are: fracture mode (effects on the appearance of the fracture have been noted when only negligible change of properties occurred), reduction of area of notched specimens, ultimate strength of notched specimens, reduction of area of unnotched specimens, elongation of unnotched specimens, and ultimate strength of unnotched specimens. Only for metals in the extremely embrittled category is there a reduction of ultimate tensile strength of unnotched specimens in hydrogen. The fact that this property is not affected by hydrogen for metals in the other embrittlement categories simply reflects the relationship noted previously between rate of loading (straining) and the time for crack initiation and extension, remembering that crack blunting and branching slow crack growth considerably in these metals. In fact, it appears that in many cases, surface cracks do not form until the ultimate tensile strength is reached (that is, necking begins).

Although the ultimate strengths and ductilities determined from tension tests in hydrogen on unnotched and notched specimens of susceptible materials are of limited direct usefulness in design, these tension tests are valuable as rapid and economical screening tests which provide a good indication of the relative degrees of embrittlement of different metals by hydrogen environments (that is, as shown in Tables 1 through 4). For design purposes, the tensile properties determined in hydrogen can be used as a guide for establishing additional safety factors to compensate for hydrogen environment embrittlement.

It is suggested that a recommended stress concentration factor be established for notched specimens used for the evaluation of hydrogen environment embrittlement so that results from different investigations can be compared more effectively. Figure 15 shows the reduction of notch strength in 10 000-psi hydrogen as compared to 10 000-psi helium for ASTM A533-B steel as a function of stress concentration factor.

Tests are in progress at Rocketdyne to determine the strength and ductility at which surface cracks initiate during tension tests on unnotched specimens in high-pressure hydrogen. Consideration is being given to the use of this crack initiation strength and ductility in place of the normal ultimate tensile strength and ductility for the design of hydrogen systems. The assumption is that in hydrogen the maximum available strength and ductility is that associated with the initiation of surface cracks.

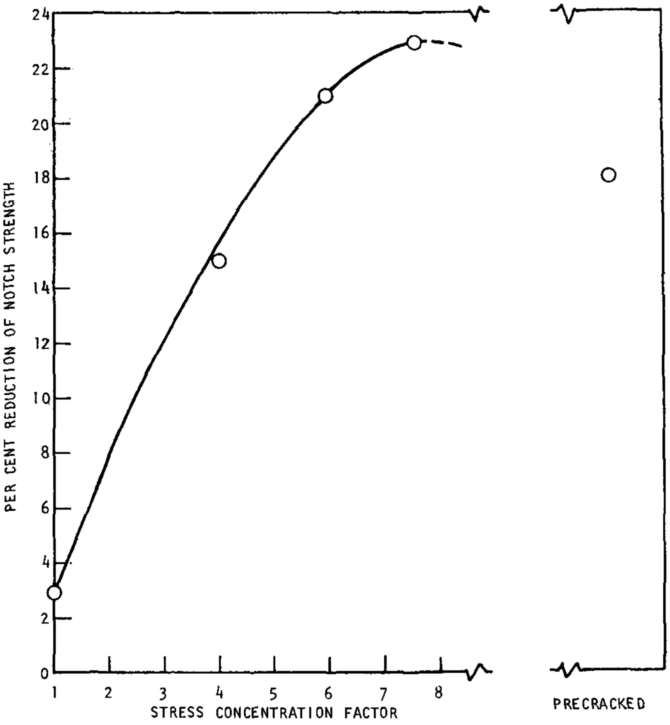

FIG. 15—*Reduction of notch strength as a function of stress concentration factor for ASTM A533-B in 10 000-psi hydrogen.*

For hydrogen to cause surface cracking, it seems axiomatic that the hydrogen must contact the metal surface. Therefore, it appears reasonable that the critical deformation for initiation of surface cracking in hydrogen is, at minimum, that surface deformation required to rupture the oxide layer so that the hydrogen can contact the metal surface. At Rocketdyne [*8*], specimens were tension tested in high-pressure hydrogen after abrasion in hydrogen to remove the oxide layer. The specimens were not exposed to air between abrasion and tension testing. The specimens so tested had a much larger number of surface cracks than specimens abraded in air before testing in hydrogen. The amount of plastic deformation at crack initiation was not determined. However, a certain amount of plastic deformation of the metal surface still was required before surface cracking initiated in the specimens abraded in hydrogen.

Fracture Mechanics Properties

High-pressure hydrogen has its greatest effects on crack behavior. Thus, the fracture mechanics approach is a natural one to apply to hydrogen systems.

The fracture toughness parameter, K_{Ic}, is considered generally to be a

TABLE 5—*Average K_{Ic} and K_{th} values for various metals in 5000-psi hydrogen and helium at room temperature.*

Material	Environment	K_{Ic} ksi $\sqrt{\text{in.}}$	K_{th} ksi $\sqrt{\text{in.}}$	K_{th}/K_{Ic}
Inconel 718 1725, 1325 to 1150° F	He	71	53	0.73
	H_2	...	13	0.18
Inconel 718 1925, 1400 to 1200° F	He	108[a]	102	0.94
	H_2	100	35	0.33
Inconel 625	He	76[a]	...	...
	H_2	61[a]	...	...
A286 stainless steel	He	132[a]	...	...
	H_2	91[a]	<103[b]	<0.78
Ti-5Al-2.5Sn ELI	He	72	63	0.88
	H_2	...	31	0.43

[a] Not valid K_{Ic} according to ASTM 399.
[b] Stress at $K_{th} > \sigma_y$.

property of a given material and not affected by the environment, including hydrogen environments. Direct evidence that K_{Ic} is not affected by hydrogen environments, particularly high-pressure hydrogen environments, is limited. The definition of K_{Ic} is important in this respect. If popin occurs, K_{Ic} should not be affected by a hydrogen environment. But, a K_{Ic} determined using the secant intercept method may well be affected by a high-pressure hydrogen environment and the time to perform the K_{Ic} test may be more critical in hydrogen than in air or inert environments. If K_{Ic} is to be determined in high-pressure hydrogen, it is important that the precrack be extended by cycling at low stress levels in hydrogen before beginning the K_{Ic} test. Otherwise, the initiation of crack movement in hydrogen would be a function of the rupturing of the surface oxide layer.

As expected, considerable effects of high-pressure hydrogen on K_{th}, the threshold stress intensity for sustained-load flaw growth, have been found [*1*]. Table 5 contains results of K_{th} tests on various metals in 5000-psi hydrogen recently completed at Rocketdyne. These tests were performed with the apparatus shown in Figs. 11 and 12. In the tests, the load (displacement) on the specimen was increased until crack movement was first observed and then the displacement was held constant, or reduced to minimize the possibility of specimen failure and crack branching. It is interesting to note that crack growth occurred in hydrogen but not in helium in A286, which has been classified as negligibly embrittled (Table 4) on the basis of tension tests. However, crack growth in the K_{th} tests in hydrogen occurred only with loads large enough to cause yielding, and the crack growth was very slow, which explains why tension tests did not show any effect of hydrogen on A286. Considerable crack branching occurred in Inconel 625 in hydrogen.

Cyclic and sustained load crack growth rates have been found to be considerably faster in hydrogen than in air or inert environments for metals susceptible to hydrogen environment embrittlement [*1*]. However, few determinations of crack growth rates have been performed with fracture mechanics type specimens in high-pressure hydrogen.

Probably the most serious basic problem in performing fracture mechanics tests in hydrogen is the increased tendency for crack branching in hydrogen. This crack branching is advantageous, but consideration must be given to whether the crack branching occurring in fracture mechanics specimens will occur to the same degree in actual structures in hydrogen.

Fatigue and Creep Properties

With smooth specimens, the most severe property degradation in high-pressure hydrogen occurs in tests involving plastic strain. Thus, considerable reductions of stress-rupture strengths and cycles to failure in low-cycle fatigue (strain cycling) tests in hydrogen are found [*12*].

The reduction of high-cycle fatigue properties by hydrogen environments was also reported by Harris and VanWanderham [*12*]. However, the tests were not typical high-cycle fatigue tests since the cycles to failure were in most cases below 10^5 cycles and the maximum stresses were high, usually above the yield strength. It is expected that the effect of hydrogen environments on typical low stress, high-cycle fatigue will not be as significant. In high-cycle fatigue, the strain per cycle is small; therefore, the effect of hydrogen on the number of cycles to crack initiation may be small, and the main effect of the hydrogen would be on crack propagation. But generally, in high-cycle fatigue, approximately 90 percent of the time to failure is occupied with crack initiation.

Summary

Since hydrogen environment embrittlement by high-pressure gaseous hydrogen is an environmental effect, it is essentially in testing for this effect that the test environment in every way, but particularly with regard to hydrogen purity, be well characterized, controlled, and reported. Standards for hydrogen purity must be established and for the present the use of MSFC-SPEC-356A is recommended. Care must be exercised in purging test systems of impurity gases and in sampling the hydrogen at the test location for analysis. Procedures for purifying hydrogen to the desired levels for high-pressure test systems have been developed. Specimen preparation, particularly surface preparation, must also be characterized, controlled, and reported.

The simplest method of testing for high-pressure hydrogen effects on metals involves the use of hollow cylindrical specimens internally pressurized with hydrogen. Such specimens are advantageous for such tests as creep and low-cycle, high-cycle, and thermal fatigue tests. Other types of tests, in particular notched tensile and fracture mechanics tests to determine the effects of high-pressure hydrogen, require the use of a pressure vessel around the specimen or a portion of the specimen. The simplest such system entails sealing the specimen directly to the pressure vessel wall with the specimen ends extending out of the pressure vessel for attachment to the loading system. With this technique, the temperature is limited to relatively low temperatures by the capabilities of the seals and steps must be taken to accurately compensate for seal friction and pressure effects.

For many tests, for example, at elevated temperatures, it is necessary to accommodate the entire specimen (and grips) inside a pressure vessel with the loading ram extending out of the vessel. In this case, a load cell should be located inside the vessel so that the test load can be measured more accurately without the necessity of compensating for seal friction and pressure effects. The larger pressure vessel required and the attendant greater difficulties in loading and unloading specimens makes this testing slower and more costly particularly at cryogenic or elevated temperatures. Provision must be made for maintaining sliding seals, load cells, and strain measuring devices at approximately room temperature when testing at elevated temperatures.

Results of tension tests in high-pressure hydrogen are difficult to apply directly in design because of the formation and growth of surface cracks during testing. However, tension tests on both unnotched and notched specimens in high-pressure hydrogen are valuable as fairly rapid and economical screening tests of susceptibility to hydrogen environment embrittlement and can be used as a guide to setting additional safety factors to compensate for this embrittlement. Consideration is being given to the determination of strength and plastic deformation at which surface cracks initiate for use in place of the normal ultimate tensile strength and elongation for design purposes. With smooth specimens, the most severe property degradation in high-pressure hydrogen occurs in tests involving plastic strain. Thus, considerable reductions of stress-rupture and low-cycle fatigue strengths are found.

Since high-pressure hydrogen has its greatest effect on crack behavior, the fracture mechanics approach is a natural one to apply to hydrogen systems. In some tests, it is important to extend the precrack in hydrogen by cycling at low stress levels before beginning the test. A complication in the testing of fracture mechanics specimens in high-pressure hydrogen is the greater tendency toward crack branching in hydrogen. The implication of this branching to actual structures needs consideration.

Acknowledgments

The test equipment, procedures, and results described in this report were developed under various National Aeronautics and Space Administration contracts with W. B. McPherson, George C. Marshall Space Flight Center, as Technical Monitor. The following personnel have made valuable contributions in the development of test equipment and procedures; G. E. Dyer, H. G. Hayes, R. D. Lloyd, and G. V. Sneesby.

References

[*1*] Jewett, R. P., Walter, R. J., Chandler, W. T., and Frohmberg, R. P., "Hydrogen-Environment Embrittlement of Metals," A NASA Technology Survey, NASA CR-2163, National Aeronautics and Space Administration, Washington, D. C., March 1973.
[*2*] Hofmann, W. and Rauls, W., *Welding Journal*, Vol. 44, May 1965, pp. 225s–230s.
[*3*] Sawicki, V. and Johnson, W., personal communication, Cornell University.
[*4*] Frick, V., Janser, G. R., and Brown, J. A., *Space Shuttle Materials*, Vol. 3, Proceedings of Conference, Society of Aerospace Material and Process Engineers, Azusa, Calif., 1971, p. 597.
[*5*] Liu, H. W., Hu, Ya-lung, and Ficalora, P. J., "Catalytic Dissociation and Hydrogen Assisted Cracking," paper presented at 1973 Western Metal and Tool Conference (WESTEC), 12–16 March 1973; also abstract in WESTEC 1973 Conference Abstracts, American Society for Metals, Metals Park, Ohio, p. 5.
[*6*] Engelhard Industries, Inc., Sales Brochures, 113 Astor St., Newark, N. J.
[*7*] Walter, R. J., *Instrumentation Technology*, Vol. 14, No. 9, 1967, p. 84.
[*8*] Walter, R. J. and Chandler, W. T., "Effects of High-Pressure Hydrogen on Metals at Ambient Temperatures," final report on Task 7 of NASA Contract NAS8-19, Rocketdyne Division, Rockwell International, Canoga Park, Calif., Report No. R-7780-1, R-7780-2, and R-7780-3, Feb. 1969.
[*9*] Lysyj, I. in *Proceedings*, Instrument Society of America, 1963, p. 41.
[*10*] Honnigford, J. B., masters' thesis, Rensselaer Polytechnic Institute, Troy, N. Y., 1958.
[*11*] Lorenz, P. M., "Effect of Pressurized Hydrogen Upon Inconel 718 and 2219 Aluminum," Report No. W9-13.2, American Society for Metals, Metals Park, Ohio, 1969.
[*12*] Harris, J. A., Jr., and VanWanderham, M. C., "Properties of Materials in High-Pressure Hydrogen at Cryogenic, Room, and Elevated Temperatures," annual report on NASA Contract NAS8-26191, Pratt and Whitney Aircraft, Division of United Aircraft Corp., West Palm Beach, Fla., June 1971.

J. A. Harris, Jr.,[1] *and M. C. VanWanderham*[1]

Various Mechanical Tests Used to Determine the Susceptibility of Metals to High-Pressure Hydrogen

REFERENCE: Harris, J. A., Jr., and VanWanderham, M. C., "**Various Mechanical Tests Used to Determine the Susceptibility of Metals to High-Pressure Hydrogen,**" *Hydrogen Embrittlement Testing, ASTM STP 543,* American Society for Testing and Materials, 1974, pp. 198–220.

ABSTRACT: The use of hydrogen as a rocket fuel has been successfully established; however, it has also been established that many metals are degraded in one or more of their properties by environmental gaseous hydrogen. The degree of degradation may range from slight to extreme, depending on the metal being analyzed and the type of test or tests used. Many important variables, such as environment, stress, temperature, and time must be considered in selecting the test to be used to determine the susceptibility to gaseous hydrogen. This report will discuss several different types of tests, such as: (1) tensile (smooth and notched), (2) strain-controlled, low-cycle fatigue, (3) high-cycle fatigue, (4) creep-rupture, and (5) fracture toughness, used to determine degradation of specific material properties and enable general observations in regard to the susceptibility of various materials to hydrogen degradation.

KEY WORDS: hydrogen embrittlement, degradation, mechanical properties, smooth tensile, notched tensile, low-cycle fatigue, high-cycle fatigue, creep rupture strength, fracture toughness, helium gas, hydrogen gas, elevated temperature, iron containing alloys, nickel containing alloys, titanium containing alloys, susceptibility

Premature or unexpected failures of pressure vessels had occurred for some time before they were attributed to the presence of hydrogen in the material or operating environment. Most of the failures were in steel components and were characterized as brittle failures, thus giving rise to the term hydrogen embrittlement, a terminology that seems to be accepted generally. The use of hydrogen as a fuel for space flights has placed an emphasis upon establishing the effects of environmental hydrogen

---

[1] Senior project materials testing engineer and general supervisor, Applied Mechanics Section of the Materials Development Laboratory, Florida Research and Development Center, Pratt & Whitney Aircraft, West Palm Beach, Fla. 33405.

upon materials. Early hydrogen-fueled rocket engines experienced no major problems attributed to hydrogen effects. This may have been due to low operating pressures, inhibitors present due to operating conditions, or just good fortune in the selection of materials. As performance requirements and operating pressures increased, use of high-strength alloys and lightweight designs became necessary. To substantiate these designs, extensive investigations have been conducted into the effect of hydrogen upon the mechanical properties of materials, specifically those properties used for design.

The authors have conducted mechanical property tests, both under in-house and the National Aeronautics and Space Administration (NASA)-Marshall sponsorship, of several alloys in high-pressure gaseous helium and hydrogen. These investigations have been aimed primarily at obtaining properties for engineering design purposes. The major effort has been to document, rather than explain, the phenomenon. Metallographic evaluations of failed specimens in these programs have revealed that many alloys do not display characteristics typical of brittle failures; in fact, some display ductile fracture characteristics. For this reason, the authors prefer the term "hydrogen degradation" when speaking of mechanical property reduction due to hydrogen environments. This paper pertains to the results of mechanical property tests on three classes of alloys, with the objective of viewing these tests as indicators of sensitivity to hydrogen degradation.

Experimental Procedure

Six types of mechanical property tests have been conducted in high pressure gaseous hydrogen at room and elevated temperatures. The same tests were also conducted in high-pressure gaseous helium to provide a basis for establishing property degradation. The six tests included: smooth and notched ($K_t = 8.0$) tensile, low-cycle fatigue, high-cycle fatigue, creep-rupture, and fracture toughness. Test specimens used in this program were designed and machined in general conformance with ASTM standards, where applicable.

Specimens

Surfaces of all specimens were finished to an average roughness of 16-μin. rms, or less, except for one outer surface of the fracture toughness specimens that was machined to a maximum roughness of 32-μin. rms in accordance with ASTM Test for Plane-Strain Fracture Toughness of Metallic Materials (E 399-70 T). Gage sections of specimens were polished prior to testing. Typical test specimens used to establish mechanical properties in high-pressure gaseous environments are illustrated in Fig. 1 and are briefly described next. Details of specimens are discussed in Ref *1*.[2]

---

[2] The italic numbers in brackets refer to the list of references appended to this paper.

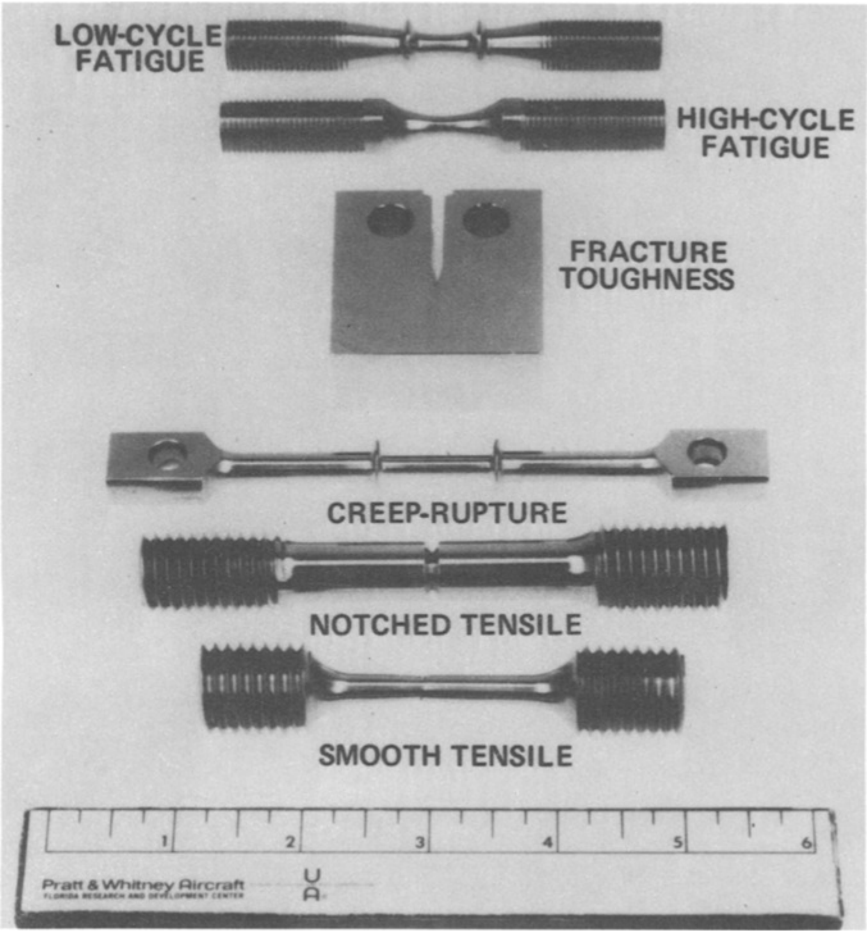

FIG. 1—*Typical test specimens used to determine effect of high-pressure gaseous hydrogen on mechanical properties of materials.*

The low-cycle fatigue specimen is cylindrical. It incorporates integral machined extensometer collars and a semihourglass gage section and is used for strain-controlled tests. A calibration procedure relates the maximum axial-strain-to-collar deflection during both the elastic and plastic portions of the strain cycle. Specimen length is 101.6 mm (4 in.), with minimum gage diameter of 5.334 mm (0.210 in.) and 12.7-mm (0.5-in.) diameter threads. This specimen is also described in Ref *2*.

The high-cycle fatigue specimen is cylindrical, with an hourglass gage section for axial-load-controlled tests. Specimen length is 101.6 mm (4 in.), with a minimum gage diameter of 4.572 mm (0.180 in.) and 12.7-mm (0.5-in.) diameter threads.

The fracture toughness specimen is a compact tensile type, with a chevron crack starter notch in accordance with ASTM Method E 399–70 T. Test rig configuration limited specimens to maximum dimensions of 47.62 by 45.72 by 19.05 mm thick (1.800 by 1.875 by 0.750 in.). Fracture toughness values obtained from this specimen are reported as K_{IE} (engineering) unless plane-strain validity requirements are met.

The creep-rupture specimen is cylindrical, with integral machined extensometer collars and flat-pinned ends. The specimen design was based upon the work of Penny et al [3]. Overall length is 139.7 mm (5.5 in.), with a gage section 25.4 mm (1.0 in. long), and 5.08 mm (0.200 in.) in diameter. This specimen is discussed in Ref *4*.

The notch tension specimen is cylindrical, with an overall length of 120.65 mm (4.75 in.), 19.0-mm (0.75-in.) diameter threads and a major diameter of 12.7 mm (0.50 in.). The notch was designed, according to Peterson [*5*], to obtain a stress concentration factor of 8.0 and was machined by grinding. Minor diameter and root radius of the notch were 8.0 mm (0.315 in.) and 0.05 mm (0.002 in.), respectively.

The smooth tension specimen is cylindrical, with an overall length of 93.22 mm (3.67 in.), 19.0-mm (0.75-in.) diameter threads, and a straight gage section 31.75 mm (1.25 in.) long by 6.35 mm (0.250 in.) in diameter.

Test Equipment

This testing was conducted in 34.5-MN/m^2 (5000-psig) gaseous helium and hydrogen environment. Specimens were tested in this environment using heavy walled pressure vessels. Although four different vessels were used, they are all of the same general design, differing only in instrumentation connections and specimen adapters. A typical pressure vessel is shown in Fig. 2. The specimen and extensometer, or crack opening displacement (COD) gage, (where used) are mounted in a load frame internal to the vessel. The outer vessel is secured by use of a "GrayLoc" flange and seal, because of the relative ease of assembly and the reliability of the seal in high pressure. The pressure vessel incorporates a pressure compensating device to eliminate axial tensile load on the specimen due to high-pressure acting over the differential specimen and adapter areas. Both internal (to the pressure vessel) and external load cells are used; thus, the effect of friction at the seals, where the load rods enter the vessels, is known. Electrical connections for the load cells, extensometer systems, furnaces, and thermocouples are made through the vessel wall via high-pressure bulkhead connectors. During testing, the internal strain gage-type load transducer is used to obtain load information for load-strain plotting purposes.

Elevated temperatures are obtained with resistance furnaces surrounding the specimens. In the 34.5-MN/m^2 (5000-psig) gaseous environments, high-power density, multizone furnaces are required to obtain test tem-

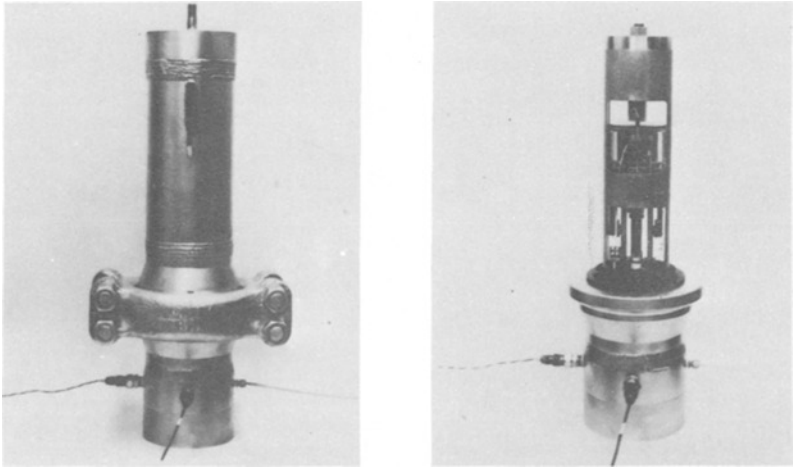

FIG. 2—*Typical pressure vessel for conducting mechanical properties tests in high-pressure gaseous environments:* (left) *closed pressure vessel and* (right) *open pressure vessel with specimen, extensometer, adapters, and half of furnace in place.*

perature and eliminate gradients due to the thermal conductivity of gaseous helium and hydrogen at this pressure. Thermocouples attached to the specimen are used to monitor and control temperature during the test. Analyses of gas samples before and after test runs indicate no detrimental contamination of test gas due to the internal furnace. To prevent possible structural damage to the pressure chamber due to overtemperature, a water jacket surrounding the outer walls provides cooling when conducting elevated-temperature tests. During testing, the vessels and test machines are located in remote test cells, which are equipped with high-pressure gas handling systems.

The testing was conducted on four test machines, each isolated in its own test cell. The fatigue tests were conducted on hydraulically actuated, closed-loop-controlled equipment. Low-cycle fatigue specimens were subjected to an all-tensile, constant total-axial strain range at a frequency of 3 to 5 cpm, which produced typical load-strain hysteresis loops. High-cycle fatigue specimens were subjected to an all-tensile axial stress range at a frequency of 20 Hz. Machine controls provided automatic system shutdown upon specimen failure.

Creep-rupture tests were conducted on a Satec Model JE creep-rupture machine, which was modified and explosion proofed. Loading was by the dead weight and lever arm system. Machine controls also provided automatic shutdown upon specimen fracture.

Tension and fracture toughness tests were conducted on a Tinius Olsen Universal Test machine, with the load frame modified to accept the high-pressure test vessel.

All test equipment loading frames are in enclosures exposed to atmospheric conditions. Control and recording apparatus for this equipment is located in adjacent block houses.

Test Procedure

As all the tests discussed herein were conducted in similar pressure vessels, the test procedure used was similar for all tests. Established procedures for specimen preparation, testing, and data reporting were adhered to, where possible.

Specimens were prepared and cleaned after machining. After inserting the prepared specimen in the load frame of the vessel, the appropriate instrumentation for the test was attached. This instrumentation consisted of extensometers, thermocouples, or COD gages, depending upon the particular test. The vessel was then sealed and subjected to a purge cycle consisting of a low-pressure nitrogen purge, evacuation, test gas (helium or hydrogen) purge, and, finally, a pressurized "pop" purge. The pop purge consists of a succession of rapid pressurizations of the vessel to a low pressure (typically, 1380 kN/m^2 [200 psi]) and releasing, while maintaining a minimum positive pressure. After purging and obtaining a pretest gas sample, high-pressure gas was introduced and maintained in the vessel until specimen temperature and gas pressure were stabilized at the desired level, and testing conducted. Upon completion of the prescribed test, pressure was vented, a posttest gas sample obtained, and, in the case of hydrogen tests, the vessel purged with nitrogen gas, opened, and the failed specimen removed. Posttest specimen measurements were obtained and test documentation completed. Gas samples were analyzed on a modified gas chromatograph with a parts-per-billion accuracy.

Experimental Program

The experimental results reported here are from a continuing program to evaluate mechanical properties of materials in high-pressure gaseous environments. Specifically, three nickel-base, two iron-base, and two titanium-base alloys were tested in 34.5-MN/m^2 (5000-psig) gaseous hydrogen at 300 K (80 F) and 366 K (200 F), or 951 K (1250 F). These alloys were also tested in 34.5-MN/m^2 (5000-psig) gaseous helium at the same temperatures to enable comparison of test results to determine degradation of properties due to the hydrogen environment.

Six types of tests were conducted: smooth and notch tensile, low-cycle fatigue, high-cycle fatigue, creep-rupture, and fracture toughness. Not all tests were conducted on each material at each temperature; however, sufficient testing was accomplished to enable observations as to an alloy's susceptibility to hydrogen degradation under different tests. The particular tests conducted and data obtained are summarized in Table 1.

TABLE 1—*Tests conducted to determine effect of high-pressure gaseous hydrogen environment upon mechanical properties.*

Type of Test	Data Obtained	Test Conditions—Parameters
Smooth tensile	0.2% yield strength ultimate strength, % elongation % reduction of area	0.005 mm/mm (in./in.)/min strain rate to yield 2.54 mm (0.10 in.)/min load rate yield to ultimate
Notch tensile ($K_t = 8.0$)	ultimate strength	2.54 mm (0.10 in.)/min load rate
Low-cycle fatigue	strain range (total and plastic) versus cycles to failure	axial total strain ranges of 0.75 to 2.20% 3, 4, or 5 cpm; mean strain is equal to one half the total strain
High-cycle fatigue	stress versus cycles to failure	axial tension-tension loading R ratio $\left(\frac{\text{min stress}}{\text{max stress}}\right) = 0.1$ 20-Hz cyclic rate
Fracture toughness	plain strain or engineering fracture toughness	compact tension specimen fatigue precracked in air 72.8 $\text{MN/m}^2\sqrt{\text{m}}$ (80.0 ksi $\sqrt{\text{in.}}$)/min load rate
Creep-rupture	elongation versus time stress versus time to failure % elongation % reduction in area	constant stress (load) at elevated temperature

Materials Tested

Three types of alloys were tested; nickel-base, iron-base, and titanium-base. The materials tested and their heat-treated conditions are listed next:

Name	Purchasing Specification	Heat Treat Condition When Tested
Nickel-base alloys:		
Inco 718	AMS 5662	solutioned at 1227 K (1750 F)[3] and solutioned at 1310 K (1900 F)[3]
Inco 625	AMS 5666	annealed at 1255 K (1800 F)
Hastelloy X	AMS 5754	annealed at 1448 K (2150 F)
Iron-base alloys:		
A286	AMS 5735	solutioned at 1255 K (1875 F) followed by age
AISI 347	AMS 5646	solutioned at 1415 K (1875 F) cold finished
Titanium-base alloys:		
Titanium 6A1-4V	AMS 4928	annealed at 1019 K (1375 F)
Titanium A110 (5A1-2.5Sn)	AMS 4926	annealed at 922 K (1200 F)

All of these materials were in the form of wrought barstock. Material was purchased from commercial sources and had standard processing and heat treatments. Acceptance tests conducted on the material as-received verified that purchasing specifications were met.

Results

Comparisons of various tests or properties versus hydrogen degradation are made in Tables 2 and 3. These comparisons are made from tests conducted in 34.5-MN/m^2 (5000-psig) gaseous helium or hydrogen for all alloys discussed here. Nickel-base and iron-base alloys were tested at 300 K (80 F) and 951 K (1250 F), and the titanium-base alloys were tested at 300 K (80 F) and 366 K (200 F). The test data are given in Tables 4 and 5.[4] Typical results are illustrated in Figs. 3 through 6. The following observations are made:

1. The 0.2 percent offset yield and ultimate strengths were not degraded at either temperature for any of the alloys discussed here.

2. The ductility (elongation or reduction in area) at ambient temperature of 300 K (80 F) was degraded for several alloys, and these same alloys also exhibited degradation when evaluated by other tests, such as notched ($K_t = 8.0$) tensile, strain-controlled low-cycle fatigue, load-controlled high-cycle fatigue, or fracture toughness. This suggests that if the ambient

---

[3] Followed by stabilization and age treatments.

[4] Test data are presented in customary units only.

TABLE 2—*Hydrogen degradation*[a] *of nickel, iron, and titanium alloys evaluated by various tests at 34.5-MN/m*^{2} *(5000-psig) pressure and 300 K (80 F).*

Type of Test	Inco 718		Alloys					
			Nickel-Base	Hastelloy	Iron-Base		Titanium-Base	
	1227 K (1750 F)[b]	1311 K (1900 F)[b]	Inco 625	X	A286	AISI 347	6–4	A110
Tensile								
0.2% Yield	ND	ND	ND	ND	ND	ND	ND	ND
Ultimate	ND	ND	ND	ND	ND	ND	ND	ND
Reduction of area	D	D	D	ND	ND	ND	D	D
Elongation	D	ND	D	ND	ND	ND	D	D
Notch tensile ultimate tensile strength ($K_t = 8$)	D	ND	ND	ND	ND	ND	D	D
Low-cycle fatigue (strain controlled)	D	D	D	D	ND	ND	ND	D
High-cycle fatigue (load controlled)	D	D	...	...	...	ND	...	ND
Fracture toughness	D	ND	ND	...	ND	ND	ND	ND

[a] Degradation (D) = hydrogen reduced the property or life (in helium) greater than 10%, or $D = \frac{H_e - H_2}{H_e} \times 100$ is >10%.

Negligible degradation (ND) = hydrogen reduced the property or life (in helium) less than 10%.

[b] Solution heat treatment temperature.

TABLE 3—*Hydrogen degradation*[a] *of nickel, iron, and titanium alloys evaluated by various tests at* $34.5\text{-}MN/m^2$ *(5000-psig) pressure and elevated temperature.*

Type of Test	Alloys							
	Inco 718		Nickel-Base 951 K (1250 F)		Iron-Base 951 K (1250 F)		Titanium-Base 366 K (200 F)	
	1227 K (1750 F)[b]	1311 K (1900 F)[b]	Inco 625	Hastelloy X	A286	AISI 347	6–4	A110
Tensile								
0.2% yield	ND	ND	ND	ND	ND	ND	ND	ND
Ultimate	ND	ND	ND	ND	ND	ND	ND	ND
Reduction of area	ND	ND	ND	ND	D	ND	D	D
Elongation	ND	ND	ND	ND	D	ND	D	D
Notched tensile ultimate tensile strength ($K_t = 8$)	ND	ND	ND	ND	ND	ND	...	D
Low-cycle fatigue (strain controlled)	ND	D	D	...	ND	ND	ND	D
High-cycle fatigue (load controlled)	D	D	...	...	...	...	...	...
Creep	D	D	D	...	D	ND	D	D
Rupture	D	D	D	...	D	ND	D	D

[a] Degradation (D) = hydrogen reduced the property or life (in helium) greater than 10%, or $D = \frac{H_e - H_2}{H_e} \times 100$ is 10%.

Negligible degradation (ND) = hydrogen reduced the property or life (in helium) less than 10%.

[b] Solution heat treatment temperature.

TABLE 4—*Room temperature (80 F) tensile properties of materials in 5000-psig pressure gaseous environment.*

					Test Results			
	Test Conditions		Load Rate, in./min		Strength		Ductility	
Material	Stress Concentration Factor	*Environment*	0 Load to *Yield*	Yield to *Ultimate*	*Yield, ksi*	*Ultimate, ksi*	EL,[a] %	RA,[b] %
AMS 5662	smooth	helium	0.050	0.100	158.7	196.2	23.5	35.8
(Inco 718)	smooth	helium	0.050	0.100	161.2	201.2	16.0	17.5
1750 F solution	smooth	helium	0.050	0.100	161.3	201.5	23.5	35.3
	8.0	helium		0.100		254.2		
	8.0	helium		0.100		247.7		
	smooth	hydrogen	0.050	0.100	151.1	180.1	5.5	9.4
	smooth	hydrogen	0.050	0.100	157.2	182.0	4.5	10.9
	8.0	hydrogen		0.100		114.1		
	8.0	hydrogen		0.100		154.2		
	8.0	hydrogen		0.100		133.6		
AMS 5662	smooth	helium	0.050	0.100	157.2	189.5	26.0	51.3
(Inco 718)	smooth	helium	0.050	0.100	155.6	186.2	25.5	49.9
1900 F solution	8.0	helium		0.100		302.8		
	8.0	helium		0.100		302.2		
	smooth	hydrogen	0.050	0.100	158.3	186.2	21.5	40.3
	smooth	hydrogen	0.050	0.100	156.4	185.6	23.5	36.6
	8.0	hydrogen		0.100		277.2		
	8.0	hydrogen		0.100		291.4		
	8.0	hydrogen		0.100		288.1		
AMS 5666	smooth	helium	0.050	0.100	92.1	147.7	46.5	62.5
(Inco 625)	smooth	helium	0.050	0.100	75.8	142.9	48.0	61.5
	8.0	helium		0.100		173.0		
	8.0	helium		0.100		190.2		

	smooth	hydrogen	0.050	0.100	102.2	140.5	23.0	30.1
	smooth	hydrogen	0.050	0.100	99.2	142.3	23.0	30.1
	8.0	hydrogen		0.100		175.2		
	8.0	hydrogen		0.100		176.8		
	8.0	hydrogen		0.100		181.8		
AMS 5735 (A286)	smooth	helium	0.050	0.100	104.4	151.5	28.5	45.5
	smooth	helium	0.050	0.100	109.4	151.5	27.0	47.5
	8.0	helium		0.100		222.8		
	8.0	helium		0.100		225.5		
	smooth	hydrogen	0.050	0.100	110.2	155.8	28.5	46.4
	smooth	hydrogen	0.050	0.100	111.2	155.6	27.0	45.8
	8.0	hydrogen		0.100		225.4		
	8.0	hydrogen		0.100		224.3		
	8.0	hydrogen		0.100		225.4		
AMS 5646 (AISI 347)	smooth	helium	0.050	0.100	69.7	102.0	38.0	70.1
	smooth	helium	0.050	0.100	63.9	99.4	36.5	70.5
	8.0	helium		0.100		170.0		
	8.0	helium		0.100		173.3		
	smooth	hydrogen	0.050	0.100	64.6	109.7	41.5	71.1
	smooth	hydrogen	0.050	0.100	67.4	108.3	39.0	70.4
	8.0	hydrogen		0.100		166.8		
	8.0	hydrogen		0.100		172.1		
	8.0	hydrogen		0.100		127.8		
AMS 5754 (Hastelloy X)	smooth	helium	0.050	0.100	48.6	106.7	54.0	63.0
	smooth	helium	0.050	0.100	44.6	103.0	53.5	62.8
	8.0	helium		0.100		127.7		
	8.0	helium		0.100		163.8		
	smooth	hydrogen	0.050	0.100	48.6	105.5	51.5	60.5
	smooth	hydrogen	0.050	0.100	50.1	105.3	54.5	66.4
	8.0	hydrogen		0.100		124.0		
	8.0	hydrogen		0.100		125.5		
	8.0	hydrogen		0.100		130.8		
	smooth	helium	0.050	0.100	145.4	151.1	15.0	45.4

TABLE 4—(Continued)

	Test Conditions		Load Rate, in./min		Test Results			
					Strength		Ductility	
Material	Stress Concentration Factor	Environment	0 Load to Yield	Yield to Ultimate	Yield, ksi	Ultimate, ksi	EL,[a] %	RA,[b] %
AMS 4928	smooth	helium	0.050	0.100	146.7	151.0	15.0	44.0
(Ti-6Al-4V)	8.0	helium		0.100		205.3		
	8.0	helium		0.100		209.5		
	smooth	hydrogen	0.050	0.100	144.1	147.8	13.5	34.0
	smooth	hydrogen	0.050	0.100	145.7	152.7	13.5	37.8
	8.0	hydrogen		0.100		189.7		
	8.0	hydrogen		0.100		183.5		
	8.0	hydrogen		0.100		178.8		
AMS 4926	smooth	helium	0.050	0.100	115.6	132.5	20.0	44.6
(A110)	smooth	helium	0.050	0.100	130.3	133.1	18.5	43.9
	8.0	helium		0.100		204.9		
	8.0	helium		0.100		197.2		
	smooth	hydrogen	0.050	0.100	121.0	134.8	14.5	35.4
	smooth	hydrogen	0.050	0.100	133.6	138.9	16.5	31.4
	8.0	hydrogen		0.100		158.2		
	8.0	hydrogen		0.100		173.3		
	8.0	hydrogen		0.100		167.1		

[a] Elongation in 1 in.

[b] Reduction of area.

TABLE 5—*Elevated temperature tensile properties of materials in 5000-psig pressure gaseous environment.*

						Test Results			
	Test Conditions			Load Rate, in./min		Strength		Ductility	
Material	Test Temperature, deg F	Stress Concentration Factor	Environment	0 Load to Yield	Yield to Ultimate	Yield, ksi	Ultimate ksi	EL,[a] %	RA,[b] %
AMS 5662	1250	smooth	helium	0.050	0.100	136.7	155.9	20.0	19.7
(Inco 718)	1250	smooth	helium	0.050	0.100	131.3	154.3	25.0	47.5
1750 F solution	1250	8.0	helium		0.100		202.5		
	1250	8.0	helium		0.100		210.5		
	1250	smooth	hydrogen	0.050	0.100	137.5	150.3	22.0	46.8
	1250	smooth	hydrogen	0.050	0.100	136.0	155.5	21.5	34.9
	1250	8.0	hydrogen		0.100		187.5		
	1250	8.0	hydrogen		0.100		196.5		
	1250	8.0	hydrogen		0.100		199.1		
AMS 5662	1250	smooth	helium	0.050	0.100	134.9	150.3	17.5	31.8
(Inco 718)	1250	smooth	helium	0.050	0.100	141.3	150.4	11.5	18.0
1900 F solution	1250	8.0	helium		0.100		190.0		
	1250	8.0	helium		0.100		196.6		
	1250	smooth	hydrogen	0.050	0.100	133.3	150.3	17.0	27.0
	1250	smooth	hydrogen	0.050	0.100	134.5	151.8	15.5	19.6
	1250	8.0	hydrogen		0.100		176.2		
	1250	8.0	hydrogen		0.100		174.7		
	1250	8.0	hydrogen		0.100		180.8		
AMS 5666	1250	smooth	helium	0.050	0.100	75.3	116.9	62.5	70.4
(Inco 625)	1250	smooth	helium	0.050	0.100	71.7	120.8	59.0	66.2
	1250	8.0	helium		0.100		150.0		
	1250	8.0	helium		0.100		135.8		
	1250	smooth	hydrogen	0.050	0.100	72.7	119.1	57.5	64.2

TABLE 5—(Continued)

Material	Test Conditions			Load Rate, in./min		Test Results			
						Strength		Ductility	
	Test Temperature, deg F	Stress Concentration Factor	Environment	0 Load to Yield	Yield to Ultimate	Yield, ksi	Ultimate ksi	EL,[a] %	RA,[b] %
	1250	smooth	hydrogen	0.050	0.100	77.4	127.4	52.5	55.9
	1250	8.0	hydrogen		0.100		146.0		
	1250	8.0	hydrogen		0.100		147.4		
	1250	8.0	hydrogen		0.100		148.0		
AMS 5735 (A286)	1250	smooth	helium	0.050	0.100	104.6	119.0	25.5	52.1
	1250	smooth	helium	0.050	0.100	104.0	122.4	29.0	54.5
	1250	8.0	helium		0.100		166.5		
	1250	8.0	helium		0.100		182.0		
	1250	smooth	hydrogen	0.050	0.100	106.7	118.9	22.0	44.6
	1250	smooth	hydrogen	0.050	0.100	122.3	109.3	25.0	46.6
	1250	8.0	hydrogen		0.100		173.5		
	1250	8.0	hydrogen		0.100		184.5		
	1250	8.0	hydrogen		0.100		186.2		
AMS 5646 (AISI 347)	1250	smooth	helium	0.050	0.100	57.8	60.4	24.5	66.3
	1250	smooth	helium	0.050	0.100	57.4	59.6	25.0	68.1
	1250	8.0	helium		0.100		104.0		
	1250	8.0	helium		0.100		102.7		
	1250	smooth	hydrogen	0.050	0.100	54.7	58.8	25.5	68.3
	1250	smooth	hydrogen	0.050	0.100	60.3	64.2	25.0	66.7
	1250	8.0	hydrogen		0.100		101.4		
	1250	8.0	hydrogen		0.100		100.0		
	1250	8.0	hydrogen		0.100		99.8		

AMS 5754 (Hastelloy X)	1250	smooth	helium	0.050	0.100	35.2	82.1	53.0	57.5
	1250	smooth	helium	0.050	0.100	33.1	77.5	53.0	57.6
	1250	8.0	helium		0.100		90.2		
	1250	8.0	helium		0.100		91.2		
	1250	smooth	hydrogen	0.050	0.100	33.9	80.8	51.5	58.2
	1250	smooth	hydrogen	0.050	0.100	34.1	80.3	51.0	48.9
	1250	8.0	hydrogen		0.100		88.6		
	1250	8.0	hydrogen		0.100		90.8		
	1250	8.0	hydrogen		0.100		91.0		
AMS 4928 (Ti 6–4)	200	smooth	helium	0.050	0.100	138.3	152.5	15.0	46.6
	200	smooth	helium	0.050	0.100	139.2	147.6	16.0	47.0
	200	8.0	helium		0.100		207.5		
	200	8.0	helium		0.100		207.5		
	200	8.0	helium		0.100		206.5		4.7
	200	smooth	hydrogen	0.050	0.100	141.0	146.3	10.5	22.6
	200	smooth	hydrogen	0.050	0.100	138.5	144.7	12.0	31.4
	200	8.0	hydrogen		0.100		209.0		
	200	8.0	hydrogen		0.100		184.4		
	200	8.0	hydrogen		0.100		183.3		
AMS 4926 (A110)	200	smooth	helium	0.050	0.100	111.8	127.6	20.5	45.4
	200	smooth	helium	0.050	0.100	113.6	132.7	17.5	46.6
	200	8.0	helium		0.100		190.5		
	200	8.0	helium		0.100		185.3		
	200	8.0	helium		0.100		187.0		
	200	smooth	hydrogen	0.050	0.100	114.4	126.0	14.0	20.8
	200	smooth	hydrogen	0.050	0.100	112.5	130.0	17.0	31.9
	200	8.0	hydrogen		0.100		160.2		
	200	8.0	hydrogen		0.100		168.0		
	200	8.0	hydrogen		0.100		175.5		

---

[a] Elongation in 1 in.

[b] Reduction of area.

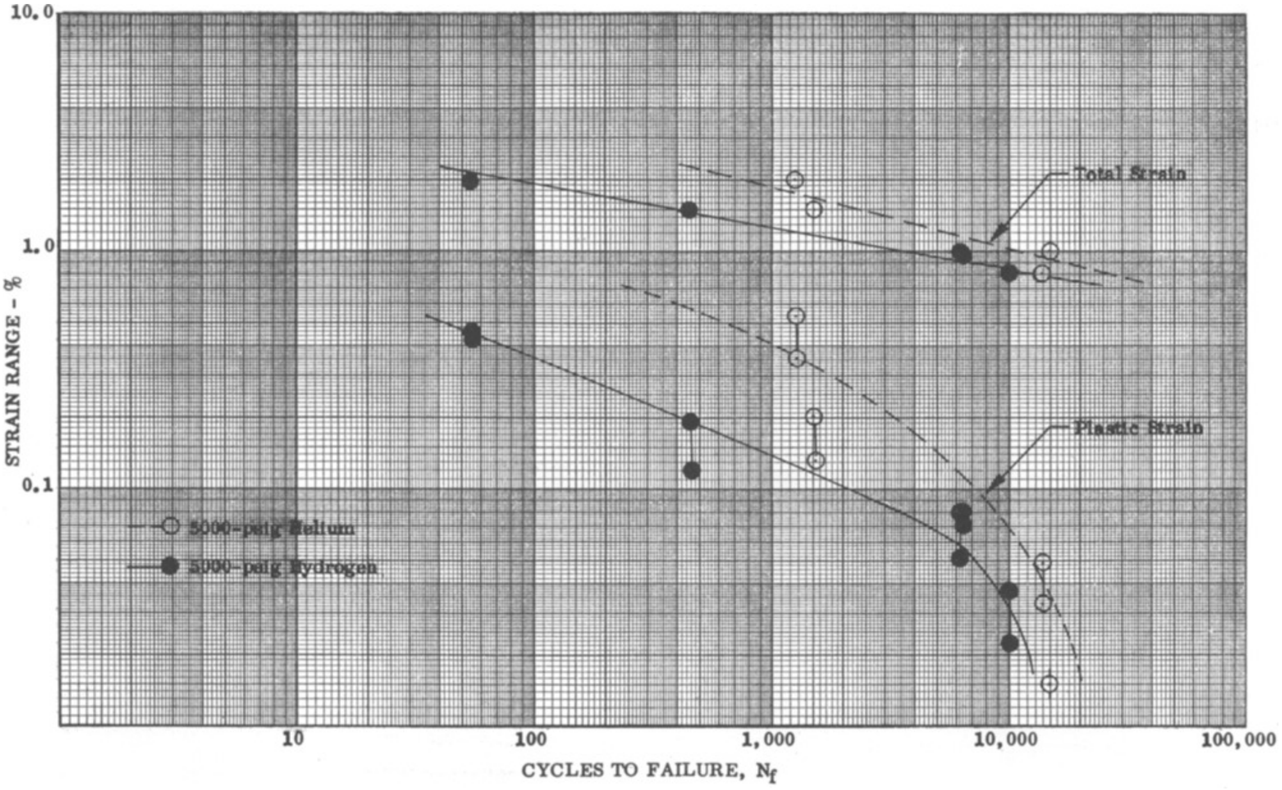

FIG. 3—*Typical effect of low-cycle fatigue life.*

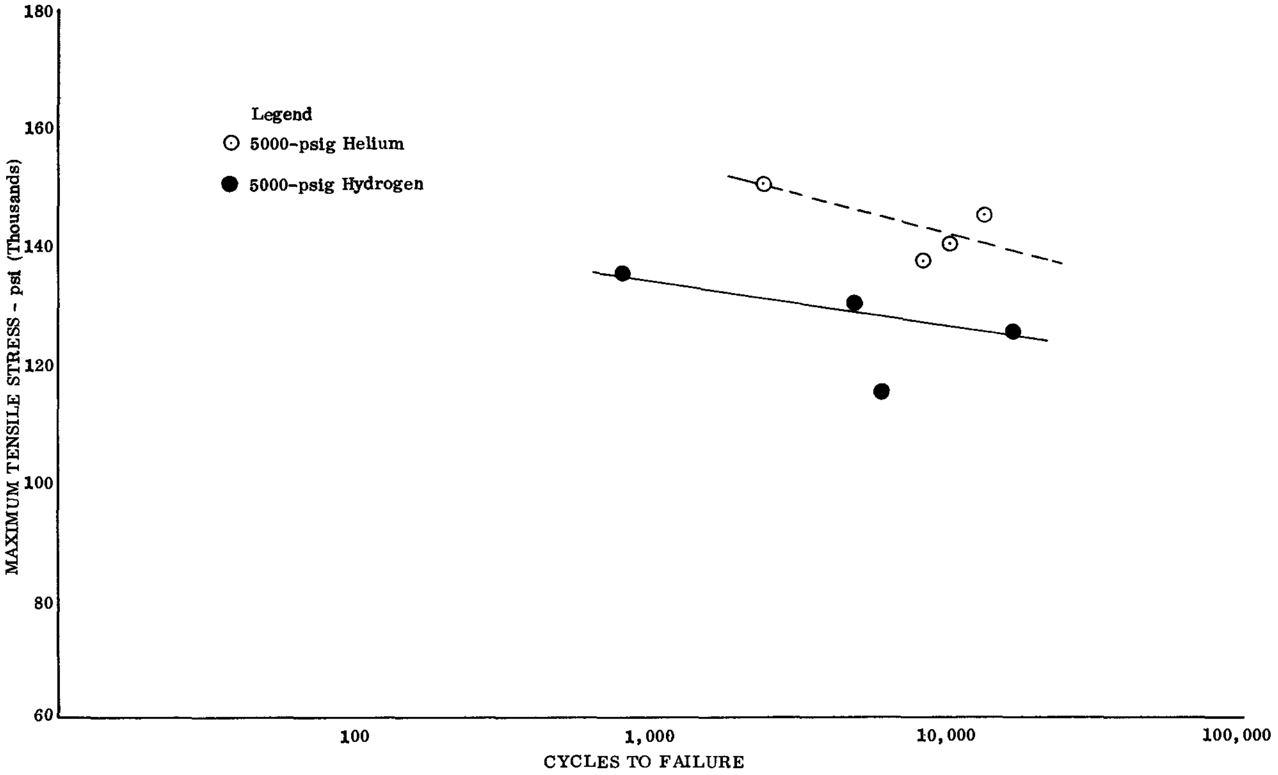

FIG. 4—*Typical effect of high-cycle fatigue life.*

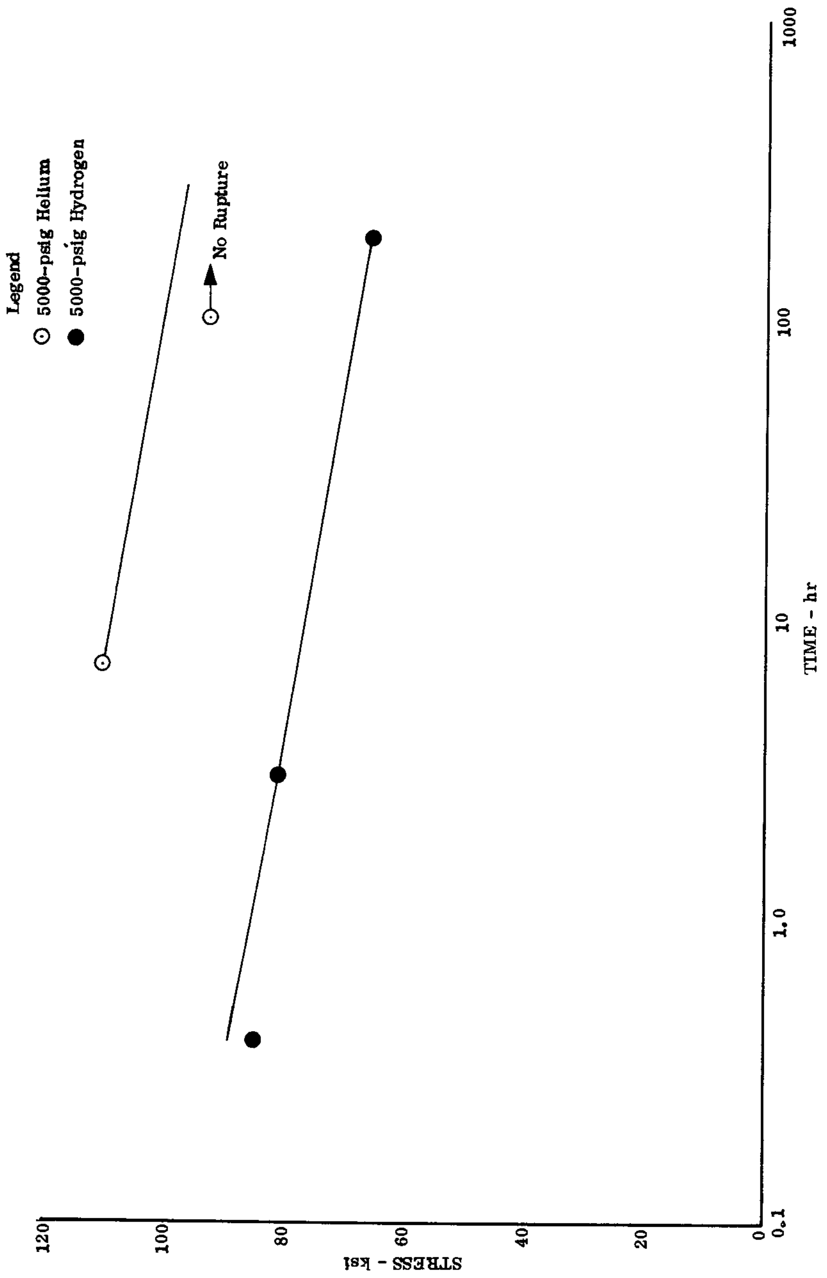

FIG. 5—*Typical degradation of stress rupture.*

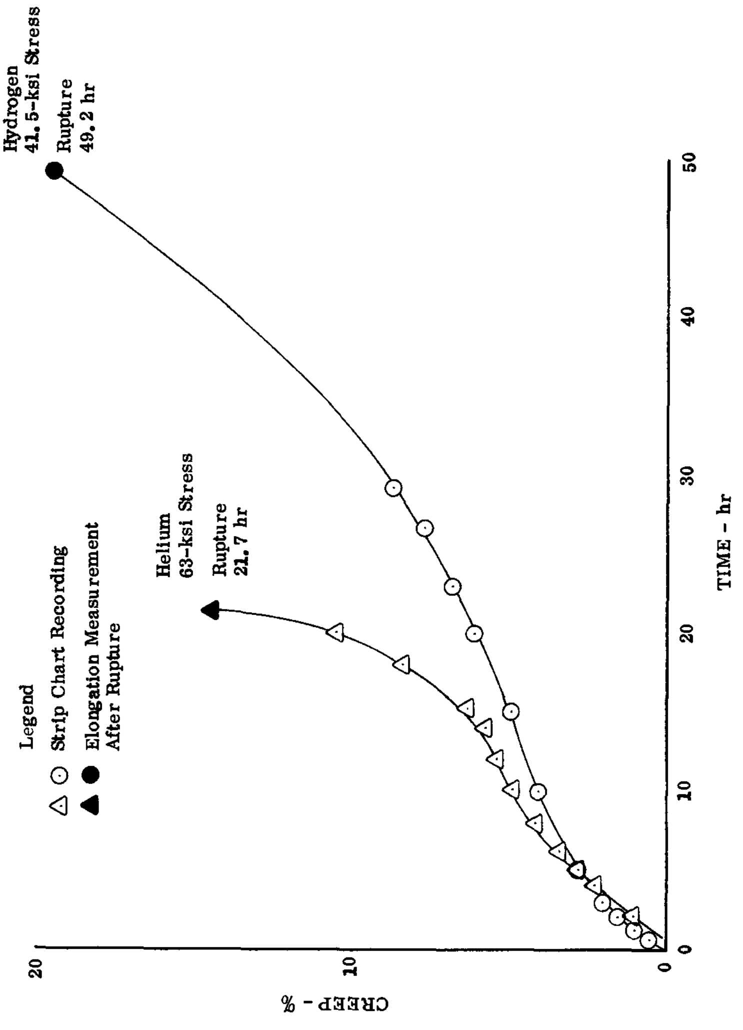

FIG. 6—*Typical degradation of creep-stress rupture.*

temperature (300 K [80 F]) smooth tensile ductility is degraded, then other properties will also show degradation. This is true for all alloys tested except Hastelloy X, which was not degraded in any tensile property, but was degraded in the low-cycle fatigue test. The iron-base alloys, A286 and AISI 347, were not degraded in ductility, nor were they degraded in the other tests.

3. A similar comparison between tensile ductility at elevated temperatures of 951 K (1250 F) for the nickel-base and iron-base alloys and 366 K (200 F) for the titanium-base alloys and the other tests does not yield the same observations. The nickel-base alloys, Inco 718 and Inco 625, were not degraded in any of the tensile properties at these temperatures; however, they were degraded when evaluated with other tests such as low- and high-cycle fatigue and creep and rupture.

4. It is known that the material microstructure has a significant effect upon the degree of gaseous hydrogen degradation. The degree of degradation depends on the type of test used. This is illustrated by the different response of the two heat treatments of Inco 718 in the different tests. This material was of the same heat, the different microstructures resulting primarily from the two solution heat treat temperatures. This effect has also been documented on Inco 718 low-cycle fatigue properties in Ref *2*, where a fine grain, recrystallized structure had orders of magnitude greater low-cycle fatigue life at 1 percent total strain, 34.5-MN/m^2 (5000-psi) gaseous hydrogen, and ambient temperatures of 300 K (80 F) than did coarse-grained, predominantly unrecrystallized structure.

Conclusions

The authors' purpose in conducting these tests was to establish the degree of degradation in mechanical properties due to the hydrogen environment and to provide design information for these conditions. The materials are those that are proposed for use in hydrogen-fueled spacecraft applications. No specific attempt was made to screen materials simply for environmental hydrogen degradation, however; the following conclusions can be made:

1. No one type of test will always determine the susceptibility or the degree of susceptibility to hydrogen environment embrittlement or degradation.

2. If the ambient temperature 300 K (80 F) smooth tensile ductility (elongation or reduction in area) is degraded in hydrogen, then some other properties will be degraded.

3. However, if the ambient temperature 300 K (80 F) smooth tensile ductility is not degraded, it does not mean that other properties are not degraded. (Refer to Hastelloy X.)

4. Tests that expose the material to high stresses or plastic strain, and

time, such as fatigue and creep-rupture tests, are the most severe tests for hydrogen degradation susceptibility.

Discussion and Recommendations

The authors believe that no one test will provide enough data to evaluate the degree of hydrogen degradation to be used in analyzing a structure from a design-material-life standpoint. For the individual responsible for a structure that must operate in a hydrogen environment, there can be no substitute for a test that will supply data appropriate to the particular loading spectrum expected. In this case, a test that simply indicates susceptibility to hydrogen degradation is of no real value; the test must also provide some measure of the degree of degradation on a meaningful property. Considering the many different types of tests discussed herein and others now being used to evaluate the susceptibility to hydrogen environment embrittlement, and considering testing variables, such as specimen size, loading conditions, temperature, pressure, reproducibility, economics, and, especially, comparability of data, it is recommended that the smooth tension test be used to determine the susceptibility to hydrogen environment degradation. This test may be performed at ambient temperature 300 K (80 F) and in low-pressure hydrogen. The yield and ultimate strength will probably not indicate degradation; however, the ductility, easily measured after the test is completed, will serve as a guide to the susceptibility to hydrogen degradation. This type of test is one of the least expensive to conduct and produces results easily comparable to the work of other investigators.

The hydrogen pressure level is an important variable and will influence the results. Also the strain or loading rate is very important and these two variables should be further evaluated before this type test is standardized. It is believed that a much slower strain rate, especially in the plastic range, should be used in a standardized tension test than that used in conducting the tests reported here.

Acknowledgments

The authors wish to express their appreciation to the many people of the Pratt & Whitney Aircraft Florida Research and Development Center, Materials Development Laboratory, who formed the Project Group that conducted this testing under the cognizance of W. B. McPherson, National Aeronautics and Space Administration, Materials Division, Marshall Space Flight Center, Alabama.

References

[*1*] VanWanderham, M. C. and Harris, J. A., Jr., "Properties of Materials in High Pressure Hydrogen at Cryogenic, Room, and Elevated Temperatures," Contract NAS8-26191, Annual Report, PWA FR-4566, 30 June 1971.

[2] VanWanderham, M. C. and Harris, J. A., Jr., "Low Cycle Fatigue of Metals in High Pressure Gaseous Hydrogen at Cryogenic Ambient and Elevated Temperatures," presented to the 1971 WESTEC Conference, Los Angeles, Calif.

[3] Penny, R. K., Ellison, E. G., and Webster, G. A., *Materials Research and Standards*, Vol. 6, No. 2, Feb. 1966, p. 76.

[4] Harris, J. A., Jr., Schratt, J. F., and VanWanderham, M. C., "Creep-Rupture Properties of Materials in High Pressure Gaseous Hydrogen at Elevated Temperatures," presented to Third National SAMPE Technical Conference, Oct. 1971, Huntsville, Ala.

[5] Peterson, R. E., *Stress Concentration Design Factors*, Wiley, New York, 1953.

J.-P. Fidelle,[1] *R. Bernardi,*[1] *R. Broudeur,*[1] *C. Roux,*[1] *and M. Rapin*[1]

Disk Pressure Testing of Hydrogen Environment Embrittlement

REFERENCE: Fidelle, J.-P., Bernardi, R., Broudeur, R., Roux, C., and Rapin, M., "**Disk Pressure Testing of Hydrogen Environment Embrittlement,**" *Hydrogen Embrittlement Testing, ASTM STP 543*, American Society for Testing and Materials, 1974, pp. 221–253.

ABSTRACT: The rupture appearances and pressures are compared for clamped disks, biaxially stressed to rupture under upward increasing pressures of helium or of an embrittling fluid such as gaseous hydrogen isotopes. Usually the downward surface is available for observation during the test in progress, but it can be exposed to a second embrittling medium. Factors studied include: (*a*) for the materials; chemistry (aluminum, cobalt, chromium, copper, iron, nickel, platinum, titanium, uranium, zirconium, etc., base), surface condition, thermomechanical processing, welding, etc., (*b*) for the testing conditions (−196 to −450°C), H_2 pressure, purity, pressure increase rate, etc. Low-cycle fatigue and delayed failure tests can also be conducted and discontinuous cracking monitored by various techniques, especially permeation.

The disk pressure test (DPT) can be used for selection and quality control of bulk materials, protective coatings against hydrogen environment embrittlement (HEE), and their processing. Materials selection is made according to screening tests of increasing severity. The DPT shows evidence of other causes of embrittlement and their synergistic effects with HEE, which is quite important. Other advantages of DPT, such as sensitivity, versatility, rapidity, simplicity of operation and maintenance, safety, low cost of specimens and equipment, etc., are outlined and compared to other methods.

KEY WORDS: hydrogen embrittlement, pressure, biaxial stresses, hydrogen, purity, temperature, strain rate, delayed failure, crack propagation, permeability, alloys, coatings, screenings, quality control, materials selection

Basically, the disk pressure test (DPT) is the same test as that used for testing internal hydrogen embrittlement (IHE) [*1*],[2] but, instead of comparing unembrittled to embrittled materials, here we compare materials under nonembrittling and embrittling conditions.

---

[1] CEA, Centre d'Etudes de Bruyères-le-Châtel, France.

[2] The italic numbers in brackets refer to the list of references appended to this paper.

The idea of the test first came after failures of high-strength (HS) steel pressure vessels which cracked during pressurization under hydrogen gas (GH_2) pressures five to ten times smaller than the bursting pressures when pressurized with helium. As effects of the same order of magnitude could be observed on plates also, such a geometry was found appealing to start a materials evaluation program using much cheaper specimens than pressure vessels, even miniaturized.

Most experiments have been carried out applying a gaseous pressure of hydrogen or of its isotope deuterium upward to a disk, but we have also used mixtures of gases or liquids. Other experiments have also been made recently, placing the aggressive fluid (a liquid or GH_2) on the upper surface of the disk and stressing by means of helium pressure on the lower surface.

Before any experiment, the test line is pumped and flushed several times by helium under 20 bars[3] then by GH_2 when it has to be the testing medium.

General Equipment and Specimens

Table 1 summarizes the general equipment and specimens. The basic cell has been described previously [*1*, *2*] ,the other cells will be described with the tests for which they have been used. They are made of austenitic stainless steel, which is A286 in case of the low- and elevated-temperature cells. Each cell is interchangeable within the test line and does not require any change in the remainder of the equipment. The general equipment is the same one described previously, but an additional storage tank for hydrogen under high pressure, up to 2 000 bars. GH_2 is 99.995 percent pure with $H_2O \leq 5$ vpm, $O_2 \leq 5$ vpm.

Unless the influence of surface condition is studied especially, the disks are generally lapped. On a trial basis, the most frequently used thickness, 0.75 mm (30 mils), has been found to be a good compromise between easy, reproducible machinability, sensitivity, and test rapidity. Reproducible, thin specimens are more difficult to machine while thicker specimens need longer test times due to the higher rupture pressures and the need for reducing the pressure increase rate in order to keep pace with the rate of hydrogen entry.

At room temperature (RT) it is possible to test up to 20 standard disks a day.

Appearances of the Ruptured Disks

Of course, it depends on many factors. In the case of relatively homogeneous materials we may mention: chemistry, thermomechanical treatments, surface condition, hydrogen activity (pressure and purity in case

---

[3] 1 bar = 0.987 atm = 14.51 psi.

TABLE 1—*Various cells and specimens used.*[a]

Cell	Specimen Sizes, mm		Present Temperature Range	Present Maximum Pressure
	Diameter	Thickness		
Basic	40 to 58	0.2 to 1.8	20 to 180° C	1600 bars at RT and below; 600 bars at 400° C
Low temperature	40 to 58	0.2 to 1.8	−196 to 180° C	
Elevated temperature	40 to 58	0.2 to 1.8	20 to 450° C (planned to 600° C)	
Low-cycle fatigue	40 to 58	0.2 to 1.8	can be done on the other cells	
Mini	8	0.15 to 0.4	20 to 180° C	1600 bars at RT
Large	133	0.5 to 5	20 to 180° C	

[a] 58-mm-diameter and 0.75-mm-thick disks will be used hereafter unless stated otherwise.

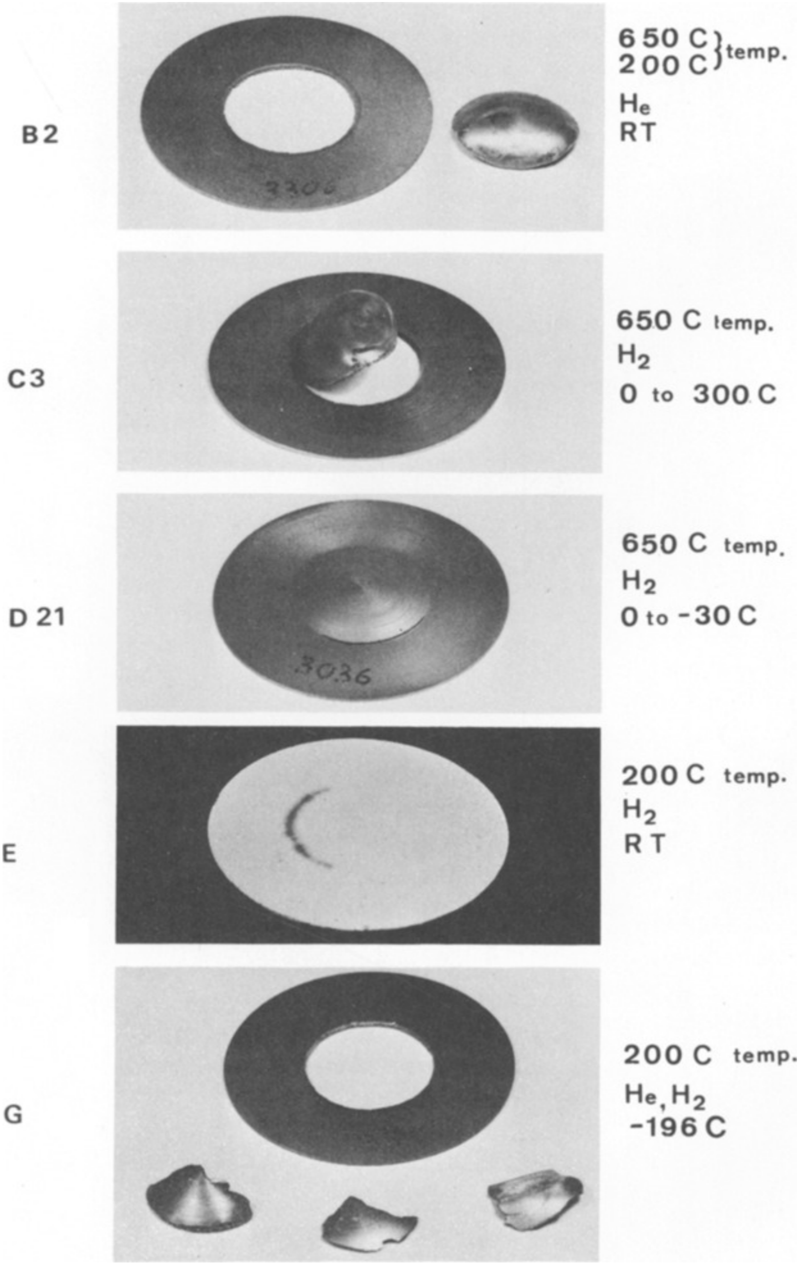

FIG. 1—*Appearance of 35NCD16 disks tested under various conditions.*

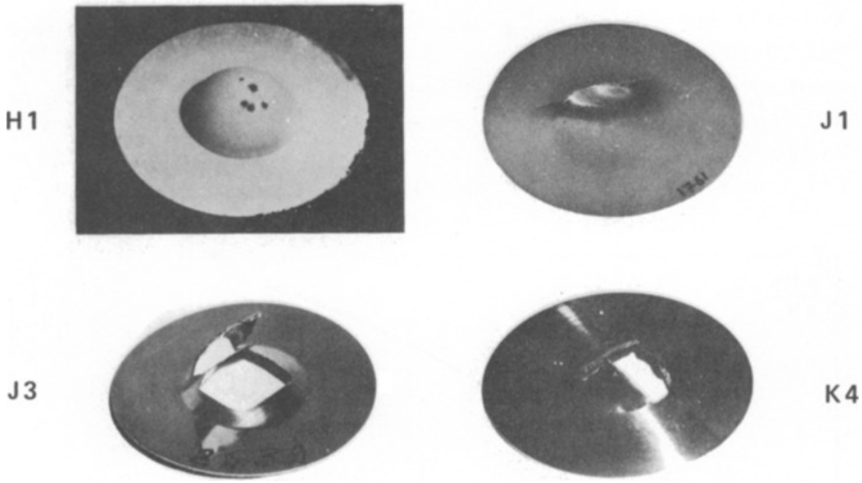

FIG. 2—*Rupture appearance on heterogeneous materials*

of GH_2), temperature, loading rate (pressure increase rate), etc. Most tests have been run with the pressure and the eventual embrittling medium on the same side (about 6 000 tests in seven years, covering 70 materials in various conditions). From them it has been possible to rationalize a chart of growing embrittlement appearances, including 14 basic cases. Figure 1 gives instances in the case of 35NCD16 (0.41C, 4.28Ni, 1.97Cr, 0.53Mo) steel, tempered at 200° C (tensile strength) = 194.3 kg/mm^2) or 650° C (TS = 72.7 kg/mm^2). Embrittlement grows from B2(He) to E(H_2 – 200° C tempering) as the plastic strain at rupture decreases. *G* indicates low temperature embrittlement, which is moderate owing to the nickel content of this steel.

Materials with important heterogeneities can influence rupture appearances in a way which bring them into evidence (Fig. 2).

H1: cupola plus tiny holes at the $M_{23}C_6$ precipitates, matrix interfaces on 870° C sensitized Type 304, He, H_2

J1: cracking at the anchorage plus cracks parallel to the rolling direction on HS carbon steel, H_2

J3: cupola plus ruptures parallel to the crossed rolling directions on cold-rolled Pt-25Ir alloy, He, H_2

K4: ruptures parallel and normal to the weld axis of diametrally welded U-1.5Mo alloy, H_2

Influence of the Nature of Materials (testing materials for relative hydrogen gas embrittlement (HGE) susceptibility)

Materials are screened means for tests of increasing severity. Figure 3 gives results of the first screening test for various materials. All of them were 0.75 mm thick, except nickel (0.40 mm), IN 744 (0.50 mm), ground CG 27 (0.85 mm), and lapped plus polished CG 27 (0.82 mm). The common pressure increase rate, 65 bars/min, was slow enough to provide sufficient sensitivity and sort materials into three main preliminary categories (they include a few more materials which could not be mentioned on Fig. 3 due to lack of space).

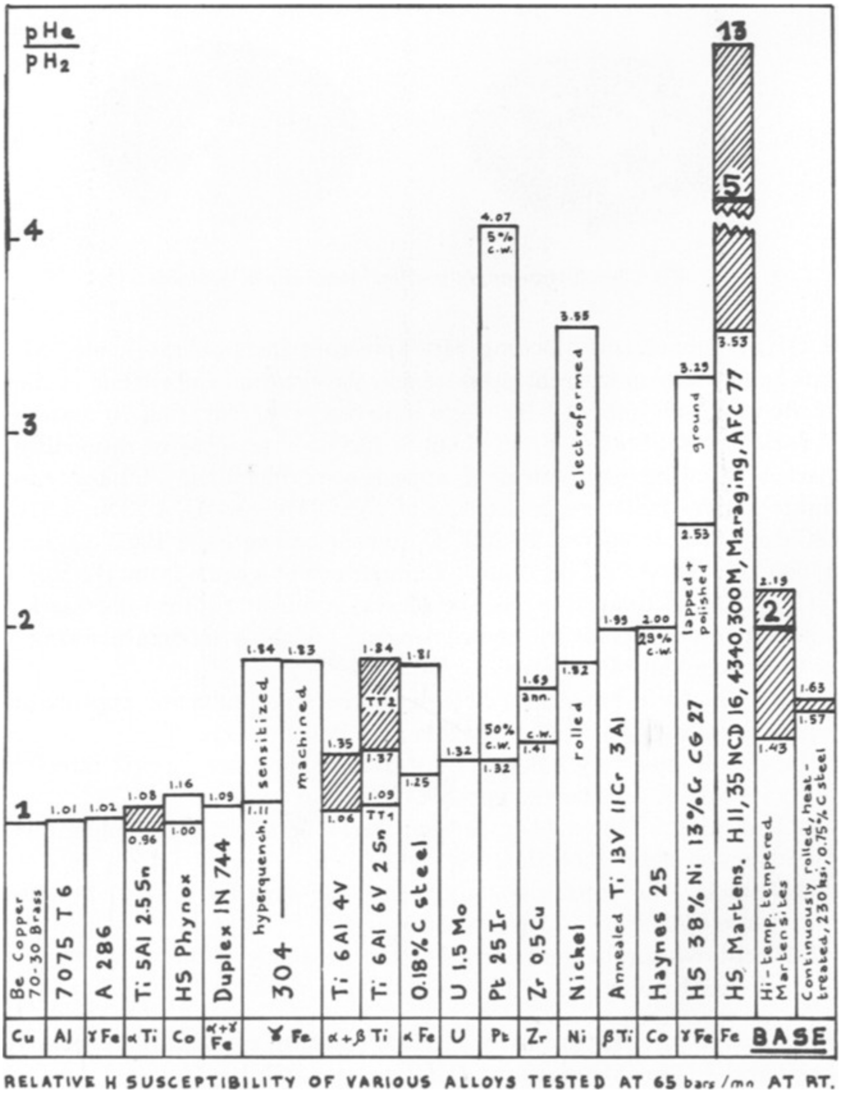

FIG. 3—*Relative hydrogen susceptibility of various metals and alloys tested at 65 bars/min at room temperature.*

TABLE 2—*Composition in weight percent.*

	C	Co	Cr	Ni	Fe	Mo	Mn	Si	W	La
HS 188	0.08	39.6	22	22	1.5		0.75		14	0.05
Phynox	0.125	39.49	19.75	17.26	15.33	5.64	1.28	0.23		

Little or No Sensitivity

1. *Aluminum base:* 7075-T6.
2. *Cobalt base:* Haynes 188 (HS 188) and French alloy Phynox.

Compositions in weight percent mechanical properties and more detailed DPT results are given for these alloys in Tables 2 and 3. Phynox is hardened twice: by cold work and ordering and thermal treatment of the cold-worked material.

Selection criterions are successively: (*a*) low hydrogen embrittlement (low $p\text{He}/p\text{H}_2$), (*b*) high biaxial resistance (high $p\text{He}$), and (*c*) high yield point (YP). Materials 2 and 3 appear the most interesting ones. Further selection between them will be made on the basis of: (*a*) more severe HGE tests and (*b*) other properties than resistance to HGE. It will be noted that cold work decreases HGE, while raising the YP, contrary to what is observed, for instance, on steels when YP is raised by thermal treatment at lower temperatures. However, too much cold work detrimentally affects the biaxial strength of the material.

3. *Copper base:* Beryllium copper [*2*], 70–30 brass.
4. *Iron base:* Types 304, 316, 310 austenitic steels.
   AGT (13Ni, 13Cr), X 203 (21Cr, 20Ni, 20Co) austenitic steels.
   A286 age hardened austenitic steel [*2*].
   IN 744 duplex austeno-ferritic steel (26Cr, 6.5Ni).
   Type 430 ferritic steel.

Solution treated and quenched Type 304 is embrittled very little during the regular DPT: $p\text{He}/p\text{H}_2 = 1.11$, which is similar to the ratio $\text{UTS}_{\text{He}}/\text{UTS}_{\text{H}_2} = 1.13$ found by Benson et al [*3*] for notched tension specimens of a similar material tested under 10 000 psi GH_2 and helium. However, machining ([*4*] and Fig. 3) and rolling induce a martensitic transformation which makes the specimens magnetic and also causes a greater sensitivity to hydrogen embrittlement (HE). In rolled 0.33-mm-thick disks, a ratio $p\text{He}/p\text{H}_2 = 4.62$ has been found which approaches that found on HS martensitic steels with similar thicknesses.[4]

Sensitization by holding 700° C for 3 h followed by a slow cooling is

---

[4] Cold work percent = $100 \times (t_o - t_f)/t_o$ where t_o and t_f are the initial and final thicknesses of rolled material.

TABLE 3—*Mechanical properties and disk pressure test results.*

Material		Thermomechanical Treatment		YP, kg/mm^2	TS, kg/mm^2	E, %	pHe, bars	pH$_2$, bars	pHe/pH$_2$
HS 188	1	8.4% CW		93.7	111.2	30.8	987	787	1.24
	2	38.7% CW		131	143.9	11.2	874	760	1.15
Phynox	3	23% CW	+3h 520 C	130	144.1	9.2	860	768	1.12
	4			130	145	9.6	890	717	1.24
	5	36% CW	+7h 520 C	143.5	165.8	6.4	686	547	1.23
	6	46% CW		148.5	199	1.2	330	330	1
	7	23% CW + anneal 10 h at 700 C		54.9	106.7	54.3	980	940	1.04

[a] CW = cold worked. See footnote 4.

known to induce sensitivity to intergranular corrosion. It also causes intergranular hydrogen cracking ([*5*] and Fig. 3).

5. *Titanium base:* Ti-5Al-2.5Sn alloy [*2*].
   Ti-6Al-6V-2Sn ($\alpha + \beta$) alloy, treated 2 h at 860° C, quenched and tempered 4 h at 595° C [*2*].
6. *Zirconium base:* Unalloyed zirconium [*6*].
   Zircaloy 2 (Zr-1.5Sn) [*6*].

Moderate Sensitivity

1. *Cobalt base:* Pure rolled cobalt, $p\text{He}/p\text{H}_2 = 1.29$.
2. *Iron base:* 0.18C ferro-pearlitic steel. However, as this material has a banded structure, the degree of embrittlement depends appreciably on the orientation of the pearlite bands, $p\text{He}/p\text{H}_2$ ranging from 1.83 to 1.25, whether they are perpendicular or parallel to the disk plane: (*a*) fast-quenched and high-temperature tempered martensitic steels and (*b*) continuously rolled and heat treated 230-ksi XC 75 (0.75C) and XC 65 (0.65C) carbon steels. Long sheets of these steels are used for prestressing concrete buildings, around nuclear reactors. (In that instance the (hydrogen environment embrittlement) hazard was that of hydrogen generated by corrosion of steel.) These steels appear less sensitive than the martensitic steels achieving a similar strength level, the only means of thermal treatment [*7*].
3. *Nickel base:* Rolled nickel [*2*].
4. *Platinum base:* 50 percent cold-worked Pt-25Ir alloy.
5. *Titanium base:* T-6Al-4V ($\alpha + \beta$) alloy treated 1 or 2 h at 800° C [*2*].
6. *Uranium base:* U-1.5Mo alloy [*8*].
7. *Zirconium base:* Zr-0.5Cu alloy [*6*].

High or Very High Sensitivity

1. *Cobalt base:* Haynes 25. The solution treated material is quite sensitive to HGE: $p\text{He}/p\text{H}_2 = 2.52$. Cold work decreases HGE, but, unfortunately, too much cold work also severely reduces biaxial resistance.
2. *Chromium base:* 60Cr-40Fe alloy [*2*]. Sigma phase in austenitic, and ferritic steels is not only brittle *per se* but is also hydrogen embrittled.
3. *Iron base:* Medium and high-strength steels and badly processed high-temperature tempered (relatively low-strength) steels.

The wrong processing can be due to: (*a*) Austenitizing at too high temperatures which allows exaggerated grain growth. (*b*) A sluggish quench, which forms brittle upper bainite [*9*] (this needs some ingenuity to avoid in large forgings, such as those used for some large chemical synthesis reactors), (*c*) A sluggish cooling after tempering, which is also a serious matter to avoid in thick specimens, and (*d*) Tempering in the tempered martensite embrittlement temperature range ([*10*] and Fig. 4 on 35NCD16 steel).

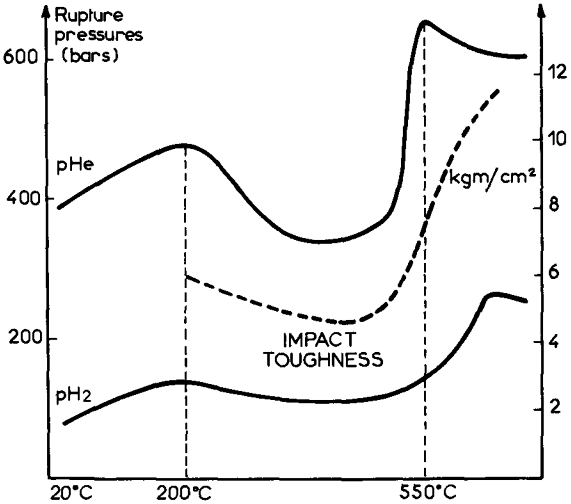

FIG. 4—*Influence of the tempering temperature on the impact strength and rupture pressures* p*He and* pH_2 *of 35NCD16 steel.*

Results of the DPT have been calibrated versus industrial experience, and it has been found that steels with a $p\text{He}/p\text{H}_2$ ratio greater than two were troublesome during their service life, whereas no hydrogen induced delayed failure has been noticed after several years for others with a ratio smaller than two. For instance, steels commonly used for GH_2 storage under pressure have a ratio ranging between 1.40 and 1.55. Attempts to noticeably decrease the weight of commercial cylinders means of higher strength steels (tempered at lower temperatures) have been unsuccessful as the ratio two was exceeded, and accordingly hydrogen induced delayed failures were experienced.

Hydrogen sensitivity of 260 to 280-ksi HS steels is high, ranging from 3.5 to 13; however, maraging steels generally appear more sensitive than less alloyed HS steels (Table 4). 194-ksi CG 27 (38Ni, 12.5Cr, 5.4Mo, and 2.33Ti) [*2*]: this austenitic material is hardened twice: 16 h at 790° C + 16 h at 650°C, and like sensitized Type 304 and Inconel 718 its hydrogen sensitivity is derived from the precipitates at the grain boundaries.

4. *Nickel base:* Electroformed nickel [*2*].
5. *Platinum:* Solution treated + 5 percent cold-worked Pt-25Ir alloy.
6. *Titanium base:* Annealed Ti-13V-11Cr-3Al alloy.

Ti-6Al-6V-2Sn ($\alpha + \beta$) alloy, treated 1 h at 750 °C [*2*].

Then materials with apparently none, little, or moderate sensitivity are further submitted to tests of increasing severity to find out the limits of their resistance within the area of potential utilization. These tests favor crack initiation especially. Then materials which are only initiation

TABLE 4—pHe/pH_2 *ratios for various high-strength steels tested under standard conditions.*

Steel	pHe/pH_2[a]	Number of Batches Tested
230° C tempered 35NCD16	[3.5 to 5.35]	5
200° C tempered 35NCD16	3.85 [4 to 5] 7.18	6
H 11	[3.6 to 5.7]	5
300 M (4340 with Si)	5.24	1
250 maraging	4.7 [6.4 to 7] 12.90	8
AFC 77 (maraging with Cr)	4.7 to 7.85	2

[a] The usual range is between brackets, extreme values are outside 35NCD16 (typically) includes 0.40C, 4.30Ni:, 1.93Cr, 0.51Mo.

resistant but not crack propagation resistant appear affected (for instance titanium alloys), while materials resistant to crack propagation will come out unaffected or slightly affected (70–30 brass, beryllium copper, 7075-T6, Type 310, A286) (Table 5).

Here it is worth to point up that the so-called initiation resistance is not actually a bulk property of materials, since discontinuous crack propagation involves a discontinuous succession of initiations. Initiation resistance is rather due to surface poisoning or surface oxides which prevent hydrogen entry (as in the case of titanium alloys). Therefore, the aim of

TABLE 5—*Initiation or increase of HGE during increased severity tests.*

Material	Tests of Increasing Severity at RT				Test Above RT
	Tests at Low Strain Rates	Delayed Failure	Over-stretching	Low-Cycle Fatigue	
70–30 brass	no		no		
Beryllium copper	no			no	
7075 T-6	no	no	yes moderate		
A286, 310	no	no	no	no	yes moderate
Phynox					yes moderate
Ti-5Al-2.5Sn	yes moderate	yes moderate		yes drastic	yes drastic
Ti-6Al-6V-2Sn		yes drastic		yes drastic	yes drastic
Zircaloy 2	yes moderate				
U-1.5Mo		yes drastic			

increased severity tests is to overcome spurious inhibition effects when they restrain hydrogen entry during the regular DPT.

It can be done several ways: (*a*) by increasing exposure times, (*b*) by increasing temperature, and (*c*) by producing a severe localized plastic deformation (not dissimilar to that taking place at a crack tip).

On the other hand, it is possible to take advantage of the spurious inhibition effects when their effectiveness and reproducibility is improved well enough to afford a consistent protection against HGE [*11*]. Therefore, on the most sensitive materials, tests were performed to determine if HE could disappear when tested under milder conditions than those of the standard test, and whether protection against HGE could be possible.

The special cells needed for some of these further tests, the typical results obtained, as well as the influence of various factors on HGE, are given next.

Influence of Hydrogen Purity

This can be studied easily. Table 6 gives results of tests where the air was not evacuated before running the hydrogen tests.

In a low-strength steel, HGE is curtailed almost completely, but, unfortunately, this embrittlement reduction decreases as strength level and hydrogen sensitivity increase. Small degrees of apparent exceptions are due to the simultaneous increase of oxygen concentration at rupture, this being approximately four times greater at the end of the last test than at the end of the first one; then, embrittlement of HS steels is still very large. This does not actually question the results obtained on HS steel fracture mechanics specimens for which oxygen pressures as low as 6.10^{-3} atm could stop the cracking in 1-atm GH_2 completely [*19*]. In

TABLE 6—*Influence of oxygen contamination on HGE of steels.*

Material	pHe, bars	pH_2, bars	pH_{2c}, bars	vpm, O_2[a]	pHe/ pH_2	pHe/ pH_{2c}	E/E_c[b]
0.09C-3.5Ni, 73 ksi steel 0.60-mm thick	420	310	410	512	1.39	1.02	10.77
35NCD16							
650° C tempered 173 ksi	560	300	365	575	1.86	1.53	1.33
550° C tempered 189 ksi	570	192.5	295	712	2.96	1.93	1.37
200° C tempered 282 ksi	540	140	167.5	1254	3.85	3.22	1.07
350 ksi maraging	380	67.5	105	1989	5.63	3.62	1.13

[a] O_2 concentration at rupture.

[b] $E = (p\text{He} - pH_2)/p\text{He}$ $E_c = (p\text{He} - pH_2 \text{ contaminated})/p\text{He}$

TABLE 7—*Influence of abrasion before testing on HGE of Zr-0.5Cu alloy.*

State of Material	Not Abraded			Abraded		
	pHe, bars	$p\mathrm{H}_2$, bars	$p\mathrm{He}/p\mathrm{H}_2$	pHe, bars	$p\mathrm{H}_2$ bars	$p\mathrm{He}/p\mathrm{H}_2$
Cold worked	531	376	1.41	514	223	2.30
Annealed	530	312	1.69	525	203	2.58

this experiment the specimens included an open crack, and the crack tips are at a thermodynamically attractive location for oxygen to migrate and sit steadily, blocking hydrogen sorption. On the other hand, hydrogen-oxygen competition on smooth specimens is not restricted to one point, and oxygen cannot restrain hydrogen entry well enough to prevent embrittlement of noticeably sensitive materials. Therefore, smooth specimens are more suitable than precracked specimens for realistic studies on the influence of impurities on HGE.

Influence of Surface Condition

The DPT appreciates the influence of surface condition sensitively (see Fig. 5 about 35NCD16HS steel). Similar effects are found on HS age hardened CG 27 austenitic steel ([*2*] and Fig. 3). In Type 304L, machining induces a martensitic transformation, making the material noticeably sensitive to HGE ($p\mathrm{He}/p\mathrm{H}_2 = 1.83$).

On materials like titanium, zirconium, uranium alloys surface oxides afford protection against HGE. Abrasion of oxide on a Zr-0.5Cu alloy, just before testing, makes this material more sensitive (Table 7). The moderate sensitivity of a U-1.5Mo alloy during the standard DPT ($p\mathrm{He}/p\mathrm{H}_2 = 1.32$) even disappears when the material is protected by polishing in a Monti bath; this is an oxidizing bath including H_3PO_4, CrO_3, and C_2H_5 OH [*8*].

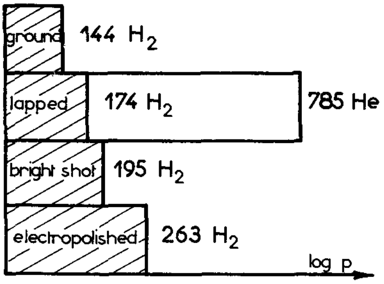

FIG. 5—*Influence of surface preparations on the rupture pressures (bars) of 35NCD16 HS steel.*

Influence of Thermomechanical Processing

Instances of the influence of thermal treatment have already been given for Type 304 and 35NCD16; other instances will be given later when dealing with the influence of temperature and pressure of martensitic steels on HGE.

Nowadays there is still an important problem for good and accurate processing of martensitic steels. Quite often a given heat treatment applied to a given strength level gives some scatter on elongation percent (E%). Of course, this ductility scatter affects the ultimate biaxial strength of materials tested under helium. Table 8 shows that the effect is even more pronounced when disks are tested under GH_2. This hints that these tests can be useful for quality control of materials, either usable in the presence of GH_2 such as the 650° C tempered material, or not usable, such as the other ones. For standard disks, minimum rupture pressures should be demanded (220 bars GH_2 for the 200° C tempering and 400 bars for the 650° C tempering). Lower pressures would indicate unsufficient quality, detrimental for whatever application is considered.

Unless it induces a transformation to a more hydrogen sensitive phase (as in 304 stainless steel), sufficient cold work appears beneficial for reducing HGE at RT. Also steels brought to a given strength level by a combination of rolling and heat treatment are less HGE sensitive than steels brought to this level by heat treatment only. Heat treatment only means lower tempering temperatures and probably less thermodynamical stability, hence, a smaller hydrogen resistance. The last two points present a great deal of practical interest, and further investigations will determine whether they keep true during slow strain rate and static fatigue tests.

TABLE 8—*Influence of ductility scatter on ultimate biaxial strength of 35NCD16 steel, tempered at various temperatures and tested under* GH_2.[a]

Tempering temperature	200° C			230° C		
Elongation, %	9.73	8.4	7	8	7.33	6.8
pHe, bars	980	890	650	867	785	666
pH_2, bars	245	180	130	210	174	124
$p\mathrm{He}/pH_2$	4	4.94	5	4.18	4.51	5.35

Tempering temperature	400° C		550° C			650° C		
Elongation, %	8.4	6.6	11.2	10.5	7.6	15.1	13.6	10.7
pHe, bars	615	530	777	670	650	690	710	599
pH_2, bars	207	93	230	160	140	410	351	270
$p\mathrm{He}/pH_2$	2.97	5.70	3.38	4.18	4.78	1.68	2.02	2.19

[a] Each material has been tempered twice for 2 h.

TABLE 9—*Influence of cold work on rupture pressures of Phynox standard disks.*

CW, %	YP, kg/mm^2	TS, kg/mm^2	*E*, %	*p*He, bars	*p*H$_2$, bars	*p*He/*p*H$_2$
23	98.1	130.4	19.2	810	653	1.24
46	145.5	168.8	5	357	337	1.06

However, while there are materials for which cold work does not decrease the ultimate biaxial strength in the cold-worked range investigated (Zr-0.5Cu, Pt-25Ir), it does for the cobalt alloys we have investigated (Tables 3 and 9). A similar trend has also been observed to a lesser extent on 13Cr-13Ni and 21Cr-20Ni-20Co stable austenitic steels. Therefore, although in some ranges cold work will be useful by raising the YP and decreasing the HGE, its use has to be limited properly for such materials.

Here it is proper to point up that the work hardening we have considered was made by rolling. As demonstrated by Wiester et al [*13*] localized cold work, such as that induced by stamping or grinding, is extremely detrimental, most likely because of the tensile stresses induced at the boundaries of the work hardened zones.

Influence of Welding

Welding [*4*, *14*] is frequently necessary to join parts of a structure but may have a detrimental influence on its resistance to HGE [*4*, *14*], by promoting more sensitive microstructures (alpha-titanium alloys) or by irregularities of the weld acting as stress raisers. Quite frequently the cracking of hydrogen pressure vessels starts from such areas [*15*].

In order to test the influence of welds on HGE, we use diametrally welded 58-mm-diameter disks. The DPT can be used to: (*a*) select weldable alloys, (*b*) make a choice among different welding processes, and (*c*) evaluate different welding sequences of a welding process, for further use in the presence of GH$_2$. Table 10 illustrates how the DPT could be used for selecting welding processes for Type 304L:

TABLE 10—*Influence of machining and welding on HGE of 304L.*

	No Machining			Machined	
Welding Process	*p*He, bars	*p*H$_2$, bars	*p*He/*p*H$_2$	*p*H$_2$, bars	*p*He/*p*H$_2$
Electron beam welding	730	560	1.30	383	1.90
Microplasma	703	510	1.38	360	1.95

Electron beam welding (EBW) has been preferred to microplasma which gives a somewhat smaller pHe and larger relative HE. HE of welded 304L is especially due to delta-ferrite retained from high temperature[5], but, when EBW is performed slowly enough so that thermal conduction plays an important role, then the importance of delta-ferrite is minimized and HGE decreases to the level of unwelded material. Machining to remove weld irregularities did not prove to be beneficial but rather detrimental, inducing a surface transformation to martensite which is more sensitive to HE. Therefore, slow EBW was selected without machining off the weld reliefs.

When welding causes embrittlement, cracking occurs in the embrittled zone, but it is sometimes useful to get more quantitative information. Then, a minicell is used to test very small disks (maximum diameter: 8-mm, useful diameter: 5 mm) which are taken out from the fusion zone, the heat affected zone, and the base metal at given distances from the weld axis and are tested under helium and GH_2 [*4*]. Such a cell can also be used for testing the HE of disks taken with different orientations from HS steel wires. Again, it was found that, for a given strength level, thermomechanically processed materials were more HGE resistant than steels for which the strength level results only from thermal treatment [*16*].

Another potential use of this cell is failure analysis. Quite frequently, the complex shape of failed specimens, nonhomogeneous thermal exposures, nonhomogeneous corrosion, etc. do not permit sampling out regular test specimen, and the only localized mechanical property available is microhardness. At some extent the situation is circumvented by the use of 5 mm useful diameter disks which enable the plotting of local biaxial ductility versus situation.

Influence of Pressure

To test it, we apply GH_2 partial pressures and go to rupture applying an additional increasing partial pressure of helium. In HS steels 35NCD16 [*2*] and 4330, there are two main regions separated by a round elbow:

1. Low pressure regions where there is a drastic influence of pressure, starting well below 1 psi, the total rupture pressure ($p\mathrm{He} + p\mathrm{H}_2$) falls steeply.

2. Higher pressure regions where there is a small influence of hydrogen activity on the stress threshold at which HGE occurs (Table 11).

In the case of 4330 treated to about half of the previous strength level, there is an immediate small decrease of $p\mathrm{He} + p\mathrm{H}_2$ when $p\mathrm{H}_2$ is comprised between one and five bars, but then it decreases very slowly and almost linearly (Table 12).

---

[5] Although, not very sensitive to HE, delta ferrite at least acts as a short path for hydrogen entry.

TABLE 11—*Influence of GH_2 partial pressure on total rupture pressure* ($pHe + pH_2$) *of 200° C tempered, 253 ksi, 4330.*

pH_2, bars	0	0.25	1	4	16	87.5
$pHe + pH_2$	750	230	180	145	115	87.5

We have recently started to study the influence of pressure by applying a given pressure of GH_2 disks downward and going to rupture by applying an increasing pressure of helium upward. This technique gives embrittlement data in good agreement with those exposed.

To overcome the fact that by first applying a large pressure of GH_2 the disks could negatively bulge or even embrittle when made of a hydrogen sensitive material, the same pressures of GH_2 and helium are applied downward and upward at the same rate, which prevents stressing the disks. Then an additional helium pressure is added upward at the chosen rate to reach rupture or any differential pressure upward or downward chosen for delayed failure experiments. If the upward pressure is progressively decreased, then the disks can be strained to rupture under a constant GH_2 pressure, provided this and the initial pHe applied was large enough.

Influence of Temperature

For tests between 20 and 180° C it is possible to place a regular cell in a thermostatically controlled oven. Beyond this range we use thermally insulated A286 steel cells with unwelded copper seals. In every instance temperature is measured on the specimen.

Low temperatures between RT and −196° C are achieved by flowing a mixture of liquid nitrogen and compressed air through a jacket around the testing cell (Fig. 6). Elevated temperatures are achieved by means of two heating plates above and below the cell (Fig. 7). Figure 8 gives the influence of temperature on HGE of 35NCD16: tempered at 650° C TS = 194.3 kg/mm^2 (276.5 ksi) and tempered at 200° C TS = 107.5 kg/mm^2 (153 ksi) [*17*].

HGE appears after −130° C for the first tempering, increases progressively, then, after a very flattened maximum between −40 and −10° C, decreases sluggishly to 50° C. After that it remains constant within the experimental error limits, at least until +300° C. It will be noted, however,

TABLE 12—*Influence of GH_2 partial pressure on total rupture pressure* ($pHe + pH_2$) *of 680° C tempered, 128 ksi, 4330.*

pH_2, bars	0	5	100	200	327.5
$pHe + pH_2$	520	495	440	385	327.5

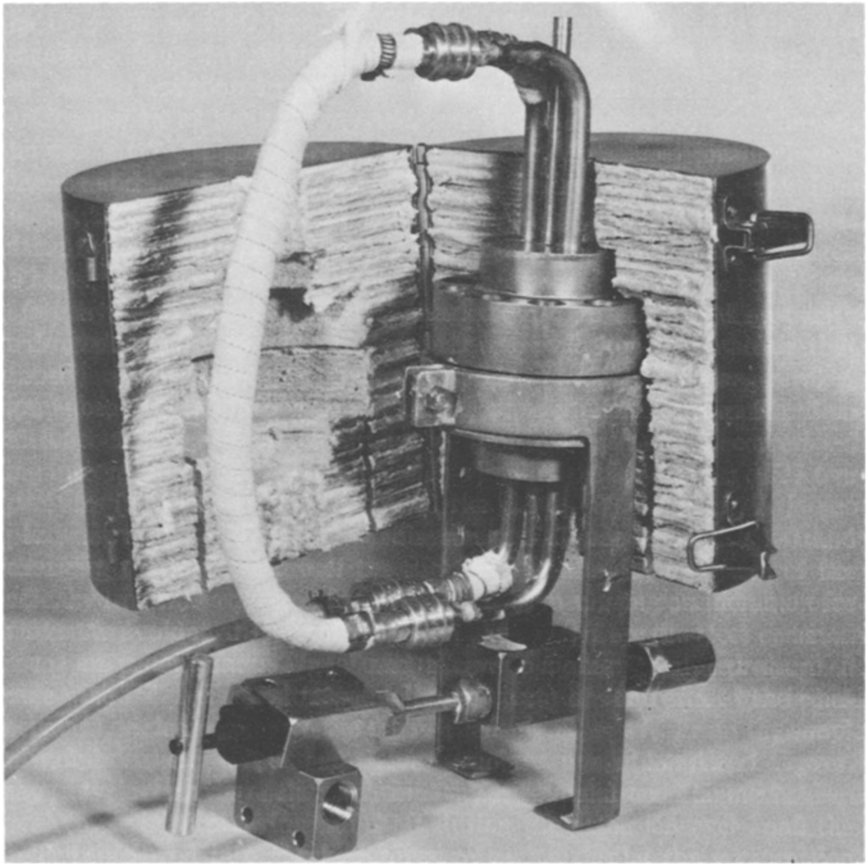

FIG. 6—*Low-temperatures cell.*

that the ratio pHe/pH_2 is always smaller than two, indicating a tolerable sensitivity.

HGE appears as soon as −145° C for the second tempering is reached, increases steeply, then, after a maximum near −40° C, decreases slowly and thus keeps very important at +300° C. The transition noted at low temperatures reflects the synergistic effect of low-temperature embrittlement and HGE, this one disappearing as the other one appears (shaded portion in Fig. 8). Due to the nickel percent content of the steel, such an effect is not observed for the high-temperature tempered material.

The embrittlement drop noticed at about 200° C for the HS material is probably because this is also the tempering temperature for this material. Above 200° C HGE increases rapidly at first then it decreases, but only slowly because then the material has entered the tempered martensite embrittlement range. This contention is substantiated by electron frac-

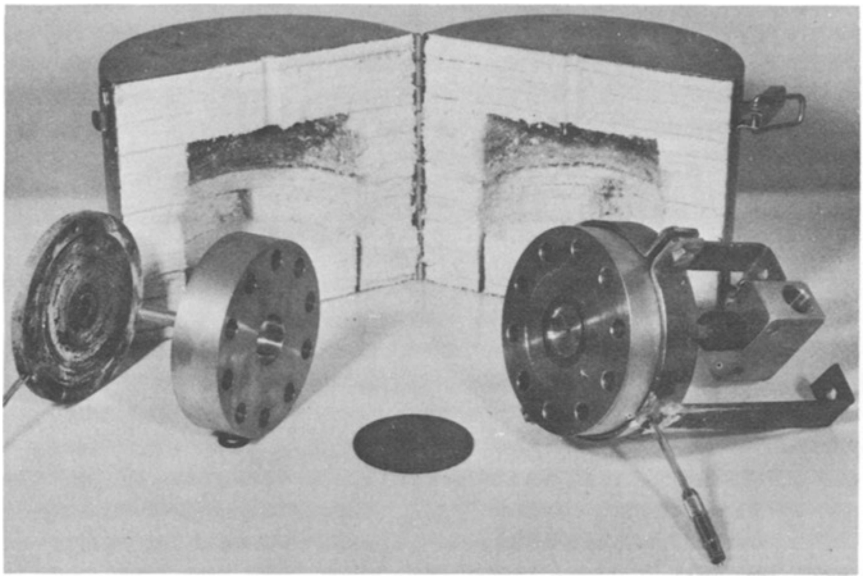

FIG. 7—*Elevated-temperatures cell.*

tography. Whereas fracture is transgranular for the material embrittled at room and medium temperatures, it is intergranular for the material tested at 300° C. This is the regular shift observed when embrittling effects of tempering are superimposed to those of HE [5, 9].

The influence of temperature has also been studied on nickel between 20 and 180° C [2], Inconel 718 [18], Phynox, and A286. Preliminary

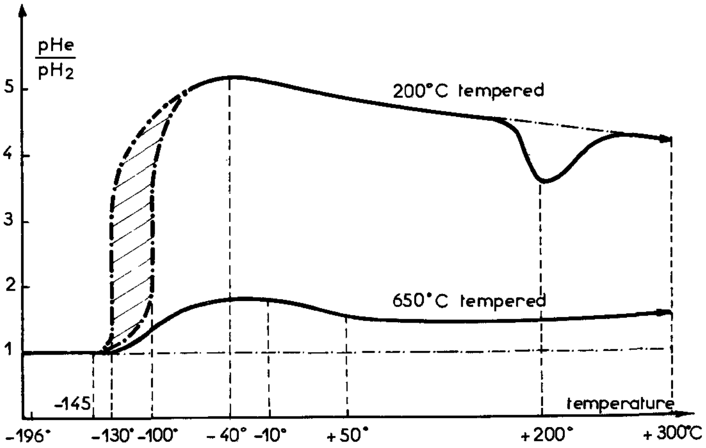

FIG. 8—*Influence of temperature on HGE of 35NCD16 steel.*

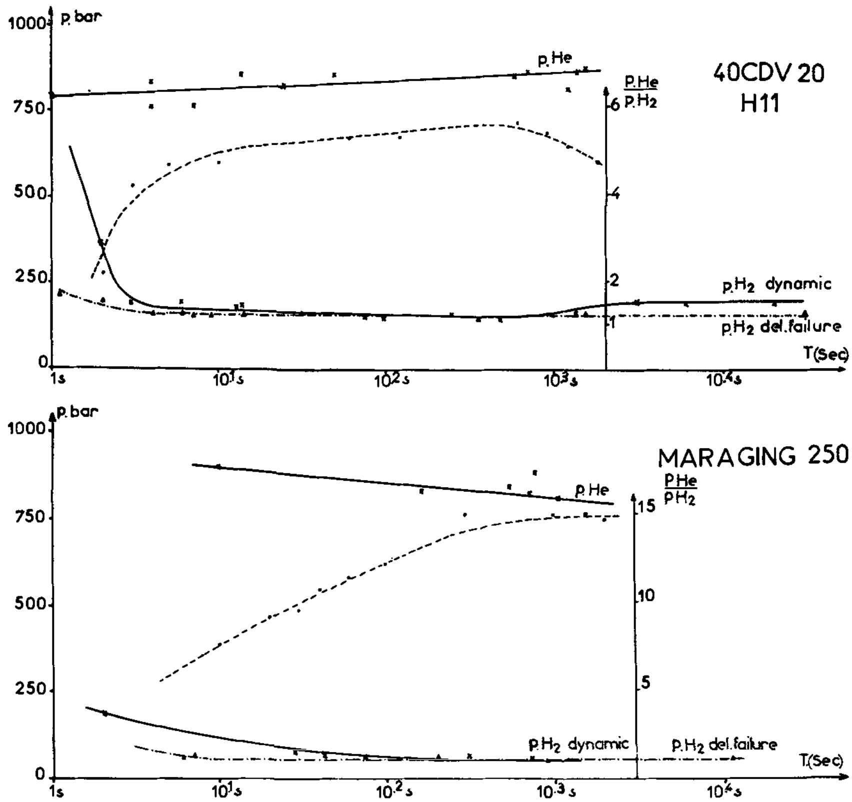

FIG. 9—*Delayed failure curves and influence of the pressure increase rate on HGE of H-11 and 250 maraging steel.*

results indicate some embrittlement of this material at about 300° C ($p\text{He}/p\text{H}_2 = 1.25$).

Influence of Strain Rate

This has been investigated on two HS steels (Fig. 9). At high pressure increase rates, there is little embrittlement; however, when they are decreased, embrittlement increases rapidly for H 11 and somewhat less rapidly for 250 maraging steel, owing to the smaller RT D_H in this steel: $D_H = 2.1 \times 10^{-8}$ cm² s^{-1} for H 11 [*19*] and $D_H = 3 \times 10^{-9}$ cm s^{-1} for 250 maraging steel.[6] These results are in good agreement with those obtained on 35NCD16 and 350 maraging steels, cathodically charged

---

[6] Admittedly, in the present tests environmental hydrogen is dragged inside of the metal by dislocations more than by regular diffusion [*20, 21*], but, at some extent, the speed of dislocations has to be turned up to hydrogen diffusivity to get a maximum efficiency.

over different periods; $D_H = 5 \times 10^{-8}$ cm^2 s^{-1} in 35NCD16, which is close by D_H in H 11. Therefore, 35NCD16 is more quickly saturated than maraging and at first appears more embrittled when charged disks are tested under helium. Then IHE of maraging overshoots that of 35NCD16 when it gets saturated [*1*]. The same explanation is also valid for Ti-5Al-2.5Sn. Hydrogen diffusivity is low near RT, $(D_H)_{70\ C} = 2.9 \times 10^{-10}$ cm^2 s^{-1} [*22*], and HGE is more noticeable at lower *dp/dt* (pressure increase rates): $p\text{He}/p\text{H}_2 \leq 1.08$ for $dp/dt = 89$ bars/min and $p\text{He}/p\text{H}_2 = 1.31$ for $dp/dt = 20$ bars/min. The second ratio can be compared to the ratio 1.23 of the notch tensile strengths of the same alloy tested under 684 bars (10 000 psi) helium and GH$_2$ found by Walter and Chandler [*23*].

Delayed Failure Experiments

Although HGE is relatively less time dependent than IHE, the claim that HGE is not time dependent is not correct. Would it be so, then HGE would not be so much of a problem for the industry, and there would not be so much need to worry about it. As a matter of fact, delayed failures caused by GH$_2$ have been shown for a long time by Hofmann and Vogt on a reinforcing steel [*24*].

We have carried out delayed failure experiments on 252-ksi H-11 250 maraging steel (Fig. 9), and on several other martensitic steels. Delayed failure racks are shown in Fig. 10. During these experiments, GH$_2$ pressure

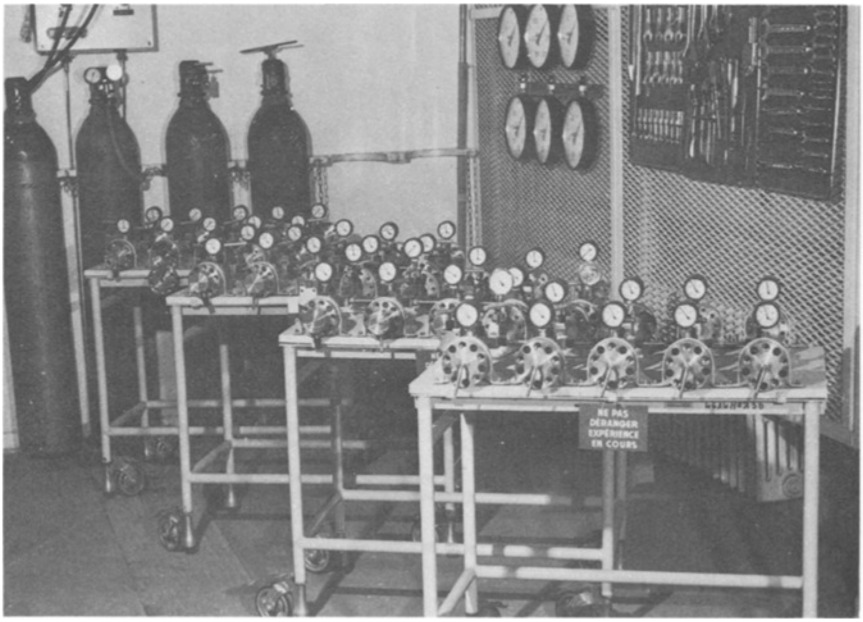

FIG. 10—*Delayed failure racks.*

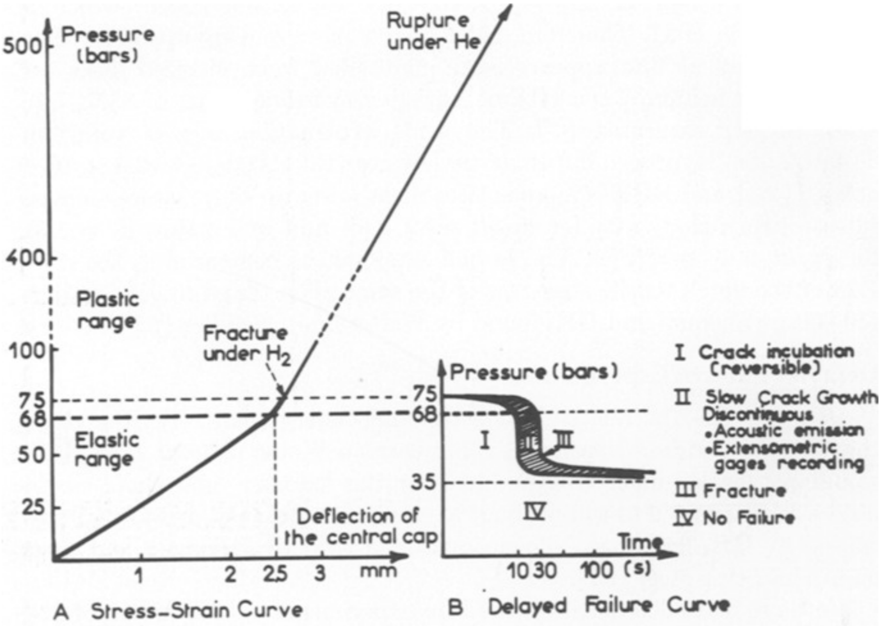

FIG. 11—*Stress-strain and delayed failure curves for 2 mm thick 35NCD16 HS steel disks.*

is applied rapidly so that it is possible to reach pressures higher than the maximum pressure attained during rupture tests conducted at 65 bars/min or below. Figure 9 indicates that the delayed failure limit seems to merge with the limit rupture pressure obtained during tests conducted at more and more reduced rates. This information is being confirmed by other experiments in progress, which presents a great potential interest in saving the time spent on long delayed failure experiments.

Other experiments have been carried out on 2-mm-thick plates of 285 ksi, 200°C tempered, 35NCD16 (Fig. 11) [*25*]. Owing to the relatively slower hydrogen impregnation than on regular thickness specimens, a clean S-shaped delayed failure diagram could be recorded, similar to those reported by Troiano et al [*26*] for IHE. It includes three parts: (1) incubation, (2) discontinuous crack propagation which can be monitored by acoustic emission or discontinuous recordings of extensometric gages placed on different parts of the specimens, and (3) fast fracture. Comparing the two parts of Fig. 11 it will be noted that delayed failure can take place well below the pressure beyond which macroscopic yielding occurs. This does not question the well-known fact that HE requires some plastic deformation [*27*, *28*], but this deformation needs not take place on a macroscopic scale and only need take place near the tip of internal flaws, which preexist in such HS materials. This is confirmed by the fact that prestressing with a neutral gas to a pressure equal to the hydrogen delayed failure limit of unprestressed material raises this limit for prestressed material. Thus, cold work by prestressing appears to be an effective way to reduce HGE further.

Hydrogen enters materials even below the delayed failure limit. Disks which had not failed after 2 h exposure to 30 bars of GH_2 were tested under helium, after evacuating GH_2 and flushing the upward chamber several times with helium. The disks broke under a mean pressure of 215 bars, while uncharged material did not fail under 700 bars of helium. Such checkups are useful to indicate what safety margin would be present if a material, previously exposed to GH_2 and apparently unembrittled, had to be stressed to higher stress levels after removal of GH_2.

Permeation is another sensitive way to follow incubation and discontinuous crack propagation. This has been discussed at length in earlier papers as well as the influence of temperature [*10, 17, 29, 30*]. In HS steels, discontinuous crack propagation comes out as discontinuous permeation increases. In the experiments depicted by Fig. 12, permeated gas was collected daily by means of a Töpler pump and measured by gas chromatography. The differences between the initial and final permeabilities at RT indicate irreversible damage. It is also possible to monitor cracking continuously by means of a mass spectrometer [*31*]. Permeation is an especially suitable technique for studying HGE in progress, and one

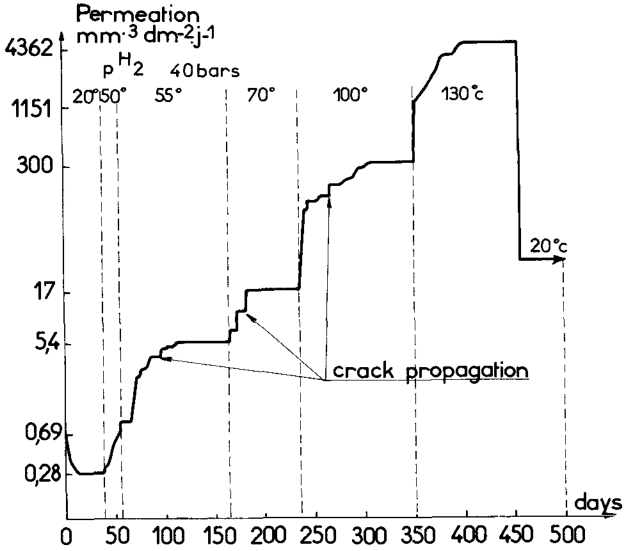

FIG. 12—*Discontinuous permeation increases in 2 mm thick 35NCD16 HS steel disks, exposed to GH_2 under pressure at various temperatures. Note the irreversible effect of crack propagation on permeability.*

advantage of the disks is to leave one side of the specimen available for such measurements.

Experiments have also been carried out on Ti-5Al-2.5Sn and zirconium alloys when hydriding takes place, and, since diffusion through compact hydrides is slower than through bulk materials, surface hydriding causes permeation to drop appreciably before rupture [*6*, *15*].

In delayed failure tests run on U-1.5Mo alloys between 20 and 100° C, rapid cracking without detectable hydriding was observed at lower temperatures and high stresses induced by high pressures, while under lower pressures at higher temperatures the material started hydriding then broke when its thickness had been sufficiently reduced by corrosion. Such tests are run in an inert gas vented glove box to avoid uranium hydride fires when the cell is broken down, but only the delayed failure cells need to be inside of the glove box, the remainder of the equipment being outside.

Another potential use of such a glove box is abrasion in an inert gas atmosphere of oxide coated materials, such as titanium, zirconium, and uranium alloys, immediately before testing under GH_2. Admittedly, these material are so much reactive with oxygen that oxides may reform to some extent, but abrasions made under less favorable conditions, for example, in air, followed by tests on Zr-0.5Cu alloy indicate that they do not reform sufficiently to prevent increased HGE of abraded specimens (Table 7).

Low-Cycle Fatigue

This program in progress now has been initiated because it had been found that if during delayed failure experiments the applied pressure decreased due to a small leak or a RT change, ruptures occurred quite frequently as the pressure was adjusted back, indicating that changing stresses are more critical than plain static stresses.

During the first experiments disks have been cycled *n* times between O-bars and a fraction, generally ½, of the GH_2 rupture pressure during a regular dynamic test; then, they have been strained to rupture. Tests

TABLE 13—*Influence of the number of low-cycle fatigue cycles on the final rupture pressure.*

Material	pHe, bars	$p\text{H}_2$, bars	$p\text{He}/p\text{H}_2$	n, cycles	pHe, bars	$p\text{H}_2$, bars	$p\text{He}/p\text{H}_2$
Beyllium copper	535	535	1	20	530	530	1
A286	609	589	1.02	40	no significant change		1.02
280-ksi 35NCD16	703	103	7.18	10		77	
Ti-5Al-2.5Sn	430	408	1.05	39[a] 48	365	200 150	1.82 2.43
Ti-6Al-6V-2Sn	437	399	1.09	10	545	276	1.98

[a] Rupture under GH_2 occurred between 39 and 48 cycles.

TABLE 14—*Overstretching results for 7075 T-6.*

pHe, bars	pH_2, bars	$p\mathrm{He}/pH_2$	π	pHe, bars	pH_2, bars	$p\mathrm{He}/pH_2$
287	283	1.01	246	199	165	1.21
			249	211	169	1.25

have been conducted with helium too, in order to differentiate between the effects of cycling under a neutral gas and those due to GH_2 (Table 13). Except for Ti-5Al-2.5Sn, cycling was not carried out long enough for failures to occur during cycling, because the tests had to be carried out manually, but they would have likely occurred for the other two sensitive materials 35NCD16 and Ti-6Al-6V-2Sn, considering that they are already seriously affected after only ten cycles. These preliminary results have been found encouraging enough so that an automated cell has been designed and is presently under evaluation.

Overstretching

This test has been initiated during a program conducted at Case-Western Reserve University in order to investigate the role of HE in stress corrosion cracking [*32*]. It has been used for materials displaying negligible sensitivity during the regular dynamic test: 70–30 brass and 7075-T6. During the test, materials are bulged under a pressure, π, about 85 to 90 percent of the rupture pressure, then pressure is applied in the opposite direction to rupture. A severe plastic deformation takes place at the anchorage which should favor HE if there is any sensitivity, even small, of the material to hydrogen.

No embrittlement could be detected for 70–30 brass. Table 14 shows the results obtained for 7075-T6, indicating that under conditions of severe plastic deformation, similar to those existing near the tip of a stress corrosion crack, EHE is made possible.

Other Sources of Environmental Hydrogen Embrittlement (EHE)

Hydrogen isotopes, deuterium, and tritium also induce HGE [*2, 5, 6, 7, 8, 10, 11, 20, 25, 29*], which generally decreases in the following order $H \rightarrow D \rightarrow T$. In each case the same test cells can be used, but, in the case of the radioactive isotope tritium, they are placed in an inert gas vented glove box.

The DPT is not only usable for HGE but also for other sources of EHE such as water or acids [*1*]. The aggressive medium can be placed on the same side as pressure, on the other side, or even on both sides. Delayed failure experiments have been carried out on HS steel disks exposed to water saturated, pressurized helium on one side, tô study the problem of light tanks filled with a neutral gas under high pressure. Usually high-pressure gases are wet, which is a potential source of corrosion generated hydrogen. Helium pressure was 80 percent of the rupture pressure during the dynamic test. When 300 vpm of oxygen were present with moisture, disks cracked between six and ten days, and traces of corrosion were present on the open cracks. In the absence of oxygen, stress corrosion cracking was completed in three weeks, conspicuous traces of corrosion being absent on the cracks.

Protection Against HGE and Hydrogen Absorption

In equipment where HEE and especially HGE cause a problem, several kinds of protection measurements can be attempted:

1. Choice of materials with a good bulk resistance to HE.

2. Alter conditions of operation, when possible. For instance, with reactors working at elevated temperatures under GH_2 pressures, periodically vent the hydrogen out and outgas absorbed hydrogen in order to prevent critical accumulation inside of the material.

3. Alter design to put threads or other stress concentrators outside of the hydrogen chamber.

4. Have a surface in contact with GH_2 as smooth and free from tensile stresses as possible. When possible, shot peening will be helpful by creating compression stresses in surface layers and will help to decrease the effective tensile stresses during service in the presence of GH_2.

5. Fretting the inner shell or prestressing it will also be effective.

6. When tolerable, add inhibitors to the hydrogen supplying phase, such as buffers to liquids in order to prevent acidity or traces of oxygen to titanium alloys exposed to GH_2 near RT. Similarly when purity is not critical (for instance, when GH_2 later reacts with oxygen) GH_2 could be stored under high pressure in large ordinary steel vessels after oxygen contamination.

7. Separate the mechanical resistance and the resistance to hydrogen by using low permeability liners and vented means of wormholes in the resistant outer shell; however, this should not be made of HS steels as it has been determined that even quite low GH_2 pressures can affect these materials. Liners can be made of austenitic steels, aluminum alloys, beryllium copper, and materials which the DPT has demonstrated to have a low permeability to GH_2 [*30*].

In large reactors, the weight of the liner itself can cause the liner to buckle under its own weight; therefore, it is necessary either to increase the thickness of the liner or to use materials with a reasonably high YP. Then beryllium copper is attractive but cannot be used in the important instance of NH_3 and related synthesis. Age hardened HS aluminum alloys can have YP double that of Type 304, but they cannot be used too far above RT, which would cause overaging. On the other hand age hardened A286 steel has a high YP (90 ksi) and can be used at elevated temperatures, but it is difficult to weld when thick. Cobalt austenitic alloys such as Haynes 188 and Phynox, appear to be an attractive alternate solution, usable at even higher temperatures although more expensive.

8. Use of coatings: (*a*) corrosion resistant coatings which will curtail corrosion and corrosion induced hydrogen generation and (*b*) coatings with a low permeability to GH_2. We have studied (*b*) with DPT in HS steels, especially 230° C tempered 35NCD16 HS steel [*33*, *34*]. Coatings need not possess noticeable mechanical resistance like thick vertical liners, but a very low permeability is even more critical since hydrogen permeating the coatings cannot be vented outside. Besides that, coatings must: not detrimentally affect the substrate, while being processed, have a small or negligible hydrogen sensitivity, not be porous, not be cracked, be thick enough, be cohesive and adhesive to the substrate, and be able to deform with the substrate. At first DPT studies helped to select low permeability materials with negligible hydrogen sensitivity: aluminum, gold, cadmium, copper, indium, 18–15 stainless steel, tin, and zinc. Despite its noticeable hydrogen sensitivity, nickel was not excluded at first because its sensitivity is still smaller than that of the HS steel substrates and because nickel flashes are used frequently between the substrate and the main coating.

During the tests, the coated sides of the disks are exposed to a GH_2 pressure at least equal to that which would cause immediate failure of uncoated materials. Defective coatings will afford limited or no protection, not to mention coatings which permanently embrittle the substrate and which have already been eliminated to date [*33*, *34*, *35*]. On the other hand, excellent coatings can afford protection for months and years.

Vacuum sputtered 18–15 austenitic stainless steel, aluminum, and gold were not successful, although aluminum and gold gave some interesting results [*34*], but the scatter was too large because this kind of coating cannot exceed 10 to 20 μm thicknesses without affecting coating cohesion, and the chances remain too big that random defects go throughout the coating thickness. Fortunately electrolytic coatings better avoid this shortcoming as they can reach up to 70 μm easily.

Zinc platings were rapidly eliminated because they permanently embrittled the substrate. Buffered zinc definitely provided some protection ranging from four days to more than two years, but results were not reproducible. Nickel and nickel plus gold gave reproducible but bad results. Nickel did not come out as good material either as a self standing coating or as a flash under another coating.

Duplex cadmium coatings[7] gave excellent results when tested under the pH_2 which would cause immediate failure in the absence of coatings.

---

[7] According to the idea, qualitatively proposed by Johnson et al [*36*], these coatings include a first coarse grained layer (C), nonembrittling after baking, then a fine grained, bright cadmium layer (B) which does not embrittle when C is thick enough.

(30 C + 10 B) μm cadmium coated disks	failed after more than two years (812 to 819 days).
(30 C + 20 B) μm cadmium coated disks	did not fail after more than five years at RT. started to fail after about two years at 60° C. generally failed after about five months at 100° C.

The coatings with 20-μm bright cadmium have been more effective than those with 10 μm. For more than two years no failure took place even for disks stressed under GH_2 pressures higher than the rupture pressures pH_2 for uncoated disks. After removing GH_2, unfailed disks were stressed under helium, and the rupture pressures were equal or close to pHe for unexposed disks, indicating the efficiency of 20-μm coatings in reducing hydrogen entry.

Although temperature increase decreases HE due to a given amount of internal hydrogen, on the other hand, it accelerates and increases hydrogen entry, which explains acceleration of delayed failures with increasing temperature. Nevertheless, services without failure, for several months at 100° C and for more than a year at 60° C are still of interest for materials which would have cracked rapidly in the absence of coatings.

Similar tests have been conducted with duplex (25 + 25)-μm copper coatings, giving interesting results, although less reproducible and allowing delayed failures to be observed after only a few days. However the addition of a third layer of 3 μm of indium gave a better resistance, since the first delayed failure among four specimens was observed after 518 days, whereas the other specimens are still resisting after 1260 days.

Chemically deposited chromium was a failure in 35NCD16 because of its brittleness [*34*]. On the other hand, such a material diffused into 18Ni maraging steel builds up an austenitic layer resistant to hydrogen entry *in situ* [*37*]. Preliminary results indicate that such a technique should be usable to fight HGE of maraging disks, resisting between 6 h and more than 640 days under a hydrogen pressure that would have caused immediate failures otherwise. Unfortunately the program had to be terminated before further testing could be done in order to improve reproducibility with thicker austenitic layers.

Discussion

Advantages of the Disk Pressure Test

As indicated in the previous paragraphs, the DPT can be used for materials and processing selection, and instances have been given noticeably for iron- and cobalt-base alloys. The DPT can be employed to study factors influencing service behavior (temperature, GH_2 pressure, time, etc.). Typical cases where the test has been used include:

1. Steel selection for commercial GH_2 cylinders.

2. Materials and processing selection for welded pressure vessels, filled with high-pressure GH_2 (up to 1500 bars), and operated between RT and +130°C.

3. Selection of steels for chemical synthesis reactors using pure GH_2 under high pressure between −50° C and elevated temperatures.

4. Materials and processing selection for coatings designed to protect HS steels against HGE at RT and above.

5. Selection of steels (sheets and wires) for prestressing concrete.

6. Materials and operating conditions selection for welded steel vessels containing wet neutral gases under pressure.

The DPT can be used for quality control (materials and processing). Instances have been given especially in the case of 35NCD16 tempered at various temperatures. Usually the test is performed three times for each material under each condition, and reproducibility is ±2 to 3 percent; this can reach ±1 percent or less for very precisely processed, high quality materials. Generally it becomes ±5 to 10 percent for ultra HS steels and can reach ±20 to 25 percent for inaccurately processed, low quality materials. Of course, this is not due to the testing procedure or to the equipment but to the material itself, and it is also registered during less sensitive tests anyway. In such instances tests are performed at least five times for each condition.

The general advantages of the DPT have already been indicated previously [*1*]: (1) sensitivity, (2) flexibility, (3) possibility of investigating several causes of embrittlement, including IHE, HEE, and other embrittlement mechanisms different from those due to hydrogen and their synergistic effects (this is quite important since we must avoid running into another cause of embrittlement which cannot be revealed by the investigation technique used), (4) rapidity, (5) simplicity of operation and maintenance, (6) simplicity of test specimens, and (7) economy.

We will review some of these points again and will especially insist on points specific of the DPT, when used for testing HEE:

1. Possibility of using pressures up to 1600 bars (23 200 psi) on such a deleterious gas as hydrogen. Despite this high pressure, safety is high, principally because of the reduced size of the test cells and small volumes of gas involved.

2. Sensitivity. Table 15 compares results obtained with the DPT and the notch tensile test (NTT) under 10 000 psi GH_2 [*23*]. The agreement is quite good especially when you considered that results were obtained by different investigators using only equivalent materials. In two instances (410 stainless steel and nickel— the DPT data are more sensitive than the NTT ones, but this is due to the smaller thicknesses of the disks used in these cases, which better evidence environmental effects at the considered loading rate (65 bars/min). If NTT under 10 000-psi gas and DPT on 30 mils thick disks appear to have the same sensitivity, there

TABLE 15—*Comparison NTT/DPT (30 mils thick disks are used unless stated otherwise).*

	NTT		DPT
Materials	$(N_{He}-N_{H_2})/N_{He}\times 100$	N_{He}/N_{H_2}	pHe/pH_2
Maraging	88	7.33	6.4 to 7
410	79	4.76	6.77 (8 mils thick specimen)
H 11	76	4.16	3.6 to 5.7
Inco 718	54	2.17	2.27
Nickel	30	1.43	1.82 (16 mils thick specimen)
Ti-6Al-4V annealed	25	1.33	1.25 to 1.35
SAE 1020	20	1.25	1.25 (0.18C steel)
Ti-5Al-2.5Sn	19	1.23	1.13 (fast) to 1.31 (slow)
304 ELC	13	1.15	1.11 (304L)
A286	3	1.03	1.02 (fast) to 1.03 (slow) (XN26)
310	3	1.03	1.03
7075 T-73	2	1.02	1.01 (fast) to 1.02 (slow) 7075-T-6
316	0	1.0	1.0
OFHC copper	0	1.0	1.0 (7030-brass)

are other factors, listed from 3 to 8, which make the DPT more advantageous.

3. In contrast with the tension test under pressure, complete leak free behavior is not guaranteed on the mobile part of the test specimen. This prevents altering the results due to friction forces. Also, the seals can be used many times, and low-cycle fatigue as well as studies at low and high temperatures need a simpler equipment than when sliding seals have to be used.

4. In contrast with most of the other test methods, a side of the specimen is generally available for physical measurements while the test is in progress.

5. Possibility of studying the effects of two independent sources of HEE simultaneously, for instance, GH_2 upward and salt water downward.

6. Possibility of getting a direct relationship between hydrogen brittleness and permeability on the same specimens. Means of permeation measurement crack propagation during delayed failure tests can be monitored as well as incubation and the influence of various factors.[8]

7. The test specimen geometry is especially convenient for testing inhibotors, surface treatments, and coatings designed to delay and slow down HEE (studies to increase incubation time). In recent years incubation studies and smooth specimens have been discounted by a number of authors because, during delayed failure experiments on smooth specimens, cracking was preceded by a irreproducible incubation period, which could be long enough to give the impression of a lack of sensitivity to HEE. There is no doubt that crack propagation studies on precracked speci-

---

[8] Of course, other techniques such as acoustic emission and extensometric gages are usable and have been effectively employed.

mens are important, but it would be a shortsighted attitude not to study the incubation mechanism just because knowledge of this phenomenon is not yet mastered. Indeed studies with the purpose of increasing incubation can offer interesting solutions to fight HEE in the frame of industrial problems. As shown before in oxygen contaminated GH_2, smooth specimens are more realistic than precracked specimens, which in this specific case can give correct but unrealistic results leading to overoptimistic interpretations.

8. Economics. Of course, most of the preceding points are of economical advantage, either quite direct or more indirect, such as time and safety considerations. The cost of the equipment is also moderate and was $8500 in 1971. This is somewhat higher than the cost of the equipment used only for testing IHE [*1*], because of the need for an additional high pressure tank for GH_2. This amount is about the price of a 400-lb table tension machine, which is an equipment with much more limited potentialities and is not sold to run tests with GH_2 under pressure anyway.

In delayed failure experiments, the rupture cell is the only thing to be duplicated, which not only saves money but also space (Fig. 10), while the ubiquitous pressure applies load wherever it is needed without duplicating mechanical loading devices.

Finally the cost of the specimens is quite low: about $8 for steel disks against about $25 for notched tension specimens and even more for more sophisticated specimens. This is a key factor since, as with a car, operation eventually costs more than the purchase.

Acknowledgments

The authors would like especially to thank A. R. Troiano, M. F. McGuire, R. N. Gest, E. Bachelet of Case-Western Reserve University, Cleveland, Ohio, L. Bretin of Creusot-Loire, Le Creusot for many helpful discussions, R. Chevalier and R. Martinou, Snecma, Corbeil for electroplating specimens, B. Marandet, C. Pirrovani, and A. Maës for their contribution to the tests.

References

[*1*] Fidelle, J.-P., Broudeur, R., Pirrovani, C., and Roux, C., this symposium, pp. 34–47.

[*2*] Fidelle, J.-P., Allemand, L.-R., Roux, C., and Rapin, M. in *Hydrogen in Metals*, J.-P. Fidelle and M. Rapin, Eds., Valduc, France, 1969, p. 131.

[*3*] Benson, R. B., Jr., Dann, R. K., and Roberts, L. W., Jr., *Transactions*, Metallurgical Society, American Institute of Mining, Metallurgical, and Petroleum Engineers, Vol. 242, 1968, p. 2199.

[*4*] Poirier, J., Fidelle, J.-P., and Roux, C., in *Electron Beam Welding and Melting*, Interbus, Paris, 1971, p. 529.

[*5*] Fidelle, J.-P., Legrand, J., and Couderc, C., "A Fractographic Study of Hydrogen Gas Embrittlement in Steels," Paper F-71-8. Fall Meeting, Detroit, Mich. American Institute of Mining, Metallurgical, and Petroleum Engineers, Oct. 1971.

[*6*] Poirier, J., Fidelle, J.-P., and Roux, C., "Behavior of Zirconium and Its Alloys

Versus Hydrogen and Deuterium Under Pressure," GMC 18-69-103, Part II, CEA, Bruyères-le-Châtel, France, 1969.

[*7*] Poirier, J. and Fidelle, J.-P., "Hydrogen Embrittlement of Low-Alloyed High-Strength Steel Sheets," GMC 15-70-124, CEA, Bruyères-le-Châtel, France, 1970.

[*8*] Poirier, J., Fidelle, J.-P. and Rapin, M., "Behavior of Uranium and Its Alloys Versus Hydrogen and Deuterium Under Pressure," GMC 18-69-103, Part III, CEA, Bruyères-le-Châtel, France, 1969.

[*9*] Legrand, J., Couderc, C., and Fidelle, J.-P. in *Hydrogen in Metals*, Science Industrie, Paris, Ed., Chatenay-Malabry, France, 1972, p. 316.

[*10*] Fidelle, J.-P., Allemand, L.-R., Deloron, J., and Roux, C., *Mécanique Electricité*, Vol. 52, 1969, p. 27.

[*11*] Fidelle, J.-P., Broudeur, R., and Clauss, A. in *Hydrogen in Metals*, J. P. Fidelle and M. Rapin, Eds., Valduc, France, 1969, p. 324, ORNL-TR-2448, Oak Ridge National Laboratory, Feb. 1971.

[*12*] Hancock, G. G. and Johnson, H. H., *Transactions*, Metallurgical Society, American Institute of Mining, Metallurgical, and Petroleum Engineers, Vol. 236, 1966, p. 513.

[*13*] Wiester, H. J., Dahl, W., and Hengstenberg, H., *Archiv für Eisenhüttenwesen*, Vol. 34, 1963, p. 915.

[*14*] *Metal Progress*, May 1971, p. 90.

[*15*] Allemand, L.-R., Fidelle, J.-P., and Rapin, M. in *Hydrogen in Metals*, J.-P. Fidelle and M. Rapin, Eds., Valduc, France, 1969, p. 241.

[*16*] Poirier, J. and Fidelle, J.-P., "Demonstration of Metals Sensitivity to Hydrogen Means of Very Small Disks. Application to Various High-Strength Steels," GMC 13-69-98, CEA, Bruyères-le-Châtel, France, 1969.

[*17*] Fidelle, J.-P., Broudeur, R., and Roux, C. in *Hydrogen in Metals*, Science Industrie, Paris, Ed., Chatenay-Malabry, France, 1972, p. 350.

[*18*] Bachelet, E., "Research in Progress," Case-Western Reserve University, Cleveland, Ohio, 1972.

[*19*] Bretin L., Labo Creusot-Loire, Le Creusot, France, private communication, 1972.

[*20*] Fidelle, J.-P., Roux, C., and Rapin, M., *Mémoires Scientifiques de la Revue de Métallurgie*, Vol. 66, 1969, p. 833, BISI Translation 8242, 1970.

[*21*] Fidelle, J.-P., Broudeur, R., Tanon, A., and Roux, C., "Role of Hydrogen in Stress Corrosion Cracking of Austenitic Steels in Chloride Solutions. Establishment of a Possible Mechanism Applicable to this Kind of Cracking," Symposium on Stress Corrosion Cracking and Hydrogen Embrittlement, Paris, April 1971, Report 4361, French Atomic Energy Commission, 1972.

[*22*] Dexter, A. H., Derrick, R. G., and Louthan, M. R., Jr., *Corrosion*, National Association of Corrosion Engineers, Vol. 27, 1971, p. 466.

[*23*] Walter, R. J. and Chandler, W. T., "Effect of High-Pressure Hydrogen on Metals," Fall Meeting, Detroit, Mich., American Society for Metals, Paper D8-14.2, Oct. 1968.

[*24*] Hofmann, W. and Vogt, J., *Archiv für Eisenhüttenwesen*, Vol. 35, 1964, p. 551.

[*25*] Jolly, N., Le Gallo, P., Bretin, L., and Fidelle, J.-P., "Extensometric Measurements on 35NCD16 High-Strength Steel Disks Strained to Rupture Under Increasing Argon or Hydrogen Gas Pressure," GMC 14-70-123, CEA, Bruyères-le-Châtel, France, 1970.

[*26*] Steigerwald, E. A., Schaller, F. W., and Troiano, A. R., *Transactions*, Metallurgical Society, American Institute of Mining, Metallurgical, and Petroleum Engineers, Vol. 215, 1959, p. 1048.

[*27*] Bastien, P. and Azou, P., *Compte Rendus*, Académie des Sciences, Vol. 232, 1951, p. 69.

[*28*] Hofmann, W. and Rauls, W., *Archiv für Eisenhüttenwesen*, Vol. 32, 1961, p. 169.

[*29*] Fidelle, J.-P., Allemand, L.-R., Tanon A., and Rapin, M., *Mémoires Scientifiques de la Revue de Métallurgie*, Vol. 65, 1968, p. 241, BISI Translation 6702, Jan. 1969.

[*30*] Fidelle, J.-P., Allemand, L.-R., Rapin, M., and Hocheid, B. in *Hydrogen in Metals*, J.-P. Fidelle and M. Rapin, Eds., Valduc, France, 1969, p. 209.

[*31*] Fidelle, J.-P., Panel Discussion, this symposium.

[*32*] Gest, R. N. and Troiano, A. R. in *Hydrogen in Metals*, Science Industrie, Paris, Ed., Chatenay-Malabry, France, 1972, p. 427.

[*33*] Fidelle, J.-P., Deloron, J. M., Roux, C., and Rapin, M., *"Influence of Surface Treatments and Coatings on Pressurized Hydrogen Emgrittlement of High-Strength Steels, Case of 35Ni-Cr-16Mo Steel,* Hannover Buchdruckwerkstätten, West Germany, Sept. 1968, p. 192, NASA TT-F-12-099, Feb. 1969.

[*34*] Fidelle, J.-P., Deloron, J. M., Roux, C., and Rapin, M., *Métallurgie et la Construction Mécanique*, Vol. 101, 1969, p. 341.

[*35*] Brunetaud, R., Chevalier, R., and Martinou, R. in *Hydrogen in Metals*, J. P.-Fidelle and M. Rapin, Eds., Valduc, France, Sept. 1967, p. 83.

[*36*] Johnson, H. H., Schneider, E. J., and Troiano, A. R., "The Recovery of Embrittled Cadmium Plated Steel," WADC-TR-57-430, Case Institute of Technology Cleveland, Ohio, June 1957.

[*37*] Pinard-Legry, G. and Montuelle, J., "Protection of High-Strength Martensitic Steels Against Corrosion Means of Surface Austenitization," Colloque Cefracor-Irsid, Paris, Dec. 1967.

R. L. Kesterson [1]

Effects of Irradiation and Oxygen on Hydrogen Environment Embrittlement of Selected Alloys

---

REFERENCE: Kesterson, R. L., **"Effects of Irradiation and Oxygen on Hydrogen Environment Embrittlement of Selected Alloys,"** *Hydrogen Embrittlement Testing, ASTM STP 543,* American Society for Testing and Materials, 1974, pp. 254–263.

ABSTRACT: Testing in 10-MPa (1500-psi) hydrogen did not reduce the notched strength of irradiated Inconel 718 or A286; however, irradiated Ti-5Al-2.5Sn suffered reductions in notched strength of 6.9 percent. Likewise, irradiated CW 301 stainless steel lost 81 percent of the notched strength in 10-MPa (1500-psi) hydrogen. For hydrogen pressures of 175 KPa (25 psi), impurity levels of 15-ppm oxygen do not seriously inhibit embrittlement of CW 301 stainless steel and a loss of 42 percent of notched strength is observed. With 150-ppm oxygen, the notched strength is reduced only 7.5 percent. Both Inconel 625 and molybdenum TZM were found to be subject to hydrogen embrittlement.

KEY WORDS: hydrogen embrittlement, irradiation, notch strength, notch tests, nuclear reactors, oxygen

Data generated by Walter and Chandler [*1*][2] and others indicate that most of the materials that the nuclear engine for rocket vehicle application (NERVA) reactor relied upon for structural support were subject to hydrogen embrittlement. To study this phenomenon, both Westinghouse Astronuclear Laboratory (WANL) and Aerojet Nuclear Systems Company (ANSC) initiated various testing programs.

The NERVA reactor employs ultrapure hydrogen at about 7 MPa (1000 psi) as a propellant which is heated by the nuclear core to about 2500 K (4000° F). Added to these hostile conditions in which structural materials must function is the presence of a strong radiation flux and the resulting specie of reactive atomic hydrogen. Information on the effects

---

[1] Engineer, Offshore Power Systems, Jacksonville, Fla. 32211.

[2] The italic numbers in brackets refer to the list of references appended to this paper.

of atomic hydrogen at these pressure levels is nonexistent; however, data generated [2] with atomic-molecular gas mixtures at low pressures indicate that the effect can be quite significant, both on the degree of embrittlement and on the temperature range of susceptibility. This paper discusses the available results from initial programs which have been completed.

Materials and Procedures

Six materials were chosen for the first series of tests, Inconel 625 and 718, CW 301 stainless steel, Ti-5AL-2.5Sn, A286, and molybdenum TZM. The chemistries of these alloys are listed in Table 1. The heat treatment and mechanical histories of these materials are reported in Table 2. The Inconel 718, A286, and Ti-5AL-2.5Sn specimens were taken from bar stock and were tested as round bar specimens. The Inconel 625, CW 301 stainless steel, and molybdenum TZM specimens were made from 0.048 (0.019), 0.089 (0.035), and 0.041 (0.016) cm (in.) thick sheet, respectively.

Initial programs [3] concerned the testing of previously irradiated specimens in a high-pressure, high-purity hydrogen atmosphere. The A286, Inconel 718, and Ti-5Al-2.5Sn specimens were standard notched buttonheads with a notch radius of 0.025 mm (0.001 in.) and a K_T of about 8. The CW 301 stainless steel pin loaded notched sheet specimen design is shown in Fig. 1. End tabs were welded on the specimens for support during testing. In the irradiation portion of the test program, crosshead speeds of 0.036 and 0.024 cm/min were used on the buttonhead and sheet specimens, respectively.

Tension tests were performed in stainless steel pressure chambers with

TABLE 1—*Material chemistries.*

Element	Inconel 625[a]	Inconel 718	CW 301 Stainless Steel	Ti-5Al-2.5Sn	Molybdenum TZM[a]	A286
Fe	2.5	19.02	73.33	0.14	0.01	52.53
Ni	61	52.54	7.1	...	...	26.43
C	0.05	0.04	0.10	0.01	0.01	0.05
Cr	21.5	18.21	17.65	...	...	14.7
Ti	0.02	0.91	...	91.8	0.40	1.99
Al	0.02	0.60	...	5.44	...	0.27
Zr	...	...	...	...	0.08	...
Cb/Ta	3.6	5.22	...	...	...	...
Mo	9.0	3.06	0.24	...	99.4	1.27
Sn	...	...	...	2.47	...	...
Mn	...	0.10	0.99	...	...	1.68
Si	...	0.13	0.45	...	...	0.65
Cu	...	0.01	0.10	...	...	...

[a] Chemical analysis of typical mill furnished material.

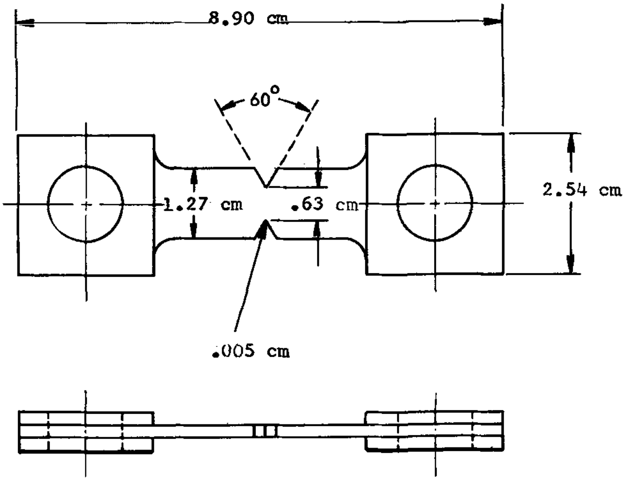

FIG. 1—*CW 301 stainless steel notched sheet specimen.*

Instron testing machines. The hydrogen gas for the high-pressure tests was obtained by passing high-purity bottled hydrogen through catalytic deoxygenation units, activated charcoal, and alumina adsorbents at 77 K and a 10-μm filter. The low pressure, 175-KPa (25-psi) test incorporated ultrapure bottled hydrogen passed through a liquid nitrogen cold trap. The hydrogen used in these tests met the Marshall Space Flight Center specification MSFC SPEC-356A requirements for purity.

The load produced by the pressure differential was corrected for by placing a slight load on the fixtured specimen, pressurizing the chamber, and adjusting the load a predetermined amount until a plateau was

TABLE 2—*Material Histories.*

Material	Condition
Inconel 625	mill annealed
Inconel 718	1065° C–1 h air cooled to ambient 732° C–8 h 649° C–12 h
Ti-5Al-2.5Sn	vacuum annealed 760° C–1 h
CW 301 stainless steel	full hard–as received
Molybdenum TZM	mill stress relieved
A286	982°C–1 h 732° C–16 h

reached. At this point the specimen was slack in the grips, and the measured compression load represented the pressure differential. For the high-pressure irradiated test, the pull rods penetrated the vessel using triple O-ring seals. The friction load of these seals was compensated for by increasing the load until another plateau was reached while the specimens were still slack within the grips. This second plateau represented both the loads produced by the pressure differential and the sliding seal load present during the constant deflection test. For the lower pressure, 175-KPa (25-psi) tests, there were no sliding seals, and the pull rod penetrated the vessel through stainless steel bellows of very low spring rate. The load factor attributed to the bellows was less than 0.5 kg and was deemed negligible.

Most of the initial testing was done at the General Dynamics facilities at Fort Worth, Texas. The test specimens were irradiated at 333 K (140° F) in the National Aeronautics and Space Administration (NASA)/Plum Brook reactor to a nominal fast fluence of 1.5×10^{20} n/cm^2 ($E > 1$ MeV). About six months lapsed between the irradiation and the testing.

A major mechanism [4] influencing the gaseous hydrogen embrittlement reaction is the concentration of oxygen in the hydrogen gas. The oxygen reacts with the surface adsorption sites and, if in sufficient quantity, will inhibit completely the absorption of hydrogen and thus prevent embrittlement. Using notched specimens of CW 301 stainless steel, the effects of various amounts of oxygen impurity levels were determined. The tests were done in the 175-KPa hydrogen test chamber, and the oxygen levels were increased up to 150 ppm by volume. The various oxygen-hydrogen atmospheres were produced by evacuating the chamber, back-filling with hydrogen and evacuating again, introducing controlled volumes of oxygen, and finally pressurizing with hydrogen.

Tension tests on notched molybdenum TZM specimens were performed in 175-KPa (25-psi) hydrogen. The test specimens were 0.041 cm (0.016 in.) thick and had a notch radius of 0.0025 cm (0.001 in.). Tabs were spot welded onto the pin loaded end for support. The crosshead deflection rate was varied to measure strain rate effects. All specimens were loaded initially at a rate of 0.0127 cm/min (0.005 in./min) until a stress level of 690 MN/m^2 (100 ksi) after which the deflection rate for some tests were adjusted to a lower value, and the test proceeded to completion.

Tests in 175-KPa (25-psi) hydrogen were performed on 0.048-cm (0.019-in.)-thick unnotched Inconel 625 sheet specimens. The strain rate was 0.003 cm/cm/min. Both the uniform (strain prior to necking) and fracture strain (total strain) were recorded. The difference between these strains was calculated and found to be more sensitive to the test environment than the other measured parameters. The information so generated is characteristic of gross plastic deformation and crack propagation conditions.

Results and Discussion

Irradiation Effects

The data generated in the irradiation-hydrogen test are listed in Table 3. As shown by the data, the titanium alloy sustained an average loss in notched strength (helium versus hydrogen) of 6.9 percent. This result compares to a reported 19 percent loss in 70-MPa (10 000-psi) hydrogen [*1*], a 17 percent loss in 35-MPa (5000-psi) hydrogen [*5*] and a 10 percent loss in 9.5-MPa (1400-psi) hydrogen [*6*]. From these data, it was assumed that in the case of Ti-5Al-2.5Sn the prior irradiation does not increase the degree of embrittlement.

The average notched tensile strengths of irradiated A286 specimens increased by 1.8 percent when tested in 10-MPa (1500-psi) hydrogen compared to 10-MPa (1500-psi) helium. This slight increase was judged not to be significant. Unirradiated specimens have been reported to be unaffected by gaseous hydrogen at 70 MPa (10 000 psi) [*1*].

TABLE 3—*Results of* H_2 *irradiation tests.*

Material	Test Environment, 10 MPa (1500 psi)	Ultimate Strength, MN/m^2 (ksi)	Average Loss from He, %
Ti-5Al-2.5Sn irradiated	He	1220 (177)	
		1200 (174)	
	H_2	1150 (166)	
		1130 (164)	
		1140 (165)	
		1080 (156)	6.9
A286 irradiated	He	1865 (270)	
		1870 (271)	
	H_2	1925 (279)	
		1876 (272)	
		1870 (271)	
		1930 (280)	+1.8
CW 301 stainless steel irradiated	He	1705 (247)	
		1700 (246)	
	H_2	328 (47.6)	
		341 (49.4)	
		324 (46.9)	81
Inconel 718 irradiated	He	2050 (298)	
		1980 (287)	
	H_2	1990 (289)	
		2040 (296)	0
Inconel 718 unirradiated	3.5 MPa H_2	1860 (269)	
	10 MPa H_2	1830 (265)	

TABLE 4—*Effect of oxygen content on hydrogen embrittlement of CW 301 stainless steel.*

Test Environment, 175 KPa	Notched Strength, MN/m^2 (ksi)	Reduction from Air-Argon, %
Air-Argon	1590 (230.5)	
	1610 (233.8)	
	1605 (232.4)	
H_2	900 (130.4)	
	934 (135.1)	
	924 (133.9)	42.5
15 ppm O_2	930 (134.8)	41.8
30 ppm O_2	1070 (157.0)	32.5
45 ppm O_2	1180 (171.2)	26.1
60 ppm O_2	1230 (179.6)	22.6
105 ppm O_2	1395 (202.9)	12.7
150 ppm O_2	1475 (214.4)	7.5

The effects of gaseous hydrogen on the mechanical properties of Inconel 718 have been studied by numerous investigators [*1, 5, 6*]. Reductions in notched strengths from 0 to 54 percent have been observed depending upon the gas pressure, temperature, heat treatment, and material lot. Results from the Inconel 718 tests indicate that there was no measurable effect of the hydrogen test environment as compared to helium in the irradiated tensile properties. Two unirradiated tension specimens were tested in 3.5 and 10-MPa hydrogen; however, there were no tests done in helium to provide comparison. The data indicate an increase in strength, even when tested in hydrogen, attributed to irradiation. A proposed explanation [*3*] for this result concludes that neutron irradiation of Inconel 718 produces effects similar to the solutioning effects which produce a structure less susceptible to hydrogen embrittlement.

The notched tensile strength of CW 301 stainless steel sheet specimens was reduced severely by testing in an ultrapure hydrogen environment. Irradiated specimens tested in 10-MPa hydrogen lost 80 percent of their strength. Likewise, unirradiated specimens tested in 175-KPa hydrogen lost about 42 percent of the notched tensile strength. Unpublished data [*7*] on cryostretched 301 stainless steel sheet indicate a loss of ambient fracture toughness, K_Q, of 82 percent when tested in 7-MPa hydrogen. From the data generated so far on 301 stainless steel, it can be conclusively stated that in the cold-worked condition, this material is very susceptible to hydrogen embrittlement.

Oxygen Impurity Effects

The effects of various oxygen impurity levels on the notched tensile strengths of CW 301 stainless steel were measured, and the data are tabulated in Table 4. In pure hydrogen at 175 KPa, the notch strength was

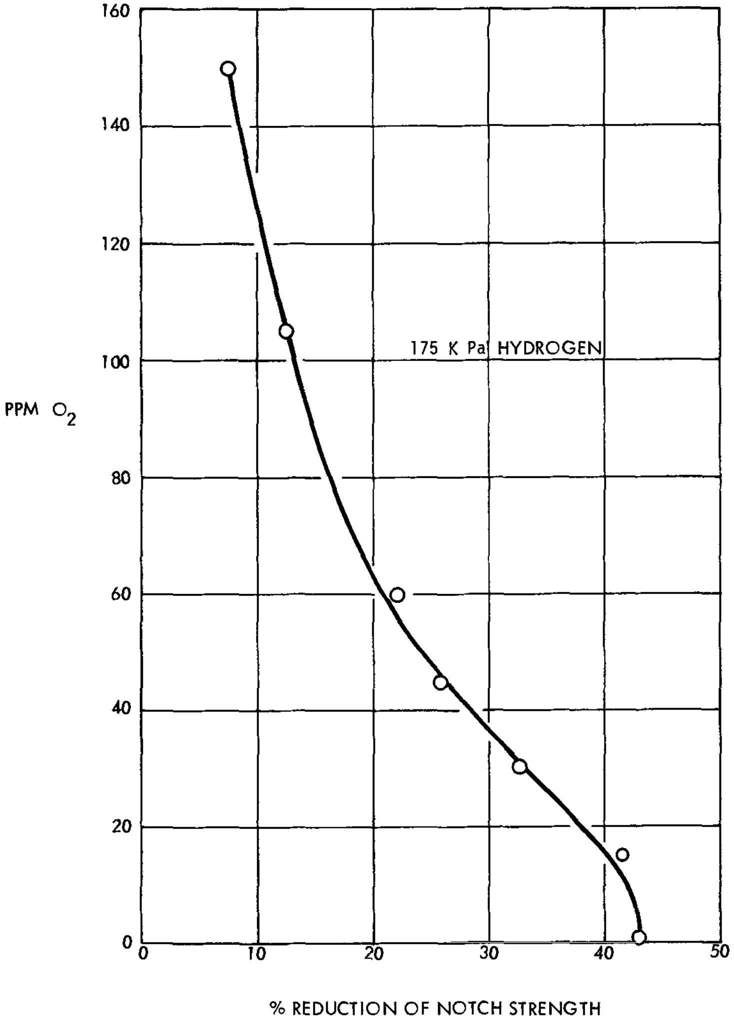

FIG. 2—*Effect of oxygen impurity on CW 301 stainless steel.*

reduced by 42.5 percent. Previously reported tests [*3*] done at higher pressures resulted in greater losses in strength, again emphasizing the significance of the test pressure.

The results of the oxygen impurity tests are displayed graphically in Fig. 2. The graph depicts the effects of various amounts of oxygen on the percent reduction in notch strength due to the hydrogen gas test environment. The data indicated that for exposures to 175-KPa hydrogen, oxygen impurity concentrations as high as 15 ppm had little effect on the reaction mechanisms. Likewise, oxygen levels of 150 ppm effectively limit the embrittlement to an 8 percent loss in notched strength.

It is emphasized that these data were generated at a pressure of 175 KPa. If the number of available adsorption sites is assumed to remain relatively constant as the pressure increases, then it is reasonable to postulate that the inhibiting ability of a specific oxygen level will also increase. This postulation is based on the fact that as the pressure is increased, the actual concentration of oxygen per unit volume also increases; therefore, more oxygen is available to "poison" the adsorption site.

Inconel 625 and Molybdenum TZM

Data from tests on Inconel 625 in 175-KPa hydrogen and air-argon atmospheres are reported in Table 5. The air-argon mixture was achieved by pressurizing the ambient air-filled chamber with argon. The test environment thus produced consisted of about 8 percent oxygen by volume. The data indicated that the relatively low-pressure hydrogen atmosphere significantly reduced the average yield strength, while only slightly reducing the ultimate strength and elongation. The measured differences between uniform strains and fracture strains were affected significantly by the test environment. The strain between reaching ultimate load and at fracture was reduced by 50 percent in the hydrogen atmosphere. Although this type of data is of little value in design calculations, it does provide a very sensitive method of screening for susceptibility to hydrogen embrittlement.

Data obtained from tests on molybdenum TZM notched sheet specimens

TABLE 5—*Effect of hydrogen on Inconel 625 (unnotched).*

Test Atmosphere, 175 KPa (25 psi)	0.2% Yield, MN/m^2 (ksi)	Ultimate Strength, MN/m^2 (ksi)	Uniform Strain, %[a]	Fracture Strain, %[b]	ΔStrain, %[c]
Air-Argon	546 (79.2)	1017 (147.4)	49.10	53.73	4.63
	524 (76.9)	1013 (147.1)	48.90	54.70	5.80
Average ($\bar{X}$)	535 (78.1)	1015 (147.2)	49.00	54.22	5.22
Hydrogen	422 (61.2)	971 (141.2)	47.20	51.05	3.85
	522 (75.6)	996 (144.5)	49.10	51.58	2.48
Average ($\bar{X}$)	472 (68.4)	984 (142.9)	48.15	51.32	3.17
$\frac{\text{X Hydrogen}}{\bar{\text{X}}\text{ Air-Argon}}$	0.876	0.969	0.981	0.946	0.608

[a] Strain at maximum load (prior to neck down).
[b] Strain at failure.
[c] Fracture strain minus uniform strain.

TABLE 6—*Effects of hydrogen and strain rate on notched molybdenum TZM sheet.*

Test Atmosphere, 175 KPa (25 psi)	Crosshead Deflection Rate, cm/min[a]	Notched Ultimate Strength, MN/m^2 (ksi)	Chart Elongation, mm[b]
Air-Argon	0.0127	1012 (146.7)	1.6
	0.0127	988 (143.1)	2.2
Hydrogen	0.0127	959 (139.0)	0.19
Air-Argon	0.0127/0.00127	900 (130.4)	2.3
	0.0127/0.00127	914 (132.5)	1.6
Hydrogen	0.0127/0.00127	920 (133.3)	0.91
	0.0127/0.00127	914 (132.5)	0.84
Air-Argon	0.0127/0.0005	920 (133.3)	1.8
Hydrogen	0.0127/0.0005	878 (127.3)	1.1
	0.0127/0.0005	828 (120.0)	0.79

[a] First rate until a stress of 690 MN/m^2 (100 ksi) is obtained, second rate to failure.
[b] Specimen deformation measured from load-deflection chart.

are listed in Table 6. As indicated, the notched strength was reduced by testing in the hydrogen environment from 0 to 7.5 percent, depending upon the strain rate. Likewise, the recorded elongation of the notched specimen was reduced from 46 to 90 percent, depending upon the strain rate. Admittedly, some of this information is based on only single data points; thus, the accuracy of some of the comparisons is degraded. However, a general result of these tests is the indication that molybdenum TZM sheet is definitely susceptible to gaseous hydrogen embrittlement even at relatively low pressures.

Conclusions

1. Irradiated A286 does not experience a loss in notched strength when tested in 10-MPa hydrogen; likewise, the irradiated Inconel 718 material tested did not decrease in notched strength when tested in hydrogen.
2. The notched strength of irradiated CW 301 stainless steel was degraded severely by about 81 percent when tested in 10-MPa hydrogen.
3. Irradiated Ti-5Al-2.5Sn material experienced normal losses in notched strength of 6.9 percent.
4. At hydrogen pressures of 175 KPa, oxygen impurity levels as high as 15 ppm did not seriously inhibit hydrogen embrittlement of CW 301 stainless steel.
5. The yield strength of Inconel 625 sheet was reduced by 12 percent when tested in 175-KPa hydrogen. The ultimate strength and elongation were reduced by 2 and 5 percent, respectively.
6. The differences between uniform strains and fracture strains of

specimens tested in air-argon and hydrogen is a sensitive measure of hydrogen embrittlement susceptibility.

7. Molybdenum TZM sheet is embrittled by gaseous hydrogen; reductions in notched strengths of 7.5 percent were observed.

Acknowledgments

The irradiated data, herein reported, were generated under the direction of D. Winterich of NASA/Plum Brook, M. Davidson of Aerojet Nuclear System Company, and J. K. Miles and R. L. Burtnett of General Dynamics and is gratefully acknowledged. This program was performed for the NERVA project under the direction of NASA-AEC Space Nuclear Propulsion Office.

References

[*1*] Walter, R. J. and Chandler, W. T., "Effects of High Pressure Hydrogen on Metals at Ambient Temperature," Report No. R-7780-1, Rocketdyne, Division of North American Rockwell Corp., Canoga Park, Calif., Feb. 1969.

[*2*] Nelson, H. G., Williams, D. P., and Tetelman, A. S., *Metallurgical Transactions*, 1971, Vol. 2, pp. 953–959.

[*3*] Miles, J. K. and Burtnett, R. L., "Hydrogen Embrittlement of Irradiated Alloys," Report No. FZK-379, General Dynamics Corp., St. Louis, Mo., May 1971.

[*4*] Hancock, G. G. and Johnson, H. H., *Transactions*, Metallurgical Society, American Institute of Mining, Metallurgical, and Petroleum Engineers, Vol. 236, April 1966, p. 513.

[*5*] Harris, J. A., Jr., and VanWanderham, M. C., "Properties of Materials in High Pressure Hydrogen at Cryogenic, Room and Elevated Temperatures," Report No. FR-4566, Pratt and Whitney Aircraft Div., United Aircraft Corp., West Palm Beach, Fla., June 1971.

[*6*] Walter, R. J., Hayes, H. G., and Chandler, W. T., "Mechanical Properties of Inconel 718, Waspalloy, A286, and Ti-5Al-2.5Sn ELI in Pure Gaseous H_2," Report No. R-8187, Rocketdyne, Division of North American Rockwell Corp., Canoga Park, Calif., April 1970.

[*7*] Forman, R., private communication, National Aeronautics and Space Administration-Manned Spacecraft Center, Tex.

CLOSING COMMENTARIES

STP543-EB/Jan. 1974

J.-P. Fidelle [1]

Closing Commentary—IHE-HEE: Are They the Same?

I certainly agree that internal hydrogen embrittlement (IHE) and hydrogen environment embrittlement (HEE) are the same on an atomic scale, HEE being caused by hydrogen absorption. This has been demonstrated by a number of investigators in the case of steels [*1–4*];[2] we have also seen this for pure nickel and titanium alloys [*2*]. I wish to point up that the relatively large hydrogen pickups (up to 2.5 ppm) observed after short tests at room temperature are not consistent with room temperature diffusivities and have to be explained by hydrogen being drawn inwards by dislocations [*5*] generated either at the surface (Fisher's sources) or near the surface (Sumino's sources). Disputation of this point [*4*] cannot be accepted because these authors failed to consider that the dragging efficiency of a dislocation is strain rate dependent. Direct evidence of the role of dislocations in the transport of hydrogen has been supplied [*6*].

In the case of steels and nickel, we have also noticed that hydrogen pickup qualitatively increased in the same way as nickel percent, suggesting again that HEE had to be related to the bulk properties of the materials [*2*]. Most of our hydrogen absorption experiments have been double checked by running disk pressure tests with the isotope deuterium (D), since D absorption cannot be mistaken for scatters in the amount of residual hydrogen.

Since stresses are triaxial inside of the metal but only biaxial at the surface, I feel that cracking initiates below the surface. However, subsurface cracking is very difficult to detect for HEE, because, in this case, the hydrogen concentration decreases from the surface producing the optimum compromise between stress state and hydrogen concentration at a place closer to the surface than would occur with IHE.

As pointed up earlier [*5*] in the case of a notched, precracked specimen, subsurface initiation of HEE is unlikely to be detected since the maximum

---

[1] CEA, Centre d'Etudes de Bruyères-le-Châtel, France.

[2] The italic numbers in brackets refer to the list of references appended to this paper.

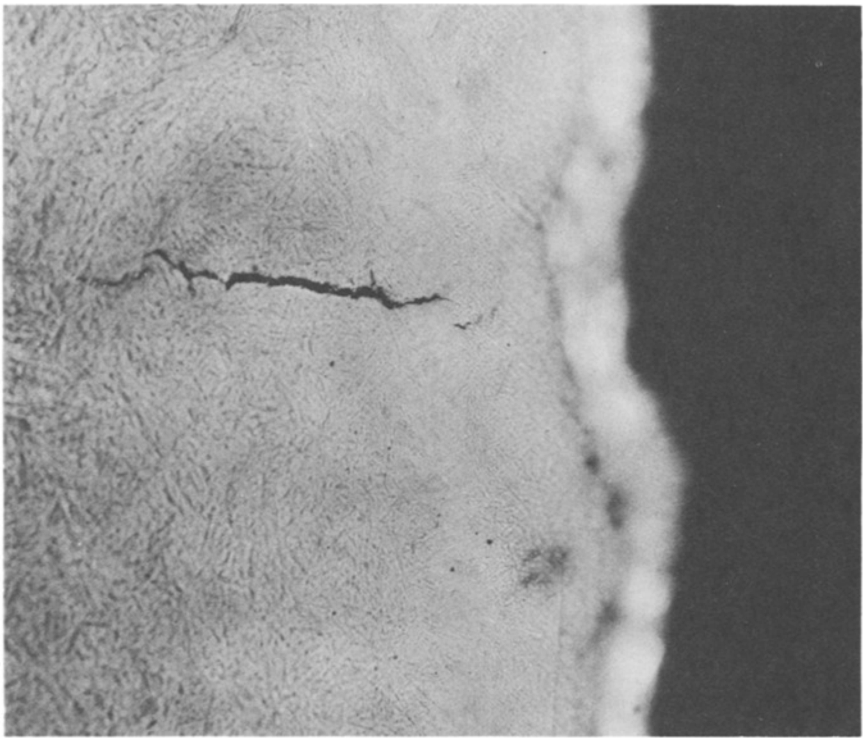

FIG. 1—*An internal secondary crack.*

hydrogen concentration is too close to the crack tip and results in the impression of surface initiation. Therefore, to evidence subsurface initiation, it is better to use smooth specimens and test conditions where the initiated crack does not burst immediately into a wide open crack ([*2*], Fig. 15, [*5*], Fig. 3).

Figure 1 shows an internal secondary crack developed, in a 30 μm coarse cadmium coated 35NCD16 high-strength steel disk which failed after 139 days exposure of the coated side to 125 bars H_2 at room temperature. Of course, such specimens had been baked, ensuring the absence of hydrogen embrittlement before testing [*7*]. Figure 2 suggests subsurface initiation in an aluminum coated 35NCD16 high-strength steel disk which failed at 145 bars during a dynamic test (the coating had an average thickness of 14 μm deposited by vacuum sputtering which could not induce any hydrogen entry into the substrate). In this instance, HEE occurred at a hole in the coating or at a place of reduced thickness. Polishing of two adjacent cross sections of the disks with these kinds of cracks generally showed the cracks progressively disappearing. Although not generally presented in the open literature, hydrogen gas induced delayed fractures of

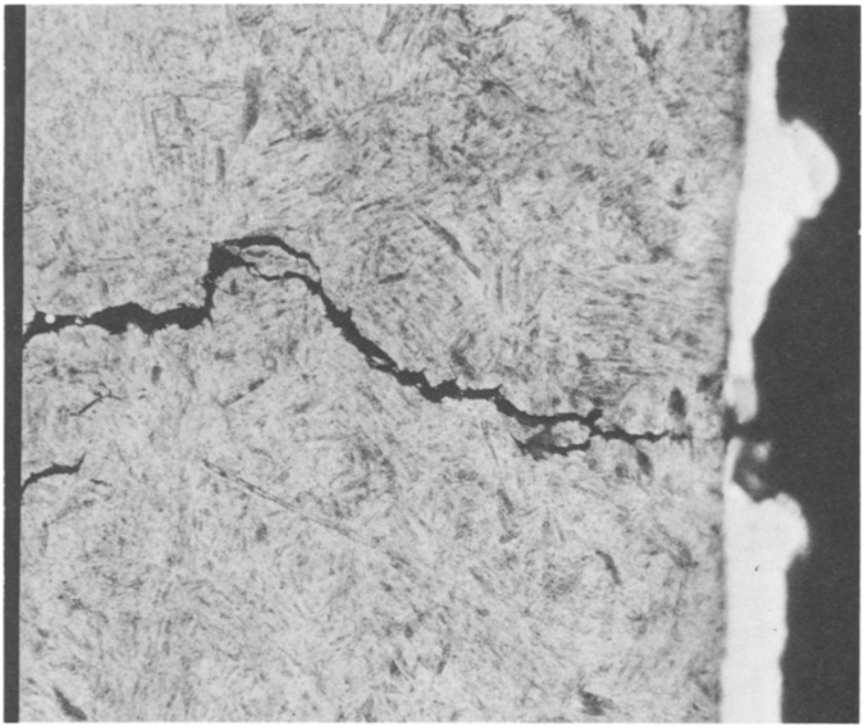

FIG. 2—*A subsurface initiation.*

thick-walled chemical reactors clearly have suggested subsurface initiation. See the incomplete ellipse shaped striations on Fig. 3. Surface initiation of hydrogen cracking would give only half ellipses and fatigue stretched half ellipses.

Figure 4 shows discontinuous permeation increases due to discontinuous crack propagation in 35NCD16 high-strength steel exposed to 230 bars deuterium gas at 70°C. Permeation indicates hydrogen absorption and would not be observed if crack propagation was due only to hydrogen adsorption on fresh external surfaces. Shortly before fracture occurs,

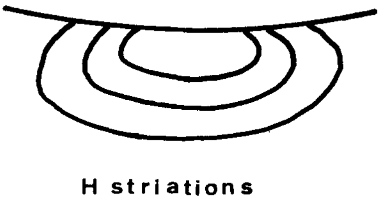

FIG. 3—*Ellipse shaped striations.*

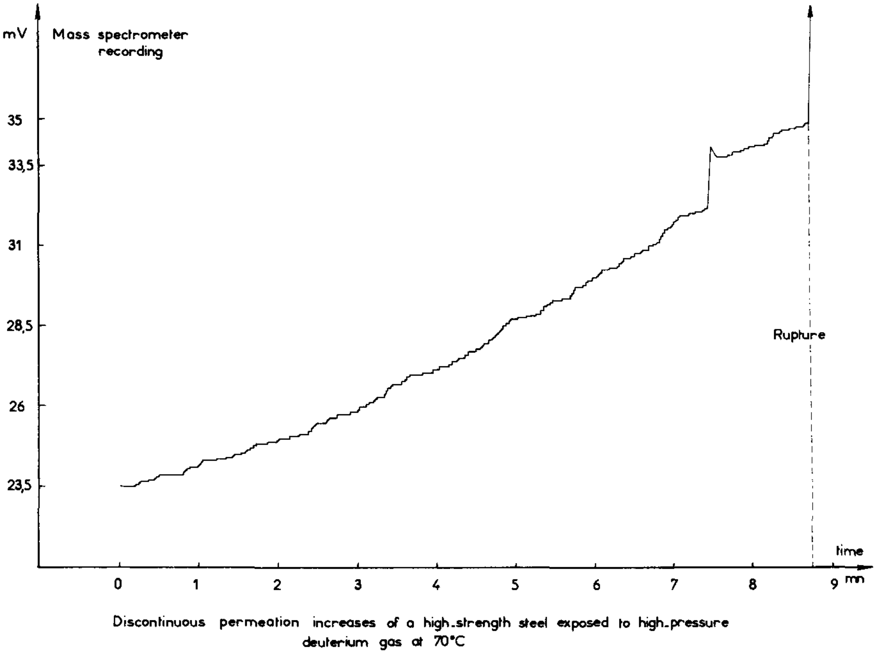

FIG. 4—*Discontinuous permeation increases of a high-strength steel exposed to high-pressure deuterium gas at 70° C.*

a permeation peak raises, followed by a permeation decrease, indicating the burst of an internal crack releasing gas to the outside. Cracking and sudden gas release shortly before final fracture have also been confirmed by acoustic emission.

Although IHE and HEE are basically facets of the same phenomenon, there are differences in the way they come out:

1. In HEE, hydrogen distribution is different from that of homogeneously charged specimens, and, accordingly, the crack initiation sites are different. They can become similar only when charged before testing. IHE has not led to a homogeneous distribution. This case is frequent in cathodic charging of specimens where diffusivity is low at room temperature.

2. In the case of IHE, there is a closed system, whereas in the case of HEE, hydrogen is poured into the specimen until the very last stage of fracture.

3. Influence of elevated temperatures: As temperature increases, HEE disappears even when care has been taken to plate the specimens in order to avoid hydrogen escape. This way, Graville et al [*8*] could see HEE disappear at 290°C in a 30NCD14 high-strength steel (0.30C, 3.5Ni, Cr, Mo). But in a similar steel, 35NCD16 (0.38C, 4.3Ni, Cr, Mo) tempered to high- and low-strength levels, we have found HEE to be still present at 300°C [*9*].

At this temperature the ratio of disk rupture pressures under helium and H_2 is 4.20 for the high-strength condition and 1.60 for the low-strength condition. In the last instance, the ratio is the same at 50°C.

Sensitivity to a fixed hydrogen amount may well decrease as temperature increases, but not hydrogen entry, and this is why HEE still occurs at higher temperatures than those where IHE has vanished. Besides, it is obviously important to the industry that this point has some theoretical importance. The role of hydrogen in stress-corrosion cracking has been excluded by a number of investigators because of the different responses of stress-corrosion cracking and IHE to increased temperatures. The results show the inconsistency of the argument that IHE and stress-corrosion cracking are the things to be compared. It appears that many stress-corrosion cases cannot be discounted as HEE instances on a temperature argument basis.

4. Influence of low temperatures: Although IHE has been reported down to −196°C for 4340 [*10*] and to −269°C (4.2 K) for 310 stainless steel [*11*], in the case of the 35NCD16 high-strength steel, embrittlement caused by molecular hydrogen was found to disappear at −145°C during disk pressure tests conducted at a pressure increase rate of 65 bars/min [*9*]. Tests in progress with disks deformed at lower strain rates might decrease this minimum temperature, but, since lowering temperature curtails hydrogen entry, embrittlement caused by molecular hydrogen is likely to disappear above low temperatures where internally present hydrogen still causes hydrogen embrittlement.

5. Influence of strain rates: Unless contamination by extraneous impurities occurs, slow strain rates should increase HEE even more than IHE, because, in the first case, hydrogen will enter as long as the test is in progress. On the other hand, high strain rates will not allow sufficient hydrogen entry [*4*, *12*]. HEE will disappear sooner than IHE when strain rate increases.

References

[*1*] Vennett, R. M. and Ansell, G. S., *Transactions*, American Society for Metals, Vol. 60, 1967, p. 242.

[*2*] Fidelle, J.-P., Allemand, L.-R., Roux, C., and Rapin, M. in *Hydrogen in Metals*, J.-P. Fidelle and M. Rapin, Eds., Valduc, France, 1969, p. 131.

[*3*] Benson, R. B., Jr., Dann, R. K., and Roberts, L. W., Jr., *Transactions*, Metallurgical Society, American Institute of Mining, Metallurgical, and Petroleum Engineers, Vol. 242, 1968, p. 2199.

[*4*] Fricke, E., Stüwe, H.-P., and Vibrans, G., *Metallurgical Transactions*, Vol. 2, 1971, p. 2697.

[*5*] Fidelle, J.-P., Roux, C., and Rapin, M., *Mémoires Scientifiques de la Revue de Métallurgie*, Vol. 66, 1969, p. 833, BISI Translation 8242, 1970.

[*6*] Broudeur, R., Fidelle, J.-P., and Auchère, H. in *Hydrogen in Metals*, Chatenay-Malabry, France, May 1972, p. 106.

[*7*] Fidelle, J.-P., Broudeur, R., Pirrovani, C., and Roux, C., this symposium, pp. 34–47.

[8] Graville, B. A., Baker, R. G., and Watkinson, F., *British Welding Journal*, June 1967, p. 337.
[9] Fidelle, J.-P., Broudeur, R., and Roux, C., *Hydrogen in Metals*, Chatenay-Malabry, France, 1972, p. 350.
[10] Steigerwald, E. A., Schaller, F. W., and Troiano, A. R., *Transactions*, Metallurgical Society, American Institute of Mining, Metallurgical, and Petroleum Engineers, Vol. 218, 1960, p. 832.
[11] Whiteman, M. B. and Troiano, A. R., *Corrosion*, National Association of Corrosion Engineers, Vol. 21, 1965, p. 54.
[12] Fidelle, J.-P., Bernardi, R., Broudeur, R., Roux, C., and Rapin, M., this symposium, pp. 221–253.

STP543-EB/Jan. 1974

H. G. Nelson[1]

Closing Commentary—IHE-HEE: Are They the Same?

The terms internal hydrogen embrittlement (IHE) and hydrogen environment embrittlement (HEE) are used to relate the original location of hydrogen within a system to a degradation in the fracture behavior of a metal structure (either the crack initiation or the growth stage of fracture). Because these phenomena are the combination of a number of processes involved both in the transport of hydrogen and its interaction with the metal lattice, they are complex. To say such complex phenomena are always the same or are always different would be equally absurd. Instead, my answer to this closing question must be to indicate briefly under what conditions IHE and HEE are similar and are different.

The processes of hydrogen transport (required to get hydrogen from its original position in the system to some location within the metal lattice to cause embrittlement) will, of course, always be different for IHE and HEE, because by definition the original location of hydrogen is never the same. Whether or not this difference plays a role in the separation of the two phenomena is determined by the rates of such processes as adsorption, dissociation, absorption, which occur only in HEE. If these processes are rapid compared with the transport processes common to both IHE and HEE, they will have no direct influence on the rate of degradation or the degree of embrittlement. If, however, one or more of these processes are slow compared with the common processes, HEE will exhibit the rate kinetics of the slowest, and IHE and HEE will be different under seemingly similar conditions.

Once hydrogen is in the metal lattice, further hydrogen transport will occur by processes common to both phenomena. Even here, IHE and HEE need not be the same. Both the location of the degrading hydrogen-metal interaction and the rate of hydrogen transport in the metal lattice will be influenced by such factors as the stress state of the material and dislocation motion. Hydrogen well within the metal lattice (IHE) and hydrogen in the

---

[1] Ames Research Center, National Aeronautics and Space Administration, Moffett Field, Calif. 94035.

metal lattice near an external surface (HEE) will invariably see different stress states and differing degrees of dislocation activity, and, thus, will interact within the metal structure at different locations at different rates. As pointed up by Fidelle, this rational is supported by the tendency for cracks to initiate near an external surface in HEE and well within the metal lattice in IHE.

Hydrogen, once at the location where it can interact with the metal lattice to cause embrittlement, will interact in the same manner whether or not its origin was within the metal lattice or the environment. Degradation will occur because of a reduction in bond strength of the metal lattice, the formation of a brittle metal hydride, or the precipitation of molecular hydrogen at some internal cavity. Even here, although the interaction mechanisms on the atomic scale are identical, situations do exist which preclude their importance in both phenomena. One example is the possible rupture of the metal lattice by the formation of an extremely high pressure in an internal cavity by the precipitation of molecular hydrogen. In IHE, such pressures can be conceived as the result of severe nonequilibrium conditions but would seem impossible under normal conditions of HEE. Another example is "fast strain rate embrittlement" sometimes observed in IHE. Here, hydrogen originates in the metal lattice as a brittle hydride phase, and hydrogen transport does not occur. Such a phase cannot be present when hydrogen is only present in the environment.

In summary, IHE and HEE may or may not be similar, depending on the specific constraints of the system under consideration. Certainly the interaction mechanisms on the atomic scale are many times the same. Macroscopically, however, because both IHE and HEE involve other considerations such as hydrogen transport processes, location of the hydrogen-metal interaction, the stress state of the metal lattice, the form and degree of dislocation activity in the metal lattice, etc., the overall phenomena are generally different—different to the extent that embrittlement is not the same function of temperature, is not the same function of microstructure, and in fact may exhibit little or no physical similarities.